OXIDATION OF AQUEOUS HUMIC SUBSTANCES BY OZONATION

by

Aslıhan Kerç

B.S. in Env. Eng. İstanbul Technical University, 1993

M.S. in Env. Eng. Marmara University, 1996

Submitted to the Institute of Environmental Sciences in partial fulfillment of the requirements for the degree of

Doctor

of

Philosophy

in

Environmental Technology

Boğaziçi University

2002

OXIDATION OF AQUEOUS HUMIC SUBSTANCES BY OZONATION

APPROVED BY:

Prof. Miray Bekbölet.....
(Thesis Supervisor)

Prof. Ferhan Çeçen.....

Prof. Ahmet M. Saatçi.....

Prof. Hasan Z. Sarıkaya .....

Prof. Orhan Yenigün .....

DATE OF APPROVAL.....24.12.2002.....

Dedicated to my family...

ACKNOWLEDGMENTS

I express my gratitude to Prof. Miray Bekbölet, my thesis supervisor for her guidance, support, patience, encouragement and help throughout my thesis. It was an opportunity for me to share her expertise during this study.

I will always be grateful to Prof. Ahmet M. Saatçi, who not only acted as a co-advisor in my thesis, but also guided me throughout my academic career with a never ending patience. I would also like to express my appreciation to the other members of my thesis jury Prof. Ferhan Çeçen, Prof. Hasan Z. Sarıkaya and Prof. Orhan Yenigün for their valuable time and comments.

The experiments in this study were conducted in Marmara University Environmental Engineering Laboratory and Boğaziçi University Institute of Environmental Sciences Laboratory. I want to thank all the laboratory staff for their helps.

I am thankful to Mr. Ercüment Aktuz for his encouragements during my studies and generous helps especially in the analysis conducted with gas chromatography.

I would like to thank Mr. Erhan Bağrıaçık for developing the software used in the ozone measurement system. I appreciate the guidance and help provided by Ms. Ceyda Uyguner in photocatalytic oxidation experiments.

Special thanks are extended to my all friends in Marmara University and Boğaziçi University for their support.

The financial support provided by the Research Fund of Boğaziçi University Project No. 02 Y 105D is gratefully acknowledged.

ABSTRACT

OXIDATION OF AQUEOUS HUMIC SUBSTANCES BY OZONATION

Chemical oxidation techniques have been used in water treatment for the removal of Natural Organic Matter (NOM), which are known to produce halogenated organic compounds in the finished waters upon chlorination. Besides its disinfection power, ozonation have been employed especially for its oxidation potential for the degradation of natural organics. Several studies in the literature have shown that although being a powerful oxidant, ozone is ineffective for the oxidation of recalcitrant organics like carboxylic acids. The accumulation of carboxylic acids in the solution upon ozonation makes the complete mineralization impossible or unfeasible. Therefore, in this study ozonation was combined with photocatalytic oxidation for the removal of humic acids, which comprise an important portion of natural organic compounds.

The first part of this study covers the ozonation kinetics, in which ozone mass transfer into aqueous solutions and ozone demand, accumulation and decomposition phases in humic acid solutions were evaluated. An empirical model was proposed for defining the humic acid degradation with ozonation.

The proceeding sections cover the combination of ozonation with photocatalytic oxidation. These two oxidation processes were applied in a sequential system in which ozonation was applied as a pretreatment stage for partial oxidation of humic acids prior to photocatalytic oxidation using TiO_2. Langmuir-Hinshelwood kinetics as well as the first order degradation kinetics was studied for defining the photocatalytic oxidation of humic acids. Pretreatment by ozonation resulted in increased first order degradation rates during the photocatalytic oxidation stage. Adsorption characteristics of the humic acids solutions on the catalyst (TiO_2) surface were also evaluated for better understanding of the removal processes. The results of the adsorption studies were analyzed using the Freundlich adsorption model.

UV absorbance and color were the parameters used to monitor the humic acid degradation during oxidation. The effects of oxidation processes on the humic acid molecules were assessed using molecular size distribution obtained by ultrafiltration of the oxidized humic acid samples. Trihalomethane formation potential (THMFP) was also another parameter measured to demonstrate the oxidation efficiencies achieved.

The combined oxidation resulted in complete mineralization of organics (~99 per cent), whereas organic matter oxidation efficiency achieved by only ozonation was 80 per cent, pointing out the accumulation of ozone resistant organics in humic acid solutions.

KISA ÖZET

SUDAKİ HÜMİK MADDELERİN OZONLAMA İLE OKSİDASYONU

Kimyasal oksidasyon teknikleri, klorlama sonucunda çıkış sularında halojenli organik bileşikler meydana getirdiği bilinen Doğal Organik Maddelerin (DOM) giderimi için su arıtımında kullanılmaktadır. Ozonlama, dezenfeksiyon gücünün yanısıra özellikle doğal organik maddeleri parçalama potansiyeli için kullanılmaktadır. Literatürdeki çeşitli çalışmalar göstermiştir ki güçlü bir yükseltgen olmasına rağmen ozon, karboksilik asit gibi dirençli organiklerin oksidasyonunda etkisizdir. Ozonlama sonucunda çözeltide karboksilik asit birikimi tam mineralizasyonu imkansız ya da uygulanamaz kılmaktadır. Bu sebeple, bu çalışmada doğal organik maddeler içerisinde önemli bir kısım teşkil eden hümik asitlerin giderimi için ozonlama, fotokatalitik oksidasyon ile birleştirilmiştir.

Bu çalışmanın ilk kısmı, sıvı çözeltiler içine ozonun kütle transferinin, hümik asit çözeltileri içinde ozon ihtiyacı, ozon birikimi ve ozon bozunması safhalarının incelendiği ozonlama kinetiğini kapsamaktadır. Ozonlama ile hümik asitlerin parçalanmasını tanımlamak için ampirik bir model önerilmiştir.

Sonraki bölümler, ozonlamanın fotokatalitik oksidasyon ile birleştirilmesini içermektedir. Bu iki oksidasyon prosesi, ozonlamanın TiO_2 kullanılan fotokatalitik oksidasyon öncesinde hümik asitlerin kısmen oksidasyonu için ön arıtma olarak kullanıldığı ardışık bir sistemde uygulanmıştır. Hümik asitlerin fotokatalitik oksidasyonunun tanımlanması için kinetik çalışmalar yapılmış, birinci derece bozunma kinetik modelinin yanısıra Langmuir-Hinshelwood modeli kullanılmıştır. Ozonlama ile ön arıtım, fotokatalitik oksidasyon aşamasında birinci derece bozunma hızlarının artmasını sağlamıştır. Giderim proseslerinin daha iyi anlaşılabilmesi için hümik asit çözeltilerinin kataliz (TiO_2) yüzeyine adsorplanma özellikleri de incelenmiştir. Adsorpsiyon çalışmalarının sonuçları, Freundlich adsorpsiyon modeli kullanılarak analiz edilmiştir.

UV absorbansı ve renk, oksidasyon esnasında hümik asit bozunmasını izlemek için kullanılmış olan parametrelerdir. Oksidasyon proseslerinin hümik asit molekülleri üzerindeki etkileri, oksitlenmiş hümik asit numunelerinin ultrafiltrasyonu ile elde edilen molekül büyüklüğü dağılımı ile incelenmiştir. Trihalometan formasyon potansiyeli (THMFP) de elde edilen oksidasyon verimlerinin gösterilmesi için kullanılan diğer bir parametredir.

Birleştirilmiş oksidasyon sonucunda organiklerin tamamen mineralizasyonu (yüzde ~99) sağlanmıştır. Sadece ozonlama ile elde edilen organik madde oksidasyonu verimi ise yüzde 80'dir; bu durum hümik asit çözeltilerindeki ozona dayanıklı organiklerin birikimini göstermektedir.

TABLE OF CONTENTS

LIST OF FIGURES

LIST OF TABLES

1. INTRODUCTION

It is well documented that most surface and ground waters contain natural organic matter. The organic matter in water results from elutriation of the soil and also from biological, chemical, and photochemical reactions in water that occur due to the presence of algae, animal and vegetable by-products. Some of the organic constituents in water can be listed as humic substances, carboxylic acids, amino acids, and carbohydrates. Humic substances, which are polymerized organic acids (humic and fulvic acids), are the main organic constituents in natural waters. Humic substances contribute to 30 to 50 percent of dissolved organic carbon (DOC) in natural waters (Langlais *et al.*, 1991).

Chlorination of the surface waters containing natural organic matter is a cause for the formation of halogenated organics. Haloacetic acids and trihalomethanes are the most common halogenated organic compounds formed as a result of chlorination process. The trihalomethane levels in potable waters are strictly monitored in Europe and the United States due to their carcinogenic and mutagenic effects.

Several oxidation methods have been studied for the removal of trihalomethane precursors from natural waters. Preozonation is one of these oxidation methods and has a great deal of application in many water treatment plants to achieve the Trihalomethane Formation Potential (THMFP) removal due to the high oxidation potential and reactivity of ozone with the various organic and inorganic compounds. Recent literature covers the application of Photocatalytic Oxidation processes (PCO) for the removal of trihalomethane (THM) precursors.

In this study oxidation of aqueous humic acids were evaluated. Ozonation as well as its combinations with photocatalytic oxidation were used for humic acid degradation. It is known that some of the end products of ozonation like carboxylic acids are refractory for further oxidation with ozone alone. Therefore, the limited capability of ozone in complete mineralization of natural organics was aimed to be increased by using photocatalytic

oxidation with TiO_2. It should be noted that photocatalytic oxidation is a destructive removal process rather than being a phase transfer. Water purification processes involving chemical destruction of the contaminant are gaining an increasing interest than the processes involving phase transfer of the contaminant (e.g., from liquid to solid such as activated carbon, or from liquid to gas in the case of air stripping of volatile contaminants) (Ollis *et al.*, 1989). Ozonation and photocatalytic oxidation were combined in a sequential system in which ozonation was employed for pretreatment of humic acids by partial oxidation. The degree of partial oxidation was adjusted by applying varying ozone dosages and described by percent organic matter degradation and color reduction. The effects of the combined oxidation process on the removal of THMFP as well as THM precursors were evaluated. Determination of molecular size distribution using ultrafiltration through membrane filters before and after the oxidation processes were employed to assess the changes in the molecular composition of organic matter.

2. THEORY

2.1. Natural Organic Matter

Natural organic matter (NOM) is a term used to describe the complex matrix of organic material present in natural waters. The NOM in natural waters significantly influences many aspects of water treatment, including the performance of unit processes (Oxidation, coagulation, adsorption), application of disinfectants and biological stability. As a result, NOM affects potable water quality in the areas of disinfection by-product formation, biological regrowth in the distribution system, color and tastes and odors. NOM can be divided into humic and nonhumic fractions (Owen *et al.*, 1995);

i) The humic fraction is more hydrophobic in character and comprises humic and fulvic acids.

ii) The nonhumic fraction is less hydrophobic in character and comprises hydrophilic acids, proteins, amino acids and carbohydrates.

In terms of chemical properties and implications for water treatment, the fraction of NOM specified as humic substances is considered to be the most important. Humic fraction of NOM may constitute 50 percent or more of total organic carbon (TOC) of surface waters.

NOM in water is generally derived from living or decayed vegetation and microbial decomposition processes. The source of the NOM in water supplies greatly influences the composition of the organic matter. An important source of organic matter in freshwater supplies is algal and cyanobacterial biomass, which is mostly aliphatic and totally devoid of lignins. In contrast, organic matter originating from soils is derived from terrestrial vegetation, which has high lignin content. Lignin has a predominantly aromatic structure. Consequently, NOM of soil origin tends to have a higher aromatic fraction than NOM of

aquatic origin. The location and age of the soil derived NOM also influences the organic matter's composition (Goel *et al.*, 1995).

2.1.1. Humic Substances

The common yellow to brown coloration of freshwaters is associated with dissolved organic matter (DOM) of the type commonly referred to as "humic substances". It is related to the organic matter of soil but is only partly of soil origin. Humic substances account for 40-80% of the dissolved organic matter in water; they are an important and ubiquitous fraction. Typical freshwater concentrations may be in the range of 1-25 mg/L expressed as DOC. The term humic substances are defined as the product of a heteropolycondensation of carbohydrates, proteins, fatty acids, lignins, tannins and many other materials depending on their origin (Gjessing, 1976). Aquatic humic substances have been shown to produce THMs on chlorination and to affect the transport and fate of other organic and inorganic species through partition/adsorption, catalytic and photolytic reactions.

Humic substances are structurally complex, polyelectrolytic, dark colored organic acids that are found in soils, sediments and natural waters. They have been classified into three fractions based on water solubility (Suffet and MacCarthy, 1989; Thurman and Malcolm, 1983):

i) Humin is the fraction not soluble in water at any pH value. It is a humic-like polymer that cannot be alkaline extracted from soil or sediment.

ii) Humic acid is not soluble under acidic conditions (pH<2) but becomes soluble at higher pH.

iii) Fulvic acid is soluble at all pH conditions.

The synthesis of humus is based on plant residues, and the most important compounds in this respect are lignin, carbohydrates, and proteins. They are the most important class of naturally occurring complexing agents. These are degradation-resistant materials formed during the deposition of vegetation that occur as deposits in soil, marsh sediments, peat, coal, lignite, or in almost any location where large quantities of vegetation have decayed.

They are commonly classified on the basis of solubility. The term humic substances are defined as the product of a heteropolycondensation of carbohydrates, proteins, fatty acids, lignins, tannins and many other materials depending on their origin (Gjessing, 1976).

Humic substances are high-molecular-weight macromolecules. Humic acids probably have molecular weights of 100 000 or higher (Trussell and Umphres, 1978). These substances contain a carbon skeleton with a high degree of aromatic character and with a large percentage of the molecular weight incorporated in functional groups, most of which contain oxygen. The elementary composition of most humic substance is within the following ranges: C, 45-55 %; O, 30-45 %; H, 3-6 %; N, 1-5 %; and S, 0-1 %. The terms *humin, humic acid,* and *fulvic acid* do not refer to single compounds but to a wide range of compounds of generally similar origin, with many properties in common (Manahan, 1991).

The analytical methods used for the separation of humic substances include capillary gas chromatography and liquid chromatography. Mass spectroscopy and carbon-13 nuclear magnetic resonance spectroscopy (^{13}C-NMR) are the methods used for the identification of humic substances. Aquatic NOM can be characterized by degree of aromaticity (measured by ultraviolet absorbance, fluorescence or carbon-13 nuclear magnetic resonance (^{13}C-NMR)), N:C ratio, amino acid content; molecular weight and morphology observed by transmission electron microscopy (TEM) (Krasner *et al.*, 1996).

Humic substances in natural waters are considerably more difficult to isolate, primarily due to low concentration of humic substances in water as compared to concentrations in soils and sediments (Malcolm and MacCarthy, 1986). There are analytical problems regarding the isolation of humic substances because:

i) soil organic matter is a complex mixture of many organic substance;
ii) sodium hydroxide extracts many of the substances, including simple organic compounds, inorganic compounds, and complex mixtures of polysaccharides and humic substances;
iii) humic substances themselves are complex mixtures that represent products of microbial degradation, chemical polymerization and oxidation.

The main physicochemical properties of the aquatic humic substances include:

- a strong reactivity with halogens, leading to a high consumption of chlorine in potable water treatment and production of several volatile and nonvolatile halogenated organic compounds, some with a strongly mutagenic nature;

- a significant adsorbability on solids such as activated carbon and alumina, but also on mineral colloids, which is likely to modify the performance of the coagulation/ flocculation process;

- possible complexation with trace metals, which is likely to make them more soluble and hinder their removal, or a possible complexation with coagulant metals, inducing the precipitation of the humic matter during the clarification process; and

- the possibility that the humic substances might combine with organic micropollutants, including some pesticide which can cause them to be more soluble in natural water.

2.1.2. Humic Acids

In natural waters, humic and fulvic acids are the major two types of humic substances. Humic and fulvic acids are, by the simplest definition, the sodium hydroxide extract of soil. Typical number average molecular weights of aquatic humic acids are 2000 – 3000 Daltons, whereas the molecular weights of soil humic acids are reported to be as large as several hundred thousand Daltons (Suffet and MacCarthy, 1989).

Aquatic humic acids posses many chemical properties that arise from the presence of several functional groups in their complex structure about which little are known. Humic acids consist of a skeleton of alkyl/aromatic units cross-linked by a variety of functional groups such as carboxylic, phenolic and alcoholic hydroxyls, ketone and quinone groups (Gaffney *et al.*, 1996). The model structure of humic acid molecule is presented in Figure 2.1 showing the aromatic base and functional groups.

Humic acids act as natural photosensitizers in heterogeneous as well as homogeneous solutions yielding active oxygen species such as $^1O_2$, HO·, HO_2· and O_2 ·⁻ (Leifer, 1988; Zepp *et al,* 1981). They impart yellow color, exhibit acidic character, are chemically complex in nature and behave like polyelectrolytes in aqueous medium, therefore they may initiate detrimental reactions. Consequently, the removal of humic acids constitutes the major task in water treatment.

Naturally occurring humic acids possess partially aromatic structure with significant amounts of unsaturated sp^2 hybridized carbon (e.g. aromatic carbon). They also contain volatile organic compounds that have become entrapped in polymeric network. Therefore, humic acids are considered to be polydisperse and heterogeneous with respect to size and shape as well as charge.

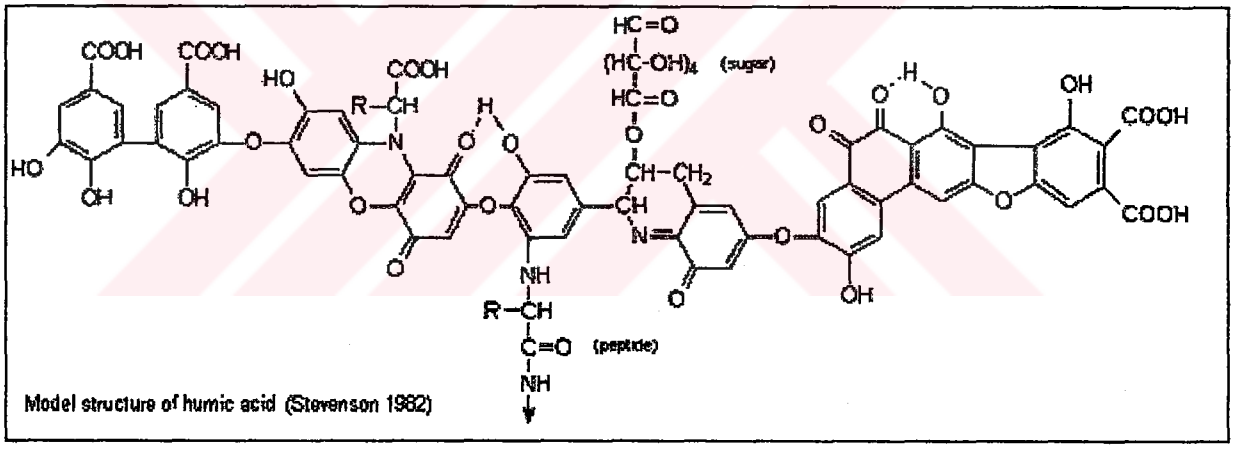

Figure 2.1. Humic acid molecular structure (Stevenson, 1982)

There are various studies in the literature regarding the elemental composition of humic substances. The characteristics of the reference humic substances as isolated and defined by the International Humic Substance Society (IHSS) are tabulated in Table 2.1. Humic acid and fulvic acid contain basically the same amount of C, H and O, but they are known to differ in the number of carboxylic and phenolic functional groups. Both of them also contain nitrogen, sulfide, phosphorous and ash. The nitrogen content of the reference humic acid is about 1 per cent, whereas it is less than 1 per cent for fulvic acid. S and P contents in both fulvic and humic acids are less than 1 per cent.

Table 2.1. Elemental composition of reference aquatic humic and fulvic acids (Langlais *et al.*, 1991)

	% C	% H	% O	% N	% S	% P	% Ash
Fulvic Acid	53.75	4.29	40.48	0.68	0.50	0.01	0.82
Humic Acid	54.22	4.14	39.00	1.21	0.82	0.01	3.19

Malcolm and MacCarthy (1986) have defined the elemental composition of Aldrich humic acid sodium salt, which was also used in this study (Table 2.2).

Table 2.2. Elemental composition of Aldrich humic acid

% C	% H	% O	% N	% S	% P	Total	% Ash
68.98	5.26	43.45	0.74	4.24	<0.05	122.7	31.21

2.2. Formation of Trihalomethanes

It is well documented that disinfection of natural waters with aqueous chlorine results in drinking waters that contain organically bound halogen, TOX (total organic halide). A portion of this TOX is composed of volatile, relatively hydrophobic organohalides such as trihalomethanes, principally chloroform (Rook, 1974). Another portion is composed of hydrophilic organohalides, principally di- and trichloroacetic acids. It is attractive to hypothesize that rupture of phenolic rings contained in natural aquatic humic material by aqueous chlorine is the principal formation pathway for TOX.

The health aspect of drinking water, with respect to the chlorination step in the purification process has been a major concern in recent years. Chlorine has been the principal disinfectant used in the world, as it is cheap and effective in maintaining the residual necessary for destroying the bacteria throughout the distribution system. However,

this kind of disinfection became a suspect as trihalomethanes (THMs) are found in finished waters.

The most common THMs in chlorinated drinking waters are, chloroform, bromodichloromethane, dibromochloromethane, and bromoform. Among four of them, chloroform is the most suspected carcinogen THM.

In 1975, Rook gave a more complete presentation of the various factors influencing the formation of trihalomethanes. Later EPA presented the results of the National Organics Reconnaissance Survey (NORS) showing that THMs could be found in almost all finished water. In 1976 the USA National Cancer Institute published results showing that at high doses chloroform, the most common THM could cause cancer in rats. This was soon followed by USEPA ban on the use of chloroform as an additive in the preparation of food and drugs. Finally, maximum contaminant level (MCL) was set to 100 μg/L as total trihalomethanes by US Safe Drinking Water Act. However, USEPA has decreased the level to 80 μg/l and recently proposed a new MCL as 50 μg/l for total trihalomethanes.

With recent advances in the identification of chlorination by products and their health effects, a greater emphasis has been paid upon the removal of trihalomethane precursors as well as THMs from drinking waters.

A number of researchers have tried to correlate humic acid or raw water characteristics to trihalomethane formation potential (THMFP) in an effort to find a useful surrogate parameter for THMFP or to better understand the chemical nature of THM formation from natural organic matter.

Reckhow *et al.* (1990) studied the THMFP of ten aquatic humic and fulvic acids isolated from natural systems. Yields of TOX, chloroform, trichloroacetic acid, dichloroacetic acid, dichloroacetonitrile and 1,1,1-trichloropropanone were measured at pH 7 and 12. Aquatic humic acids produced more of these compounds except 1,1,1-trichloropropanone and chlorine consumption and by product formation were related to fundamental chemical characteristics of the humic materials.

In the study of Kavanaugh *et al.*(1980), an empirical kinetic model of THM formation was studied. Concerning this study, the formation of THMs can be described as follows:

$$3A + B \xrightarrow{k_n} C$$

where A = HOCl, B = TOC and C = Total THM, while k_n is the n-order overall rate constant for reaction. The rate expression for the formation of THMs is given by

$$\frac{dC}{dt} = k_n[B][A]^m \qquad (2.1)$$

assuming that the rate of formation is first-order with respect to TOC and m-order with respect to HOCl.

Urano *et al.* (1983) studied the formation of THM in aqueous solution of humic acid under various conditions and obtained the following rate equation:

$$[THM] = k\,(pH\text{-}a)\,[TOC]\,[Cl_2]_o^{\,m}\,t^n \qquad (2.2)$$

Here, *[THM]* is the concentration of total THM after t hours. *[TOC]* and $[Cl_2]_o$ are the concentration of total organic carbon and chlorine dose, k is the reaction rate constant; and a, m and n are parameters. The values of k, a, m and n for humic acid as reagent were reported as k: 8.2×10^{-4}, a: 2.8, m:0.25 and n: 0.36.

A mechanism for THM formation may be explained using the reactions between methyl ketones and halogens in the presence of base. Multiple halogenations always occur at the carbon of the methyl group because introduction of the first halogen (owing to its electronegativity) makes the remaining α hydrogens on the methyl carbon more acidic. When methyl ketones react with halogens hydroxide ion attacks the carbonyl carbon atom of the trihalo ketone and causes a cleavage at the carbon-carbon bond between the carbonyl group and the trihalomethyl group. This cleavage ultimately produces a carboxylate ion and a haloform (i.e. $CHCl_3$, $CHBr_3$). The reaction pathways for the haloform formation are

presented in the below figure (Solamons, 1992).

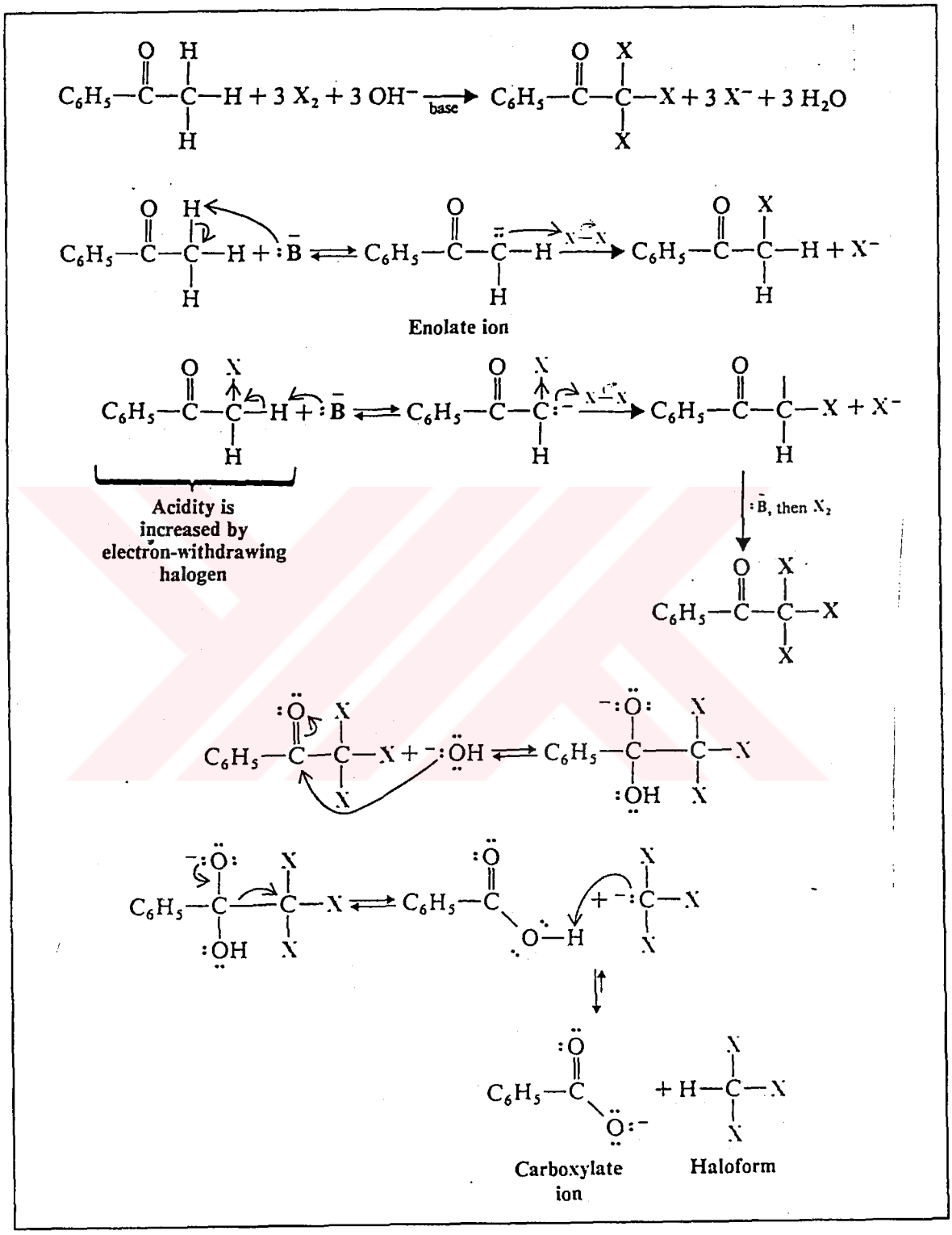

Figure 2.2. Haloform formation pathways (Solamons, 1992).

2.2.1. Methods for Removing Trihalomethane Precursors

Techniques for removing THM precursors, which are basically the natural organic compounds, are classified as clarification, source control, aeration, adsorption, ion exchange, biological degradation and oxidation. In chemical oxidation most widely used oxidants are ozone and chlorine dioxide. Photocatalytic oxidation with TiO_2 has been proven to be an effective method for the oxidation of humic acids (Bekbolet *et al.*, 1996). The advanced oxidation processes, which depend on the formation of hydroxyl radicals (OH·), are applied for total elimination of organic compounds both in water and wastewater treatment. Highly reactive OH· species attack non-selectively to almost all organics and result in rapid degradation. Hydroxyl radical is known to be the most powerful oxidizing species after fluorine and it has an oxidation potential of 2.80 V. Combinations of various oxidation techniques are applied in advanced oxidation processes. These processes include ozone/ ultra-violet irradiation, ozone/titanium dioxide, ozone/titanium dioxide/UV, ozone/hydrogen peroxide, ozone/γ-rays (^{60} Co). (Kusakabe *et al.*, 1990 ; Backlund, 1992; Arai *et al.*, 1986; Allemane *et al.*, 1993; EPA, 1981). These combined processes involve in most cases generation and subsequent reaction of hydroxyl radicals.

The hydroxyl radical is a short-lived, extremely potent oxidizing agent, capable of oxidizing organic compounds mostly by hydrogen abstraction. This reaction generates organic radicals, which by addition of molecular oxygen yield peroxyl radicals. These intermediates initiate thermal (chain) reactions of oxidative degradation, leading finally to carbon dioxide, water and inorganic salts (Legrini *et al.*, 1993).

$$HO\cdot + RH \rightarrow R\cdot + H_2O$$

$$R\cdot + O_2 \rightarrow RO_2\cdot \rightarrow \rightarrow$$

$$HO\cdot + RX \rightarrow RX^{\cdot +} + HO^{-} \rightarrow \rightarrow CO_2 + H_2O$$

Based on the reactivity of hydroxyl radicals the oxidative degradation of humic acid should follow the above expressed scheme in general. Thereby resulting in the removal of THM precursors (Bekbolet and Ozkosemen, 1996).

2.3. Ozonation

2.3.1. Ozone Chemistry and Fundamental Aspects

Ozone (O_3), a colorless gas at room temperature, is an allotropic form of oxygen (O_2). Ozone is characterized by strong oxidizing properties. It is very unstable at ambient temperatures and pressures and decomposes very rapidly to oxygen.

Ozone has a characteristic odor, which can be detected by most humans at low concentrations (0.02 ppm by volume), far below the levels of acute toxicity. It is moderately soluble in water, with solubility depending on the temperature of the water and ozone concentration in the feed gas. As temperature increases, ozone becomes less soluble and less stable in water; however, the disinfection and chemical oxidation rates remain relatively stable (EPA, 1981).

Ozone is a highly reactive gas formed by electrical discharges in the presence of oxygen as follows:

$$3O_2 + energy \rightarrow 2O_3$$

Substantial amount of energy is required to split the stable oxygen-oxygen covalent bond to form ozone molecule.

Ozone discovered by Schonbein in 1840, has extremely important significance in various environmental health areas including air pollution, water pollution, and industrial hygiene studies.

Like oxygen, ozone is a supporter of combustion and is one of the most powerful oxidizing agents, attacking almost all organic compounds. Ozone has an oxidation potential of 2.07 V, whereas this value is 1.36 for chlorine.

Ozone which is one of the most reactive gases known -in fact the fourth most powerful oxidizing agent known (only F_2, F_2O, and O· are better) is thought to have a mechanism of oxidation related to the following reaction:

$$O_3 \longrightarrow O_2 + O\cdot$$

where nascent oxygen produces a high-energy oxidation via a free radical reaction (Evans, 1972).

2.3.2. Ozonation in Drinking Water Treatment

Ozone has been used since 1903 for the treatment of drinking water. Ozone has been considered as an alternative disinfectant to chlorine especially after 1974, when it was discovered that chlorine reacts with natural organics in water to form a group of potentially carcinogenic compounds. Number of ozonation applications increase as standards for chlorinated by-products become more stringent. Ozonation is mostly used in the preoxidation step for the oxidation of organics and taste and odor removal purposes rather than disinfection. A significant decrease in the THM concentrations in the finished drinking waters have been reported when prechlorination is replaced with preozonation in drinking water treatment plants.

Ozone, which is an effective disinfectant at low concentrations, reacts with reduced inorganic compounds and with organic material. When compared with chlorination, the difference is the addition of an oxygen atom, instead of a chloride atom to the organics, the end result being an environmentally acceptable compound. Once this ozone demand has been met, the ozone reacts vigorously with bacteria and viruses. It is reported to be more effective than chlorine in inactivating resistant strains of bacteria and viruses (Peavy *et al.*, 1985).

The required ozone dosage to obtain a certain degree of disinfection in drinking waters is strongly dependant on the organic content of the water. Therefore, determination of ozone dosage and the contact time is a complicated issue in the environmental

engineering literature. Ozone transfer into water and chemical reactions occur simultaneously in the gas-liquid contactors. The hydraulic characteristics of the ozone contact chambers, the method of ozone gas transfer into the liquid including the diffuser type and configuration are the factors affecting the efficiency of ozonation applications.

2.3.3. Ozonation Kinetics

2.3.3.1. Transfer and Decomposition of Ozone in Water. Ozone's high level of chemical energy is the driving force for its decomposition. The ozone molecule readily reverts to elemental oxygen during the oxidation- reduction reaction. (Montgomery, 1985)

When the ozone gas is introduced into water many mechanisms affect its absorption in water and its reactions with the contaminants in water. The rate of ozone decomposition is a complex function of temperature, pH, and concentration of organic solutes and inorganic constituents.

In water, ozone may react directly with dissolved substances, or it may decompose to form secondary oxidants such as OH· radicals, which then themselves immediately react with solutes. The decomposition of aqueous ozone is generally due to chain reactions involving OH· radicals. Different pathways of reactions lead to different types of kinetics. (Staehelin and Hoigné, 1985).

Figure 2.3 shows reaction pathways of ozone as they have been described by Hoigné and Bader (1976). Once ozone enters solution, it follows two basic modes of reaction: direct oxidation, which is rather slow and extremely selective, and autodecomposition to the hydroxyl radical (OH·). Autodecomposition to the hydroxyl radical is catalyzed by the presence of hydroxyl radical, by organic radicals (R·), or by high concentrations of hydroxide ion. The hydroxyl radical is extremely fast and nonselective in its oxidation of organic compounds. But at the same time, the hydroxyl radical is scavenged by carbonate and bicarbonate ions to form carbonate ($CO_3\cdot^-$) and bicarbonate ($HCO_3\cdot$) radicals. These radicals are of no consequence in organic reactions. Further, the hydroxyl radicals and organic radicals produced by autodecomposition become chain carriers and enter back into

the autodecomposition reaction to accelerate it. Thus, conditions of low pH favor the slow direct oxidation reactions involving O_3, and high pH conditions or high concentrations of organic matter favor the autodecomposition route.

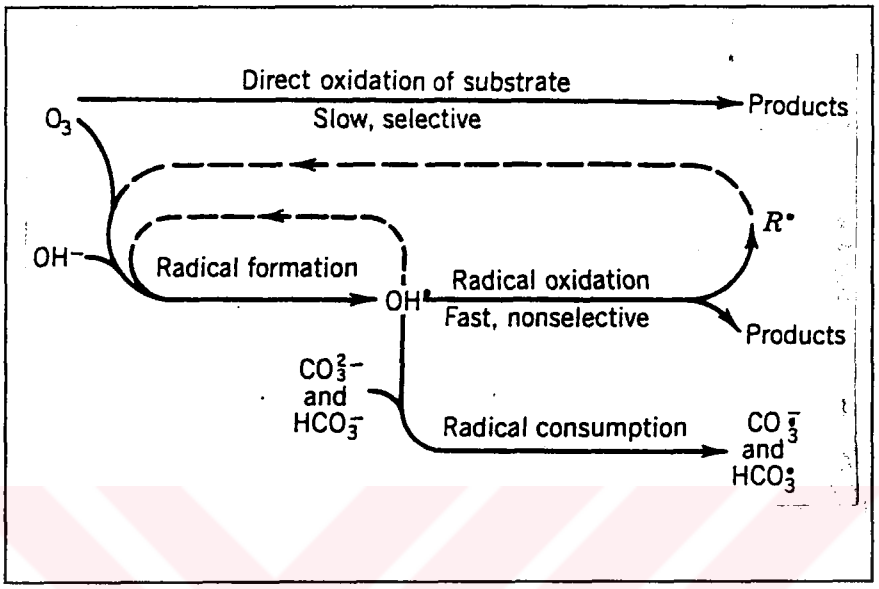

Figure 2.3. Reaction pathways of ozone (Hoigné and Bader, 1976)

Ozone is capable of oxidizing a variety of organic materials in aqueous solution. The major mechanisms contributing to the removal of organic pollutants can be identified as physical stripping (volatilization) and chemical oxidation by ozone molecules (direct oxidation) and by free radicals (indirect oxidation) (Gurol, 1985). Gurol and Singer (1983) described the process of oxidation by ozone in an ozone contactor involving the phenomenon of mass transfer with simultaneous reactions. The process was explained with the following points:

i) The interrelationship between partial pressure of the gaseous ozone and its solubility on water and the rate of mass transfer of ozone from the gas phase into solution,

ii) The kinetics of self-decomposition of ozone in water,

iii) The kinetics of the oxidation of the substrates and their oxidation products by molecular ozone.

These physical and chemical reactions can be expressed by Equation 2.3.

$$\left(\frac{d[O_3]}{dt}\right)=\left(\frac{d[O_3]}{dt}\right)-\left(\frac{d[O_3]}{dt}\right)-\sum\left(\frac{d[O_3]}{dt}\right) \tag{2.3}$$

solution	absorption from gas phase	decomposition	oxidation reactions by molecular ozone

Gurol and Singer (1982) described the change of ozone concentration in water according to its transfer into water from the gas phase and its decomposition in water as follows:

$$\frac{d[O_3]}{dt}=K_La\left([O_3]^*-[O_3]\right)-r_{O_3} \tag{2.4}$$

where K_La is the mass transfer coefficient governing the absorption of ozone by the solution, $[O_3]^*$ is the saturation concentration of ozone in accordance with Henry's law and the applied partial pressure of ozone in the gas stream contacting the solution, and r_{O3} is the rate of decomposition of ozone, it includes both self decomposition of ozone and decomposition due to reactions with other impurities in the solution. Staehelein and Hoigné (1985) have expressed the rate of ozone depletion due to the reaction of NOM within the chain cycle, including the loss of ozone by direct reaction and the initiation reaction by the following equation:

$$-\frac{d[O_3]}{dt}=\left[k_d[NOM]_d+k_i[NOM]_i\left(1+\frac{k_p[NOM]_p}{k_s[NOM]_s}\right)\right][O_3] \tag{2.5}$$

where, k_d, k_i, k_p and k_s represent the rate constants for direct, initiation, promoting and scavenging reactions. However, ozone decomposition can be simply expressed with the following first order decomposition kinetics including both direct and indirect reactions.

$$r_{O_3}=-\frac{d[O_3]}{dt}=k_{O_3}[O_3] \tag{2.6}$$

where k_{O3} represents the ozone decomposition rate constant and defined as follows:

$$k_{O_3} = k_d[NOM]_d + k_i[NOM]_i\left(1+\frac{k_p[NOM]_p}{k_s[NOM]_s}\right) \quad (2.7)$$

Yurteri and Gurol (1988) characterized the overall kinetics of dissolved ozone consumption by a first order relation with respect to $[O_3]$ and defined it as "specific ozone utilization rate", w ($time^{-1}$). The variation of w values measured in different water samples were explained in terms of the pH, alkalinity, and total organic content of the solution matrix.

In a semi-batch reactor where ozone gas in continuously added into the solution, the contact time of ozone in aqueous phase can be divided into three phases incorporating the ozone transfer from the gas phase into aqueous phase and the decomposition of ozone (Montgomery, 1985):

Phase 1: Demand phase (ozone transfer without residual)
Phase 2: Residual maintenance phase (measurable residual)
Phase 3: Decay phase (possible ozone and oxygen stripping)

During the demand phase, since the rate of ozone decomposition reactions are exceeding the ozone mass transfer into solution, no residual ozone concentration can be maintained in the solution. The length of the ozone demand phase depends on the concentration of ozone in the applied gas stream, gas flowrate, the characteristics of the ozone dissolution system, hydraulic characteristics of the reactor, temperature and the water quality. Once the ozone demand of the water has been satisfied, the applied ozone begins to accumulate in the water during the residual maintenance phase, since the mass transfer rate exceeds the decomposition rate. The ozone concentration in water can increase up to the saturation concentration governed by the Henry's Law depending on the temperature and pressure. The decay phase begins after the termination of ozone gas application into the solution.

2.3.3.2. Oxidation of Organics with Ozone. Among the organic groups which can be oxidized by ozone are olefinic and acetylenic carbon-carbon double and triple bonds; aromatic, carbocyclic and heterocyclic molecules; carbon-nitrogen and similar unsaturated groupings; nucleophilic molecules such as amines, sulfides, sulfoxides, phosphines, phosphites, etc.; carbon-hydrogen bonds in alcohols, ethers, aldehydes, amines, hydrocarbons, etc.; silicon-hydrogen, silicon-silicon, and silicon-carbon bonds; and carbon-metal bonds of various types (Evans,1972).

Natural organic matter (NOM) oxidation with ozonation is an important issue in drinking water treatment. The tasks of NOM-ozonation are (Camel and Bermond, 1998):

- Removal of color and UV-absorbance
- Increase in biodegradable organic carbon ahead of biological stages
- Reduction of potential disinfection by-product formation, including THMs
- Direct reduction of DOC/TOC levels by mineralization.

There are studies in the literature regarding humic and fulvic acid ozonations. It has been shown that ozonation of humic and fulvic acids results with TOC and UV visible absorbance reduction in high ozone dosages (Anderson *et al.*, 1986). The researches have also shown that ozonation increases the biodegradability of humic substances (Legube *et al.*, 1987).

Ozone can react with humic substances in an aqueous media by direct and radical type processes as presented in Figure 2.4. Ozone decomposition and subsequent hydroxyl radical generation are greatly affected by the type and concentration of natural NOM present in waters. Molecular ozone is expected to attack the humic material at three specific sites: carbon-carbon double bonds, aromatic rings with electron donating groups such as –OH or $–NH_2$, and sites containing complexed metals such as iron (Glaze and Wallace, 1984). Attacking as an electrophile, ozone preferentially reacts with electron rich humic acid moieties. The major source of electron rich moieties is sp^2 – hybridized carbon, such as those contained in unsaturated carbon structures, eg: aromatic, olefinic etc. Functional groups, such as hydroxyls (-OH) and amines ($-NH_2$) are electron donating and enhance the

reactivity of adjacent carbon bonds. On the other hand; functional groups such as carboxyls (-COOH) are electron withdrawing and may have tended to lessen the reactivity of adjacent bonded carbon. Therefore, the initial carbon structure and functionality have affected the reaction rate of ozone with humic acid (Bose *et al.*, 1994; Westerfoff *et al.*, 1999).

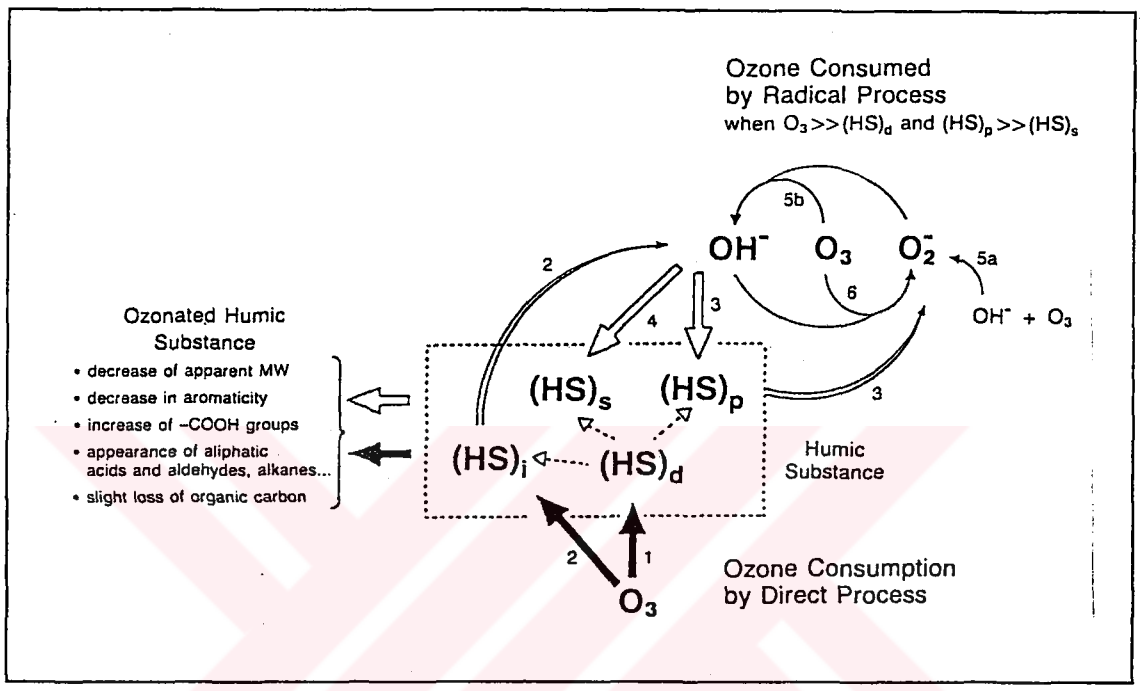

Figure 2.4. Ozone action on humic substances (Langlais *et al.*, 1991)

Ozonation of waters containing humic substances leads to the changes in the molecular structure of the humic substances. Changes occur in their functional group and carboxyl content, molecular size and hydophobicity (Bose *et al.*, 1994). Carboxylic acids, aromatics, hydrocarbons, aldehydes, ketones, aliphatic acids, esters, aliphatic alcohols, and aromatic esters are the by-products of ozonation process as determined by GC-MS analysis (Gracia *et al.*, 1996; Killops, 1986). Acetic, formic and oxalic acids have been identified as the major carboxylic acid species that form during ozonation of natural waters (Kuo, 1998).

Ozonation results in a significant disappearance of higher apparent molecular weight (AMW) material with a corresponding increase in lower AMW material. Partial oxidation products (lower MW organics) of the higher MW humic substances are less reactive with chlorine. This yields to a lower THMFP level (Amy *et al.*, 1988). Following graph indicates a destruction of THM precursors by ozone.

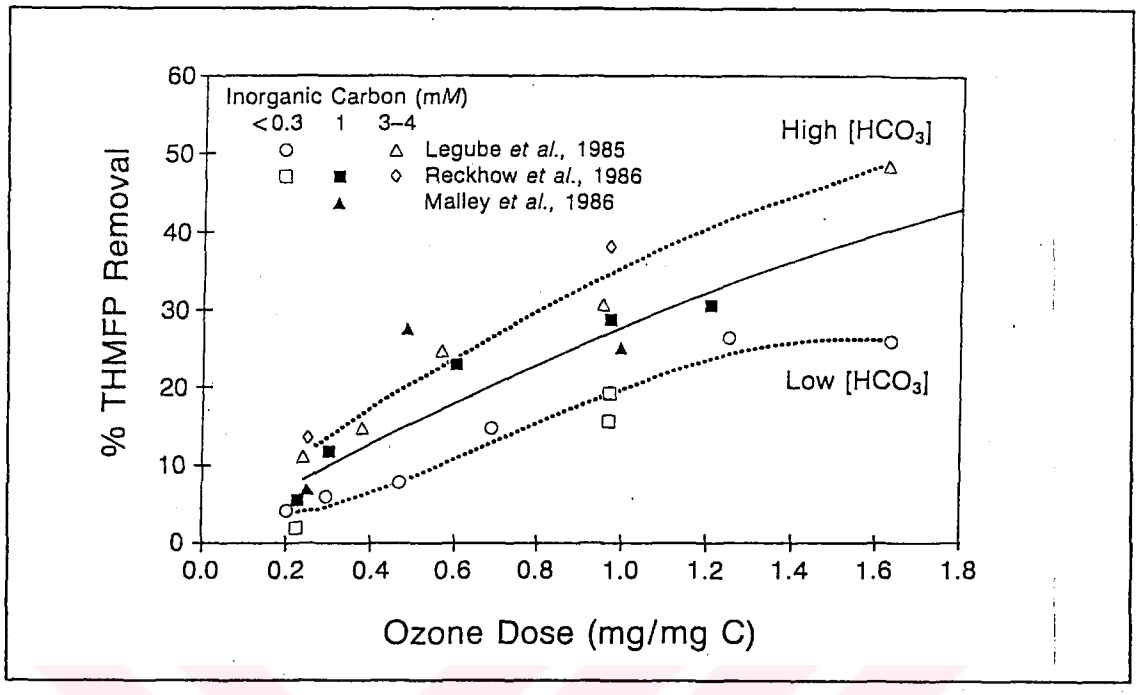

Figure 2.5. THMFP removal by ozone (Langlais *et al.*, 1991)

Due to the complex chemical structure of humic substances, their reactivity and their importance in natural waters, humic substances are assumed to react with ozone in the same way as natural waters. They react like a solution containing different concentrations of molecular ozone consumer sites, leading to the formation of radical or non-radical species, and different concentrations of hydroxyl radical consumer sites, possibly leading to a radical chain propagation. In addition to these principal reactions, there is also the reaction of ozone on hydroxide ions, leading to the formation of the hydroxyl radical and the reaction of ozone with OH, resulting in the autodecomposition of ozone in water (Langlais *et al.*, 1991).

Hoigné and Staehelin (1985) have defined the possible reactions of ozone with humic substances *(HS)* for the direct *(d)*, initiation *(i)*, promoting *(p)* and scavenging *(s)* reactions with the following scheme:

$$(HS)_d + O_3 \xrightarrow{k_d} products + O_2 + H_2O_2$$

$$(HS)_i + O_3 \xrightarrow{k_i} products..... \longrightarrow OH$$

$$(HS)_p + OH \xrightarrow{k_p} products + (O_2^- \longrightarrow HO_2)$$

$$(HS)_s + OH \xrightarrow{k_s} products$$

$$OH^- + O_3 \longrightarrow (O_2^- \longrightarrow HO_2)$$

$$O_2^- + O_3 \longrightarrow OH$$

$$OH + O_3 \longrightarrow (O_2^- \longrightarrow HO_2)$$

The reaction pathways of humic acid moieties with ozone can be described as follows:

Humic Acid Moities:

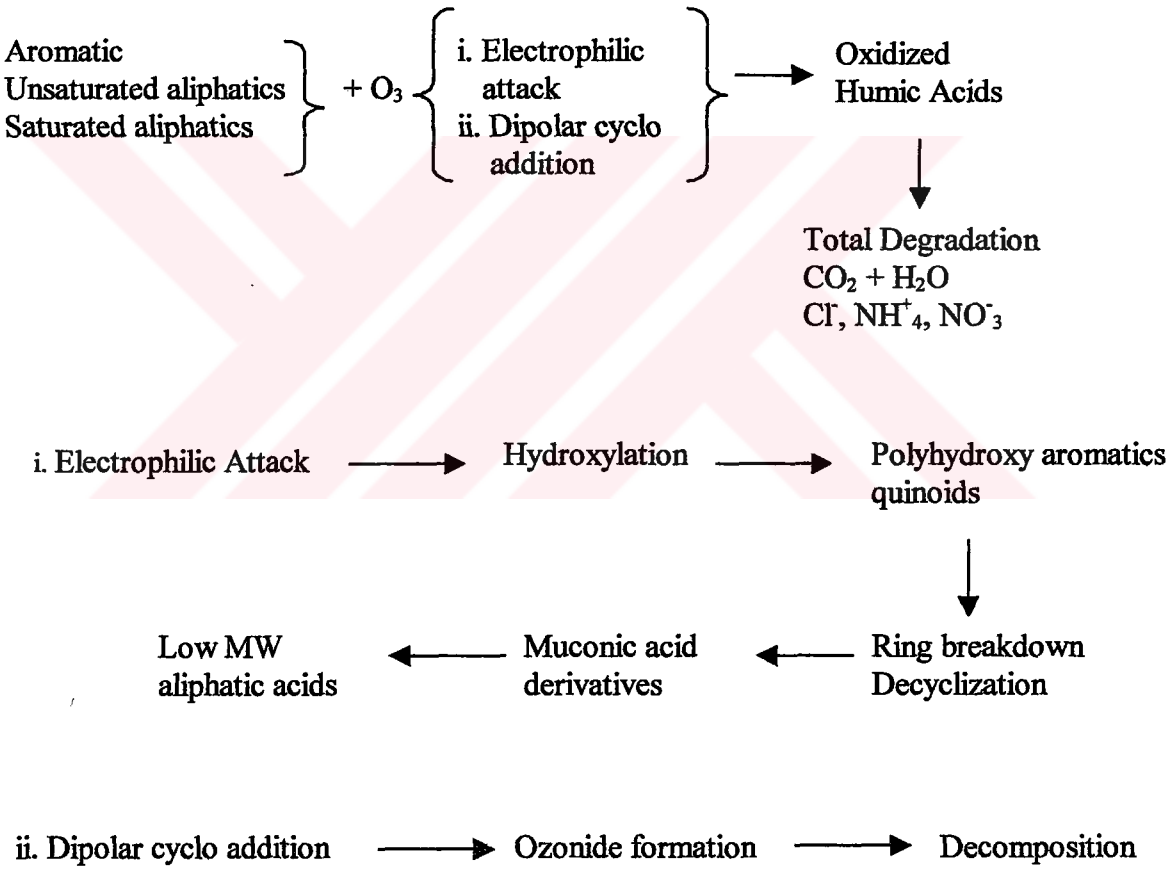

The effect of ozonation on humic substances may be summarized as formation of hydroxyl, carbonyl, and carboxyl groups; increased polarity and hydrophilicity, loss of double bonds and aromaticity; and a shift in the molecular weight distribution resulting in an increased percentage of lower molecular weight compounds. Increase in polarity and hydrophilicity due to ozonation may cause decrease in adsorbability of the humic substances on the adsorbent surfaces.

Humic acid degradation with ozonation can be defined by second order kinetic model including both organic content and ozone concentration, but it is common to express the humic acid degradation with a pseudo first order kinetic model with respect to reactive TOC concentration (Kusakabe, 1990; Takahashi, 1995).

$$-\frac{d[HA]}{dt} = k_{HA,O_3}[HA] \tag{2.8}$$

where *[HA]* represents the humic acid concentration and $k_{HA,O3}$ represents the first order degradation rate constant for humic acid.

2.4. Photocatalysis

Photocatalytic oxidation, which is an advanced oxidation process, has been applied in water, wastewater and gas treatment studies. These processes rely on oxidative degradation reactions, where organic radicals are generated upon photolysis of the organic substrate or by reaction with generated hydroxyl radicals. These radical intermediates are subsequently trapped by dissolved molecular oxygen and lead via peroxyl radicals and peroxides to an enhancement of the overall degradation process and finally to complete mineralization (Legrini *et al.*, 1993). Photocatalytic oxidation have been applied in many researches for the degradation of almost every major class of organics or halo-organic water contaminants like halogenated hydrocarbons, aromatic hydrocarbons, surfactants, herbicides, sulfide, hydrogen sulfide and several precious and base metal complexes (Ollis *et al.*, 1989). It has been shown previously that heterogeneous photocatalysis is a promising route for the degradation of humic acids under various experimental conditions simulating natural water systems (Bekbolet, 1996; Bekbolet and Ozkosemen, 1996, Bekbolet *et al.*, 1998). Eggins and coworkers (1997) and recently Palmer and coworkers (2002) have studied the effects of operational parameters on the photocatalytic degradation of humic acids. They have investigated the operational parameters like concentration, temperature, oxygen, light intensity and pH for their effects on adsorption, rate of initial degradation and mineralisation of Aldrich humic acid solution.

In the aquatic environment or in air, direct or sensitized photooxidation occur for many chemicals that can form excited states with solar radiation. The excited state reacts directly with oxygen or cleaves to form radicals, which then react with oxygen. In this photolysis process the sunlight can transform chemicals by two mechanisms:

i) Direct absorption of light by the pollutant followed by reaction.

ii) Absorption of light by other materials that react with the pollutant or mediate a reaction pathway that includes the toxicant.

Both mechanisms may involve free radicals rate reactions influenced by the color, clarity and sometimes dissolved oxygen content. At concentrations low enough that the pollutant does not absorb a substantial fraction of the incident radiation (mechanism 1) and does not significantly change the concentrations of reactive species (sensitizer, mechanism 2), the kinetics of the photolysis can be described by models that are first order in light intensity and pollutant concentration (Hutzinger, 1980). In aquatic environment the humic substances also act as photosensitizers to produce pollutant transformation.

In order to promote the pollutant degradation via production of oxidizing species, catalysts are used in photolysis processes. The term photocatalysis consists of the combination of photochemistry and catalysis and implies that light and a catalyst is necessary to bring about or accelerate a chemical transformation. ZnO, TiO_2, CdS, WO_3 are the examples for semiconductors used as photocatalysts (Serpone, 1997). The effectiveness of a catalyst is measured by its ability to accelerate electron transfer and electron distribution controls the catalytic processes. Electron density and electron redistribution between catalyst and substrate are the principle factors, which govern the activity of the surface.

In photocatalysis since the oxidation reactions are also taking place on the surface of the catalyst, photochemistry at surfaces and interphases are important for the examining of the degradation mechanisms. At interfaces the environmental chemicals behave differently than in the homogeneous phase. In general the normal molecular state provides little or no information about the properties on the surface of adsorbed molecules.

Heterogeneous photocatalysis leads to a variety of reactions in the aqueous solution including interaction between protons and semiconductor valency electrons following emission of a photon-electron, photo-annealing processes, photosorption and the related changes in occupied electron states. In order to determine the proportion of the photocatalytic effects during the material conversion of the environmental chemicals, it is necessary first of all to determine the adsorption behavior of these substances on surfaces. The adsorbed amount can be obtained by determining the adsorption isotherms at various temperatures and pressures (Hutzinger, 1980).

The advantages of photocatalysis can be summarized as follows:

i) the organic contaminants can be destroyed completely (mineralization to CO_2) in short reaction periods

ii) the method avoids formation of polycyclized products

iii) the process requires inexpensive catalysts with high turnovers which can also be supported in appropriate reactors.

2.4.1. Light Sources used in Photocatalysis

Solar radiation is effective in the photochemical reactions taking place in the natural aquatic environment. In environmental photochemistry and photocatalysis artificial radiation sources are employed to initiate photosensitized reactions. Generally, wavelengths greater than 280 nm are used for this purpose since the whole region covering the solar radiation is not essential.

Xenon arc lamps (unfiltered and filtered), mercury lamps (low, medium, and high pressure), blacklight fluorescent and daylight lamps are the radiation sources used in photochemistry. In mercury lamps increased pressure gives a broader band emission spectrum. Xenon arc lamps fit the solar radiation spectrum best over the whole range. Blacklight fluorescent lamps, which have a maximum emission at 365 nm, are widely used in photocatalysis. The use of medium-pressure mercury arc lamps is of considerable interest due to their high electrical power and emission in the UV-C, UV-B and UV-A regions (Hutzinger, 1980; Legrini *et al.*, 1993).

2.4.2. TiO_2-Photocatalyzed Oxidative Degradation

Photocatalytic degradation of organic pollutants in the presence of illuminated TiO_2 suspensions have been applied in many research studies and proven to be an effective technique in order to achieve complete mineralization. Being an inexpensive and non-toxic chemical TiO_2 is the most widely used photocatalyst. Degussa P-25 TiO_2 was proposed as the standard catalyst material by Serpone (1997). Photocatalytic degradation process basically relies on the nonselective reactivity of the oxidizing species namely ·OH radical possessing a high oxidation potential.

In the use of photocatalyst for pollutant removal, reactions always occur in the presence of oxygen from the air. The reaction starts with the exposure of TiO_2 to light. When TiO_2 is irradiated with photons of less than 385 nm, the band-gap energy (E_{bg}) is exceeded and an electron is promoted from the valance band to the conduction band and two types of carriers –electrons (e-) and holes (h+) – are generated. The resultant electron-hole pair (e_{CB}^-/h_{VB}^+) has a lifetime in the space-charge region that enables its participation in chemical reactions. The most widely postulated reactions are shown below:

Initiation reaction:

$$TiO_2 + h\nu\,(\lambda<388nm) \rightarrow h_{VB}^+ + e_{CB}^-$$

$$h_{VB}^+ + e_{CB}^- \rightarrow heat \rightarrow recombination\ reaction$$

In most materials that are electrically conductive, i.e. metals, electrons and holes immediately recombine. On semiconductors such as TiO_2, however, they survive for longer periods of time. (In fact, in certain chemically combined forms, i.e., "trapped" forms their lifetimes can be measured in hours). The ratio of the recombination rate (between electrons and holes) to the rate of production of electron-hole pairs is a good indicator of the maximum efficiency of a photocatalytic reaction (Fujishima *et al.*, 1999).

TiO_2 oxidizing power of holes is greater than reduction power of exited electrons. On the surface of catalyst, there is approximately a single layer of tightly adhering (adsorbed) water molecules. When these adsorbed water molecules are oxidized by holes, ·OH radicals,

which have high oxidizing power are formed. ·OH can then react with organic compounds initially producing free radicals. Oxidation reactions induced by h_{VB}^+ are shown below:

$$h_{VB}^+ + H_2O_{ads} \rightarrow \cdot OH + H^+$$
$$h_{VB}^+ + OH^-_{ads} \rightarrow \cdot OH$$

When molecular oxygen is present, because it also has unpaired e-, it likes to react with these free radicals, producing organic peroxyl radicals, which in addition to containing an unpaired e-, also now contain two oxygens. Reduction reactions induced by e_{CB}^- are given below:

$$e_{CB}^- + O_{2,ads} \rightarrow O_2^-$$
$$2e_{CB}^- + O_{2,ads} + 2H^+ \rightarrow H_2O_2$$
$$H_2O_{2,ads} + e_{CB}^- \rightarrow \cdot OH + OH^-$$

The generated radicals can take part in chain reactions. In a short time, organic compounds are completely degraded, i.e. converted into CO_2 and water. Meanwhile, the electrons that are produced in the electron-hole pairs are also put to work. These electrons are used to reduce (add electrons) to oxygen in the air. Because oxygen is easier to reduce than water, it will tend to be reduced, producing the superoxide radical anion $O_2\cdot^-$. The superoxide anion attaches itself to the peroxyl radicals. The resulting unstable product now contains at least four oxygens and can decompose to produce a CO_2 molecule. On the molecular scale superoxide acts like a "supercharger" greatly increasing the oxidation process, which is in fact a form of combustion. In addition, another interpretation proposed is the formation in air so-called atomic oxygen ·O, which is extremely reactive, directly acts on C-C bonds in organic matter (Fujishima *et al.,* 1999, Legrini *et al.,* 1993).

The degradation rate constants (k) obtained for photocatalytic oxidation of organic compounds is likely to be a function of illumination intensity (I) and surface activity of the catalyst. One manufacturer's TiO_2 is not the same catalyst as another's even when correction is made for surface area differences. Therefore comparisons between reactants are advised to be made for the same catalyst and the same illumination source (Ollis *et al.,*

1989). However, comparisons for different reactor configurations can be made using the overall quantum yield ($\phi_{overall}$) and relative photonic efficiency (ζ) (Calvert and Pitts, 1966; Serpone, 1997).

The overall quantum yield expresses the number of molecules (N_{mol}) undergoing an event (conversion of reactants or formation of products) relative to the number of quanta (N_{ph}) absorbed by the reactant(s) or by the photocatalyst.

$$\phi_{overall} = \frac{N_{mol}\ (mol\ s^{-1})}{N_{ph}\ (einstein\ s^{-1})} = \frac{rate\ of\ reaction}{rate\ of\ absorption\ of\ photons} \tag{2.9}$$

The notion of relative photonic efficiency was defined to compare cross-reference experiments without the errors associated with the effects of reactor geometry, light source and photocatalyst properties. This standard procedure suggests the use of a standard "secondary actinometer", which is phenol, in photocatalyzed processes. Thus

$$\zeta = \frac{Initial\ rate\ of\ disappearance\ of\ substrate}{Initial\ rate\ of\ disappearance\ of\ phenol} \tag{2.10}$$

where both (initial) rates are obtained under exactly identical conditions (Serpone, 1997).

3. MATERIALS AND METHODS

3.1. Reagents and Materials

Organic free distilled/deionized water was used for the preparation of all reagents used in the experiments. A mixed resin column was used for deionization and distilled/deionized water was also passed through an activated carbon column to remove possible organic contaminants. The conductivity of the obtained water was less than 10 microsiemens cm^{-1}.

The reagents were prepared according to the procedures outlined in the previous literature as indicated in the following sections; otherwise the procedures given in the *Standard Methods* (APHA, AWWA, WEF, 1992) are followed.

3.1.1. Humic Acid

Aldrich humic acid sodium salt was used for the preparation of humic acid solutions. Humic acid stock solution (1000 mg L^{-1}) was prepared by dissolving humic acid sodium salt in distilled/deionized water and filtering through filter paper. Humic acid stock solutions were stored in glass amber bottles. Humic acid solutions for the oxidation experiments were prepared by diluting the stock solution with distilled/deionized water.

3.1.2. Indigo Reagent

Potassium Indigotrisulfonate supplied from Aldrich was used for the preparation of indigo reagent, which was used for ozone concentration measurement in aqueous solution. Sodium dihydrogen phosphate and phosphoric acid were used as buffer and pH adjustment solutions as directed in *Standard Methods* (APHA, AWWA, WEF, 1992). The indigo reagent was discarded when its absorbance decreased to a value less than 80 per cent of its initial absorbance.

3.1.3. Chlorine Dosing Solution

The chlorine dosing solution used in the THMFP analysis was prepared using commercial NaOCl bleach with a concentration of 15-16%. The free chlorine content of the dosing solution was determined with DPD colorimetric method using HACH DR2000 spectrophotometer in accordance with *Standard Methods* (APHA, AWWA, WEF, 1992).

3.1.4. Trihalomethane Standards

A mixture of trihalomethanes containing bromodichloromethane, bromoform, chloroform and dibromochloromethane in methanol was supplied from Ultra Scientific. A certificate of analysis was obtained together with the standard THM mixtures for the exact concentration of each analyte. The certificate stated that the THM mixtures were prepared gravimetrically and the analyte concentrations were verified using high-resolution gas chromatography and/or high performance liquid chromatography. The concentrations of THM compounds in the standard mixtures are presented in Table 3.1. The standard solutions used for the calibration were prepared by diluting the concentrated mixture of trihalomethanes in n-pentane. A new standard bottle was used each time a new calibration was made.

Table 3.1. Trihalomethane concentrations in the stock standard mixture

THM Compound	Concentration, $\mu g\ mL^{-1}$
Chloroform	100.5
Bromodichloromethane	100.4
Dibromochloromethane	100.2
Bromoform	100.4

3.1.5. n-Pentane

n-Pentane, which was the solvent used in the extraction procedure for THM analysis, was supplied from Merck in 99% pure form. The solvent bottle was kept in a non-laboratory area to keep it free from any possible contaminations.

3.1.6. Titanium Dioxide

Degussa P-25 TiO_2 was used as the photocatalyst in the photocatalytic oxidation and catalytic ozonation experiments. The primary particle size was 20-30 nm, BET surface area was 50 ± 15 m^2g^{-1}. The crystal structure of the TiO_2 was composed of 70% anatase and 30% rutile.

3.2. Experimental Set-ups

3.2.1. Ozonation

An oxygen feed ozone generator (PCI Model GL-1 type) with a capacity of producing 1.1 kg ozone per day at the concentration of 2.5% by weight was employed. Tubular type ceramic porous diffusers with 10 and 15cm lengths were used to transfer ozone gas into water in the cylindrical reactor. The diffuser was placed horizontally at the bottom of the reactor. Teflon tubing was used for the ozone gas lines. The applied ozone output of the generator was adjusted by changing the electrical current of the ozone generator. In this study, the ozone application rate was kept constant at 4.8 mg O_3 min^{-1}. The flowrate and the ozone concentration of the feed gas to the reactor were 1.9 L min^{-1} (4 scfh) and 2.5 mg L^{-1} respectively. The output of the ozone generator was verified by measuring the ozone concentration in the gas phase using potassium iodide method. 10L humic acid samples were used in the ozonation experiments. The experiments were conducted at room temperature and the water temperature was 25±3 °C. The ozonated humic acid samples were continuously sent to the measurement system using a Watson Marlow 505 L peristaltic pump. Figure 3.1. shows the experimental set-up used for the ozonation experiments.

Computerized continuous ozone monitoring system (COMA), was used to measure the aqueous phase ozone concentrations. The system that consisted of peristaltic pumps for sample and reagent injection, and an online spectrophotometer provided data at every 10 seconds (Kerc and Saatci, 1996).

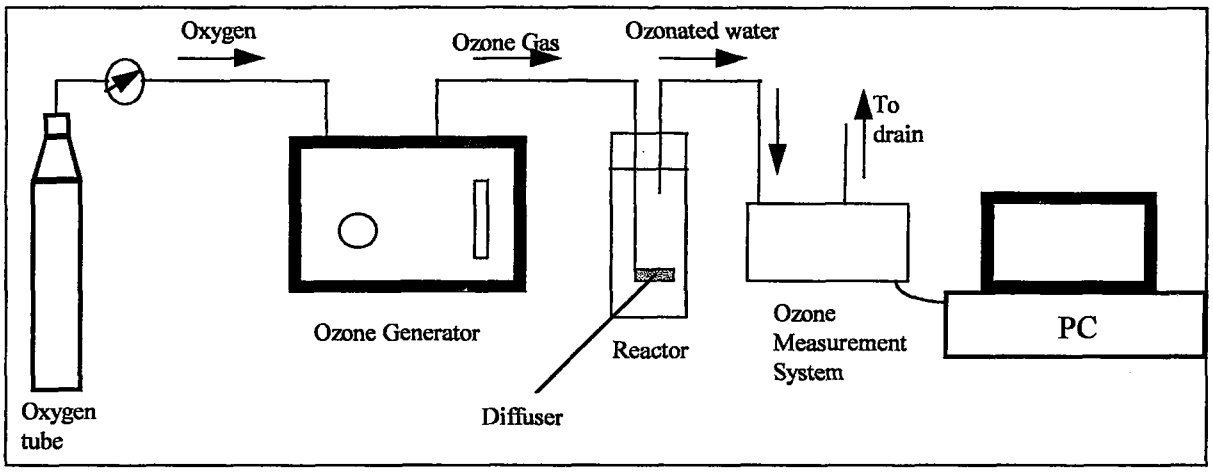

Figure 3.1. Experimental set-up for ozonation experiments

3.2.2. Photocatalytic Oxidation

A cylindrical glass photoreactor with a diameter of 7.5 cm and height of 3.5 cm was used in the photocatalysis experiments. 50 mL humic acid solutions were irradiated in the glass reactor using 125 W Black Light Fluorescent (BLF) lamp. The lamp had an output spectrum of 320 to 440 nm with a maximum emission at 365 nm. The intensity of the lamp was 2.84 x 10^{-6} E min^{-1} as measured by potassium ferrioxalate actinometry. The distance between the lamp and the liquid surface in the reactor was kept constant at 16.5 cm in all the experiments. Rectangular mirrors were used around the photoreactor to focus the light on the center of the photoreactor. The content of the reactor was continuously stirred with a IKAMAG magnetic stirrer at a constant speed to keep TiO_2 in suspension (Bekbolet, 1996).

3.3. Analytical Methods

3.3.1. Ozone Concentration Measurement

Aqueous ozone concentrations were measured using the continuous ozone monitoring system (COMA) (Kerc and Saatci, 1996), which enables the indigo colorimetric procedure in accordance with the *Standard Methods* (APHA, AWWA, WPCF, 1991). The Indigo depends on the direct proportion between the ozone concentration and the discoloration in the Indigo

dye. The discoloration was determined according to the absorbance difference occurred between the sample and the reference blank. Unozonated sample was used as the reference blank and it was treated the same way as the other samples. The absorbance values at 600 nm for ozone concentration determinations were measured at every 10 seconds using a HACH DR2000 Spectrophotometer with 2.5 cm cell path length and the measured data were recorded by the computer connected to the system; a software prepared in DELPHI was used for this purpose. The minimum detection limit for the ozone concentration was 5.3 x 10^{-3} mg L^{-1}. The following formula was used for the calculation of ozone concentrations according to the experimental measurements:

$$C_{O_3} = \frac{V_T \times \Delta A}{f \times b \times V_s} \tag{3.1}$$

where, C_{O3} = Ozone concentration (mg L^{-1})

V_T = the total volume used in the absorbance measurement (mL)

ΔA = the difference in absorbance between sample and blank

b = path length of cell (cm)

V_S = the volume of sample in V_T (mL)

f = the absorption coefficient for aqueous ozone (0.42)

3.3.2. Humic Acid

The humic acid degradation was followed by absorbance measurements at 436, 400, 280 and 254 nm wavelengths. Absorbance measurements at 436 and 400 nm were used to define the color removal in humic acid solutions. These parameters were reported as $Color_{436}$ (m^{-1}) and $Color_{400}$ (m^{-1}). Absorbance measurement at 280 nm were done to monitor the changes in the aromatic structure during degradation of humic acids and expressed as UV_{280} (m^{-1}). It is known that π to π^* transitions occur in this UV range for phenolic substances, aniline derivatives, benzoic acids, polyenes and aromatic hydrocarbons (Karanfil *et al.*, 1996). UV 254 nm absorbance measurements indicated the organic content and expressed as UV_{254} (m^{-1}). Korshin and coworkers (1999) suggested the use of absorption at 253 nm, which can be considered as the same as 254 nm, for an estimation of the degree of functionality of the aromatic structure.

PHILIPS PU 8700 Model UV-Visible Spectrophotometer and SHIMADZU UV-160 Double Beam Spectrophotometer with 1-cm quartz cells were used in the absorbance measurements. The accuracy of these two spectrophotometers was checked with respect to each other. HACH DR2000 Spectrophotometer with 2.5 cm cell was employed in some of the ozonation experiments for continuous monitoring of $Color_{436}$ during ozonation.

In the following sections, the absorbance measurements were denoted by "C" in the graphs presenting the degradation of humic acid within the oxidation periods.

3.3.3. Trihalomethane Formation Potential (THMFP) Analysis

THMFP analyses were performed in accordance with the procedure described in the *Standard Methods* (APHA, AWWA, WPCF, 1991). Commercial NaOCl bleach was used for chlorinating the humic acid samples. At the end of 24 hours incubation period in a BOSCH incubator at 20°C, the samples were analyzed for their trihalomethane concentrations.

THM analyses were performed using liquid-liquid extraction in accordance with EPA Method 502.1. n-pentane was used as the solvent in the extraction. A HEWLETT-PACKARD 5890 Model Gas Chromatograph equipped with an Electron Capture Detector (ECD) and a J&W prosteel 624 megabore (0.53 mm ID, 30 m length) column was used for the analysis. The instrumental conditions used in the gas chromatography are given below in Table 3.2.

Table 3.2. Instrumental conditions used in the gas chromatography for THM analysis

Carrier gas	Nitrogen
Gas flowrate	10 mL/min
Initial oven temperature	40 °C
Temperature increasing rate	10 °C/min
Final oven temperature	130 °C
Injection port temperature	250 °C
Detector temperature	250 °C

Hamilton fix needle syringes with a total capacity of 10 μL were used in the analysis to inject 1μL sample volumes into the instrument.

An external standard calibration procedure was followed for processing the chromatography results. n-pentane and chlorinated distilled/deionized water were also analyzed with each set of samples to monitor any contamination that may originate from the solvent, chlorine dosing solution and the glassware used. A new calibration table was prepared with new standards each time the chromatographic column was taken out and replaced back and any change in the instrumental conditions like changes in the gas flowrate, pressure occurred. The chromatographs obtained for the standards and the calibration curves are given in Appendix A.

3.3.4. Molecular Size Determination

Ultrafiltration through membrane filters of different pore sizes were applied for the separation of humic acid solutions according to molecular size regions. AMICON Model 8010 stirred cell reactor with a total volume of 10 mL was used for this purpose. The cell was operated on a magnetic stirrer. A nitrogen gas tube equipped with a pressure control valve was used to maintain the required pressures inside the cell to obtain ultrafiltration. Millipore YM and YC series cellulose membrane filters with 25 mm diameter were used with the stirred cell. The type and nominal molecular cutoffs of the membranes as specified by the manufacturer are tabulated in Table 3.3. together with the operation pressures.

The humic acid samples were also prefiltered through 0.45 and 0.22 μm cellulose filters, which were attached to 10 mL syringes prior to ultrafiltration. Filtrations were performed in a series operations and the filtrates collected from each molecular cutoff were analyzed for their absorbance values.

For the restoration of YM filters a cleaning solution containing 0.1 M NaOH and 100 ppm NaOCl was used and the filters were stored in a 10% ethanol/water solution and refrigerated. 1 M NaCl solution was used for the cleaning of YC 05 filters and they were stored in 500 ppm sodium azide and refrigerated. Filters were discarded when reduction in

the filtrate flowrate and detoriations on the filters were observed. This corresponded approximately 10 batch filtration cycles, which was also the procedure followed by Logan and Jiang (1990) for the same type of filters.

Table 3.3. Cellulose membranes used in ultrafiltration and their operating pressures

Membrane type	Nominal Molecular Weight Cutoff, Daltons (D)	Operation pressure, kg/cm^2
YC 05	500	3.5
YM 1	1,000	3.5
YM 3	3,000	3.5
YM 10	10,000	3.5
YM 30	30,000	3.5
YM 100	100,000	1.0

3.3.5. Determination of Light Intensity

Potassium ferrioxalate actinometer, developed by Hatchard and Parker (1956) was used for the determination of light intensity for the lamps employed in the photocatalytic oxidation experiments. Actinometric measurements were performed according to the procedure outlined by Mayo and Shizuka (1976). This procedure depends on the reduction of ferric iron to ferrous iron upon irradiation of the actinometer solution containing potassium ferrioxalate in sulphuric acid. The volume of the actinometer solution was chosen as 3000 mL (V_1), which is equal to the volume used in the photocatalytic ozonation experiments. The actinometer solution was irradiated in the Pyrex reactor placed on a magnetic stirrer. After irradiation for t minutes 5 mL (V_2) of the solution was pipetted into a volumetric flask of 25 mL (V_3). In succession, 2 mL of phenantroline and a volume of buffer solution equal to about one-half of the photolyte taken (2.5 mL) were added. After dilution to 25 mL with distilled/deionized water and mixing well, the solution was allowed to stand at least 30 minutes. An identical but unirradiated solution was prepared to be used as the blank and was also allowed to stand. All these operations were performed in the absence of actinometrically active light. The amount of ferrous iron (Fe^{2+}) formed by the

irradiation was measured spectrophotometrically by the formation of the red phenantroline complex and determination of optical density at 510 nm.

The following formula was used for the calculation of number of quanta per second per cell (n_{abs}):

$$n_{abs} = \frac{6.023 \times 10^{20} V_1 V_2 (OD)}{\phi_\lambda V_2 l \varepsilon t} \tag{3.2}$$

where V_1 = the volume of the actinometer solution irradiated (mL),

V_2 = the volume of the aliquot taken for analysis (mL),

V_3 = the final volume to which the aliquot V_2 is diluted (mL),

l = the path length of the spectrophotometer cell used (cm),

OD = the measured "difference optical density" of the final solution at 510 nm,

ε = the molar extinction coefficient of the Fe^{2+} complex (1.11×10^4 L mole^{-1} cm^{-1}),

t = the irradiation time of the actinometer (sec),

ϕ_λ = the quantum yield for the Fe^{2+} formation (1.21 – 1.26 for 365 nm)

An example for the calculation of light intensity according to the experimental results is presented in the Appendix B.

3.4. Experimental Procedures

3.4.1. Ozonation Experiments

Humic acid solutions in concentrations ranging between 5 – 90 mg/L were ozonated using the experimental set-up described above. The ozone application rate and the liquid volume in the reactor were kept constant in all of the experiments. Two different diffuser lengths (10 cm and 15 cm) were used in some of the ozonation experiments to demonstrate the effects of diffuser length on the ozone mass transfer and humic acid degradation

efficiencies. Experiments without using any diffuser were also conducted for this purpose.

Ozone concentrations measurements were started with the introduction of ozone gas into the reactor. 10 mL humic acid samples for absorbance measurements were collected in the course of ozonation. The total amount of volume destruction due to sample collection during the experiments was less than 10%.

3.4.2. Photocatalytic Oxidation Experiments

TiO_2 loadings used in the experiments were 0.25, 0.50 and 1.00 mg mL^{-1}. The required amounts of photocatalyst were weighed using a SCALTEC analytical balance. TiO_2 containing humic acid solutions were sonicated in Ultrasonic LC30 sonicator for 1 minute to bring the TiO_2 to suspension and to obtain homogeneous slurry. Then humic acid solutions were irradiated on a magnetic stirrer as explained in Section 3.2.2. throughout the irradiation periods ranging from 0 to 60 minutes. A separate experiment was conducted for each reaction period. At the end of reaction periods the volume loss in the reactor due to evaporation was measured and compensated with distilled/deionized water. Since the photocatalytic oxidation experiments are conducted in a reactor open to atmosphere to provide the required dissolved oxygen for the photocatalytic oxidation reactions to proceed, the evaporation loss cannot be avoided especially for long irradiation periods. However, humic acids are not volatile and they are not eliminated from the solution with evaporation and the correct concentrations are obtained by compensating this evaporation loss.

In order to separate TiO_2 from the humic acid solution, the reactor content was centrifuged for 10 minutes using HETTICH EBA 8S centrifuge at a rate of 5000 rpm. Then, the cleared liquid was filtered using 0.45 μm Millipore Millex-HA cellulose based membrane filters, which were attached to 10 mL syringes. The filtered samples were used for the further analysis.

A set of experiments was conducted as control experiments without using light source in order to demonstrate the adsorption of humic acid on the catalyst surface within the reaction time periods used in the photocatalysis.

3.4.3. Adsorption Experiments

Adsorption experiments with TiO_2 loadings ranging between 0.1 – 1.0 mg mL^{-1} were conducted to define the adsorption characteristics of humic acid on the catalyst at equilibrium. These experiments were done by continuous shaking of the humic acid-TiO_2 slurries for 24 hours in glass-stoppered flasks placed in the water bath of the shaker. A MEMMERT constant temperature, adjustable speed shaker was used for this purpose.

Absorbance measurements were made on these samples after separation of the catalyst. The results were analyzed for defining the adsorption isotherms. Freundlich and Langmuirian type adsorption isotherms are applied to the experimental data.

3.4.4. Sequential Oxidation

Sequential oxidation of humic acids was studied in a combined system including ozonation and photocatalysis. Ozonation was employed as a pretreatment step for partial oxidation of humic acid solutions prior to photocatalysis. The experimental set-up described in section 3.2.1. was used in ozonation. Partial oxidation, which was defined by percent reduction in UV_{254} and $Color_{436}$, was obtained by applying different ozone amounts. The pretreated humic acid samples were then oxidized photocatalytically as described previously in section 3.4.2.

4. RESULTS AND DISCUSSION

4.1. Preliminary Studies on Humic Acid Characterization

The preliminary studies prior to oxidation experiments for humic acid degradation were conducted using untreated humic acid solutions for determining their initial characteristics. The parameters used to monitor the humic acid degradation during oxidation processes were measured in untreated humic acid solutions in order to define the correlations with the humic acid concentrations as well as the correlations between the parameters.

Linear correlations with regression coefficients greater than 0.99 were obtained for the relations between UV_{254}, UV_{280}, $Color_{436}$, $Color_{400}$ parameters and humic acid concentrations. The graphs presenting these correlations are given in the Appendix C. However, it should be noted that these correlations are valid for the untreated humic acid solutions, in the oxidized humic acid samples it is not possible to conclude about the humic acid concentration based on the absorbance measurements.

The color parameter can also be expressed in terms of Pt-Co unit. The correlation between the $Color_{436}$ and Color (Pt-Co) were determined in a set of measurement conducted on humic acid solutions within a range of 5-50 mgL^{-1}. The obtained linear correlation is given in Appendix C.

It is known that Color values may change at different pH values (Sawyer *et al.*, 1994). Although all the experiments with humic acid solutions in this study were conducted at neutral pH values (6.0 – 7.0), a set of experiments was conducted in to monitor the pH effect. $Color_{400}$ and $Color_{436}$ parameters were measured in the same humic acid solutions by changing pH in a range of 4.5 – 7.5. Insignificant changes were observed in Color parameters within this pH range. The plot of the experimental data for 5, 10, 15 and 20 mgL^{-1} humic acid solutions are presented in Appendix C.

The total organic carbon (TOC) analysis conducted on the humic acid samples have shown that about 36 percent of the humic acid concentration contributes to TOC in Aldrich humic acid.

4.1.1. Trihalomethane Formation in Humic Acid Solutions

The initial experiments for measuring the THMFP in humic acid samples were aimed to determine the incubation period of chlorinated humic acid samples before the THM analysis. Although the *Standard Methods* (APHA, AWWA, WEF, 1992) expresses the incubation period as 24 hours, longer periods were also used in various studies in the literature like 3 days, 7 days (Reckhow and Singer, 1984; Amy *et al.*, 1987; Chiang *et al.*, 2002). Therefore in order to monitor the effects of incubation period on THMFP, an 8-days experiment was conducted on 10 mg L^{-1} humic acid samples. The humic acid samples were chlorinated using sodium hypochloride solution at a dose of 13.5 mg L^{-1}. It was important to maintain residual free chlorine at the end of the longest incubation period; therefore such a high chlorine dosage was selected. A separate sample was used for each analysis. The following graph (Figure 4.1) presents the changes in the chloroform concentrations in the chlorinated humic acid samples according to incubation period.

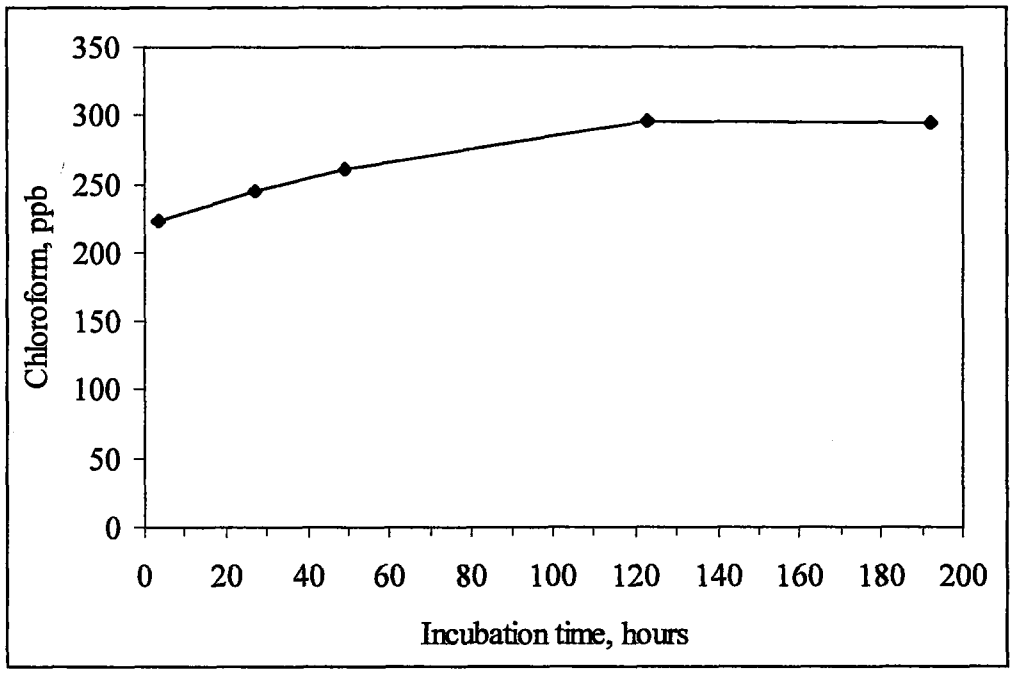

Figure 4.1. Chloroform formation in 10 mg L^{-1} humic acid solution

After 5 days incubation period no difference was observed in the chloroform formation and 85% of this ultimate formation was completed at the end of 24 hours. Therefore, 24 hours was chosen as the standard incubation period for the proceeding THMFP experiments as indicated in the *Standard Methods* (APHA, AWWA, WEF, 1992).

In each set of THMFP measurement, distilled/deionized water containing the same amount of free chlorine as the humic acid samples was incubated and analyzed as blank with the other samples. Although the gas chromatography was calibrated to measure all of the four THM compound, only chloroform and 1,2 dichlorobromomethane were detected in the blank and humic acid samples. However, the concentration of 1,2 dichlorobromomethane (12 ppb) were the same in both humic acid samples and the blank, and it did not change with increasing incubation period in neither of them. Therefore, it was concluded that the sodium hypochloride used as the chlorine dosing solution contained these THM compounds as impurities. Using another chlorine dosing solution in the analysis did not change the results. The THM concentrations originating from the chlorine dosing solution were taken into account during the analysis of the experimental data. The THMFPs were expressed only in terms of chloroform concentrations.

THMFP in 24 hours incubation period were measured in humic acid solutions. The humic acid concentrations were between 5-50 mg L^{-1}. The free chlorine concentrations were determined initially and at the end of 24 hours incubation period in order to determine the chlorine consumption (mg Cl_2/mg HA). Figure 4.2. presents the changes in chloroform concentrations (150 – 1500 ppb) with increasing humic acid concentrations (5 – 50 mg L^{-1}). The following linear correlation with a regression coefficient of $R^2 = 0.991$ was obtained for the presented experimental data.

$$[CHCl_3] = 29.30\,[HA] + 1.87 \qquad (4.1)$$

where $[CHCl_3]$: Chloroform concentration, ppb

$[HA]$: Humic acid concentration, mg L^{-1}

Equation (4.1) covers a calibration range of 5 - 50 mg L^{-1} humic acid concentration.

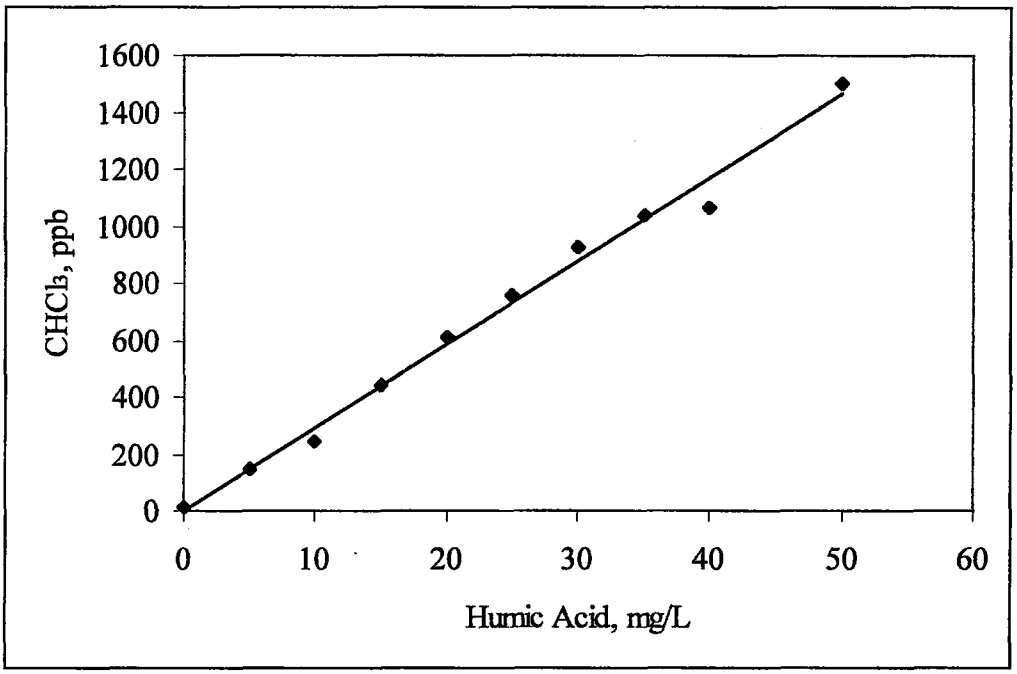

Figure 4.2. Chloroform formation in humic acid samples in 24 hours incubation period.

The results of the free chlorine measurements and chloroform measurements on the chlorinated humic acid samples were used to calculate the chloroform formation and chlorine consumption per mg humic acid. These calculations for each humic acid concentration are compiled in Table 4.1.

Table 4.1. Chloroform formation and chlorine consumption in humic acid samples

Humic Acid, mg L^{-1}	Chloroform formation, $CHCl_3$ ppb / mg HA	Chlorine consumption, mg Cl_2 / mg HA
5	29.6	0.76
10	24.9	0.51
15	29.3	0.45
20	30.5	0.42
25	30.4	0.44
30	30.9	0.38
35	29.7	0.45
40	26.8	0.44
50	30.0	0.45

Both the linear regression analysis given in Equation (4.1) and the average of the calculations for each data point as presented in Table 4.1 have shown that about 30 ppb of chloroform forms per mg of humic acid in chlorinated humic acid samples in 24 hours incubation period. In these samples the average chlorine consumption was found as 0.45 mg per mg humic acid.

4.1.2 Prediction of THMFP Using UV Absorbance and Color Parameters

It has been shown previously that UV_{254} is a good surrogate for measuring the level of THM precursors in the raw water. Linear correlations that incorporate UV_{254} and temperature can be used to calculate the THMFP (Banks and Wilson, 2002). Color was also shown to correlate to TOC and then to THM (Martin *et al.*, 1999). In this study a set of experiments were conducted to define the correlations between UV_{254}, UV_{280}, $Color_{436}$, $Color_{400}$, Color (Pt-Co) and THMFP in humic acid solutions with concentrations between 5-50 mg L^{-1}. The figures presenting these linear correlations are given in Appendix C.

Linear correlations with high regression coefficients were obtained for all the parameters studied. However, these correlations could only be used for the untreated humic acid samples, THM analysis conducted on the oxidized humic acid samples did not correlate well with these equations.

4.2. Humic Acid Oxidation by Ozonation

In order to evaluate the humic acid oxidation by ozonation, the initial studies were conducted on the change of ozone concentration in the reaction medium. Experiments were conducted using distilled/deionized water for determining the hydraulic characteristics of the ozone dissolution system. The type of the diffuser, gas flow rate, concentration of ozone in the total gas flow, water depth, mixing conditions and temperature are known to be the factors effecting the change of dissolved ozone concentration in the solution besides the chemical composition of the reaction medium.

4.2.1. Determination of Mass Transfer Coefficient

In order to determine the mass transfer characteristics of the reactor and the gas diffusers used to apply ozone into solution, ozonation experiments were conducted using distilled/deionized water. It is important to note that even in clean water, ozone decay cannot be prevented at pH ≥ 4. Therefore, in order to achieve a situation where no ozone decomposition reactions occur, the ozone mass transfer experiments are mostly conducted at pH=2 (Gottschalk *et al.*, 2000). In this study, the initial pH of the distilled/deionized water was about 5.5 – 6 and it was lowered to pH 2-2.2 using concentrated nitric acid.

Ozone gas diffusers with two different sizes were used in order to monitor the effect of dissolution equipment on the transfer of ozone from gas phase into liquid phase. Ozone concentrations in the liquid phase were continuously monitored in these experiments. The figure below presents the results of the experiments conducted with distilled/deionized water.

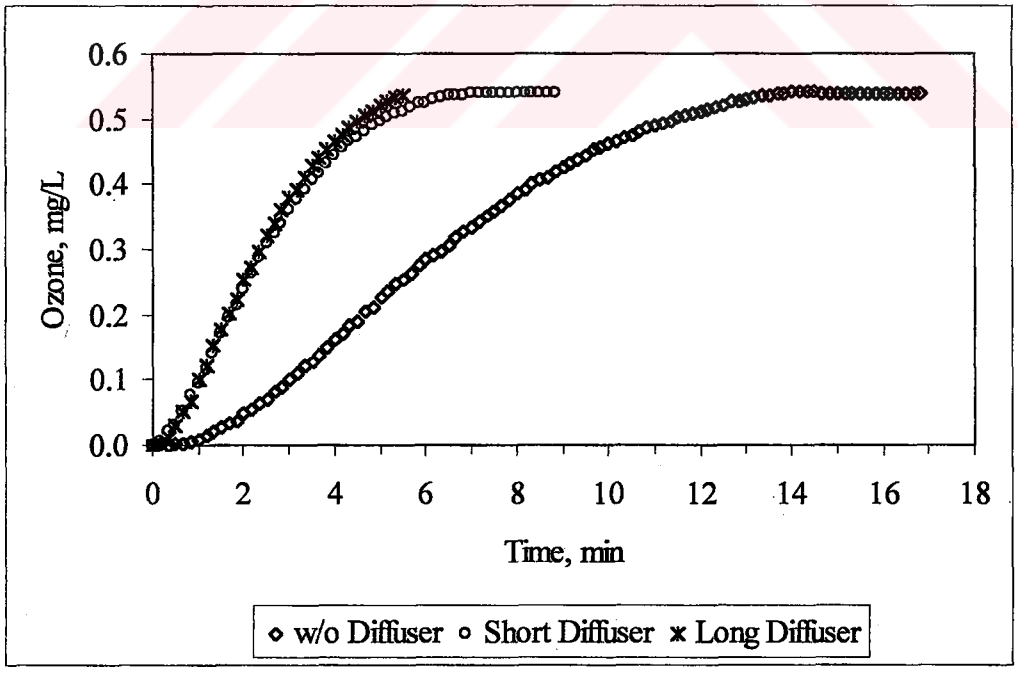

Figure 4.3. Accumulation of ozone in distilled/deionized water for three different ozone dissolution system; (i) without using any diffuser, (ii) 10 cm (short) ceramic cylindrical diffuser, (iii) 15 cm (long) ceramic cylindrical diffuser

In the experiments two tube type diffusers of different lengths (short diffuser: 10 cm and long diffuser: 15 cm) were used and in another experiment ozone was applied directly from the gas line into the reactor without using any diffuser. The other parameters like the ozone gas flow rate, ozone gas concentration, liquid volume in the reactor and temperature were kept the same in all of the experiments. Only a slight difference was observed between the short and the long diffuser in terms of ozone accumulation in water. However, when the results of the experiment conducted without using diffuser is compared with the other two experiments, it can be concluded that due to the mass transfer limitations the ozone demand phase gets longer and accumulation of ozone in the liquid phase is much more slower.

For the calculation of mass transfer coefficients (K_La), only the ozone accumulation parts of the ozone concentration data were used. The change in ozone concentration in a semi-batch reactor can be expressed by Equation (2.3) as explained previously. At pH=2, there is no self-decomposition of ozone and there are no impurities in the distilled/deionized water to react with ozone, the ozone decomposition rate (r_{O3}) in Equation (2.3) is equal to zero. Therefore, the mass transfer coefficient can be calculated from the simplified equation. Mass transfer coefficients calculated from the experimental data are given in the table below:

Table 4.2. Calculated mass transfer coefficients

Ozone Dissolution Method	Mass Transfer Coefficient, K_La (min^{-1})
Long Diffuser (15 cm)	0.28
Short Diffuser (10 cm)	0.27
Without Diffuser	0.11

Only the accumulation part of the ozone concentration data was applied for the mass transfer coefficient calculation, the ozone demand was neglected. Figures 4.4, 4.5 and 4.6 present the calculations of mass transfer coefficients for the above-explained experiments conducted with short diffuser, long diffuser and without using any diffuser respectively. The correlation coefficients for these calculations are higher than 0.99 for all the three data sets obtained using different ozone dissolution methods.

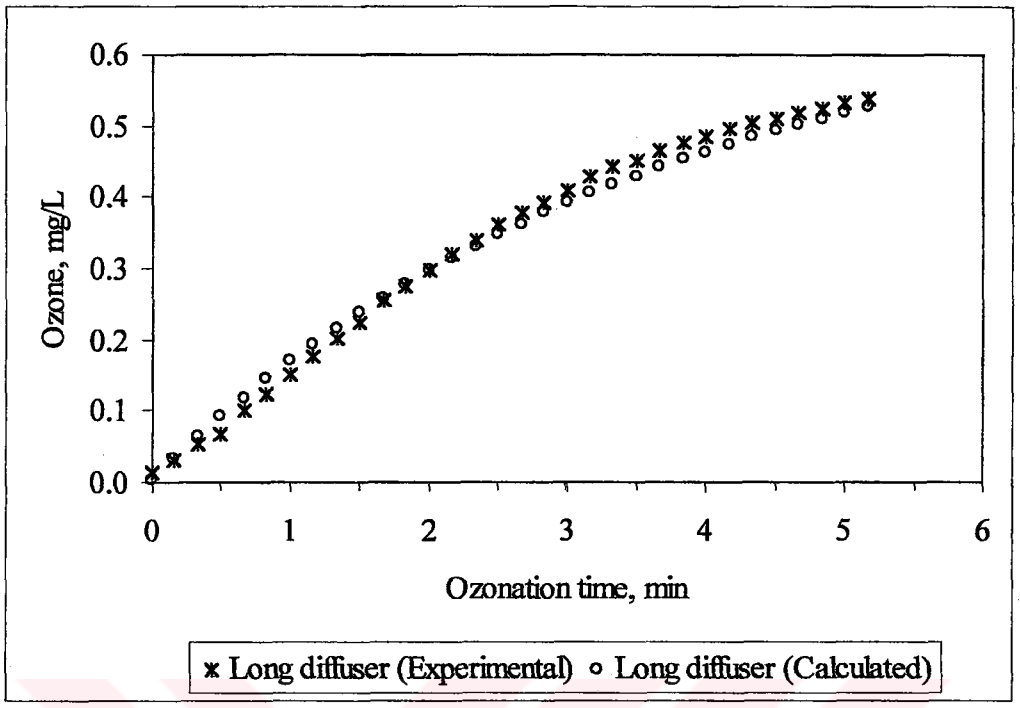

Figure 4.4. Calculation of mass transfer coefficient for the long diffuser. ($R^2 = 0.997$)

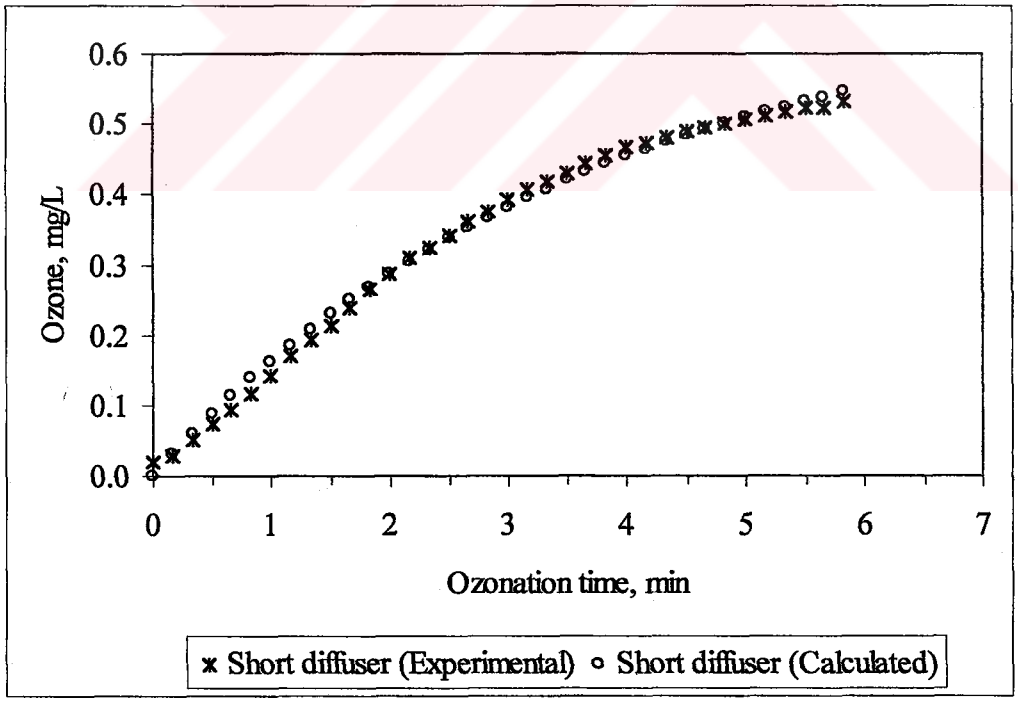

Figure 4.5. Calculation of mass transfer coefficient for the short diffuser. ($R^2 = 0.996$)

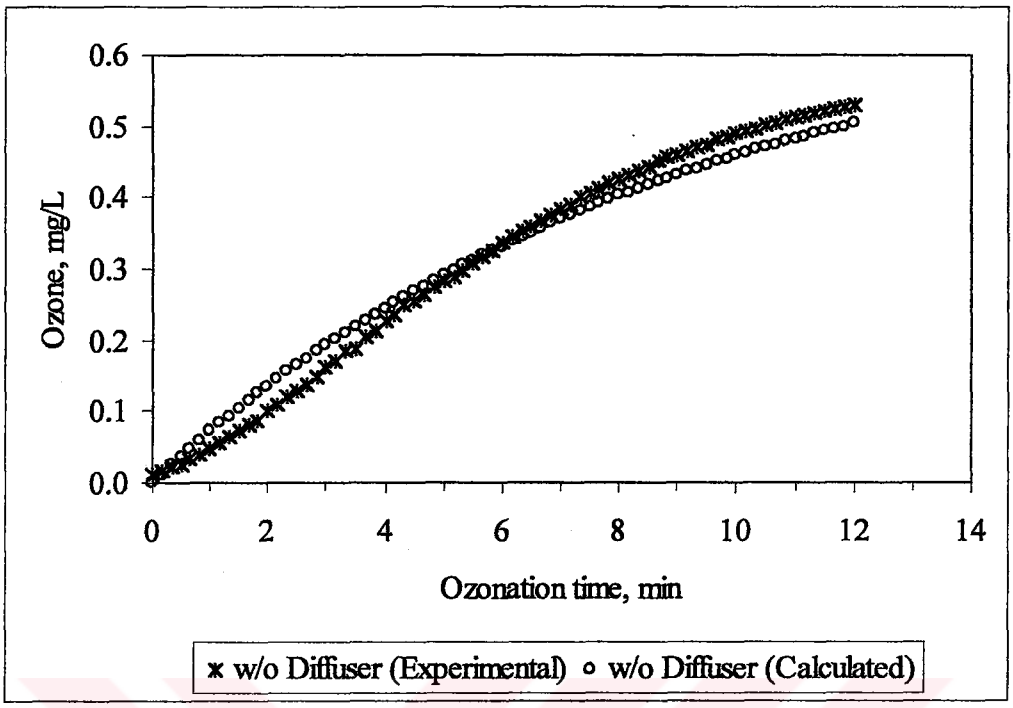

Figure 4.6. Calculation of mass transfer coefficient for no diffuser case. ($R^2 = 0.994$)

4.2.2. Effects of Dissolution System on Ozone Phases in Humic Acid Solutions

Frequent measurement of ozone concentration in a semi batch operation reactor provides accurate data for predicting the ozone demand, accumulation and decomposition phases in solution (Kerc *et al.*, 1997). In order to observe the effects of dissolution system on the demand, accumulation and decomposition phases of ozone, experiments were conducted on humic acid solutions with two diffusers of different lengths (15 cm and 10 cm) and without using any diffuser (Figure 4.7). Same humic acid concentration (10 mg L^{-1}) was used in the experiments. All of the other experimental parameters were kept the same.

When ozone gas is introduced into the reactor directly from the gas pipe without using any diffuser, the transfer efficiency to the liquid phase is very low; the maximum ozone concentration obtained was <0.04 mg L^{-1}. A difference in the ozone transfer efficiencies between the short and the long diffusers was observed. The ozone concentrations obtained in 15 minutes ozonation was 0.48 and 0.53 mg L^{-1} for the short and long diffusers respectively. This difference was not very evident in the experiments conducted with distilled/deionized water.

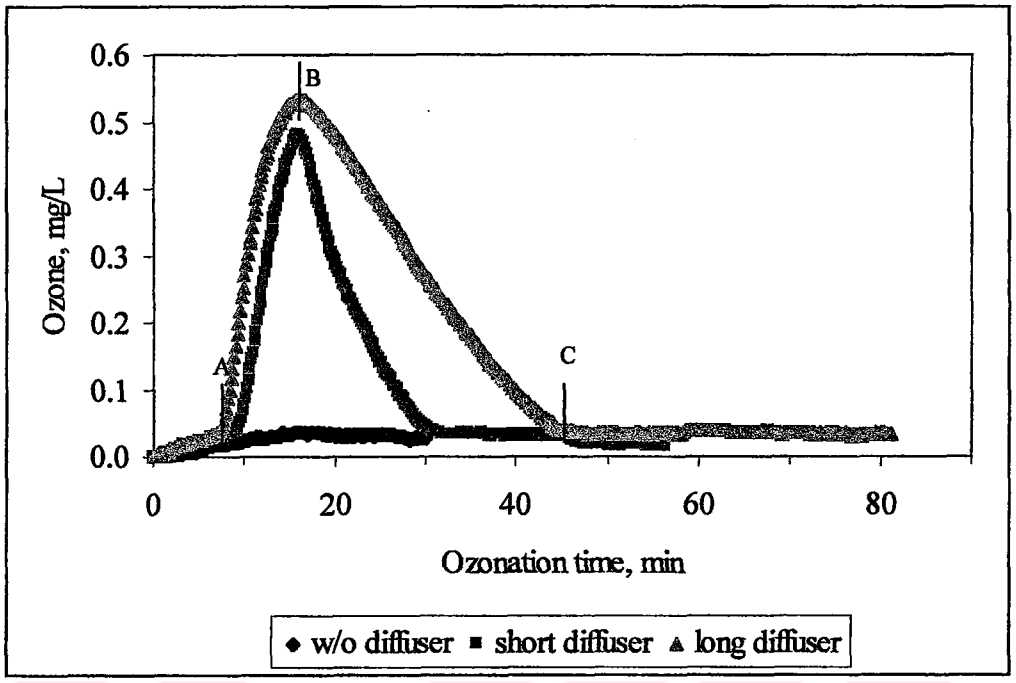

Figure 4.7. Comparison of ozone concentrations for different ozone dissolution equipment in 10 mg L^{-1} humic acid solution. (0-A: Ozone demand phase; A-B: Ozone accumulation phase; B-C: Ozone decomposition phase)

The differences in the dissolution system effects the satisfaction time of ozone demand, accumulation rate of ozone in the liquid and the final liquid ozone concentration achieved when same ozone dosages and ozonation times are applied.

4.2.3. Effects of Humic Acid Concentration on Ozone Phases

The experiments conducted on humic acid solutions with different concentrations in order to monitor the ozone demand, accumulation and demand phases have shown that initial humic acid concentration effected all the three phases. Instead of evaluating the three phases individually based on humic acid concentration an index was defined to demonstrate the differences in solutions ozonated under the same experimental conditions. The index was defined as the ratio between the total mass of ozone maintained in the solution and the total mass of ozone applied into the solution (Equation 4.2). (Tapan *et al.*, 2000). A similar index was defined as fractional ozone absorption (FOA) by Gurol (1985) for incorporating the factors controlling the removal of organic pollutants in ozone reactors.

$$Index = \frac{Ozone\ Accumulated}{Ozone\ Applied} = \frac{Area\ Under\ O_3\ Concentration\ Curve}{\frac{O_3\ Concentration\ in\ gas\ x\ Gas\ flow}{Liquid\ Volume}\ xOzonation\ time} \quad (4.2)$$

The area under the ozone concentration curve contained the ozone accumulation phase as well as the residual ozone maintained during the decomposition of ozone. The indexes calculated revealed linear correlation with the initial humic acid concentration. The use of this ozone index may be considered as a useful tool to describe the water quality parameters for the kinetic studies.

4.2.4. Evaluation of Ozone Decomposition Kinetics in Humic Acid Solutions

Ozone concentration data collected after the 15-minutes ozonation period were used to evaluate the decomposition of ozone in the liquid. Short data collection period (10 seconds) provides accurate analysis of the ozone decomposition kinetics. Most of the researchers in the literature explain the ozone decomposition with first order kinetics as given in Equation (2.6) (Gottschalk *et al.*, 2000). First order kinetics has been applied to the collected data. Figure 4.8 shows the plot of the experimental data and first order decomposition kinetics of ozone decomposition in 10 mg L^{-1} humic acid solution.

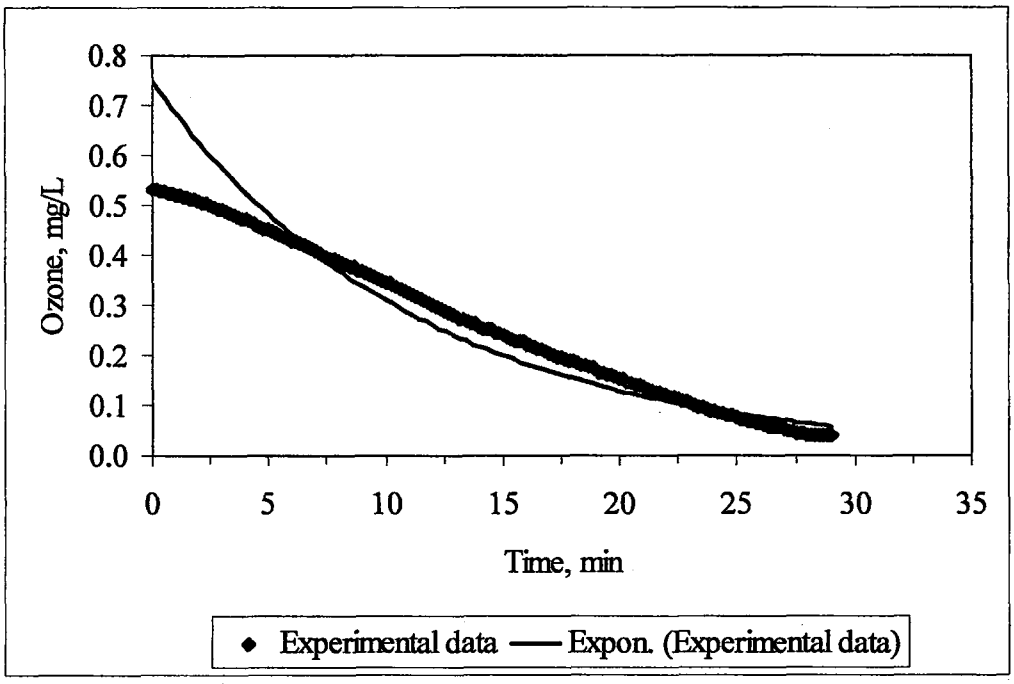

Figure 4.8. Decomposition of ozone in humic acid solution. (k_{O3}=0.088 min^{-1}, R^2=0.942)

Although the correlation coefficient (R^2) is rather high, it can be clearly observed from Figure 4.8 that the ozone decomposition data do not give a good fit to first order decomposition kinetics. Therefore, the experimental data were used to determine the exact order of the ozone decomposition kinetics in humic acid solutions as expresses with the following equation:

$$\frac{d[O_3]}{dt} = -k_{O_3}[O_3]^n \tag{4.3}$$

where, n: reaction rate order.

The best fit to experimental data was obtained for a reaction order of 0.5. The applications of the half order kinetics to the experimental data are presented in Figure 4.9.

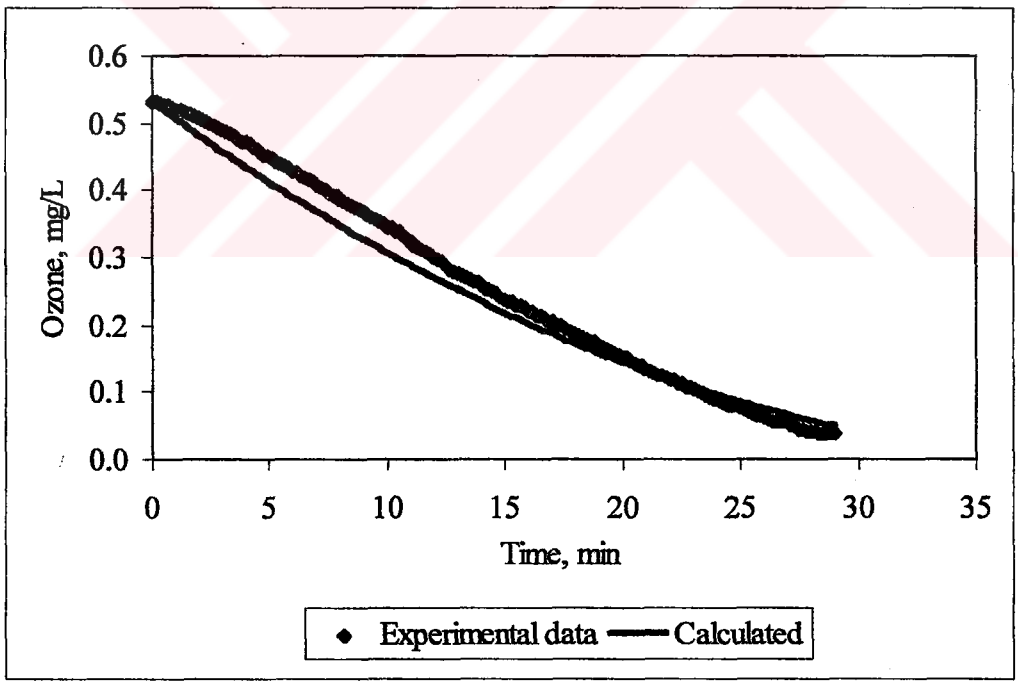

Figure 4.9. Application of half order decomposition kinetics to experimental data in humic acid solution (k_{O3}=0.035, R^2=0.994).

The half order kinetics was also applies to different initial ozone concentrations within a range of 0.3 – 1.0 mg L^{-1}. The calculated ozone concentrations using the half order kinetics resulted in correlation coefficients greater than 0.99 with the experimental data.

4.2.5. Prediction of Ozone Concentration Change in Humic Acid Solutions

As explained previously the change of ozone concentration in a solution can be expressed with Equation (2.4), which incorporates both the transfer of ozone from gas phase into liquid and the ozone decomposition in the liquid. Since the ozone decomposition rate was defined with a half order kinetics as explained in the previous section, Equation (2.4) converts in to the following form:

$$\frac{d[O_3]}{dt} = K_L a\left([O_3]^* - [O_3]\right) - k_{O_3}[O_3]^{1/2} \tag{4.4}$$

The differential equation, which defines the ozone concentration in the liquid phase, can be solved analytically.

$$\frac{1}{K_L a[O_3]} ln\left\{\frac{-K_L a[O_3] - k_{O_3}\sqrt{[O_3]} + K_L a[O_3]^*}{K_L a[O_3]^*}\left[\frac{\left(2K_L a[O_3]^*\sqrt{[O_3]} - k_{O_3} - M\right)\left(k_{O_3} - M\right)}{\left(2K_L a[O_3]^*\sqrt{[O_3]} - k_{O_3} + M\right)\left(k_{O_3} + M\right)}\right]^{k_{O_3}/M}\right\} = t - t_1 \tag{4.5}$$

where, $M = \sqrt{4\left(K_L a\right)^2[O_3]^* + k_{O_3}{}^2}$

t_1 : the ozone demand time.

The ozone demand time is the required ozonation time to satisfy the ozone demand of the solution to obtain a measurable residual dissolved ozone concentration.

The mass transfer coefficient for the gas dissolution system was determined previously using the ozone accumulation data in distilled/deionized water (Table 4.2). Half order decomposition rate constant was also calculated for the humic acid solution (Figure 4.9). These coefficients were used in the model equation to predict the ozone concentration change in humic acid solutions during ozone accumulation phase (K_La= 0.28, k_{O3}=0.035). Figure 4.10 shows the application of the model in Equation (4.5) and its comparison with the experimental data.

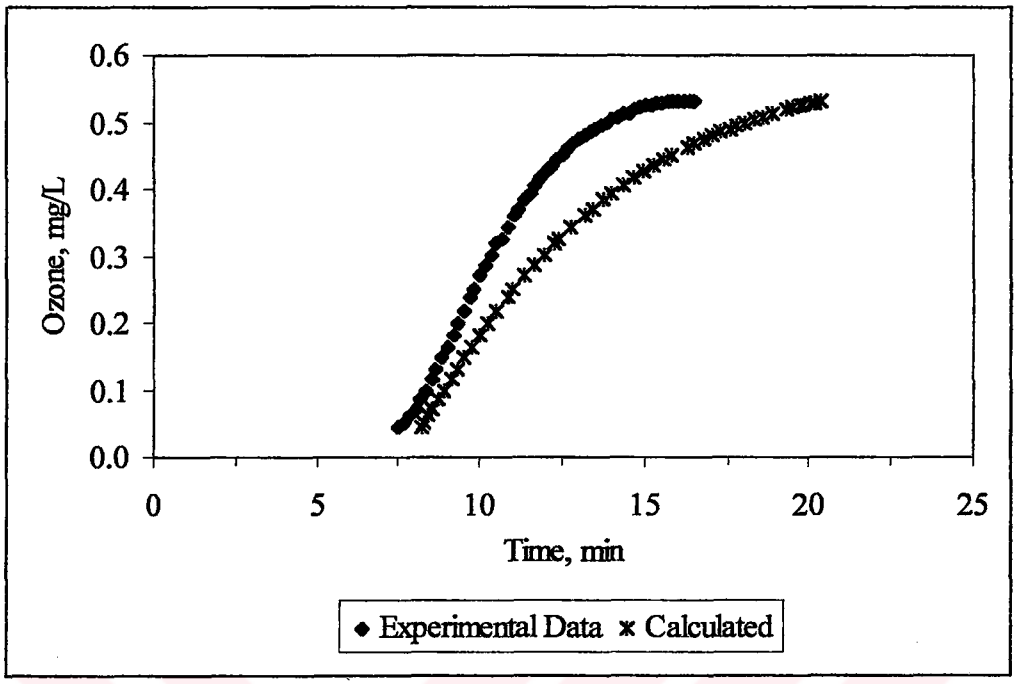

Figure 4.10. Prediction of ozone accumulation in humic acid solution (k_{O3}=0.035, K_La=0.28, Long diffuser).

4.2.6. Effects of Ozone Dissolution System on Humic Acid Degradation

Humic acid degradations with ozone oxidation were monitored in 10 mg L^{-1} humic acid solutions using different ozone dissolutions equipment. All the other experimental conditions were kept the same. The below figures show the effects of dissolution equipment on UV_{254}, UV_{280}, $Color_{400}$ and $Color_{436}$ parameters. These parameters were measured in the samples collected during ozonation.

The oxidation levels obtained using the long (15 cm) and short (10 cm) diffusers were almost the same (~80 per cent) at the end of 15 minutes ozonation period for UV_{254} reduction as presented in Figure 4.11. However, the system without any diffuser exhibited a slower oxidation and the oxidation efficiency at the end of the same ozonation period was 60 per cent. 50 per cent UV_{254} removal was obtained in less than 5 minutes when the long diffuser was employed, whereas the required ozonation time was about 7 minutes for the short diffuser case and the required ozonation time was almost double (12 minutes) when no diffuser was used.

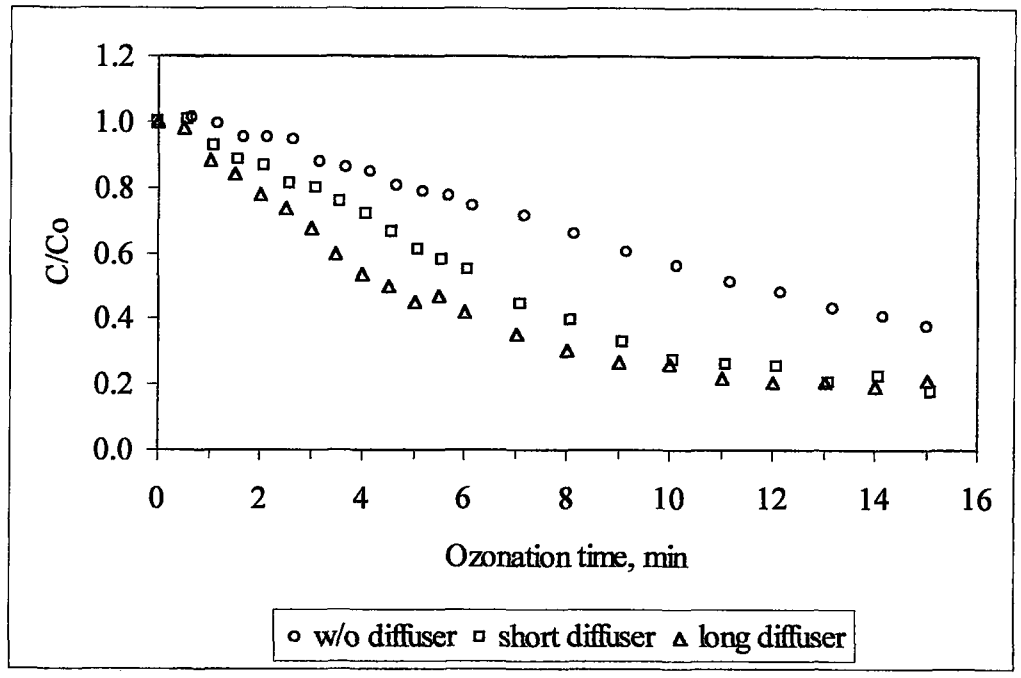

Figure 4.11. The effects of dissolution equipment on UV_{254} reduction in 10 mg L^{-1} humic acid solution with ozonation.

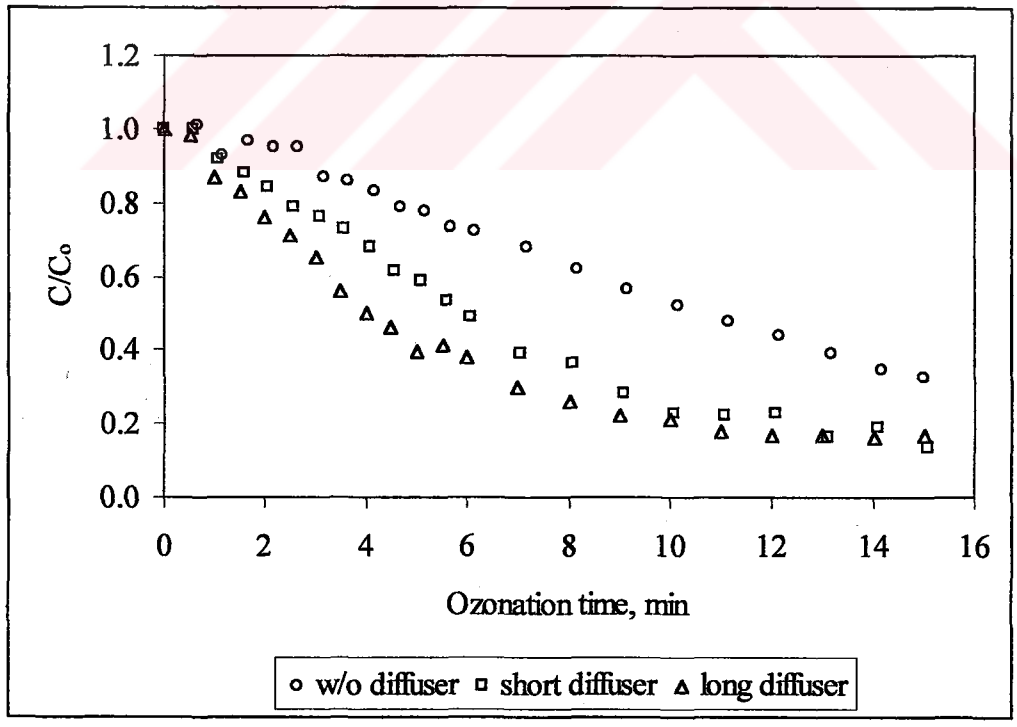

Figure 4.12. The effects of dissolution equipment on UV_{280} reduction in 10 mg L^{-1} humic acid solution with ozonation.

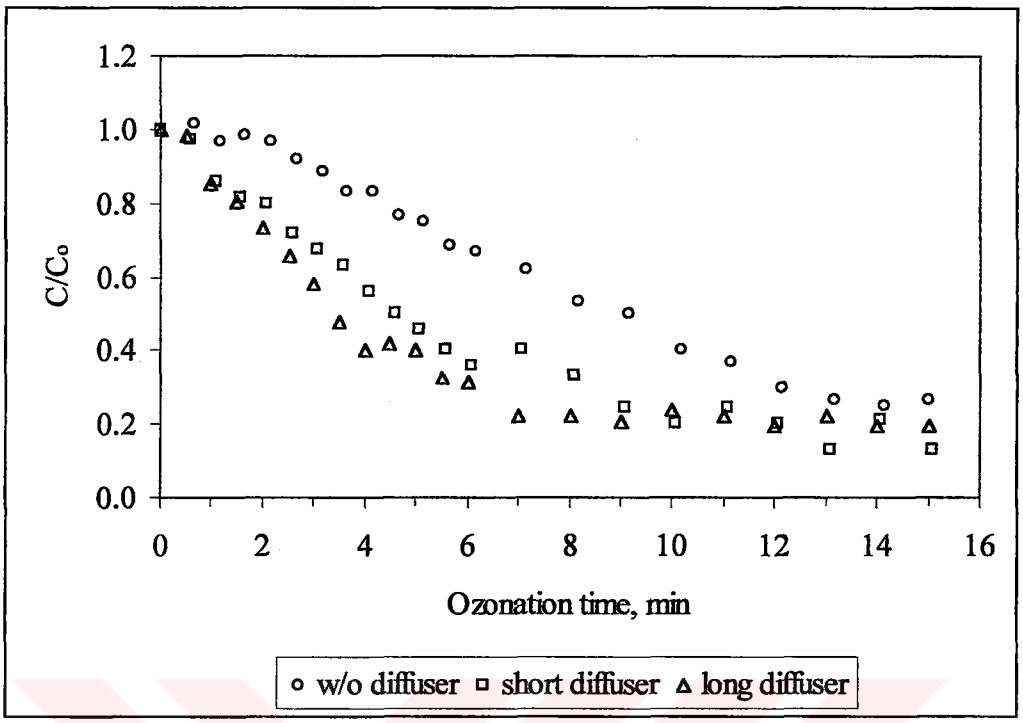

Figure 4.13. The effects of dissolution equipment on $Color_{400}$ reduction in 10 mg L^{-1} humic acid solution with ozonation.

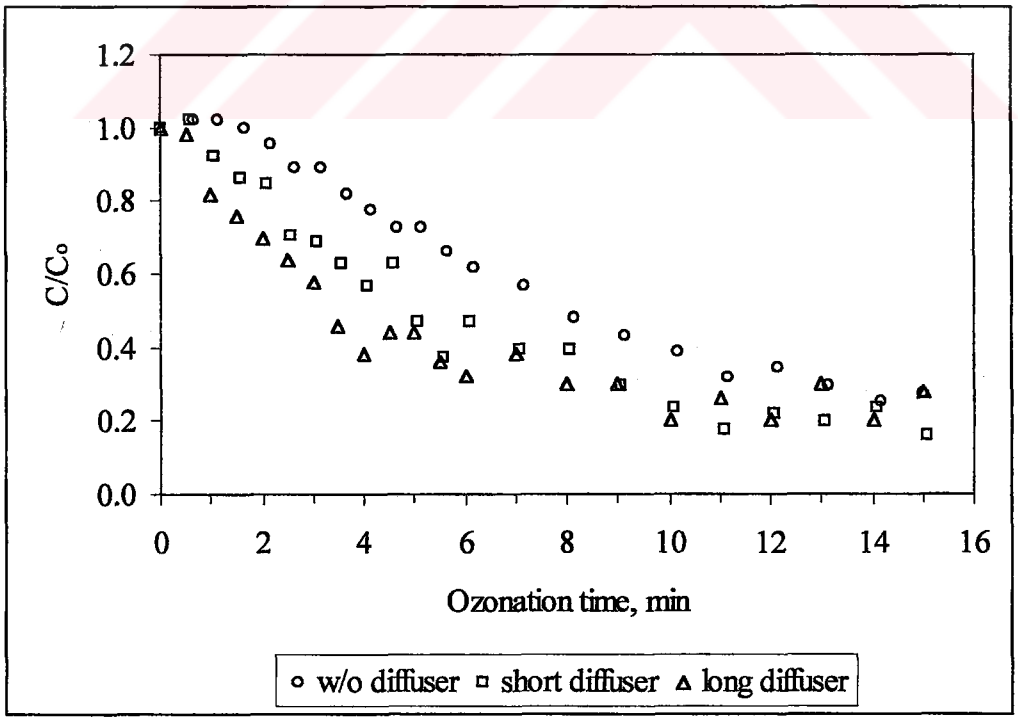

Figure 4.14. The effects of dissolution equipment on $Color_{436}$ reduction in 10 mg L^{-1} humic acid solution with ozonation.

$Color_{400}$ and $Color_{436}$ degradation profiles exhibited a similar trend and decoloration was faster than organic matter oxidation as followed with UV_{254} and UV_{280} parameters. Parallel trends were observed for reduction of UV_{254} and UV_{280}.

4.2.7. Evaluation of Humic Acid Degradation Kinetics

The simultaneous analysis of the UV_{254} data and Color data together with ozone concentration have shown that the humic acid degradation takes place mostly within the ozone demand phase. The ozone begins to accumulate in the solution after the humic acid is oxidized up to its limiting degree. The same observations are valid for all the parameters used to monitor humic acid degradation during ozonation. Similar observations were made by Ko and coworkers (1998). In the following graphs examples for UV_{254} and Color (Pt-Co) reductions in humic acid solutions are presented. Color data presented in Figure 4.16 was expressed as (Pt-Co) instead of $Color_{436}$ / $Color_{400}$ since it was obtained by on line analysis in order to obtain frequent data points. The linear correlations between these parameters can be found in Appendix C.

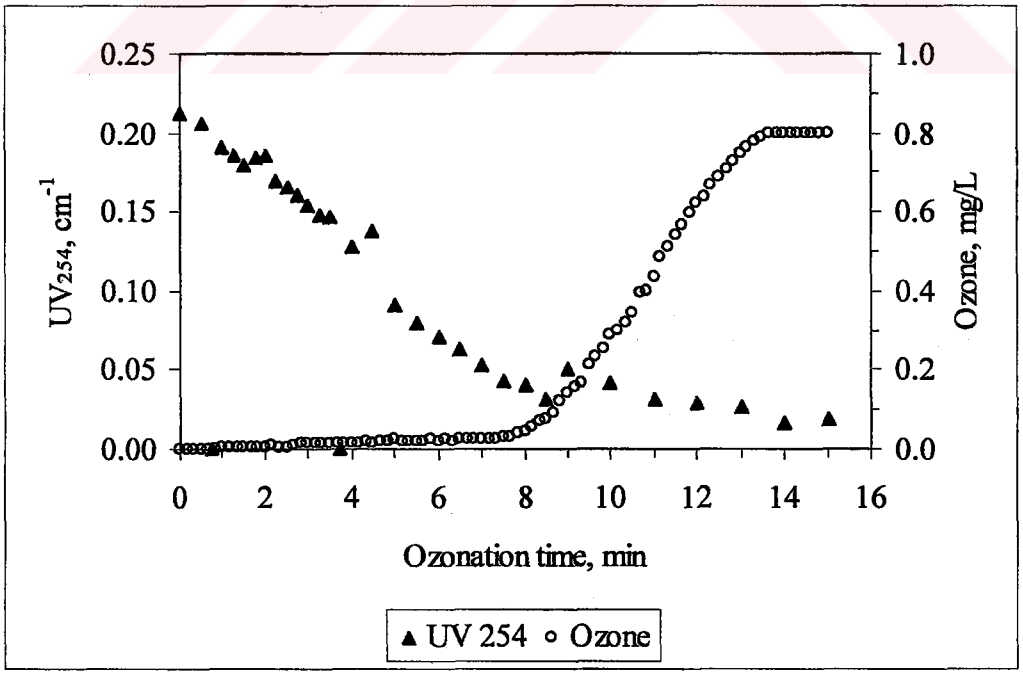

Figure 4.15. Ozone concentration and UV_{254} change during the ozonation of 10 mg/L humic acid solution.

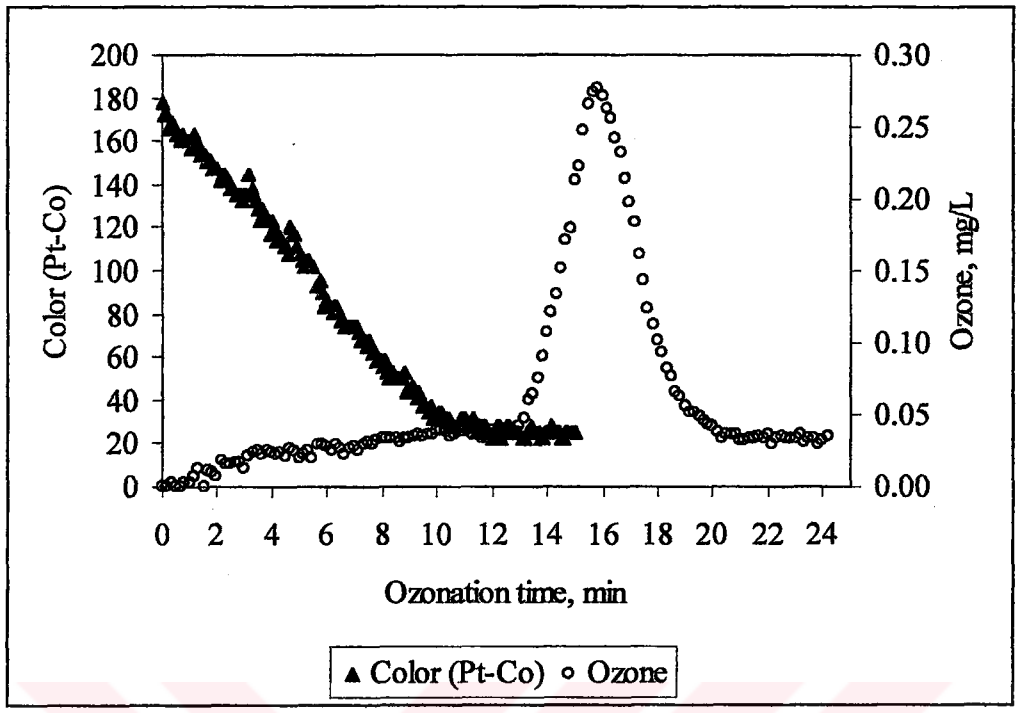

Figure 4.16. Ozone concentration and Color (Pt-Co) change during the ozonation of 15 mg/L humic acid solution.

Since, the humic acid degradation takes place within the ozone demand phase where the residual ozone concentration is zero or very low, a second order kinetic model incorporating both ozone and humic acid cannot be applied. In the literature Color and organic matter degradation rates are generally expressed with first order decomposition kinetics (Langlais *et al.*, 1991). Applications of the first order kinetics to experimental data are shown in the following example graphs in Figures 4.17 and 4.18.

First order degradation coefficients for UV_{254} and $Color_{400}$ were calculated as 0.106 and 0.124 min^{-1} respectively. The half-lives for these parameters were 6.5 and 5.6 minutes. Despite of the high regression coefficient ($R^2 > 0.97$) the first order degradation kinetics was found inaccurate especially during the early stages of the oxidation where a lag phase was observed. The rate of ozone mass transfer from the gas phase into the liquid is a factor effecting the lag phase as well as the chemical composition of the solution. The same case was observed both for decoloration and organic matter oxidation. Therefore another model, which also includes the initial lag phase and non-oxidizable portion of the model humic acid, has been searched.

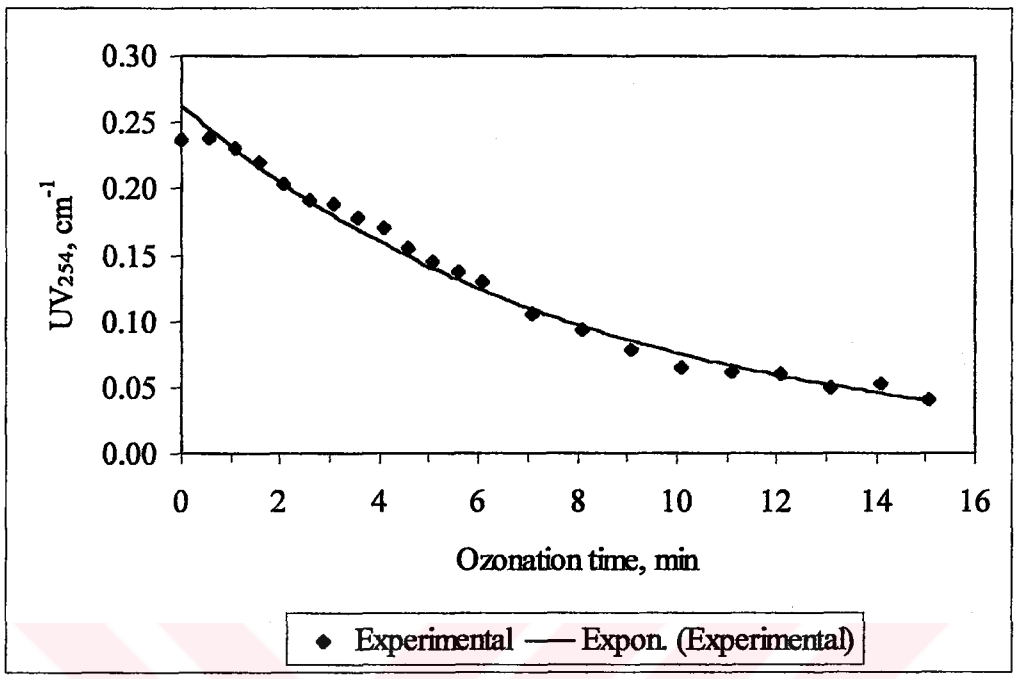

Figure 4.17. Application of first order decomposition kinetics to UV $_{254}$ data.

($UV_{254} = 0.263\ e^{-0.106\,t}$, $R^2 = 0.987$)

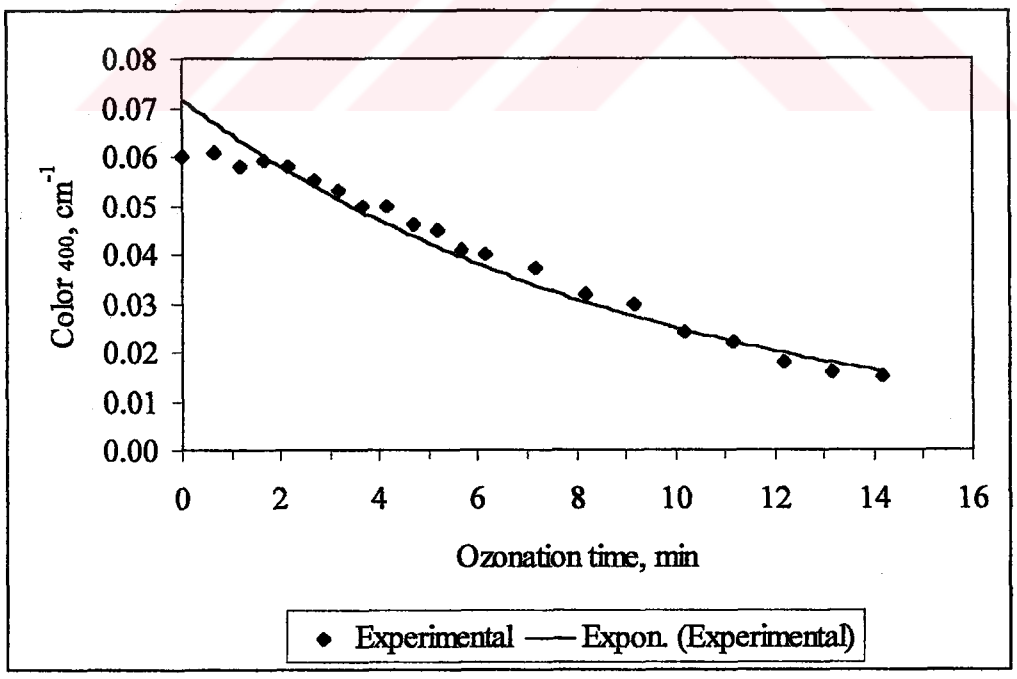

Figure 4.18. Application of first order decomposition kinetics to Color $_{400}$ data.

($Color_{400} = 0.072\ e^{-0.124\,t}$, $R^2 = 0.972$)

Evaluation of the experimental data showed that the organic matter removal due to ozonation can be expressed using the following kinetic equation (Kerc *et al.*, 2000):

$$\frac{dC}{dt} = -k(C_o - C)C \tag{4.6}$$

which can be solved to give:

$$\frac{C}{C_o} = 1 - \frac{1}{1 + e^{A - Bt}} \tag{4.7}$$

where A , B are coefficients that change according to the ozone application rate. Equation (4.7) can also be used in the modified form as:

$$\frac{C}{C_o} = 1 - \frac{D}{1 + e^{A - Bt}} \tag{4.8}$$

where *(1-D)* is the asymptotic value of C/C_o at long ozonation time.

The verification of the model has been made using the data given in the literature for NOM ozonation by other researchers. Ko and coworkers (1998) have studied the ozonation of p-hydroxybenzoic acid, which is known to be a building block in the structure of humic substances (Maximov and Kraskovskaya, 1977; Sonnenberg *et al.*, 1987). Their experimental data were applied to the above explained model with regression coefficients very close to 1.0.

The kinetic model was applied to the experimental data for the prediction of Color (Pt-Co) and UV_{254} reduction during ozonation. The following expression was determined for Color (Pt-Co) reduction:

$$\frac{Color}{Color_0} = 1 - \frac{0.87}{1 + e^{2.5 - 0.5t}} \tag{4.9}$$

The actual data obtained from the ozonation experiment of 15 mg L^{-1} humic acid solution and the theoretical values calculated using the above expression are presented in Figure 4.19. The regression coefficient between the experimental and theoretical values was 0.99.

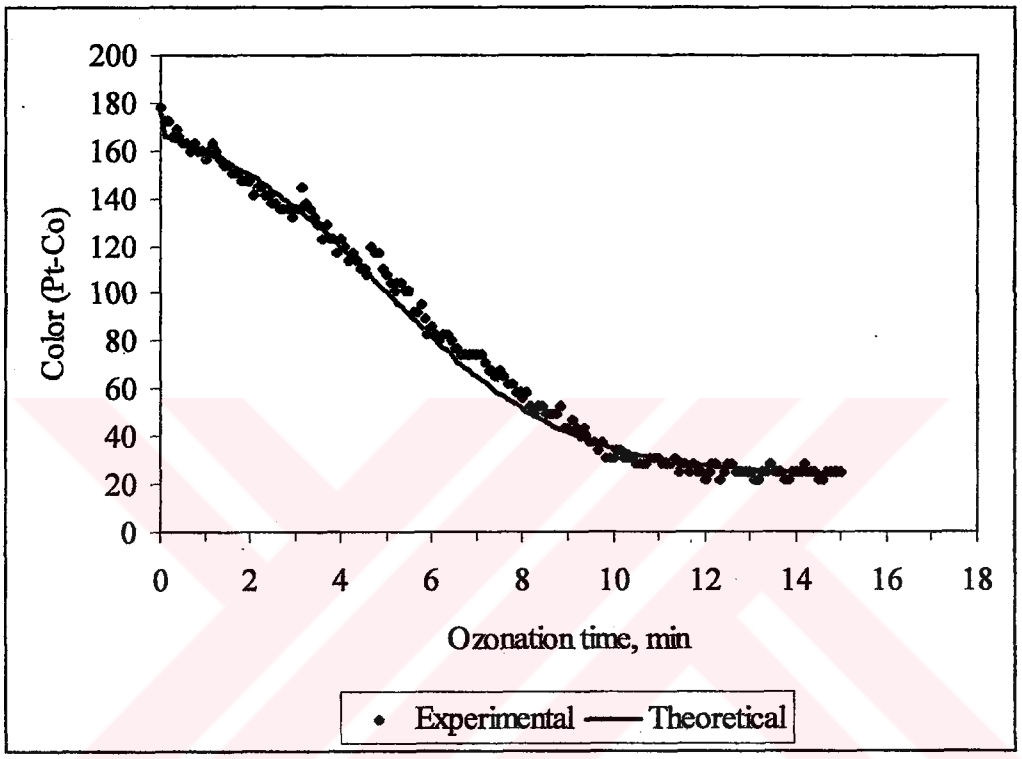

Figure 4.19. Color (Pt-Co) reduction for 15 mg L^{-1} humic acid solution during ozonation.

The same model was also applied to UV_{254} data to represent the organic matter degradation due to ozonation. The following expression was obtained for UV_{254} reduction in 10 mg L^{-1} humic acid solution:

$$\frac{UV_{254}}{UV_{2540}} = 1 - \frac{0.94}{1+e^{2.5-0.5t}} \qquad (4.10)$$

The above mentioned expression predicted the experimental values with a regression coefficient of 0.98. Figure 4.20 shows the experimental and theoretical data for UV_{254} reduction. A, B and D coefficients in Equation 4.8 were taken as 2.5, 0.5 and 0.94 respectively for the calculation of theoretical data for UV_{254}.

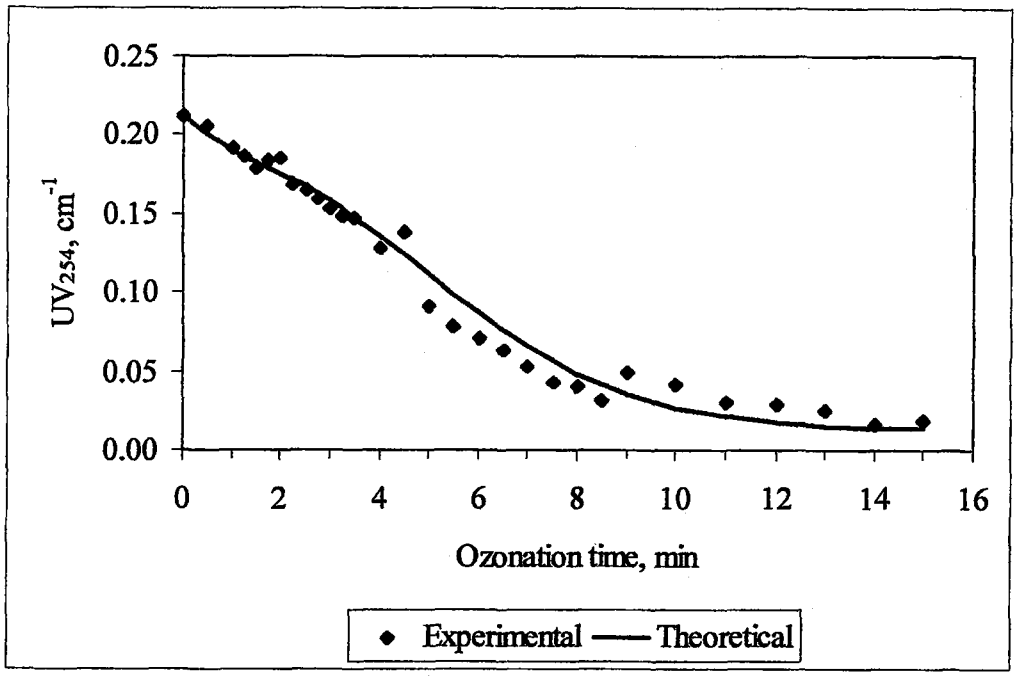

Figure 4.20. UV_{254} reduction for 10 mg L^{-1} humic acid during the ozonation period.

For the verification of the proposed model and to determine the correlations between the coefficients (*A* and *B*) and the ozone application rate, the data presented by Ko and coworkers (1998) for the reduction of UV_{254} during the ozonation of p-hydroxybenzoic acid were analyzed. They have presented their experimental data for different ozone application rates (*N*); 3.45, 2.49, 1.77 and 1.19 mg L^{-1} min^{-1}. These ozone application rates and the model coefficients determined to predict UV_{254} reduction were analyzed simultaneously. It was found that the coefficients *A* and *B* could be written as a function of the ozone application rate, *N* (mg L^{-1} min^{-1}).

$$A = 20N^{-3/2} \tag{4.11}$$

$$B = \frac{N + 0.023}{10} \tag{4.12}$$

The model described by Equation (4.8) was used for the prediction of UV_{254} reduction for the ozonation of p-hydroxybenzoic acid for different ozone application rates. Figure 4.21 presents the experimental data obtained by Ko and coworkers (1998) and the calculated values for the reduction of UV_{254}.

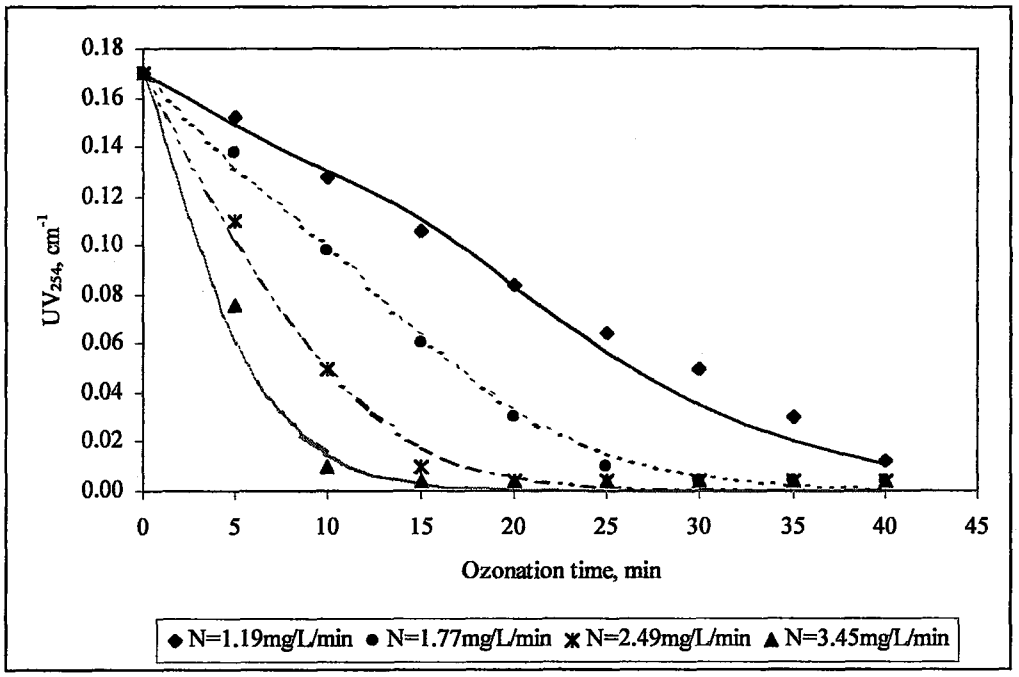

Figure 4.21. Prediction of UV_{254} reduction due to ozonation for p-hydroxybenzoic acid for different ozone application rates (Reactor volume: 15 L, p-hydroxybenzoic acid concentration: 8 mg L^{-1})

The regression coefficients for the experimental data and the calculated theoretical values were found to be greater than 0.986.

4.2.8. THMFP Reduction in Humic Acid Solution with Ozonation

THMFP was used as another parameter to assess the humic acid degradation with ozonation. THMFP measurements conducted on the samples during ozonation of humic acid solution with different concentrations have shown that similar to the other parameter (i.e. UV_{254} and Color), a lag phase occurs in THMFP reduction during the early stages of ozonation. With the increasing humic acid concentration the THMFP reduction efficiency achieved by ozonation decreases. The chloroform concentrations formed in the chlorinated humic acid samples collected during the ozonation of 5, 10, 15, 20 and 25 mg L^{-1} humic acid solutions are presented in Appendix D.

For an ozone application dose of 1 mg O_3 per mg C, the THMFP removal efficiency was calculated as 25 per cent for the experimental data of 10 mg L^{-1} humic acid ozonation.

For the same ozone dosage Reckhow and coworkers (1986) reported ~28 per cent removal and Legube and coworkers (1985) reported ~30 per cent removal in THMFP in their studies conducted on the ozonation of humic substances extracted from natural waters.

The reduction in trihalomethane precursors by ozone is basically related to several operational parameters. Humic acid structure can be considered as a huge amorphous mass of polyhetero condensate with certain functional groups protruding from its surface that may react with chlorine to produce trihalomethanes. It has been shown previously that simple methyl ketone type structures should follow haloform reaction to yield trihalomethanes. On the other hand systematic examination of the chlorination reactions of selected compounds representing the structures for the reactive groups of the humic substances has been carried out extensively (Boyce and Hornig, 1983). Of the substrates studied, structures related to 3,5 dihydroxybenzoic acid, resorcinol, orcinol and 1,3 dihydoxybenzene were found to be most efficient precursors of chloroform. The formation pathway was explained by a classical haloform type reaction mechanism but several competitive pathways were also involved.

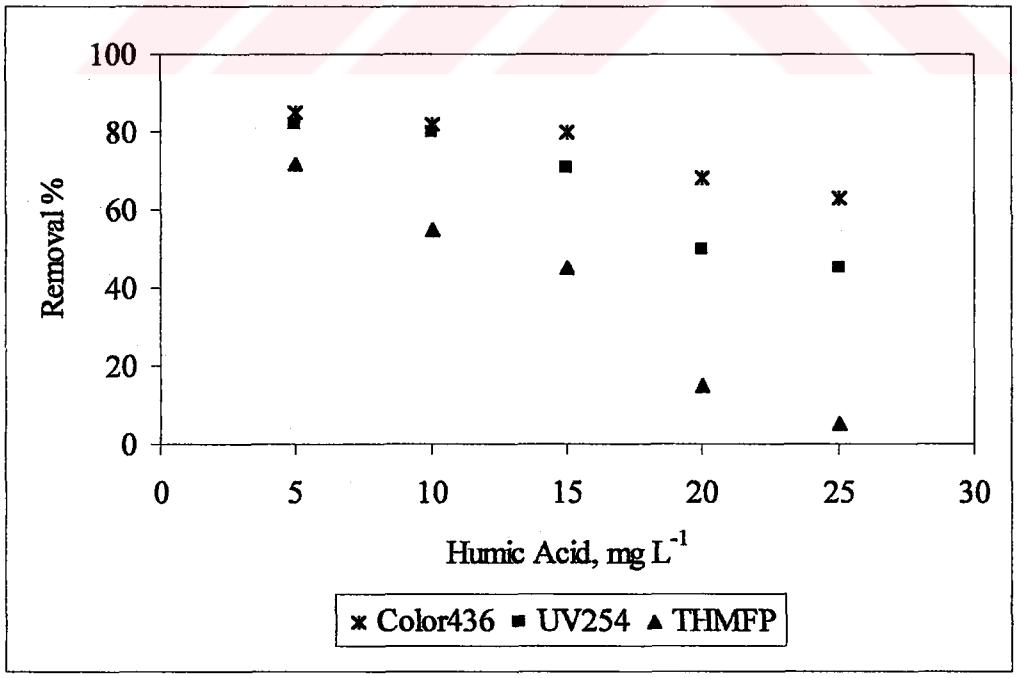

Figure 4.22. $Color_{436}$, UV_{254} and THMFP removal efficiencies obtained in humic acid solutions for an ozonation period of 15 minutes.

Since the degradation of humic acid was followed by the changes in the UV-vis spectroscopic parameters, the THMFP removal could only be related to the removal efficiencies of $Color_{436}$ and UV_{254} for an ozonation period of 15 min (Figure 4.22). For lower humic acid concentrations (5-10 mg L^{-1}) $Color_{436}$ and UV_{254} were removed by at least 80% and THMFP removal percentages were also higher than 50%. On the other hand ozonation of 15 mg L^{-1} humic acid solution resulted in lower removal efficiencies for both parameters as well as THMFP, which was 45%. The gradual decrease observed in THMFP removal for up to 15 mg L^{-1} humic acid drastically changed to a sharp decrease for 20 and 25 mg L^{-1} humic acid whereas the removal efficiencies due to ozonation were still higher than 45% for $Color_{436}$ and UV_{254}. The THM formation profiles of 20 and 25 mg L^{-1} humic acid solutions with respect to ozonation time exhibited fluctuations revealing that the groups responsible for the THM formation have different removal tendencies. Since the measured parameters were expressing the global changes in the total absorbing species present at the indicated wavelengths no direct relationship could be attained due to the THMFP removal efficiencies. For humic acid concentrations ≥20 mg L^{-1} higher ozone dosages were required to obtain significant THMFP removal efficiencies.

4.3. Sequential Oxidation of Humic Acids by Ozonation and Photocatalysis

It is well known that complete mineralization of organics cannot be achieved by ozonation within the practical ozone dosages. Through analysis of TOC before and after ozonation of humic substances at neutral pH, previous researchers observed small changes as a function of ozone dose. For an ozonation dosage of 1 mg O_3 per mg C, Reckhow (1984) has reported a TOC reduction of approximately 10 per cent, which increases as the ozone dose increases (Anderson *et al.,* 1986). Evolution of the main functional groups among humic substances has shown an increase in acidity and in the carboxylic groups, which are recalcitrant organics, upon ozonation (Langlais *et al.,* 1991; Legube *et al.,* 1989). Accumulation of carboxylic groups in the solution as a result of ozonation inhibits complete elimination of organic compounds. The prolonged ozonation of humic acid (20 mg L^{-1}) used in this study contributing to applied ozone dosages greater than 3 mg O_3 per mg C resulted in 20 per cent non-oxidizable organic content measured in terms of UV_{254}. The maximum destruction represented by TOC and specific UV absorbance ($SUVA_{254}$) for similar ozone

application rates were also reported to be <80% by other researchers (Westershoff *et al.*, 1999; Takahashi *et al*, 1995). Therefore, due to the limited capability of ozonation in obtaining higher degradation efficiencies, it is combined with photocatalysis in a sequential system for the oxidation of humic acids. Humic acid solutions were oxidized in a sequential system in which ozonation was considered as a pretreatment step prior to photocatalytic oxidation with TiO_2. There are also studies employing simultaneous application of radiation and ozone for the exhaustive degradation of humic acids (Arai *et al.*, 1986). Consecutive application of two oxidation methods was considered in this study in order to achieve low oxidation levels within shorter oxidation periods and using lower chemical dosages. 20 mgL^{-1} humic acid samples were ozonated in the pretreatment step and these partially oxidized humic acid solutions were introduced into photocatalysis step, in which the effects of different photocatalyst loadings were investigated.

4.3.1. Pretreatment of Humic Acid Samples by Ozonation

Humic acid samples with 20 mg L^{-1} concentrations were ozonated for achieving partial oxidation and altering the molecular structure of the humic acid. The experimental set-up described previously in 3.2.1 was used for the pretreatment of humic acid sample by ozonation. Different ozone application amounts were used for obtaining treated humic acid solution of different characteristics. The diffuser with 10 cm length was employed for the dissolution of ozone gas in humic acid solutions. Ozone application rate was kept constant as 4.8 mg O_3 min^{-1} in all the experiments however; the differences in the total amounts of applied ozone were obtained by varying the total ozonation time. Four partially treated humic acid samples were prepared using 3, 5, 9 and 15 minutes of ozonation periods.

Ozone concentration data obtained during the pretreatment of 20 mg L^{-1} humic acid solution with ozonation at a dose of 4.9 mg min^{-1} was used to indicate the time required for the satisfaction of ozone demand; accumulation of ozone in the aqueous solution and the decomposition of the residual ozone after the termination of ozone application. Ozonation was conducted in a total volume of 10 L humic acid solution. The three phases of ozonation process and the points where samples were collected for further oxidation with photocatalysis are shown in Figure 4.23.

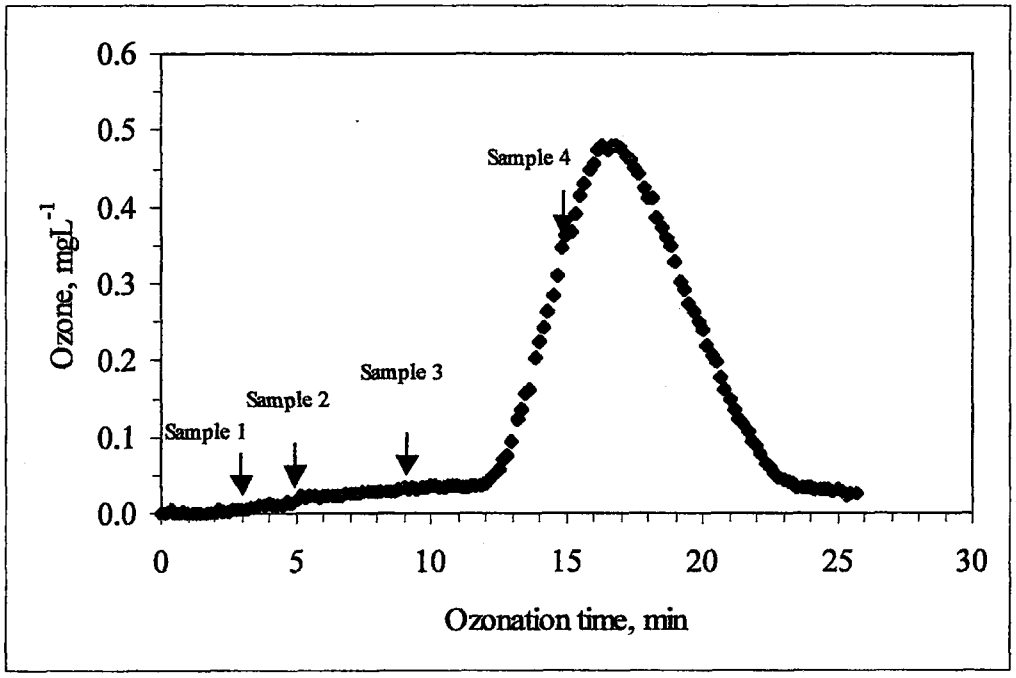

Figure 4. 23. Ozone demand, accumulation and decomposition phases for 20 mgL^{-1} humic acid ozonation and sample collection points.

As presented in Figure 4.23, samples 1, 2, and 3 were collected within the ozone demand phase, where the rate of ozone consumption reactions are greater than the ozone transfer rate into the solution from the gas phase. Sample 4 was taken during ozone accumulation phase, where ozone concentration begins to increase in the solution after the mass transfer rate exceeds the ozone decomposition rate. The applied ozone dosages (mgL^{-1} and mg O_3/mg C) and the residual ozone concentrations measured for each sample collection point is presented in Table 4.3.

Table 4.3. Ozone dosages and residual ozone concentrations in humic acid samples

Sample	Ozone dosage		Residual ozone, mg L^{-1}
	mg L^{-1}	mgO_3/mgC	
Humic acid	-	-	-
Sample 1 (S1)	1.47	0.20	0.004
Sample 2 (S2)	2.45	0.34	0.018
Sample 3 (S3)	4.41	0.61	0.033
Sample 4 (S4)	7.35	1.00	0.364

The applied ozone doses for the preparation of partially oxidized humic acid samples could be considered as equivalent to pre-ozonation ozone dosages for an effective $Color_{436}$ and UV_{254} removal (Langlais *et al.*, 1991). Based on the previous findings, dissolved ozone was rapidly consumed by humic acid during the experiments resulting in partially oxidized humic acid fragments (Kerc *et al.*, 2000). The rate of reaction between ozone and organic carbon compounds is known to be a function of carbon bonding, functional group content with aromatic compounds or compounds with e^- donating functional groups (Westerhoff *et al.*, 1999). Therefore the effect of pre-ozonation degree could be ascribed to the changes in UV_{254} and $Color_{436}$; partial oxidation by ozonation was controlled and defined based on percent degradation of these parameters in humic acid solutions. Characterization of the samples based on UV_{254}, $Color_{436}$ and the percent removal efficiencies obtained by ozonation is given in Table 4.4. The degradation profiles for UV_{254} and $Color_{436}$ are shown in Figures 4.24 and 4.25 respectively. The sample collection points are also indicated on these graphs. UV_{280} measurements conducted on the same samples have shown that UV_{280} removal rates were ~8% faster than UV_{254} and ~16% slower than the $Color_{436}$ removal rates for samples 2-4 (S2-S4). For the slightly oxidized sample (S1), the comparative results showed merely 5% changes for both of the parameters, UV_{254} and $Color_{436}$.

Table 4.4. $Color_{436}$ and UV_{254} parameters for the untreated and partially oxidized humic acid samples.

Sample	UV_{254}, m^{-1}	Per cent UV_{254} degradation	$Color_{436}$, m^{-1}	Per cent $Color_{436}$ degradation
Untreated	44.8	-	9.2	-
Sample 1	40.3	10	7.3	20
Sample 2	36.3	19	5.3	42
Sample 3	29.7	34	3.8	57
Sample 4	19.9	55	1.8	80

Pretreatment of the 20 mgL^{-1} humic acid samples with ozonation resulted in 10% - 55% UV_{254} and 20%-80% $Color_{436}$ reduction due to varying applied ozone dosages. For higher ozone application rates (obtained by ozonation times as long as 45 minutes) the maximum reduction achieved was 80% for UV_{254} and 90% for $Color_{436}$. Under extended

ozone application conditions, the resultant products are basically aldehydes and carboxylic acids that accumulate in the medium due to their resistance towards O_3 reactivity (Guittonneau *et al.*, 1996). Higher percentage removals in $Color_{436}$ than UV_{254} indicate rapid decoloration obtained in comparison to organic matter degradation obtained by ozonation. The changes in $Color_{436}$ reflected the removal of color forming chromophoric moieties of humic acid. The electrophilic attack of O_3 on phenolic groups of humic acid results in the formation of pseudo-quinoic groups and at higher O_3 doses a decrease of the quinoic groups corresponding to the break down of the aromatic cycle leads to the generation of carboxylic acids. The main contributing factor to the explanation of the mechanism of this complex reaction may be the O_3/humic acid ratio (Westerhoff *et al.*, 1999). It is also reported that acidic functional groups increase, charge density of the compounds remains relatively low and the solubility of the compounds do not increase substantially (Lambert and Graham, 1995). The acid formation should be the major indication of the release of the acidic products and this effect on pH could be followed during sample preparation due to the differences in ozonation periods. The recorded pH changes in between the samples can be accepted as insignificant under the specified experimental conditions. The highly oxidized humic acid sample exhibited only $9.5x10^{-7}$ moles H^+L^{-1}.

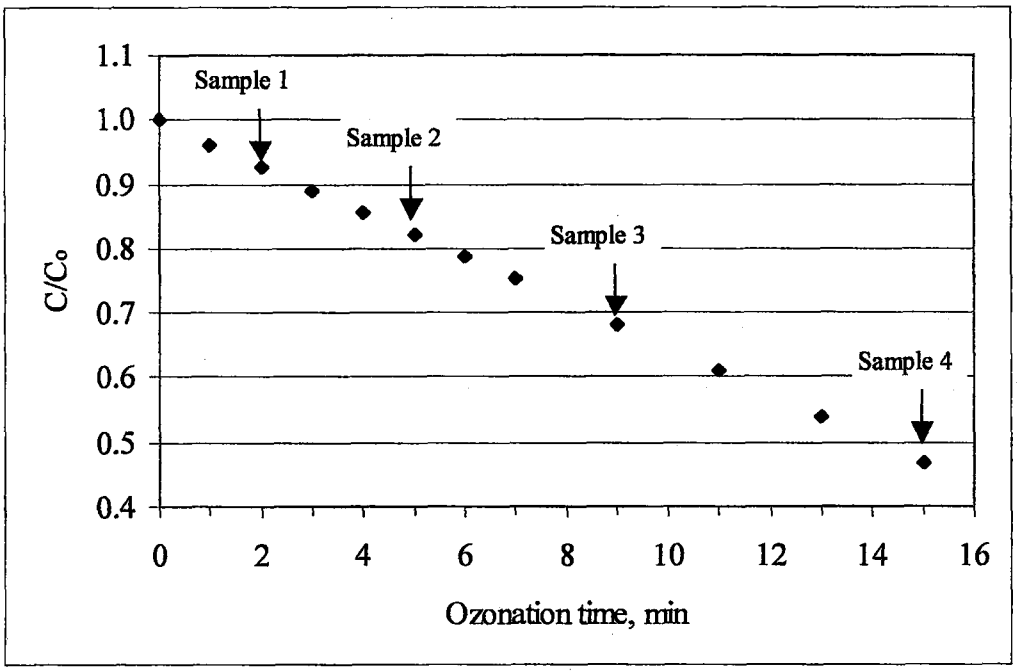

Figure 4. 24. Preparation of partially oxidized humic acid samples based on UV_{254}.

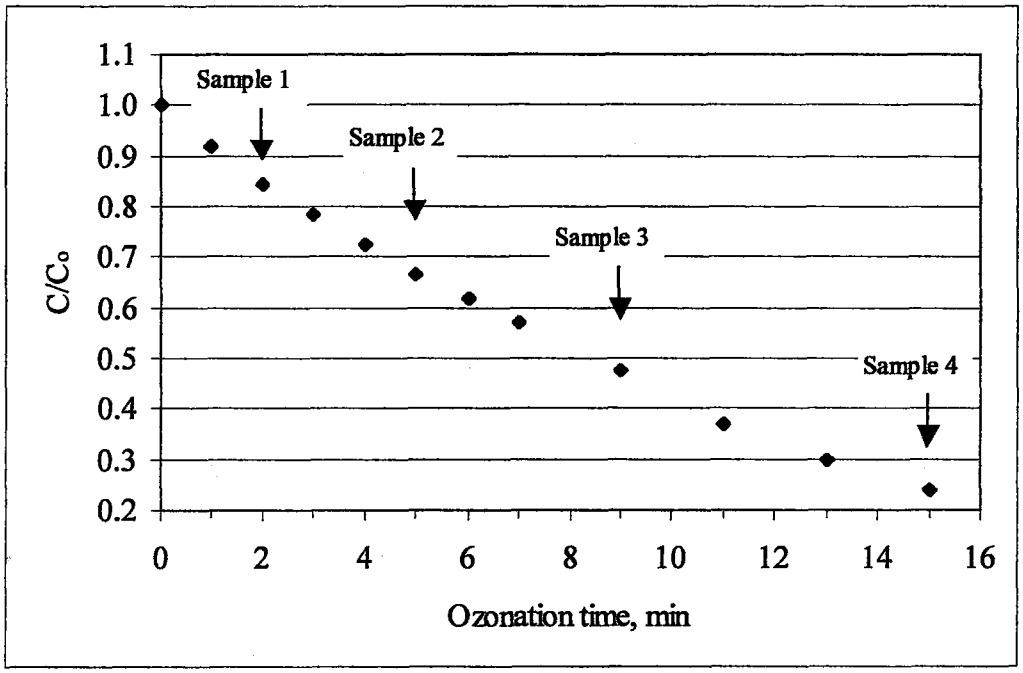

Figure 4.25. Preparation of partially oxidized humic acid samples based on $Color_{436}$.

The pH of the reaction medium determines the differential effects between the highly specific-direct molecular O_3 attack and the rapid/nonspecific-secondary free radical species attack (e.g. ·OH). Since all of the ozonation experiments are carried out under neutral pH conditions, the direct action of O_3 on humic acid is assumed to be the main route of oxidation.

Usually oxidation by pre-ozonation leads to the elimination of color and this step partly causes the degradation of the aromatic structure. Ozonation of humic acid solutions leads to a quick decolorization and a substantial decrease in UV absorbance as presented in Table 4.4. This is mainly attributed to a loss of aromaticity by depolymerization of the humic acid macromolecule.

Increase in the $UV_{254}/Color_{436}$ ratios with respect to applied ozone dosage is another indication for the faster removal of color than organic matter. $UV_{254}/Color_{436}$ ratios, TOC and specific absorbance values of the humic acid samples are presented in Table 4.5. Specific absorbance, $SUVA_{254}=UV_{254}/TOC$, is defined as the ratio between UV_{254} and TOC. Specific absorbance is used as an indication of the aromatic portion of the complex organic structure.

Table 4.5. $UV_{254}/Color_{436}$, TOC and $SUVA_{254}$ values of the untreated and partially oxidized humic acid samples.

Sample	$UV_{254}/Color_{436}$	TOC, mg L^{-1}	$SUVA_{254}$
Humic acid	4.87	7.37	6.08
Sample 1	5.52	6.55	6.15
Sample 2	6.85	5.40	6.72
Sample 3	7.82	4.33	6.86
Sample 4	11.1	3.18	6.26

The inorganic carbon contents of the humic acid samples were around 1.5 mg L^{-1} in all the samples and did not exhibit a change in relation to applied ozone dosages. The unchanged inorganic carbon content may show that complete oxidation of the organic compounds cannot be achieved by ozonation and the humic acid cannot be oxidized till carbon dioxide. The decrease in both the total carbon and total organic carbon content is possibly attributed to the formation of volatile products due to ozonation (Killops, 1986) and extensive stripping of the formed volatile products from the reaction medium with the rising ozone bubbles in the reactor.

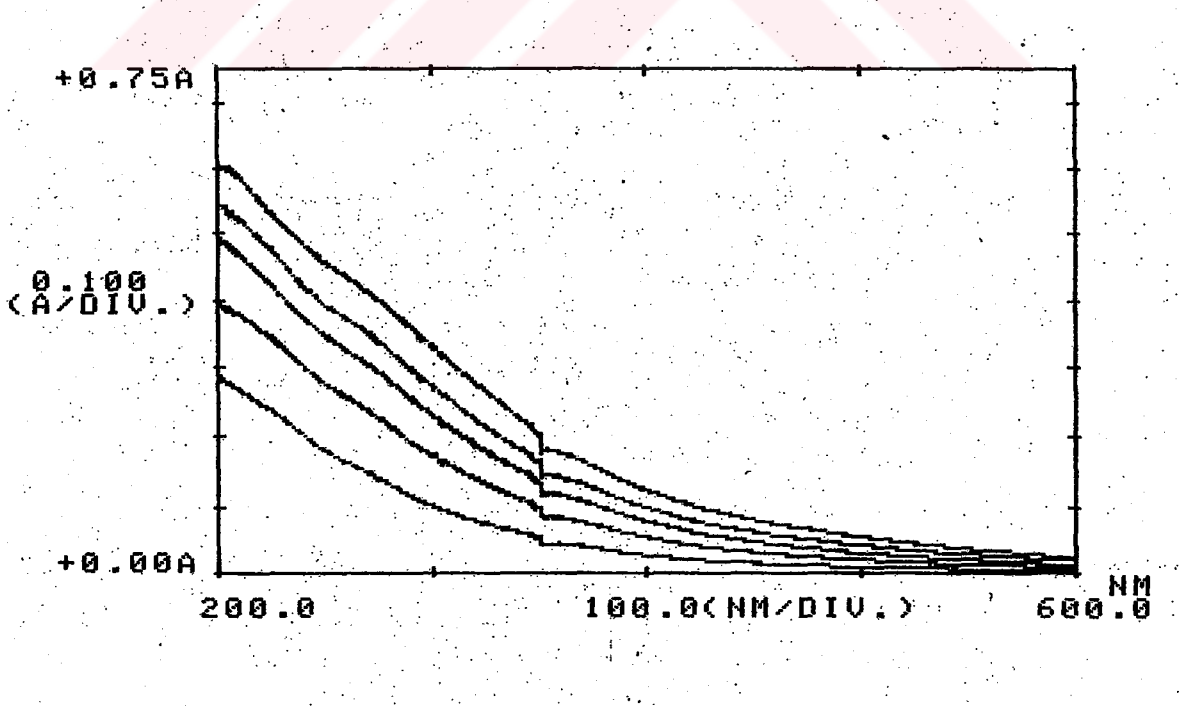

Figure 4.26. Absorbance spectrums of the untreated and four preozonated humic acid samples between 200 – 600 nm. (From top to bottom: Untreated, S1, S2, S3, S4)

The comparison of spectrums of untreated and partially treated humic acid samples between 200 and 600 nm wavelengths also shows reduction in UV-vis spectroscopic parameters obtained as a result of ozonation. The comparison of the spectrums is presented in Figure 4.26.

Similar patterns were observed in the spectrums of all the samples. The humic acid samples exhibited featureless spectrums without any characteristic maximum peak. The absorbance values continually decreased within the covered wavelength region.

4.3.2. Photocatalytic Oxidation of Humic Acid

In order to demonstrate the effects of pretreatment with ozonation on the photocatalytic oxidation of humic acid samples, the initial experiments were conducted with untreated humic acid samples. These data were used as reference for comparison with the photocatalytic oxidation of pretreated humic acid samples.

4.3.2.1. Control Experiments. Control experiments are required before the photocatalytic oxidation experiments in order to evaluate the behavior of humic acid under the controlled conditions in which no irradiation source (dark experiments) or no photocatalyst is utilized. The dark experiments provide data for the adsorption of humic acid on the catalyst within the irradiation period used in the photocatalytic oxidation experiments. In this study, 20 mg L^{-1} humic acid concentration was used in the dark experiments in which humic acid solution was stirred together with 0.5 mg mL^{-1} TiO_2 under dark conditions. Figure 4.27 presents the humic acid removal obtained in the 90 minutes dark experiment.

The purpose for conducting the dark experiments was to determine the amount of $Color_{436}$ and UV_{254} removed from the solution due to initial adsorption. 24-hours adsorption experiments were also conducted in order to assess the adsorption characteristics at equilibrium conditions. These results are presented in the proceeding sections. Reductions in $Color_{436}$ and UV_{254} at time=0 due to initial adsorption of humic acid on the photocatalyst were 73 and 70 per cent respectively. These removal efficiencies

increased to 83 and 78 percent in 60 minutes, which is the longest irradiation period in the photocatalytic oxidation experiments, and to 85 and 79 percent in 90 minutes, which was selected as an extended period. Increasing the contact time of humic acid with TiO_2 did not significantly increase the adsorption of $Color_{436}$ and UV_{254}, the majority of the adsorption was achieved at time=0. Wiszniowski and coworkers (2002) have also reported the time to reach equilibrium as 30 minutes in their experiments conducted with the Aldrich humic acid and Degussa P-25 TiO_2.

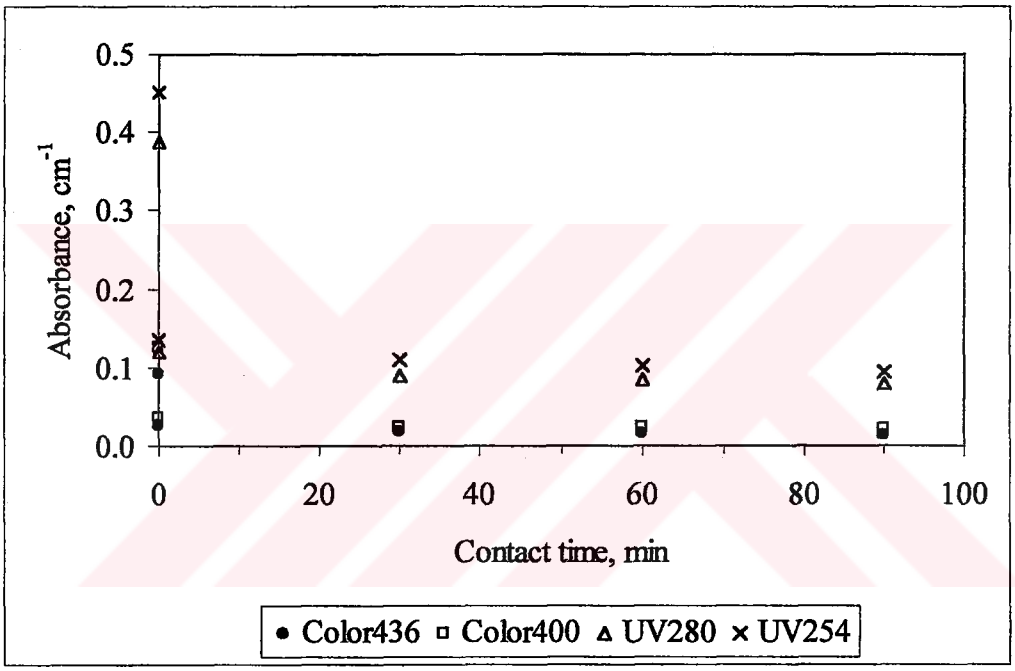

Figure 4.27. Removal of 20 mgL^{-1} humic acid under dark conditions in the presence of 0.50 mg mL^{-1} TiO_2.

The same humic acid concentration (20 mgL^{-1}) was subjected to the same dark experiment using 1.0 $mgmL^{-1}$ TiO_2 loading. In this case, humic acid adsorption based on UV_{254} was 92 per cent at time=0 and 93 per cent at 60 minutes; and remained the same at 90 minutes. 96 per cent reduction in $Color_{436}$ was achieved with initial adsorption (time=0). Similar to the previous case in 0.5 $mgmL^{-1}$ TiO_2 loading, increasing the contact time did not play an important role in additional humic acid adsorption on the catalyst.

The previous studies have also reported the changes in TOC values of the humic acid during prolonged reaction periods in dark experiments to be insignificant as 1 percent

(Bekbolet and Ozkosemen, 1996). Bekbolet and coworkers (1998) found initial reduction in Color as 50% and this high amount of adsorptive reduction was attributed to the utilization of distilled/deionized water instead of Millipore water, which is also the situation in this study. The differences in two types of waters may be caused by their conductivities. The conductivity of Millipore water is known to be <0.1 micromho cm^{-1} whereas the conductivity of the distilled/deionized water used in this study was 10 micromho cm^{-1}. The solution matrix effects the conductivity and result in different adsorption behaviors. No improvement in color removal with increased contact time of humic acid with TiO_2 was reported for the experiments conducted in the dark (Bekbolet *et al.*, 2002).

The second set of control experiments is generally conducted using irradiation source but without photocatalyst in order to find out the photodegradation of the organic contaminant. In this study experiments without using TiO_2 were not conducted, but the previous studies in the literature for direct photolysis of humic acids reported no obvious degradations (Bekbolet, 1996; Eggins *et al.*, 1997; Wiszniowski *et al.*, 2002).

4.3.2.2. Photocatalytic Oxidation Experiments. The first set of photocatalytic oxidation experiments were conducted with 20 mgL^{-1} using a TiO_2 loading of 0.50 $mgmL^{-1}$. The following Figure 4.28. presents the degradation profile for 20 mgL^{-1} humic acid solution based on UV_{254}, UV_{280}, $Color_{400}$ and $Color_{436}$.

For the photocatalyst loading of 0.50 $mgmL^{-1}$, the initial adsorptions for $Color_{436}$ and UV_{254} were measured as 74 and 70%. A persistent decrease was observed with the increasing irradiation period. The removal efficiency achieved for $Color_{436}$ was 90% for 40 minutes and 94% for 60 minutes irradiation. These removal efficiencies were found as 82% and 86% for UV_{254}.

The degradation profiles for color forming moieties as expressed by $Color_{436}$ and $Color_{400}$ exhibited similar trends. $Color_{400}$ removal efficiencies achieved in 40 minutes and 60 minutes of irradiation were 90% and 94% respectively, which are the same removal percentages for $Color_{436}$. Similarly UV_{254} and UV_{280} profiles revealed parallel trends. 84 and 88% removals were obtained in UV_{280} in 40 and 60 minutes of irradiation respectively.

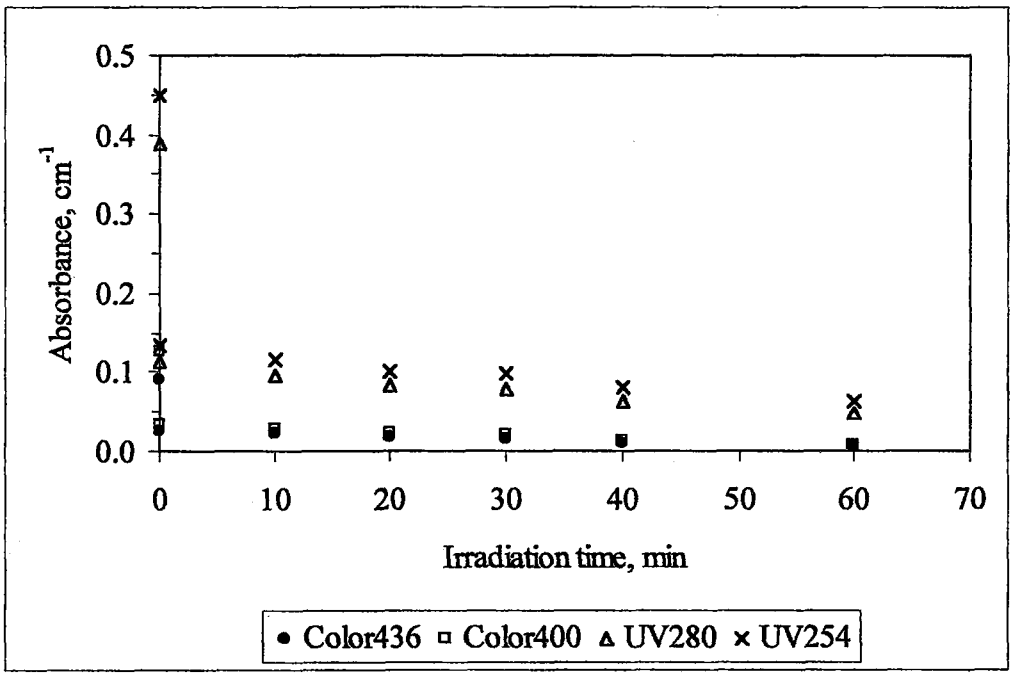

Figure 4.28. The absorbance measurements for the photocatalytic degradation of 20 mgL^{-1} humic acid for a TiO_2 loading of 0.50 $mgmL^{-1}$.

The photocatalytic degradation of humic acid is known to be explained with a pseudo first order kinetic model (Bekbolet *et al.*, 1998, Wiszniowski *et al.*, 2002).

$$-\frac{d[HA]}{dt} = k_{PCO}[HA] \tag{4.13}$$

where k_{PCO} (min^{-1}) represents the pseudo first order kinetic rate constant and *[HA]* represents the humic acid concentration expressed as absorbance measurements (cm^{-1}).

The application of the pseudo first order degradation model for UV_{254} and $Color_{436}$ data are presented in Appendix E and the model parameters are compiled in Table 4.6.

Color degradation rates were found to be faster than the UV_{254} and UV_{280} degradation rates indicating the resistance of organic containing double bonds and aromatic groups to oxidation compared to chromophoric groups. The calculated pseudo first order degradation rate constant for $Color_{436}$ was 1.4 and 1.5 times greater than those of UV_{280} and UV_{254} respectively.

Table 4.6. Pseudo first order model kinetic parameters for photocatalytic oxidation of 20 mgL^{-1} humic acid with 0.50 $mgmL^{-1}$ TiO_2.

	Pseudo first order degradation rate constant, k_{PCO} (min^{-1})	Half life, $t_{1/2}$ (min)	Apparent rate, r (m^{-1} min^{-1})
$Color_{436}$	3.99×10^{-2}	21	0.367
$Color_{400}$	4.20×10^{-2}	17	0.529
UV_{280}	2.81×10^{-2}	25	1.090
UV_{254}	2.64×10^{-2}	32	1.180

The previous studies in the literature also reports pseudo first order degradation rate constants obtained from the experiments conducted using TiO_2 Degussa P-25, but another type of commercial humic acid (Roth), which contained ~0.55 mg TOC per mg humic acid. Gonenc and Bekbolet (2001) reported the TOC degradation rate constant for the same photocalyst loading as 1.98×10^{-2} min^{-1}, which is slower than the UV_{254} degradation rate constant for Aldrich humic acid. The difference in the calculated rate constants may be addressed to the structural differences between the two commercial humic acids as well as the experimental conditions including the reactor geometry and the intensity of the irradiation source.

In order to observe the effect of photocatalyst loading on the photocatalytic oxidation of humic acids, 0.25 $mgmL^{-1}$ and 1.00 $mgmL^{-1}$ TiO_2 loadings were selected as one lower and one higher loading than the primary one, which is 0.5 $mgmL^{-1}$. Humic acid solutions with 20 mgL^{-1} concentrations were subjected to the same photocatalytic degradation experiments with these different TiO_2 loadings.

For the photocatalyst loading of 0.25 $mgmL^{-1}$, the initial adsorption (t=0 values) on TiO_2 resulted in 56% and 48% reduction in $Color_{436}$ and UV_{254} respectively. $Color_{436}$ removal efficiency achieved in 40 minutes was 90% and extending the irradiation time up to 60 minutes did not provide further removal. Similarly UV_{254} reduction did not vary for 40 and 60 minutes of irradiation and remained as 77% demonstrating that increased efficiencies cannot be achieved for prolonged irradiation periods. The remaining 23% UV_{254} shows the

insufficient capability of photocatalytic oxidation in obtaining complete organic matter mineralization under the existing experimental condition for a TiO_2 loading of 0.25 $mgmL^{-1}$. Light intensity, pH of the medium, initial humic acid concentration are among the factors effecting the level of oxidation efficiency achieved by photocatalysis. The unreacted UV absorbing centers are probably entrapped within the inner core of the complex humic acid molecule, which has aromatic conjugate double bond structure. 90% reduction in $Color_{436}$ shows the removal of functional groups that impart color to the solution. The remaining 10% $Color_{436}$ is due to nonoxidizable inert portion within the humic acid structure.

The pseudo first order rate constant for $Color_{436}$ was calculated as 3.32×10^{-2} min^{-1}. Bekbolet and coworkers (1998) found the pseudo first order rate constant as 7.71×10^{-2} min^{-1} for $Color_{436}$ degradation in the presence of 0.25 $mgmL^{-1}$ photocatalyst loading. $Color_{436}$ degradation rate constant calculated in this study for Aldrich humic acid was about half of the rate constant of Roth humic acid. In another study Gonenc and Bekbolet (2001) reported the first order rate constant for TOC removal as 1.40×10^{-2} min^{-1} for the same TiO_2 loading and Roth humic acid. When this rate is compared with the UV_{254} degradation rate in this study, which is 2.15×10^{-2} min^{-1}, Aldrich humic acid exhibits a higher degradation rate constant. The differences in the calculated rate constants may be addressed to the compositional differences between the two commercial humic acids. It is possible to use ^{13}C-NMR and IR analysis to evaluate the structural differences in humic acids (Mao *et al.*, 1998).

In order to analyze the effect of TiO_2 loading within a range and to obtain complete degradation in shorter irradiation periods another set of experiments were conducted using 1.00 $mgmL^{-1}$ photocatalyst loading. However, due to high amount of adsorption of humic acid onto the photocatalyst surface and complete blockage of the surface photodegradation could not be observed. This can be explained by low possibility of OH· radical formation as a result of the interactions of photons on the photocatalyst surface. Removal due to initial adsorption was 93% for $Color_{436}$ and 91% for UV_{254} when 1.00 $mgmL^{-1}$ photocatalyst loading was used. At the end of 60 minutes irradiation period these removals increased to 99% and 94% for the two parameters of consideration. Fluctuations in the absorbance values throughout the irradiation period ($91\pm3\%$ for UV_{254}) occurred as a result of

photoadsorption / photodesorption mechanisms between the humic acid molecules in the solution and the photocatalyst surface.

4.3.2.3. The Effect of Humic Acid Concentration on Photocatalytic Oxidation. Photocatalytic oxidation experiments were also conducted with 50 mgL^{-1} humic acid concentration in order to evaluate the degradation for a different concentration. Two different photocatalyst loadings, 0.50 and 1.00 $mgmL^{-1}$, were used in the experiments. The reason for choosing a higher concentration than 20 mgL^{-1} was studying with a concentration in which photocatalytic degradation can be observed even for 1.00 $mgmL^{-1}$ TiO_2 loading without the effect of complete adsorption of humic acid on the photocatalyst surface. The selected humic acid concentration (50 mgL^{-1}) corresponds to approximately 18 mgL^{-1} TOC, which is a TOC value that can be observed in natural surface waters. The TOC level in natural surface waters may vary from a few milligrams per liter in river waters to as much as 30 mgL^{-1} and greater in eutrophic lake waters (Langlais *et al.*, 1991).

The following Figure 4.29. presents the reduction in UV_{254}, UV_{280}, $Color_{400}$ and $Color_{436}$ parameters due to irradiation time for 50 mgL^{-1} humic acid solution when 0.50 $mgmL^{-1}$ TiO_2 loading was used. The degradation profiles for UV_{254} and $Color_{436}$ are also shown in Appendix E.

In the photocatalytic oxidation of 50 mgL^{-1} humic acid, the initial adsorptions for $Color_{436}$ and UV_{254} were measured as 31 and 9% for the photocatalyst loading of 0.50 $mgmL^{-1}$. The removal efficiency achieved for $Color_{436}$ and UV_{254} reduction was 67% and 54% respectively for 30 minutes and these efficiencies did not change at the end of 60 minutes irradiation period. This finding indicates that 0.50 $mgmL^{-1}$ photocatalyst loading is insufficient to completely oxidize 50 mgL^{-1} humic acid concentration for the specified experimental conditions. Therefore, the photocatalyst loading was increased to 1.00 $mgmL^{-1}$ in the proceeding oxidation experiment.

When a photocatalyst loading of 1.00 $mgmL^{-1}$ was used for the photocatalytic degradation of 50 mgL^{-1} humic acid solution, the reduction in $Color_{436}$ and UV_{254} parameters due to initial adsorption were 60% and 56% respectively. 30 minutes of irradiation resulted

in 70% removal efficiency for UV_{254}. Removal efficiency increased to 76% for UV_{254} in 60 minutes and no significant improvement could be achieved for prolonged irradiation periods. The maximum $Color_{436}$ removal obtained for 60 minutes irradiation was 88 % and it was also not affected with increases irradiation periods either.

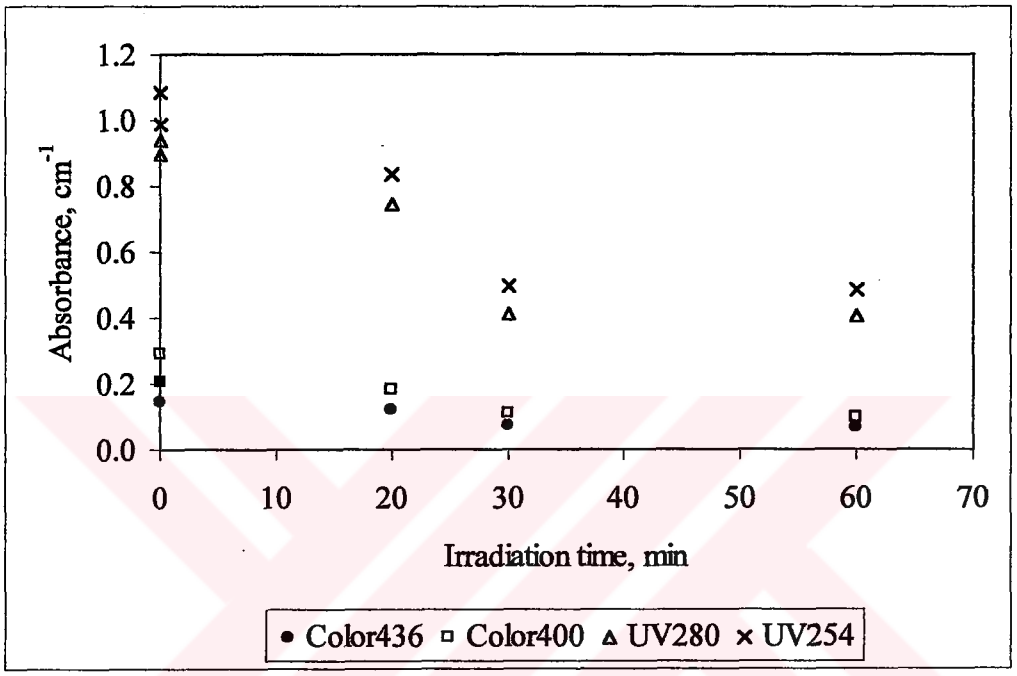

Figure 4.29. The absorbance measurements for the photocatalytic degradation of 50 mgL^{-1} humic acid for a TiO_2 loading of 0.50 $mgmL^{-1}$.

The calculated pseudo first order model parameters for the experimental data are given in Table 4.7. for the photocatalytic oxidation of 50 mgL^{-1} humic acid solution in the presence of 0.50 $mgmL^{-1}$ TiO_2. Comparison of the rate constants and half-life values showed faster degradation of color forming moieties than UV_{254} and UV_{280}. Pseudo first order degradation rate constant for $Color_{436}$ was 1.3 and 1.4 times greater than pseudo first order degradation rate constants of UV_{280} and UV_{254} respectively. The same trend was also observed for the pseudo first order degradation rate constants of 20 mgL^{-1} humic acid solution.

The effect of humic acid concentration showed itself by decreased pseudo first order degradation rate constants with increasing humic acid concentration. The calculated rate constants were changed by a factor of approximately 0.5 when humic acid concentration

was changed from 20 mgL^{-1} to 50 mgL^{-1}. The ratio of pseudo first order rate constants of 20 $mgmL^{-1}$ to those of 50 $mgmL^{-1}$ were 2.1, 2.3, 1.9 and 1.9 for $Color_{436}$, $Color_{400}$, UV_{280} and UV_{254} parameters.

Table 4.7. Pseudo first order model kinetic parameters for photocatalytic oxidation of 50 mgL^{-1} humic acid with 0.50 $mgmL^{-1}$ TiO_2.

	Pseudo first order degradation rate constant, k_{PCO} (min^{-1})	Half life, $t_{1/2}$ (min)	Apparent rate, r ($m^{-1}min^{-1}$)
$Color_{436}$	1.88×10^{-2}	37	0.393
$Color_{400}$	1.80×10^{-2}	39	0.526
UV_{280}	1.46×10^{-2}	47	1.369
UV_{254}	1.39×10^{-2}	50	1.508

When the apparent rates for two different humic acid concentrations were compared, it was observed that the initial rates for $Color_{436}$ and $Color_{400}$ parameters were almost the same, but photocatalytic oxidation of 20 $mgmL^{-1}$ humic acid concentration exhibited initial rates about 80% of the rates obtained for 50 $mgmL^{-1}$ humic acid concentration in terms of UV_{280} and UV_{254} degradation.

4.3.3. Photocatalytic Oxidation of Pretreated Humic Acid Samples

The partially treated humic acid samples using ozone oxidation as explained and characterized in Section 4.3.1 were subjected to photocatalytic oxidation under the same conditions applied for the untreated humic acid samples. For all the samples experiments were conducted using 0.25, 0.50 and 1.00 $mgmL^{-1}$ TiO_2 loadings. Since 0.25 $mgmL^{-1}$ photocatalyst loading was insufficient for complete mineralization under the experimental conditions used, 0.50 $mgmL^{-1}$ was selected as the effective photocatalyst loading for application of the pseudo first order degradation model and for comparison with other oxidation methods. The results of the experiments conducted using photocatalyst loadings of 1.00 $mgmL^{-1}$ could not be employed for the application of pseudo first order degradation model since a photodegradation could not be observed due to complete coverage of the

photocatalyst surface with the initial adsorption of the humic acid molecules. The results of these experiments were used as comparison purposes with the other results on percent removal bases.

4.3.3.1. Photocatalytic Oxidation of Humic Acid Sample 1. The partially treated humic acid sample, which was pretreated by applying 0.20 mgO_3/mgC into 20 mgL^{-1} humic acid solution was subjected to photocatalytic oxidation using TiO_2 loading between 0.25 – 1.00 $mgmL^{-1}$. Figure 4.30 presents the reductions in UV_{254}, UV_{280}, $Color_{400}$ and $Color_{436}$ parameters during the photocatalytic oxidation of Sample 1 for a TiO_2 loading of 0.50 $mgmL^{-1}$.

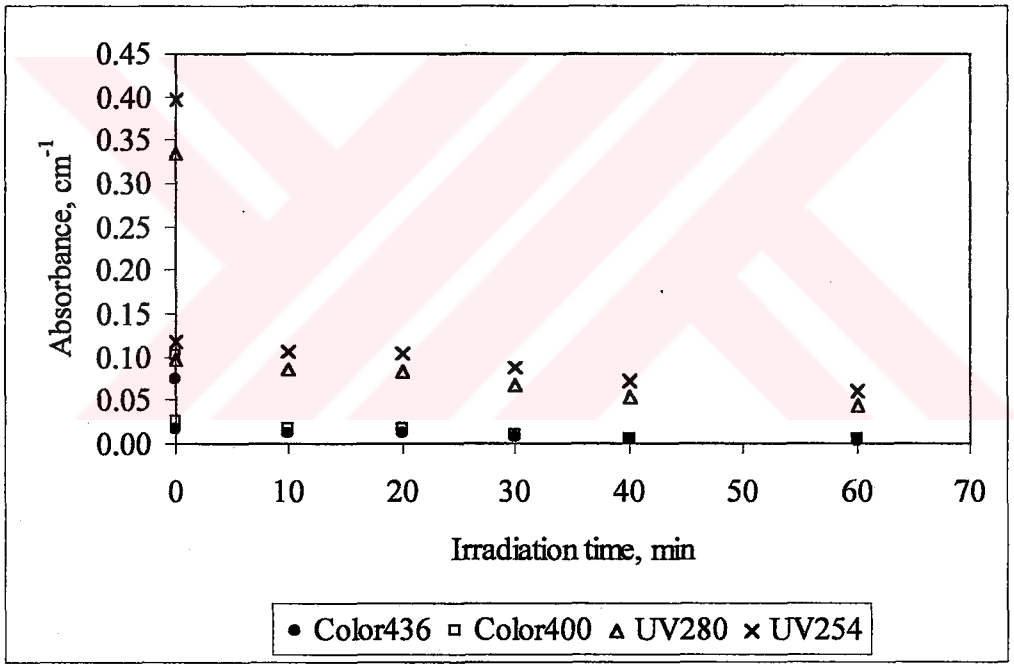

Figure 4.30. The absorbance measurements for the photocatalytic degradation of Sample 1 for a TiO_2 loading of 0.50 $mgmL^{-1}$.

The initial adsorption on the photocatalyst surface resulted in 74% $Color_{436}$ reduction and 69% UV_{254} reduction when 0.50 $mgmL^{-1}$ TiO_2 was used. For $Color_{436}$ parameter, removal efficiency achieved in 30 and 60 minutes were 90% and 96%. For UV_{254} parameter, removal efficiency achieved in 30 and 60 minutes were 78% and 85%. The degradation profiles for $Color_{436}$ and $Color_{400}$ were close to each other; similarly UV_{254} and UV_{280} exhibited parallel trends. The color forming chromophoric groups were degraded

faster than UV_{280} and UV_{254} parameters representing the aromatic groups in the humic acid structure. The degradation profiles used to calculate the parameters for first order kinetics are given in Appendix E and the model parameters are tabulated in Table 4.8.

Table 4.8. Pseudo first order model kinetic parameters for photocatalytic oxidation of Sample 1 with 0.50 $mgmL^{-1}$ TiO_2.

	Pseudo first order degradation rate constant, k_{PCO} (min^{-1})	Half life, $t_{1/2}$ (min)	Apparent rate, r ($m^{-1}min^{-1}$)
$Color_{436}$	4.72×10^{-2}	15	0.344
$Color_{400}$	4.72×10^{-2}	15	0.477
UV_{280}	2.77×10^{-2}	25	0.925
UV_{254}	2.55×10^{-2}	27	1.012

The pseudo first order degradation rate constants calculated from the experimental data were the same for $Color_{436}$ and $Color_{400}$ and very close for UV_{280} and UV_{254}. Rate constants for color degradation were 1.7 and 1.9 times greater than UV_{280} and UV_{254} rate constants respectively.

When 0.25 $mgmL^{-1}$ TiO_2 was used in the oxidation experiments, the initial adsorption on the photocatalyst surface resulted in 52% $Color_{436}$ reduction and 44% UV_{254} reduction. For $Color_{436}$ parameter, removal efficiency achieved in 30 and 60 minutes were 80% and 93%. The effect of photocatalyst loading on Color removal efficiency showed itself by only a 3% additional removal efficiency for an irradiation period of 60 minutes when the photocatalyst loading was increased from 0.25 to 0.50 $mgmL^{-1}$, the effect of increased photocatalyst loading was more significant in shorter irradiation periods. For UV_{254} parameter, removal efficiency achieved in 30 and 60 minutes were 64% and 77%.

When the photocatalyst loading was increased to 1.00 $mgmL^{-1}$, the reductions in $Color_{436}$ and UV_{254} due to initial adsorption were 93% and 88% for respectively. As a result of complete adsorption and surface blockage, photocatalytic degradation rates could not be calculated for this loading. The degradation profiles given in Figure 4.31 based on UV_{254},

UV_{280}, $Color_{400}$ and $Color_{436}$ present the complete removal by initial adsorption and ineffectiveness of increased irradiation period. The same phenomenon was observed for all of the four pretreated humic acid sample as well as the untreated humic acid sample.

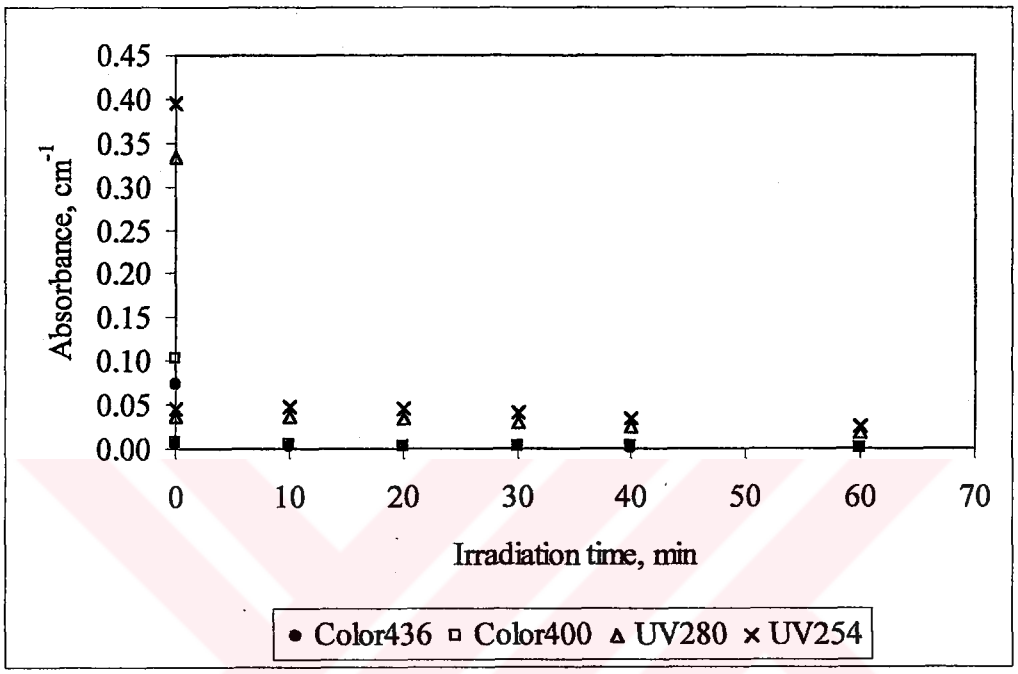

Figure 4.31. The absorbance measurements for the photocatalytic degradation of Sample 1 for a TiO_2 loading of 1.00 $mgmL^{-1}$.

4.3.3.2. Photocatalytic Oxidation of Humic Acid Sample 2. The partially treated humic acid sample, which was pretreated by applying 0.34 mgO_3/mgC into 20 mgL^{-1} humic acid solution was subjected to photocatalytic oxidation using TiO_2 loading between 0.25 – 1.00 $mgmL^{-1}$. Figure 4.32 presents the reductions in UV_{254}, UV_{280}, $Color_{400}$ and $Color_{436}$ parameters during the photocatalytic oxidation of Sample 2 for a TiO_2 loading of 0.50 $mgmL^{-1}$.

The initial adsorption on the photocatalyst surface resulted in 76% $Color_{436}$ reduction and 69% UV_{254} reduction when 0.50 $mgmL^{-1}$ TiO_2 was used. For $Color_{436}$ parameter, removal efficiency achieved in 30 and 60 minutes were 94% and 96%. $Color_{436}$ removal efficiency remained the same between 20 and 40 minutes. For UV_{254} parameter, removal efficiency achieved in 30 and 60 minutes were 79% and 87%. The degradation profiles for $Color_{436}$ and $Color_{400}$ were close to each other; similarly UV_{254} and UV_{280} exhibited parallel

trends. Color reductions were faster than UV_{280} and UV_{254} degradations.

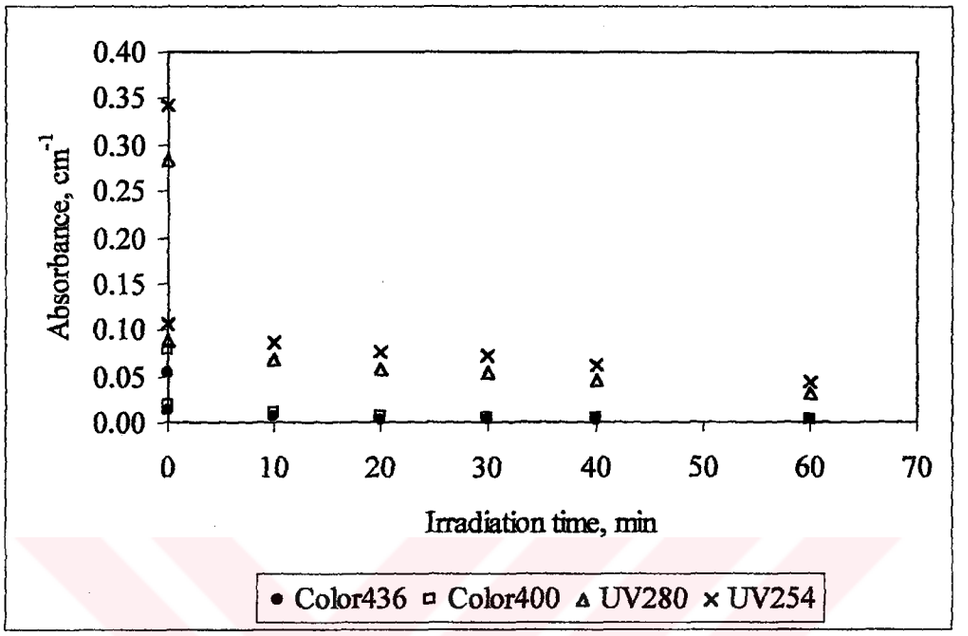

Figure 4.32. The absorbance measurements for the photocatalytic degradation of Sample 2 for a TiO_2 loading of 0.50 $mgmL^{-1}$.

The pseudo first order degradation model was applied for UV_{254} and $Color_{436}$ data. The related degradation profiles are presented in Appendix E. The model parameters, which are the pseudo first order degradation rate constants (k_{PCO}) and the half-lives ($t_{1/2}$), are compiled in Table 4.9.

Table 4.9. Pseudo first order model kinetic parameters for photocatalytic oxidation of Sample 2 with 0.50 $mgmL^{-1}$ TiO_2.

	Pseudo first order degradation rate constant, k_{PCO} (min^{-1})	Half life, $t_{1/2}$ (min)	Apparent rate, r ($m^{-1}min^{-1}$)
$Color_{436}$	4.47×10^{-2}	16	0.237
$Color_{400}$	5.11×10^{-2}	14	0.393
UV_{280}	3.02×10^{-2}	23	0.855
UV_{254}	2.76×10^{-2}	25	0.994

Pseudo first order rate constant for $Color_{436}$ degradation was 1.5 and 1.6 times greater than UV_{280} and UV_{254} rate constants respectively.

When 0.25 $mgmL^{-1}$ TiO_2 was used in the oxidation experiments of Sample 2, the initial adsorption on the photocatalyst surface resulted in 54% $Color_{436}$ reduction and 46% UV_{254} reduction. For $Color_{436}$ parameter, removal efficiency achieved in 30 and 60 minutes were 77% and 95%. For UV_{254} parameter, removal efficiency achieved in 30 and 60 minutes were 62% and 77%. The removal efficiencies were close to the removal efficiencies obtained for the photocatalytic degradation of Sample 1 in the presence of 0.25 $mgmL^{-1}$ TiO_2 loading, but the final concentrations obtained were obviously lower due to lower initial concentrations.

When the photocatalyst loading was increased to 1.00 $mgmL^{-1}$, the reductions in $Color_{436}$ and UV_{254} due to initial adsorption were 98% and 92% respectively. The pseudo first order model could not be applied to the photocatalytic degradation data due to the same reason explained previously for all the samples when 1.00 $mgmL^{-1}$ photocatalyst loading was applied. At the end of 60 minutes irradiation period, UV_{254} removal efficiency increased to 96%.

4.3.3.3. Photocatalytic Oxidation of Humic Acid Sample 3. The partially treated humic acid sample, which was pretreated by applying 0.61 mgO_3/mgC into 20 mgL^{-1} humic acid solution was subjected to photocatalytic oxidation using TiO_2 loading between 0.25 – 1.00 $mgmL^{-1}$. Figure 4.33 presents the reductions in UV_{254}, UV_{280}, $Color_{400}$ and $Color_{436}$ parameters during the photocatalytic oxidation of Sample 3 for a TiO_2 loading of 0.50 $mgmL^{-1}$.

The initial adsorption on the photocatalyst surface resulted in 73% $Color_{436}$ reduction and 65% UV_{254} reduction when 0.50 $mgmL^{-1}$ TiO_2 was used. Since the initial $Color_{436}$ value of the sample introduced into photocatalytic degradation was already low (3.7 m^{-1}) due to higher amount of ozone application compared to the previous samples, the initial adsorption removed a great percentage of this absorbance leaving a very small amount that cannot be accurately followed during photocatalysis. Therefore, pseudo first order degradation model

parameters for $Color_{436}$ and $Color_{400}$ could not be calculated for this Sample 3. For UV_{254} parameter, removal efficiency achieved in 30 and 60 minutes were 78% and 91%.

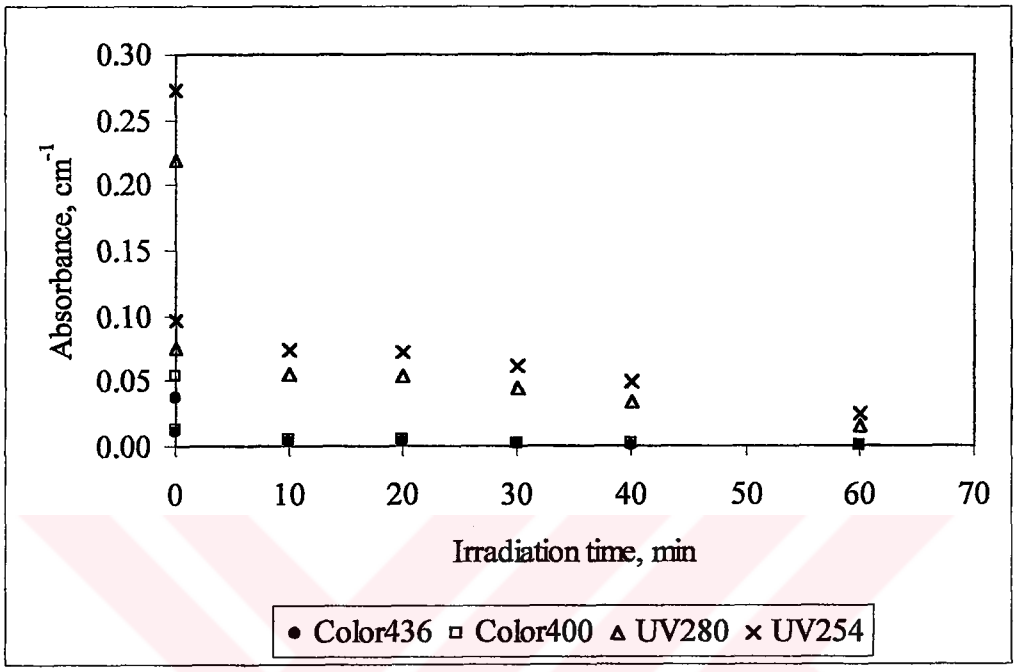

Figure 4.33. The absorbance measurements for the photocatalytic degradation of Sample 3 for a TiO_2 loading of 0.50 $mgmL^{-1}$.

The degradation profile of UV_{254} data used in the pseudo first order kinetics is presented in Appendix E. The calculated model parameters for UV_{254} and UV_{280} are shown in Table 4.10 below.

Table 4.10. Pseudo first order model kinetic parameters for photocatalytic oxidation of Sample 3 with 0.50 $mgmL^{-1}$ TiO_2.

	Pseudo first order degradation rate constant, k_{PCO} (min^{-1})	Half life, $t_{1/2}$ (min)	Apparent rate, r ($m^{-1}min^{-1}$)
$Color_{436}$	N.A.	N.A.	N.A.
$Color_{400}$	N.A.	N.A.	N.A.
UV_{280}	3.73×10^{-2}	19	0.817
UV_{254}	3.36×10^{-2}	21	0.998

N.A.: Not applicable

When 0.25 $mgmL^{-1}$ TiO_2 was used in the oxidation experiments of Sample 3, the initial adsorption on the photocatalyst surface resulted in 63% $Color_{436}$ reduction and 51% UV_{254} reduction. For $Color_{436}$ parameter, removal efficiency achieved in 30 and 60 minutes were 87% and 95%. For UV_{254} parameter, removal efficiency achieved in 30 and 60 minutes were 67% and 79%.

When the photocatalyst loading was increased to 1.00 $mgmL^{-1}$, the reductions in $Color_{436}$ and UV_{254} due to initial adsorption were 95% and 89% respectively. Further degradation of $Color_{436}$ could not be followed accurately, but it was 100% even in 20 minutes irradiation period. For UV_{254} parameter, removal efficiency achieved in 40 and 60 minutes were 92% and 96%.

4.3.3.4. Photocatalytic Oxidation of Humic Acid Sample 4. The partially treated humic acid sample, which was pretreated by applying 1.00 mgO_3/mgC into 20 mgL^{-1} humic acid solution was subjected to photocatalytic oxidation using TiO_2 loading between 0.25 – 1.00 $mgmL^{-1}$. Figure 4.34 presents the reductions in UV_{254}, UV_{280}, $Color_{400}$ and $Color_{436}$ parameters during the photocatalytic oxidation of Sample 4 for a TiO_2 loading of 0.50 $mgmL^{-1}$.

The initial adsorption on the photocatalyst surface resulted in 90% $Color_{436}$ reduction and 72% UV_{254} reduction when 0.50 $mgmL^{-1}$ TiO_2 was used. Similar to the case in Sample 3, the initial $Color_{436}$ value of the sample introduced into photocatalytic degradation was already very low (2.0 m^{-1}) due to high amount of pretreatment with ozonation. The initial adsorption removed almost all the color leaving a very small amount that cannot be accurately followed during photocatalysis. Therefore, pseudo first order degradation model parameters for $Color_{436}$ and $Color_{400}$ could not be calculated for this Sample 4.

For UV_{254} parameter, removal efficiency achieved in 30 and 60 minutes were 80% and 92%. These removal efficiencies were found to be very close to the removal efficiencies obtained for Sample 3 under the same experimental conditions. UV_{254} removal efficiencies were determined as 78% and 81% for Sample 3 for irradiation period of 30 and 60 minutes respectively.

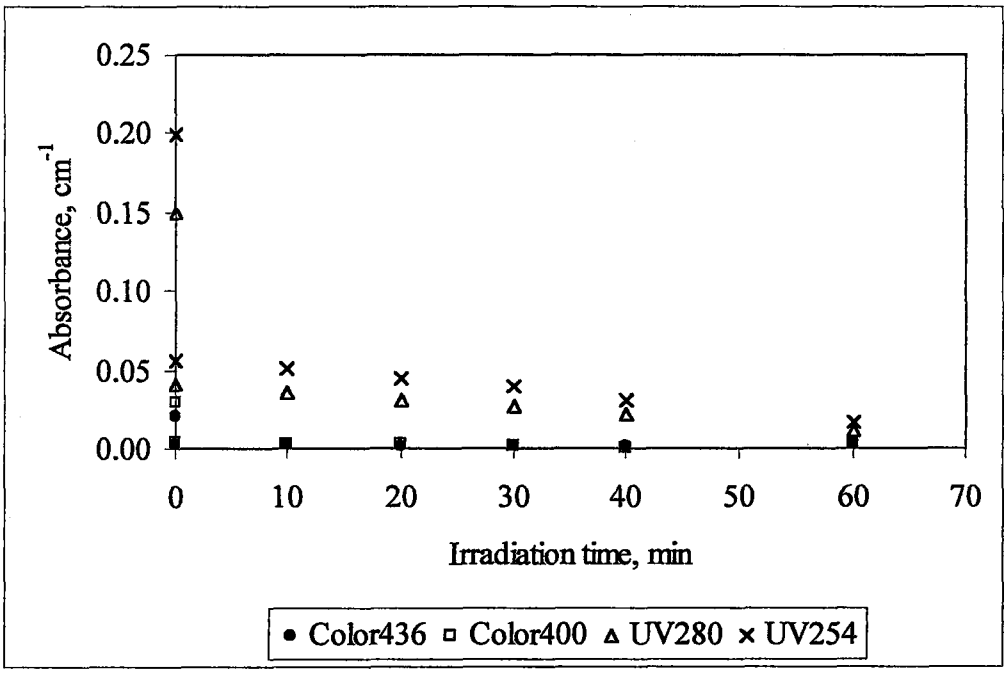

Figure 4.34. The absorbance measurements for the photocatalytic degradation of Sample 4 for a TiO_2 loading of 0.50 $mgmL^{-1}$.

Table 4.11. Pseudo first order model kinetic parameters for photocatalytic oxidation of Sample 4 with 0.50 $mgmL^{-1}$ TiO_2.

	Pseudo first order degradation rate constant, k_{PCO} (min^{-1})	Half life, $t_{1/2}$ (min)	Apparent rate, r ($m^{-1}min^{-1}$)
$Color_{436}$	N.A.	N.A.	N.A.
$Color_{400}$	N.A.	N.A.	N.A.
UV_{280}	3.63×10^{-2}	19	0.545
UV_{254}	3.50×10^{-2}	20	0.697

N.A.: Not applicable

The pseudo first order degradation model could only be applied for UV_{254} and UV_{280} parameters. The calculated model parameters are presented in Table 4.11. The degradation profile presented in Appendix E was used for the calculation of UV_{254} degradation kinetics. The calculated pseudo first order rate constant for UV_{280} was 4% higher than that of UV_{254}. It was observed that the differences between the pseudo first order degradation rate

constants for these two parameters were between 4-8% for the photocatalytic degradation of all the samples.

When 0.25 $mgmL^{-1}$ TiO_2 was used in the oxidation experiments of Sample 4, the initial adsorption on the photocatalyst surface resulted in 61% $Color_{436}$ reduction and 48% UV_{254} reduction. For $Color_{436}$ parameter, removal efficiency achieved in 30 and 60 minutes were 89% and 94%. For UV_{254} parameter, removal efficiency achieved in 30 and 60 minutes were 71% and 77%. The removal efficiencies achieved with 0.25 $mgmL^{-1}$ photocatalyst loading was very close to the removal efficiencies obtained for photocatalytic oxidation of Sample 3 under the same conditions.

When the photocatalyst loading was increased to 1.00 $mgmL^{-1}$, the reductions in $Color_{436}$ and UV_{254} due to initial adsorption were 94% and 83% respectively. Further degradation of $Color_{436}$ with increasing irradiation period could not be followed accurately. For UV_{254} parameter, removal efficiency achieved in 30 and 60 minutes were 93% and 98%.

4.3.3.5. Comparison of Photocatalytic Oxidation of Humic Acid Samples. Photocatalytic oxidation of the partially oxidized humic acid samples, which were evaluated separately in the previous sections, are compared in this section for their differences and common characteristics based on UV_{254} and $Color_{436}$ reductions depending on the irradiation periods and photocatalyst loadings. In the early stages of photocatalytic oxidation (upto ~20 minutes) fluctuations were observed in the degradation profiles due to unstable conditions of photoadsorption-photodesorption mechanisms occurring in the TiO_2 surface/solution interface. Percent removals obtained in 30 and 60 minutes photocatalytic treatment are presented below in Table 4.12 for preozonated humic acid samples as well as untreated humic acid sample.

The UV_{254} removal efficiencies obtained in 30 minutes were almost the same for all the samples, even for the untreated humic acid sample. For 60 minutes of irradiation period, slight differences in the removal efficiencies were observed for different samples depending on the applied ozone dosages. Actually, the removal efficiencies were close to each other

for the untreated humic acid sample and Sample 1 and 2, which were pretreated by low ozone dosages. Ozone is known to follow direct oxidation pathway within the pH range of these experimental conditions and the organic groups with double bonds, the chromophoric groups are the first targets of ozone oxidation. Since the humic acid solutions are pretreated with ozone prior to photocatalysis, it can be assumed that the organic groups including aromatic structures and carboxylic groups, which are more resistant to oxidation, are left in the solution for this second step of oxidation (photocatalysis). It was observed that same and even higher removal efficiencies are obtained for pretreated humic acid sample compared to untreated one. This may prove the role of unselective oxidation pathway on OH· radicals, which attack almost all organic groups, even the resistant ones.

Table 4.12. Photocatalytic removal of UV_{254} and $Color_{436}$ in untreated and preozonated humic acid samples for 0.5 $mgml^{-1}$ TiO_2 loading.

	UV_{254} removal, %		$Color_{436}$ removal, %	
Sample	t=30 min	t=60 min	t=30 min	t=60 min
Humic acid	78	86	85	93
Sample 1	78	85	90	96
Sample 2	79	87	94	96
Sample 3	78	91	97	100
Sample 4	80	92	100	100

Increased removal efficiencies were observed for $Color_{436}$ reduction in 30 minutes irradiation depending on the extend of pretreatment. Sine ozonation is known to break large organic molecules into smaller ones; the color forming groups may become more amenable for oxidation with photocatalysis. Almost complete decolorizations were observed within the 60 minutes of irradiation period, therefore no significant differences were observed for the final oxidation efficiencies for different samples at the end of 60 minutes reaction period.

For 0.25 $mgmL^{-1}$ TiO_2 loadings, UV_{254} removal rates were between 62-72% for 30-minutes and 77-80% for 60-minutes of irradiation periods; $Color_{436}$ removals for the same conditions were observed as 80-100% and 90-100%. Removal efficiencies higher than 90% were achieved even in 30 minutes irradiation for 1.00 $mgmL^{-1}$ TiO_2 loading.

The comparison of the pseudo first order kinetic rate constants for UV_{254} degradation for different samples and for different photocatalyst loadings are presented in Table 4.13.

Table 4.13. Pseudo first order kinetic model parameters for photocatalytic degradation of UV_{254} in 20 mgL^{-1} untreated and preozonated humic acid solutions.

TiO_2 loading	0.25 $mgmL^{-1}$		0.50 $mgmL^{-1}$		1.0 $mgmL^{-1}$	
Sample	k_{PCO} x10^{-2}, min^{-1}	$t_{1/2}$, min	k_{PCO} x10^{-2}, min^{-1}	$t_{1/2}$, min	k_{PCO} x10^{-2}, min^{-1}	$t_{1/2}$, min
Humic Acid	2.15	32	2.64	26	3.20	22
Sample 1	1.97	35	2.55	27	3.46	20
Sample 2	2.06	34	2.75	25	3.39	20
Sample 3	2.08	33	3.36	21	3.62	19
Sample 4	2.24	31	3.99	17	5.53	13

From a general point of view, for a TiO_2 loading of 0.50 $mgmL^{-1}$, the pseudo first order rate constants differed by 50% in relation to a pre-oxidation degree of 55% for UV_{254} and 80% for $Color_{436}$. One striking feature of the degradation data is that no significant effect (< 5%) is observed in photocatalytic rate constants for pre-ozonation removal degrees up to 35% for UV_{254} and 55% for $Color_{436}$. Further changes in humic acid structure due to the ozonation significantly altered the photocatalytic rate constants by 27% and 50% for the samples 3 and 4 respectively (Kerc *et al.*, 2003).

The calculated reaction rate constants increased with increasing photocatalyst loadings as expected. On the average the pseudo first order reaction rate constants for 0.50 mg mL^{-1} and 1.00 mg mL^{-1} photocatalyst loadings were approximately 1.5 times and 1.8 times more than the pseudo first order rate constants for 0.25 mg mL^{-1} photocatalyst loading respectively.

In general an increasing trend was observed in the rate degradation rate constants during photocatalysis with increasing ozone dosages applied in the pretreatment stage. The increase may be addressed to the structural changes obtained by ozonation and formation of smaller organic molecules that are more reactive for photocatalytic oxidation.

The comparison of the pseudo first order kinetic rate constants for $Color_{436}$ degradation for different samples and for different photocatalyst loadings are presented in Table 4.14. Increasing the TiO_2 loading in the range of 0.25 – 1.0 $mgmL^{-1}$ significantly altered the reaction kinetics by extended initial adsorption leading to surface blockage by chromophoric sites of humic acid resulting in decreased photocatalytic activity.

Table 4.14. Pseudo first order kinetic model parameters for photocatalytic degradation of $Color_{436}$ in 20 mgL^{-1} untreated and preozonated humic acid solutions.

TiO_2 loading	0.25 $mgmL^{-1}$		0.50 $mgmL^{-1}$		1.0 $mgmL^{-1}$	
Sample	k_{PCO} x10^{-2}, min^{-1}	$t_{1/2}$, min	k_{PCO} x10^{-2}, min^{-1}	$t_{1/2}$, min	k_{PCO} x10^{-2}, min^{-1}	$t_{1/2}$, min
Humic Acid	3.32	21	3.99	17	n.a.	n.a.
Sample 1	3.85	18	4.72	15	n.a.	n.a.
Sample 2	4.44	16	4.47	16	n.a.	n.a.
Sample 3	4.06	17	n.a.	n.a.	n.a.	n.a.
Sample 4	n.a.	n.a.	n.a.	n.a.	n.a.	n.a.

n.a.: Not applicable.

The reaction rate constants for $Color_{436}$ degradation also increased with increasing photocatalyst loadings as expected. On the average the pseudo first order reaction rate constants for 0.50 $mgmL^{-1}$ photocatalyst loadings were approximately 1.15 times more than the pseudo first order rate constants for 0.25 $mgmL^{-1}$ photocatalyst loading.

The OH radical bound to the semiconductor surface is a chemical equivalent to the surface trapped hole. The hydroxyl radical is able to react with almost all organic molecules thus initiate the oxidative degradation. On the other hand, since the photocatalytic oxidation reactions take place on the surface of the photocatalyst, the elementary reaction steps of humic acid (HA) on the TiO_2/water interface can be represented by the following equations:

$$O_2 + TiO_2 \rightarrow O_{2,ads}$$

$$H_2O + TiO_2 \rightarrow H_2O_{ads}$$

$$HA_{aq} + TiO_2 \rightarrow HA_{ads}$$

where, subscripts aq and ads denote aqueous and adsorbed species respectively.

In case of irradiation with light in visible region:

$$HA + h\nu \ (\lambda > 400\ nm) \rightarrow HA^*_{ads} \rightarrow sensitized\ reactions$$

The attack of the produced oxidants as ·OH/ $\cdot HO_2$ radicals may result in structural changes via hydroxylation, decarboxylation and deploymerization in humic acid molecule producing less hydrophobic, less adsorbing and less aromatic characters.

·OH radical reactions:

$$\cdot OH + H_2O_2 \rightarrow \cdot HO_2 + H_2O$$

$$\cdot OH + HA_{ads} \rightarrow \cdot A + H_2O \rightarrow via\ radical\ reactions \rightarrow \ldots\ HA_{ox} \rightarrow \ldots CO_2 + H_2O$$

Therefore, upon direct action of the oxidants, humic acid is expected to be degraded by far to the formation of CO_2 and H_2O. For prolonged irradiation periods (t>3h) photocatalysis transforms to photomineralization as followed for Sample 4 (TOC<5%).

Ozonation of humic acid solutions result in the accumulation of carboxylic acids in the solution forming the nonoxidized organic portion as explained previously. Sample 4, which was expected to have the highest amount of carboxylic acid content in relation to the highest ozone application dosage among the other samples, exhibited very low UV_{254} values at the end of 60 minutes irradiation period indicating the complete mineralization. This shows the effectiveness of photocatalysis for the degradation of carboxylic acids as also studied by previous researchers. Franch and coworkers (2002) have shown that TiO_2 photocatalysis is effective for mineralization of short-chain carboxylic diacids, as maleic, fumaric and oxalic acids. In their studies that investigates the kinetics and mechanism of carboxylic acid degradation they also point out the importance of adsorption of the organic diacids onto TiO_2 particles. Inel and Okte (1996a, 1996b, 1998a, 1998b) have shown the effective photomineralization of malonic, succinic, adipic and phthalic acids in the presence of TiO_2. The degradation rates as they have explained by zero order kinetics were higher

than the humic acid degradation rates determined in this study. The complex structure of the humic acid molecule is probably the reason for lower degradation rates in comparison to the rates obtained for pure compounds.

4.3.3.6. Application of Langmuir-Hinshelwood Kinetics for Preozonated Humic Acid Samples. It is known that the kinetics of the photocatalytic degradation of organic compounds could be suitably described by Langmuir-Hinshelwood (L-H) kinetic model due to the surface oriented nature of the reaction mechanism (Bekbolet *et al.*, 1998, Chan *et al.*, 2001, Franch *et al.*, 2002).

$$r = -\frac{d[HA]}{dt} = \frac{k_r K_{L-H}[HA_0]}{1 + K_{L-H}[HA_0]} \qquad (4.14)$$

where,

k_r : specific reaction rate constant, $m^{-1}min^{-1}$

K_{L-H} :equilibrium adsorption constant, m.

The rate of the unimolecular surface reaction is represented by r ($m^{-1}min^{-1}$) and it is proportional to the fraction of surface covered when the parent reactant is more strongly adsorbed on the surface than the products. For applying L-H kinetics, a series of humic acid solutions with concentrations between 20 – 90 mgL^{-1} were partially oxidized with ozone resulting in 50% $Color_{436}$ and 35% UV_{254} reduction in each sample prior to photocatalysis. L-H kinetic constants and the rate calculated with the initial absorbance values of Sample 3 are given in Table 4.15.

Table 4.15. L-H kinetic model parameters for preozonated humic acid. (Kerc *et al.*, 2002)

UV_{254}, 29.7 m^{-1}			$Color_{436}$, 3.8 m^{-1}		
k_r, $m^{-1}min^{-1}$	K_{L-H}, m	r, $m^{-1}min^{-1}$	k_r, $m^{-1}min^{-1}$	K_{L-H}, m	r, $m^{-1}min^{-1}$
9.43×10^{-3}	6.56	9.38×10^{-3}	0.993	0.901	0.769

The practical use of this model lies in the fact that K_{L-H} relating to the reaction rate, expresses the adsorption capacity of the organic compounds onto the TiO_2 surface. In the previous studies K_{L-H} and k_r parameters for $Color_{436}$ were reported as 0.332 and $4.99x10^{-2}$ for TiO_2 Degussa P-25 and humic acid (Roth) (Bekbolet *et al.,* 2002). Preozonation in this study showed its effect by 170% increase in K_{L-H} and more than a ten fold improvement in k_r due to the changes in molecular structure.

4.3.4. Adsorption Properties of Humic Acid Samples on the TiO_2 Surface

Surface oriented nature of the photocatalytic oxidation makes it important to evaluate the adsorption characteristics of the humic acid molecules on the photocatalyst surface. The batch adsorption experiments were conducted under dark conditions using TiO_2 loadings within a range of 0.1 – 1.0 $mgmL^{-1}$ in untreated as well as the preozonated humic acid samples. Both Langmuir and Freundlich adsorption models were applied to experimental data, however satisfactory correlations could not be attained for the Langmuir model, which is known to rule a physisorption and not a chemisorption process (Wiszniowski, 2002). Previously it has also been shown that the adsorption of humic acids can be explained with the Freundlich adsorption model (Bekbolet *et al.,* 1996). The Freundlich adsorption model is expressed as:

$$q_A = K_F C_e^{1/n} \tag{4.15}$$

where, q_A : adsorbed amount of adsorbate per mass of adsorbent ($m^{-1}g^{-1}$)

C_e: equilibrium concentration of the adsorbate (m^{-1})

K_F and $1/n$: empirical constants

The initial adsorption experiments were conducted with the untreated humic acid solutions to find out the adsorption characteristics of the unaltered humic acid molecules. The adsorption profile obtained for the untreated humic acid solution was also used for comparison purposes with the preozonated samples. The adsorption profile obtained for the untreated humic acid sample based on UV_{254} parameter is given in Appendix F. 24 hours equilibrium UV_{254} values varied between 2.4 – 34 m^{-1} for the applied photocatalyst loading

under dark conditions. $Color_{436}$ values were between 0.2 – 5.7 m^{-1} for the same conditions.

The dark adsorption experiments were also conducted with the preozonated humic acid samples (Sample 1-4). The adsorption profiles for these preozonated humic acid samples based on UV_{254} are presented in Appendix F.

24 hours equilibrium UV_{254} values for the applied photocatalyst loading of 0.1-1.0 $mgmL^{-1}$ under dark conditions varied between 3.3 – 18.5 m^{-1} for Sample 1, between 3.6 – 16.8 m^{-1} for Sample 2, between 2.7 – 18.9 m^{-1} for Sample 3 and between 5.4 – 9.7 m^{-1} for Sample 4. For the same conditions, $Color_{436}$ values were between 0.2 – 2.4 m^{-1} for Sample 1, between 0.2 – 1.9 m^{-1} for Sample 2, between 0.1 – 2.0 m^{-1} for Sample 3 and around 0.6 m^{-1} for Sample 4.

4.3.4.1. Comparison of the Adsorption Profiles and Freundlich Model Parameters in Humic Acid Samples. In order to evaluate the adsorption characteristics of the different humic acid samples in a general perspective, all the adsorption profiles obtained for the untreated and preozonated humic acid samples were plotted on the same graph in Figure 4.35 for UV_{254}.

Sample 4, to which highest amount of preozonation dosage was applied, exhibited an adsorption profile in a different region than the other samples. A correlation between the preozonation amount and the adsorption trend could not be obtained from the above adsorption profiles. 24 hours equilibrium UV_{254} absorbance values obtained for high TiO_2 loadings (1.00 $mgmL^{-1}$) were found to increase with the increasing preozonation dosages. Sample 4, which was expected to have the lowest equilibrium absorbance value due to lowest initial UV_{254} value, exhibited the highest absorbance value at the end of 24 hours equilibrium period. The changes in the hydrophobic / hydrophilic groups in the organic molecule due to ozonation may alter the adsorbability of the humic acid onto TiO_2. Similar observations were also reported in the previous studies in which the effects of ozone treatment prior to activated carbon adsorption were evaluated. It was found out that the end products of ozonation with high-polarity and solubility reduces the adsorptivity onto activated carbon (Glaze and Wallace, 1984; Sontheimer *et al.*, 1985).

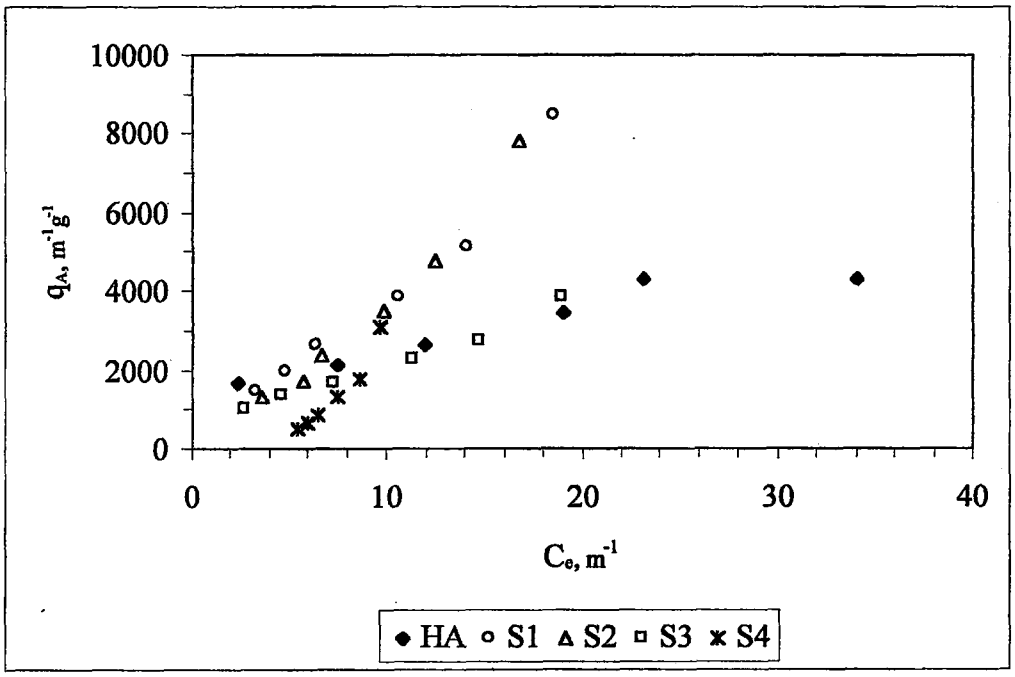

Figure 4.35. Comparison of the adsorption profiles based on UV_{254} for untreated and preozonated humic acid samples.

The isotherms revealed perfect fits to the Freundlich model especially for the untreated humic acid molecule. Degree of preozonation significantly altered the adsorption profile of humic acid on TiO_2. K_F values were in between 256 and 512 and 1/n values reflected an adsorption intensity trend towards linearity. On the other hand, for Sample 4, adsorption profile showed a cluster type accumulation in a C_e region of 5.4– 17.5 m^{-1} and a q_A region of 484-3120 $m^{-1}g^{-1}$. Therefore for comparison purposes the q_A values were calculated based on 0.5 $mgmL^{-1}$ photocatalytst loading, which corresponds to the loading that was used during photocatalytic degradation experiments. The parameters calculated for the Freundlich adsorption model for UV_{254} are presented in Table 4.16 (Kerc *et al.*, 2003).

The adsorption trend of q_A clearly explains the tendency of decreasing adsorption capacity of treated humic acid solutions on TiO_2. These results may suggest that the preozonation transformed humic acid molecule into more desorbable compounds that might migrate to the bulk solution. Bearing in mind that the structure of humic acid molecule was strongly altered due to partial oxidation by ozonation, the decreasing trend in q_A can be explained by the changes in size and the number of the functional groups taking part in surface reactions during adsorption.

Table 4.16. Adsorption properties of humic acid onto TiO_2 based on UV_{254}.

	K_F	1/n	q_A, $m^{-1}g^{-1}$
Humic acid	1102	0.39	2632
Sample 1	442	0.96	2664
Sample 2	256	1.17	2368
Sample 3	512	0.64	1696
Sample 4	-	-	880

For comparison purposes, the adsorption profiles of samples (HA, S1 – S4) for each parameter; UV_{280}, $Color_{400}$ and $Color_{436}$; are shown in Figures 4.36, 4.37 and 4.38. A cluster type accumulation was observed in the adsorption profiles of Sample 4 for all of the parameters studied. All of the samples exhibited similar adsorption trends for TiO_2 loadings greater than 0.5 $mgmL^{-1}$. However, the adsorption profiles of different samples were different from each other for lower TiO_2 loadings. The Freundlich adsorption model was also applied UV_{280}, $Color_{400}$ and $Color_{436}$ parameters. The calculated model parameters; K_F, $1/n$ and q_A, are presented in Table 4.17, 4.18 and 4.19.

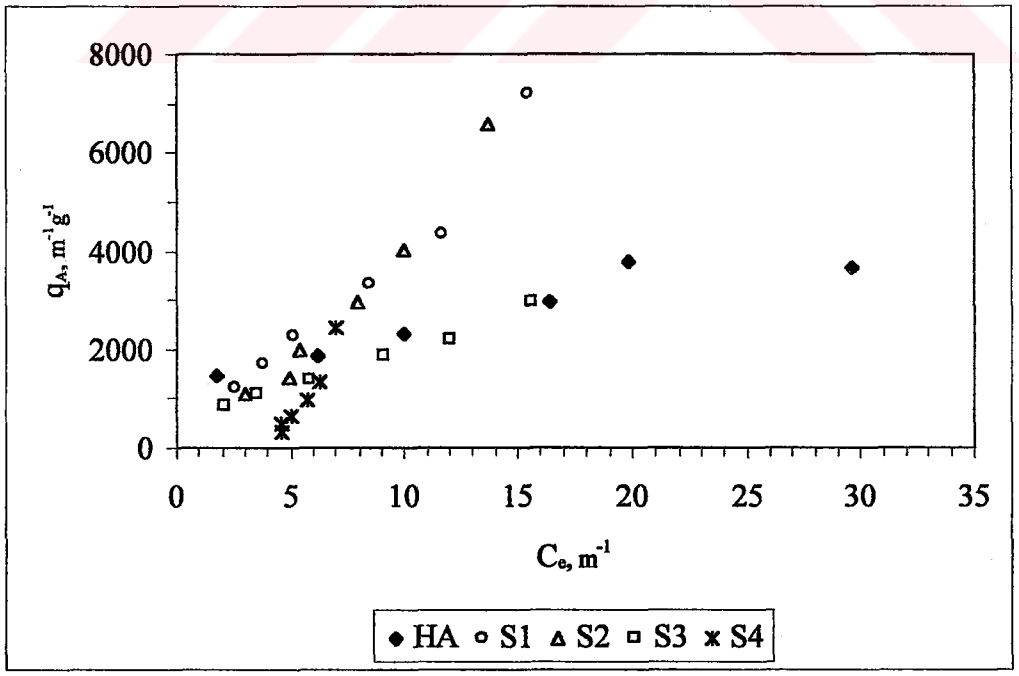

Figure 4.36. Comparison of the adsorption profiles based on UV_{280} for untreated and preozonated humic acid samples.

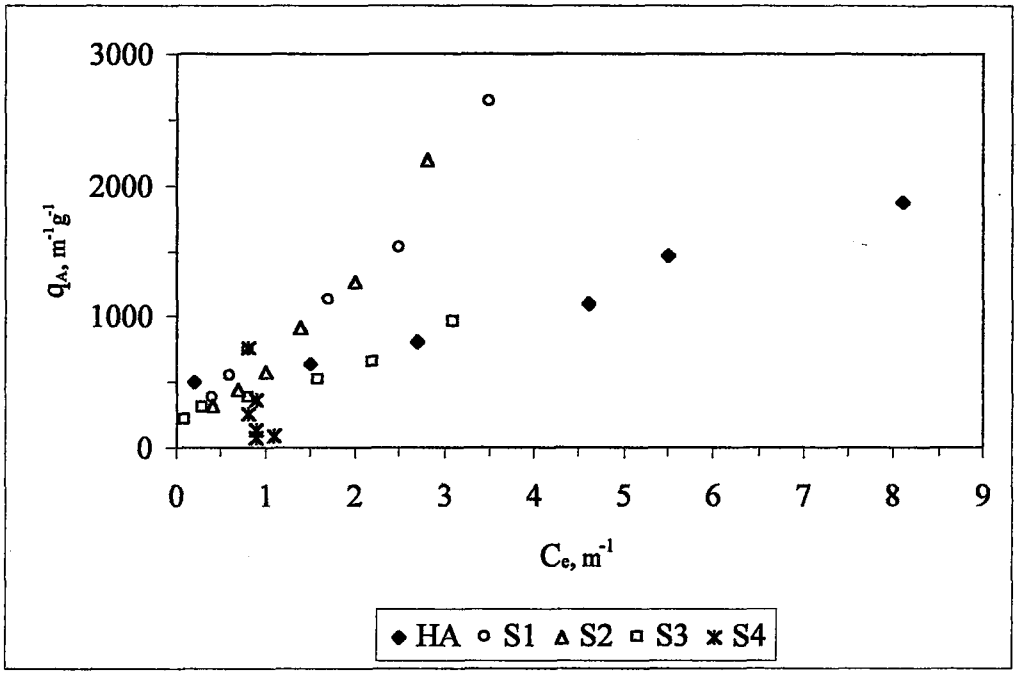

Figure 4.37. Comparison of the adsorption profiles based on $Color_{400}$ for untreated and preozonated humic acid samples.

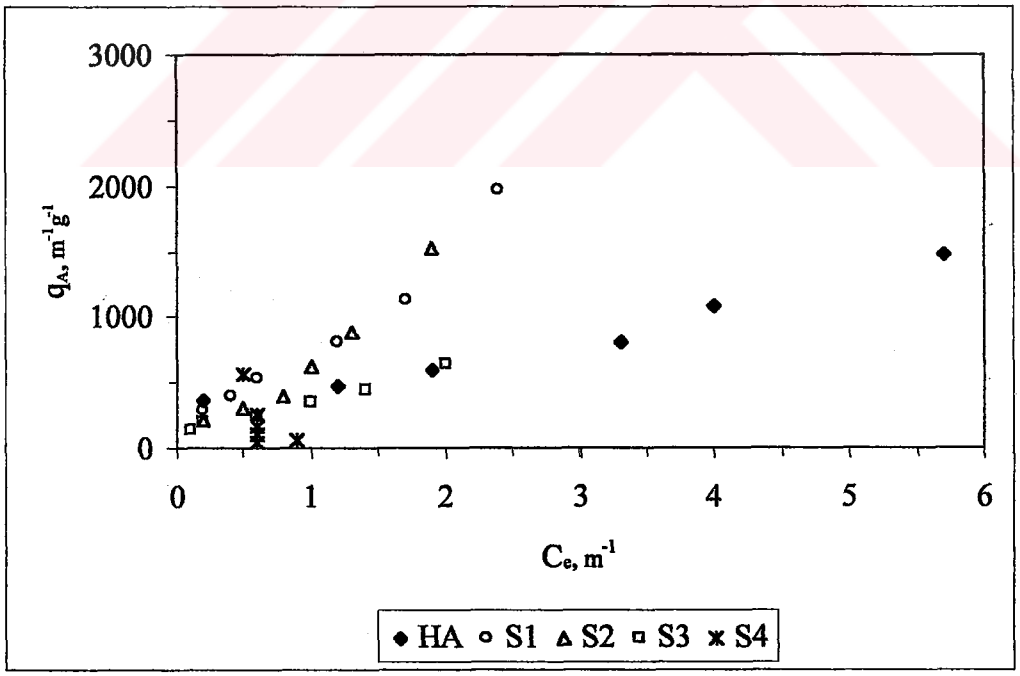

Figure 4.38. Comparison of the adsorption profiles based on $Color_{436}$ for untreated and preozonated humic acid samples.

Table 4.17. Adsorption properties of humic acid onto TiO_2 based on UV_{280}.

	K_F	1/n	q_A, $m^{-1}g^{-1}$
Humic acid	1096	0.36	2296
Sample 1	485	0.94	2264
Sample 2	252	1.21	1976
Sample 3	515	0.60	1376
Sample 4	-	-	648

Table 4.18. Adsorption properties of humic acid onto TiO_2 based on $Color_{400}$.

	K_F	1/n	q_A, $m^{-1}g^{-1}$
Humic acid	722	0.34	808
Sample 1	818	0.81	744
Sample 2	674	1.00	584
Sample 3	488	0.40	376
Sample 4	-	-	144

Table 4.19. Adsorption properties of humic acid onto TiO_2 based on $Color_{436}$.

	K_F	1/n	q_A, $m^{-1}g^{-1}$
Humic acid	568	0.39	600
Sample 1	824	0.74	536
Sample 2	663	0.85	392
Sample 3	381	0.46	240
Sample 4	-	-	104

Correlations describing the relation between the Freundlich model parameters and the preozonation dosages could not be defined. The same increasing/decreasing trends in K_F values were observed for all the parameters. 1/n values varied between 0.39 – 1.17 for UV_{254}, between 0.36 – 1.21 for UV_{280}, between 0.34 –1.00 for $Color_{400}$ and between 0.39 – 0.85 for $Color_{436}$. The untreated humic acid solution revealed 1/n values less than "1" for all the parameters indicating the unfavorable adsorption characteristics of humic acid on the TiO_2 surface. Convergence to linearity (1/n = 1) was observed for Sample 1, in which 10%

UV_{254} and 20% $Color_{436}$ degradations were initially completed by preozonation, for UV_{254}, UV_{280} and $Color_{400}$ parameters. For Sample 2, in which 19% UV_{254} and 42% $Color_{436}$ degradations were initially completed by preozonation, 1/n values were greater than "1" for UV_{254} and UV_{280}, equal to "1" for $Color_{400}$. The other samples had 1/n values less than "1" for all of the parameters studied.

For all of the parameters decreased q_A values with increasing preozonation dosages were calculated. Adsorption density (τ, $m^{-1}m^{-2}$) which is defined as the amount of adsorbate per unit are of adsorbant, may also be used for comparing the adsorptive characteristics of untreated and preozonated humic acid samples. Table 4.20 presents the calculated τ values for TiO_2 loadings of 0.50 $mgmL^{-1}$ based on UV_{254}, UV_{280}, $Color_{400}$ and $Color_{436}$ parameters. Consistent decreases in the adsorption densities were observed for all the parameters with increasing preozonation dosages except a slight increase in UV_{254} parameter in Sample 1. The decreases in the adsorption densities between the untreated humic acid and Sample 4 were determined as 67, 72, 82 and 83 per cent for UV_{254}, UV_{280}, $Color_{436}$ and $Color_{400}$ parameters respectively.

Table 4.20. Adsorption densities calculated for TiO_2 loading of 0.50 $mgmL^{-1}$.

	τ_{254} , m^{-1} m^{-2}	τ_{280} , m^{-1} m^{-2}	τ_{436} , m^{-1} m^{-2}	τ_{400} , m^{-1} m^{-2}
Humic acid	47.9	41.7	14.7	10.9
Sample 1	48.4	41.2	13.5	9.75
Sample 2	43.1	35.9	10.6	7.13
Sample 3	30.8	25.0	6.84	4.36
Sample 4	16.0	11.8	2.62	1.89

Untreated humic acid molecule contained more functional groups as deprotonated carboxylic groups leading to a strong attraction with the positively sites of TiO_2 through carboxylate linkages as well as hydrogen bonding (Wiszniowski *et al.*, 2002). The effect of ozonation on humic acid structure is mainly expressed by the decrease in size and loss of aromaticity as well as increased hydrophilicity thereby increased charge attraction. Humic acid/TiO_2 binary system is mainly governed by the binding capability of humic acid onto TiO_2 primarily due to the presence of oxygenated functional groups.

Most of the formed new groups on ozonation are strongly acidic and hydrophilic and would undergo charge attraction when brought into close proximity with the positively charged sites of TiO_2 and repulsion due to the negatively charged centers. Therefore, pH dependent deprotonation of the functional groups of humic acid and the characteristics of the titanium dioxide surface should govern the adsorption characteristics of humic acid samples. Since humic acid is considered as negatively charged at pH_{zpc}=6.3 due to the deprotonation of the carboxylic groups, the electrostatic interaction between charged humic acid segments and TiO_2 should be attractive at pH<6.3 and impulsive at pH >6.3.

$$TiOH + H^+ \rightarrow TiOH_2^+ \qquad K_{a1}$$
$$TiOH + OH^- \rightarrow TiO^- + H_2O \qquad K_{a2}$$

$$pH_{ZPC} = (pK_{a1} + pK_{a2})/2 \tag{4.16}$$

Besides Coulomb forces of attraction, favorable energetic compensation must exist; nonelectrostatic specific interactions between humic acid functional groups and TiO_2 surface should be involved for adsorption to occur. Contribution of the hydrophobic properties of humic acids may also be considered.

There are similar studies in the literature assessing the effects of ozone treatment on the adsorption characteristics of organic molecules on activated carbon. Preozonation process is known to produce lower molecular weight and more soluble DOMs relative to those in raw water. It is also shown that size of organic macromolecules is directly proportional to their molecular weight. Despite the decrease in DOM size, adsorbability of ozonated DOMs decrease because of increasing hydrophilicity. Since pH_{PZC} for activated carbon was reported to be 8.5 – 9.5, the GAC surface is expected to have a net positive charge for the studies conducted with humic acid, which has pH range 6.0 – 6.5. The chemical structure of DOMs, including the presence of functional groups that can enhance electrostatic and/or solubility effects, is known as an important parameter determining the sorption behavior of organic macromolecules by microporous adsorbents. Increases in the carboxylic, phenolic and total macromolecular acidities per DOM molecular size were shown to increase adsorption on the GAC surface. However, as the acidity increases

beyond a certain level, the enhanced DOM solubility begins to effectively compete against the electrostatic adsorption forces (Karanfil *et al.*, 1996; Kilduff *et al.*1996). The decreases in the adsorption of preozonated humic acids on the TiO_2 surface may be explained with similar mechanisms due to increases in the carboxylic and phenolic acidities with increasing preozonation dosages. Lessened attraction due to the removal of carboxylate linkages thereby may be effective in increasing the surface access of the organic molecules to enhance the reaction probability with the oxidizing species.

4.3.5. Overall Removal Obtained for The Sequential Oxidation System

Pseudo first order degradation rate constants were calculated for the overall oxidation (k_{ov}) for consecutive applications of ozonation and photocatalysis based on UV_{254}(Table 4.21). The overall oxidation time included the pretreatment of the humic acid solution with ozonation and 60 minutes of TiO_2 catalyzed irradiation period with a photocatalyst loading of 0.50 $mgmL^{-1}$.

Table 4.21. Pseudo first order kinetic model parameters for overall degradation of UV_{254}.

	Sample 1	Sample 2	Sample 3	Sample 4
$k_{ov}x10^{-2}$, min^{-1}	3.52	4.04	4.60	4.96
$t_{1/2}$, min	20	17	15	14

The apparent rate for UV_{254} degradation by ozonation (1.99 $m^{-1}min^{-1}$) was about two times faster than the rates obtained for photocatalytic oxidation (Tables 4.8 – 4.11). The overall degradation rate constants were found to be comparable with the ozonation rate constants, but they were higher than the photocatalytic oxidation rate constants. The overall oxidation exhibited half-life values less than 20 minutes. A 30 per cent decrease was observed in half-lives of Sample 1 and Sample 2 due to increased applied ozone dosages. Although rate constants for the overall oxidation were closer to those of ozone oxidation, the final oxidation levels were significantly low, exhibiting the high oxidation efficiencies of photocatalytic oxidation on the refractory organics that cannot be removed by only ozonation. The rate constant k_r calculated according to L-H model was less than both k_{PCO} and k_{ov}, explaining the significant effect of adsorption (Kerc *et al.*, 2002).

4.3.6. Molecular Size Distribution in Humic Acid Samples

Because of their importance in the aquatic systems, elucidation of the chemical structure of humic substances as well as humic acids is an important problem. The reported molecular weights for aquatic humic substances and humic acids range from 500 to more than 100 000. One of the most commonly used methods to is the ultrafiltration technique (Thurmann *et al.*, 1982). On the basis of the published studies ultrafiltration through cellulose base membranes with pore sizes ranging between 500 and 450,000 Daltons (D) as described in Section 3.3.4 was applied for assessing the changes in the molecular sizes of humic acid samples upon ozonation and photocatalysis. Humic acid sample with a concentration of 20 mgL^{-1} and the ozonated humic acid samples, which were described in section 4.3.1 were subjected to ultrafiltration through membranes in a series mode and samples from filtrates were collected after each batch of filtration as shown in Figure 4.39.

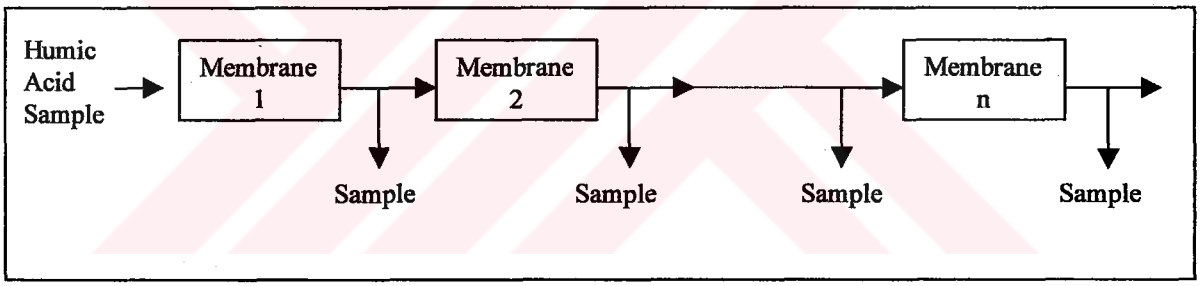

Figure 4.39. Ultrafiltration of humic acid samples in a series operation.

The use of UV-vis spectrophotometric techniques to monitor the changes in the permeate quality is proved to be of great value in measuring the concentration of humic acids (Maartens *et al.*, 1999 and Bian *et al.*, 1999). In order to evaluate the spectroscopic characteristics of untreated and pretreated humic acid samples according to different molecular size fractions, the absorbance spectrums of filtrates were compared with each other. The spectrums were plotted in a wavelength region between 200 and 630 nm to cover both ultra violet and visible regions. Two examples for the spectrums, one obtained for the untreated humic acid and the other for the preozonated humic acid sample (Sample 4) are presented in Figures 4.40 and 4.41. It should be noted that the applied ozone dosage (1 mg O_3/mg C) for Sample 4 was highest among the other samples, therefore these two examples represent two extreme conditions assessed in this study. The spectrums obtained

for the other preozonated humic acid samples (Samples 1,2 and 3) are presented in Appendix G.

In each spectrum unfiltered sample and filtrates exhibited decreasing trends in absorbance with respect to decreasing filter pore size. The spectrum with the highest absorbance represents the unfiltered sample whereas the proceeding plots represent the filtered samples through membranes in order of decreasing pore size in the below figures.

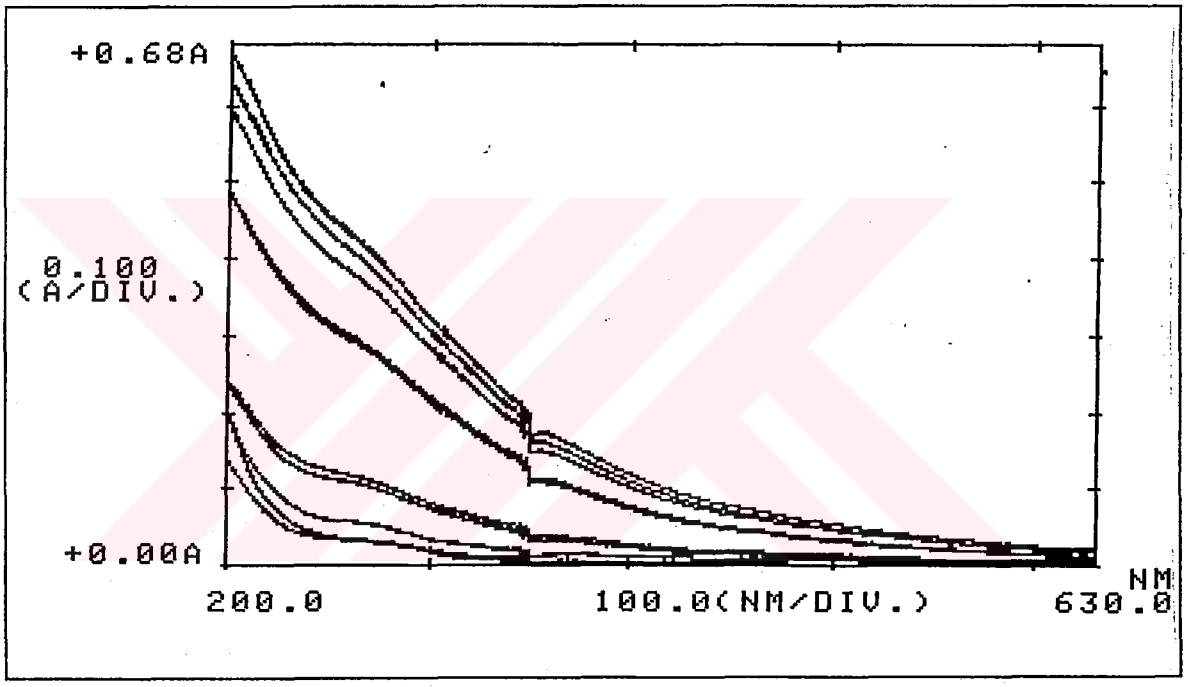

Figure 4.40. Spectrums obtained for the ultrafiltration of untreated humic acid sample through membrane filters (From top to bottom: Unfiltered humic acid sample, filtrates from membrane filters 450,000 – 500 Daltons)

The comparison of the spectrums for different humic acid samples have shown that in the untreated humic acid sample, the differences between unfiltered humic acid sample and filtrates from 450000 and 220000 could be clearly followed since the spectrums were apart from each other. As the preozonation dosage increases in Samples 1 through 4, the spectrums for the above mentioned molecular sizes merge each other indicating the smaller fraction of larger size molecules in the ozonated humic acid samples. The same comments can also be made for the fraction smaller than 100,000 Dalton. As the preozonation dosage

increases the spectrum for the filtrate from 100,000 Dalton membrane approaches to the spectrums of higher molecular size membranes. The spectrums for the untreated humic acid exhibited the greatest gap between the filtrates obtained from 100,000 and 30,000 Dalton membranes. This gap lessened as the preozonation dosage increased due to cleavage of higher molecular size organics into smaller ones. In Sample 1, 2 and 3 gaps were also observed between the spectrums of 30,000 and 10,000 Dalton membranes in addition to gap between 100,000 and 30,000. In Sample 4, which has the highest preozonation dosage, the gap shifted to 3000 and 1,000 Daltons region pointing out the accumulation of molecules in lower molecular sizes.

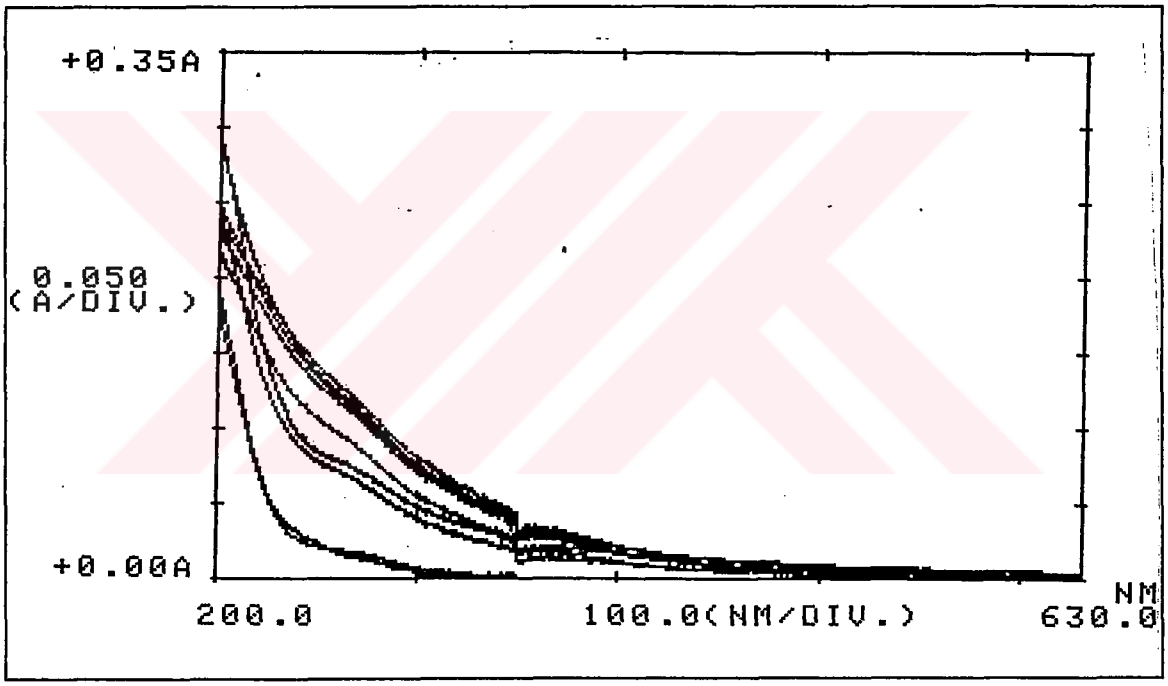

Figure 4.41. Spectrums obtained for the ultrafiltration of preozonated humic acid sample (Sample 4) through membrane filters (From top to bottom: Unfiltered humic acid sample, filtrates from membrane filters 450,000 – 500 Daltons)

The comparisons of different humic acid samples were also made based on the discrete absorbance measurements conducted on the collected samples from the filtrates of each membrane with different pore sizes. Since the UV absorbance at 254nm is considered to indicate the presence of aromatic carbon bonding and oxygenated functional groups, the use of UV_{254} measurements are reported extensively to explain molecular size distributions of humic substances (Gjessing *et al.*,1998, Cho *et al.*,1999 and Siddique *et al.*, 2000).

Strong correlations between the molar absorptivity, total aromaticity and the average molecular weights at 280 nm have been observed in previously published studies (Peuravuori and Pihlaja, 1997, Chin *et al.*, 1994). The absorbance of visible light near 400 nm is related to the intensity of the yellow color caused by extended chromophoric systems in conjugated structures. On the other hand, absorbance measurements at 465 nm and 656 nm are also used to explain the organic matter concentrations in relation to size effects (Maartens *et al.*, 1999).

The absorbance data were used for calculating the percent distribution of each molecular size region for UV_{254}, UV_{280}, $Color_{436}$ and $Color_{400}$ parameters. The measured absorbance values and the percent distributions are presented in the following figures for the untreated and preozonated humic acid samples (S1-S4) based on the absorbance parameters.

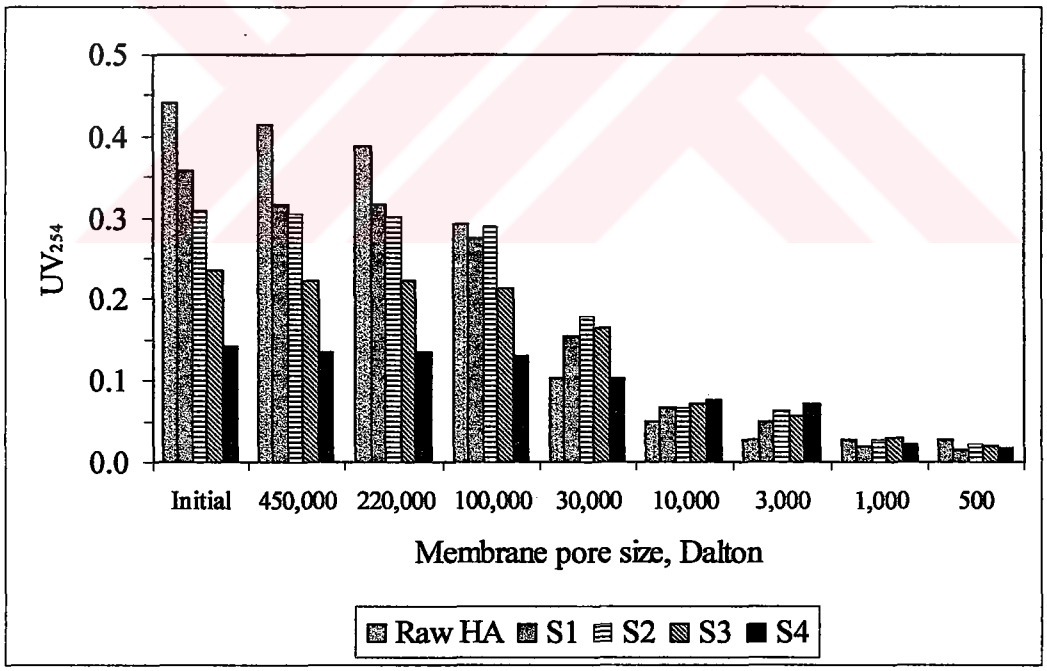

Figure 4.42. UV_{254} (cm^{-1}) change in untreated and preozonated humic acid samples upon ultrafiltration through membranes with different pore sizes.

The molecular size region in which the highest percentage of UV_{254} located is shifted towards the smaller molecular size regions in relation with the applied preozonation as presented in Figure 4.43 with the percentage peaks. For the untreated raw humic acid

solution about 43% of the molecules are in the 30,000 – 100,000 Dalton region. As the applied ozone dosage increases this region moves to right; for Sample 3 it is between 10,000 – 30,000 and for Sample 4 it is between 1,000-3,000 Dalton region with a percentage of 34.

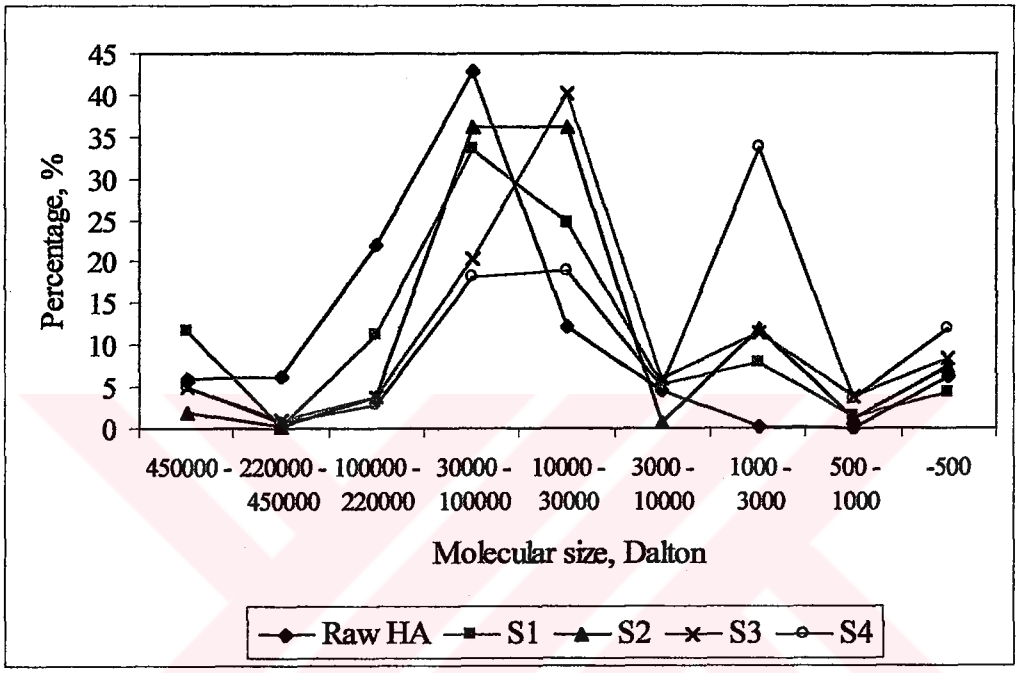

Figure 4.43. Percent distribution of UV_{254} in untreated and preozonated humic acid samples according to different molecular sizes

The molecular size regions for UV_{280} parameter showed similar patterns with UV_{254}. The highest percentages were between 30,000 and 100,000 Daltons for the untreated raw humic acid and between 1,000 and 3,000 Daltons for Sample 4.

Similar observations are also valid for the other parameters measured. UV_{280}, $Color_{400}$ and $Color_{436}$ absorbance measurements as well as their percent distributions according to different molecular sizes are presented in the following figures (Figures 4.44 – 4.49). The molecular size regions determined in the humic acid samples were almost the same based on different parameters measured. Sample 1 and Sample 2, which were the humic acid samples ozonated with the lowest ozone dosages exhibited similar molecular size regions. The significant differences were observed between molecular size regions of the untreated humic acid sample and Sample 4.

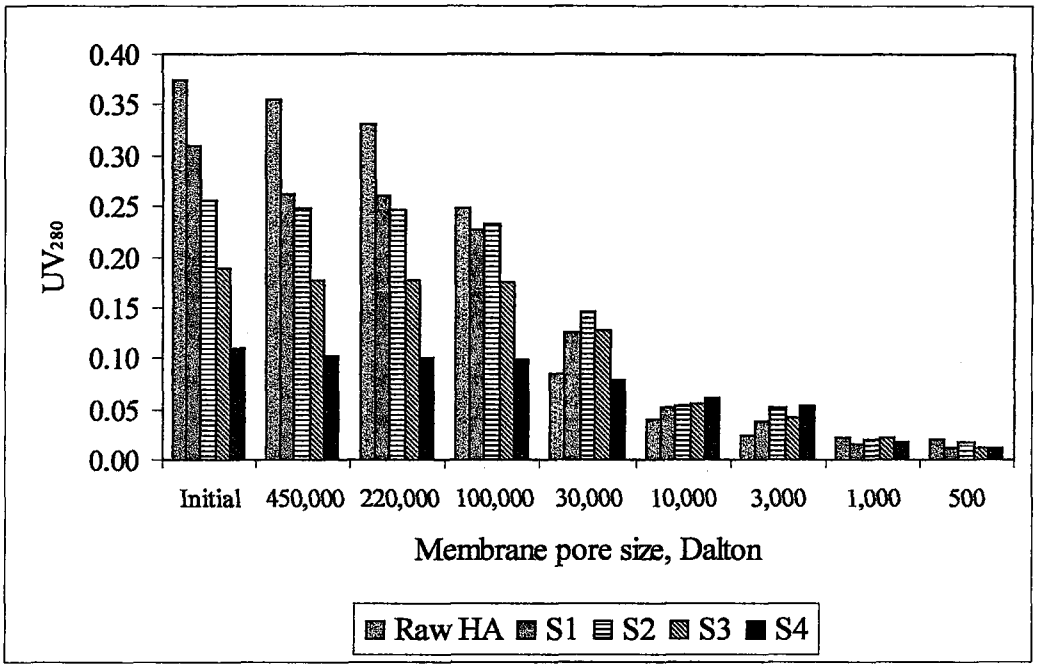

Figure 4.44. UV_{280} (cm^{-1}) change in untreated and preozonated humic acid samples upon ultrafiltration through membranes with different pore sizes.

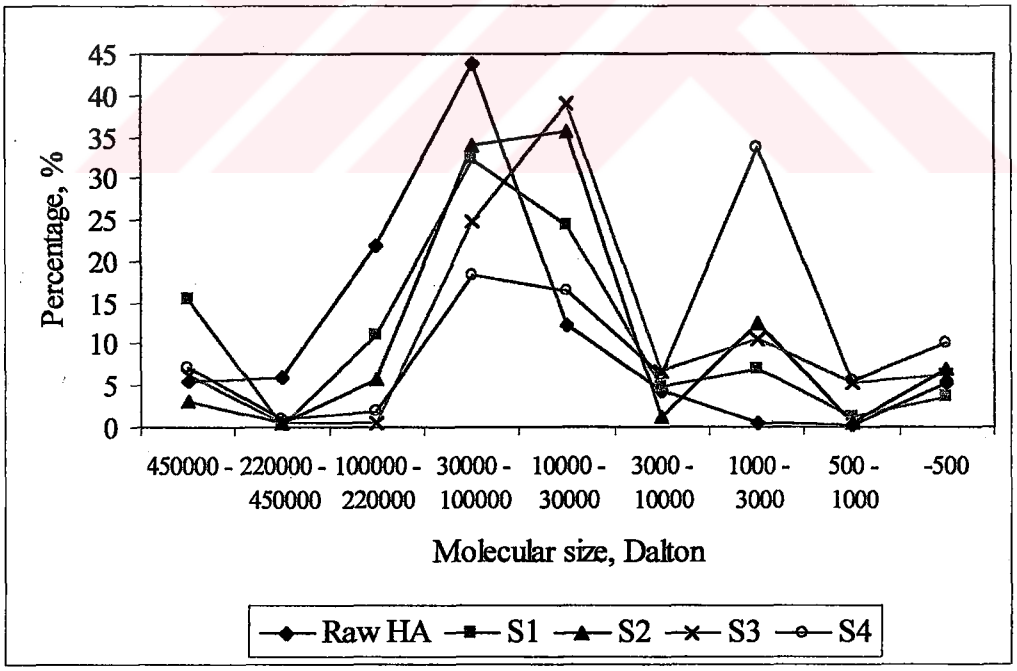

Figure 4.45. Percent distribution of UV_{280} in untreated and preozonated humic acid samples according to different molecular sizes.

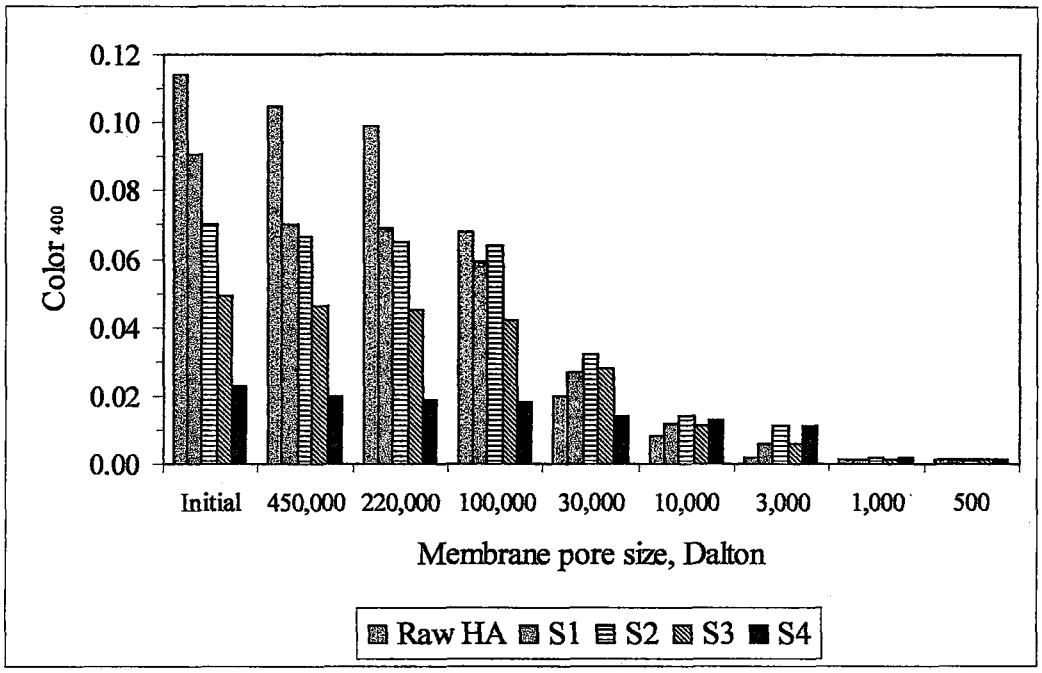

Figure 4.46. $Color_{400}$ (cm^{-1}) change in untreated and preozonated humic acid samples upon ultrafiltration through membranes with different pore sizes.

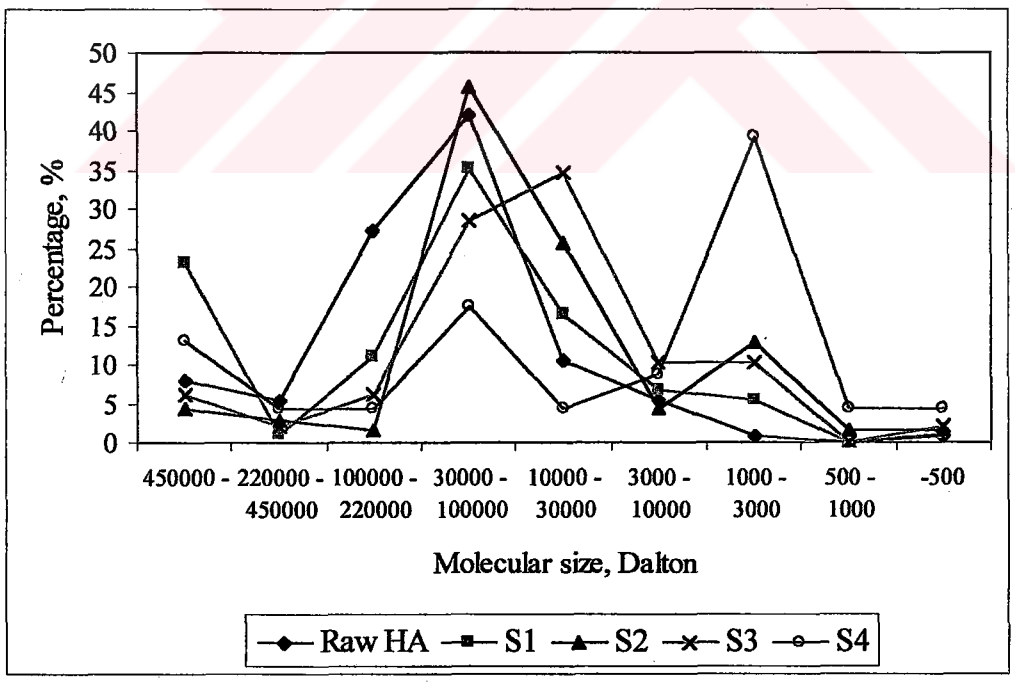

Figure 4.47. Percent distribution of $Color_{400}$ in untreated and preozonated humic acid samples according to different molecular sizes.

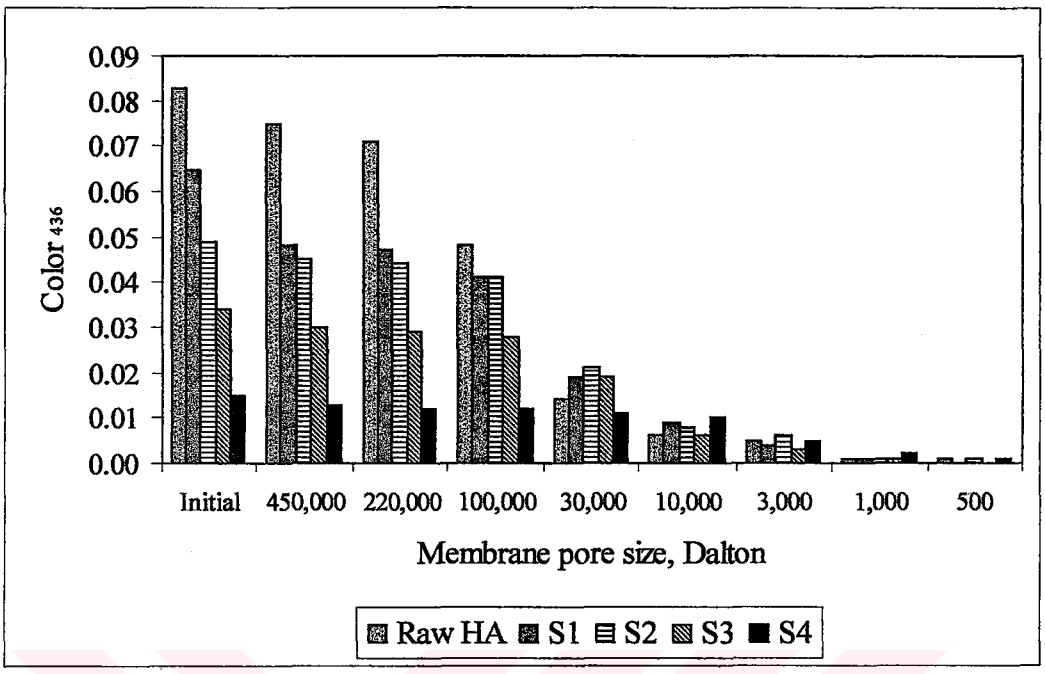

Figure 4.48. $Color_{436}$ (cm^{-1}) change in untreated and preozonated humic acid samples upon ultrafiltration through membranes with different pore sizes.

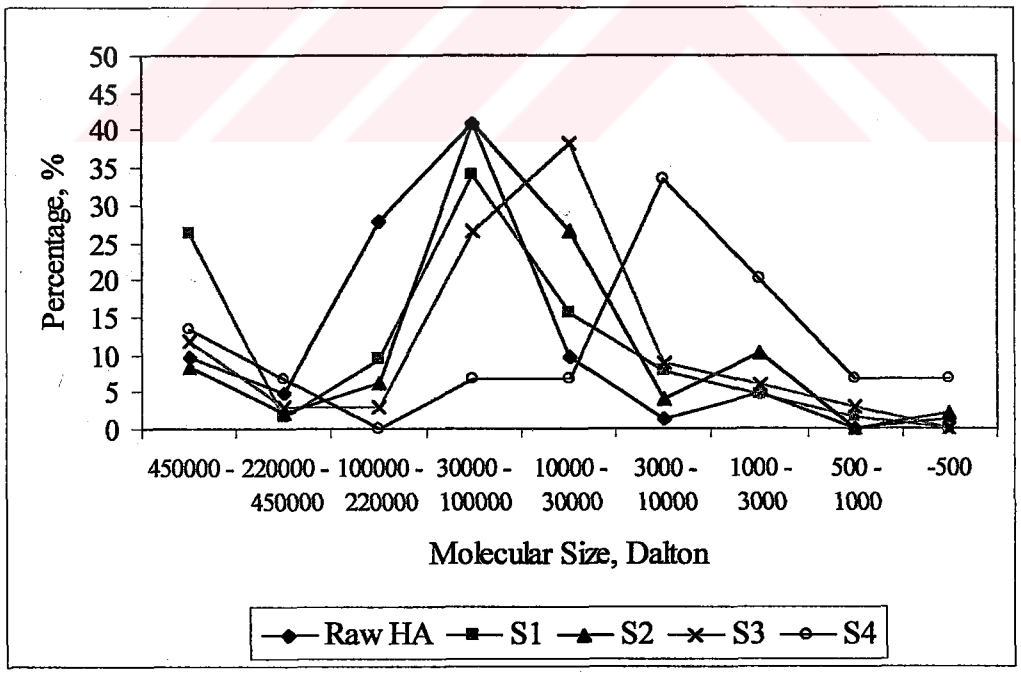

Figure 4.49. Percent distribution of $Color_{436}$ in untreated and preozonated humic acid samples according to different molecular sizes

Both $Color_{400}$ and $Color_{436}$ data have shown that the filtrates from 1,000 and 500 Dalton membranes did not contain any color. Therefore it may be concluded that the chromophoric groups in the natural organic matter are greater than 1,000 Dalton. For the color parameters, the molecular size region where the highest percentage observed was between 30,000 and 100,000 in the untreated humic acid sample, Sample 1 and Sample 2. This highest percentage region moved to between 10,000 and 30,000 region in Sample 3. All these samples showed similar trends both for $Color_{400}$ and $Color_{436}$ parameters, but for Sample 4, the highest percentage region was between 1,000-3,000 Dalton region for $Color_{400}$ and between 3,000-10,000 Dalton region for $Color_{436}$.

The highest percentage regions for UV_{254} and UV_{280} parameters also matched with those of $Color_{400}$ and $Color_{436}$ parameters.

In order to describe the molecular size regions where each sample was distributed, the percentages passing from each filter was calculated with reference to the initial unfiltered values. The graphs constructed with the calculated values also indicate the percentages of the molecules less than each filter pore size. The following graphs were used to determine the molecular size regions based on UV_{254}, UV_{280}, $Color_{400}$ and $Color_{436}$ parameters.

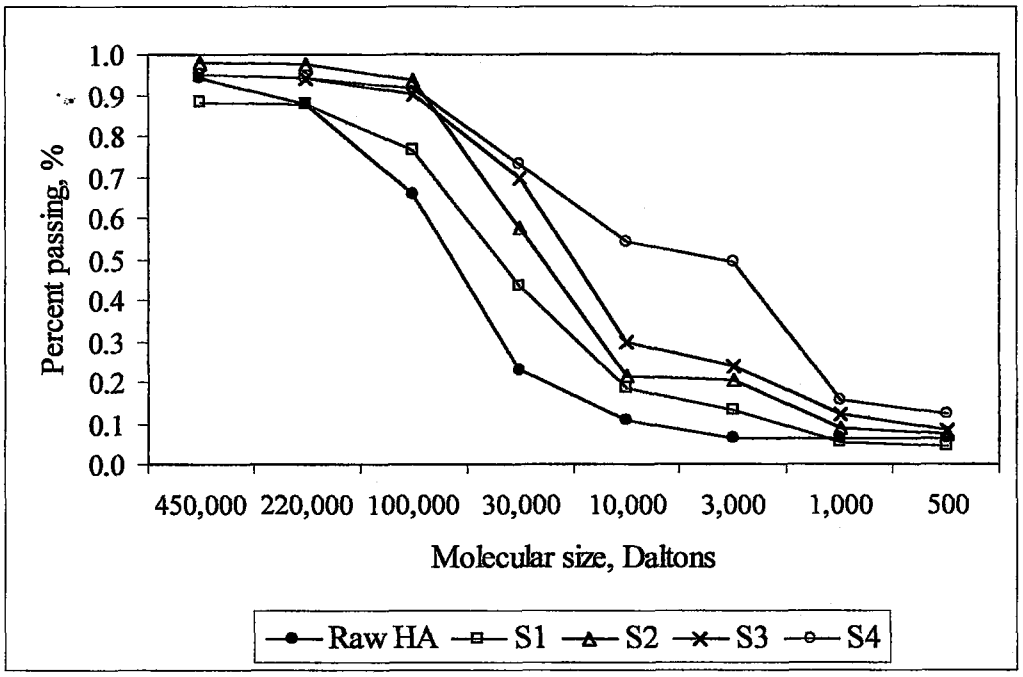

Figure 4.50. Percent passing from each filter pore size based on UV_{254} measurements.

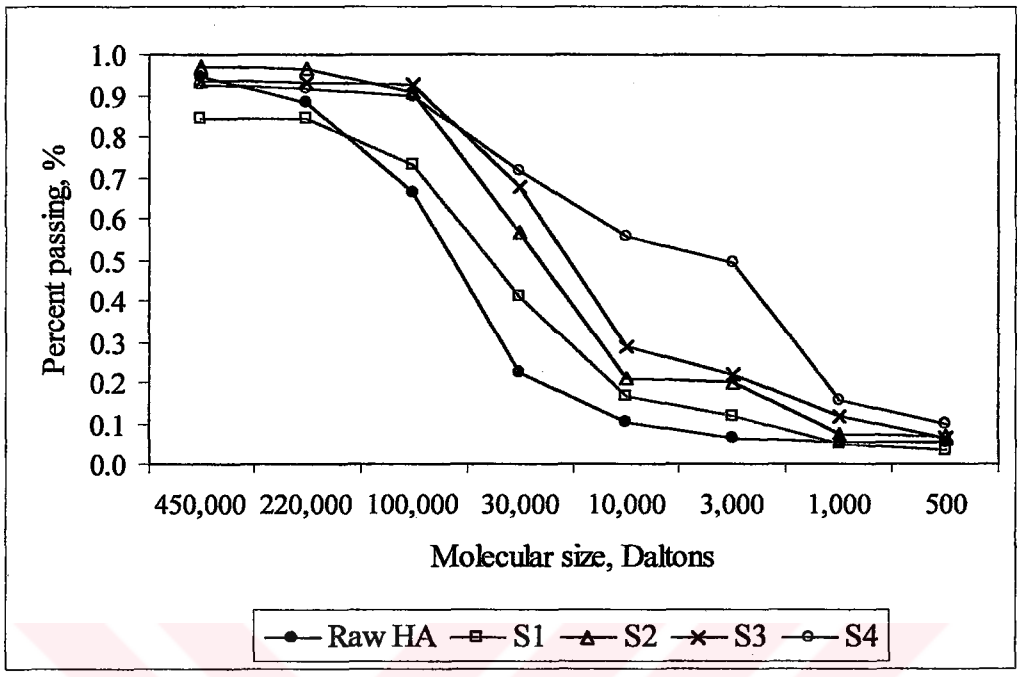

Figure 4.51. Percent passing from each filter pore size based on UV_{280} measurements.

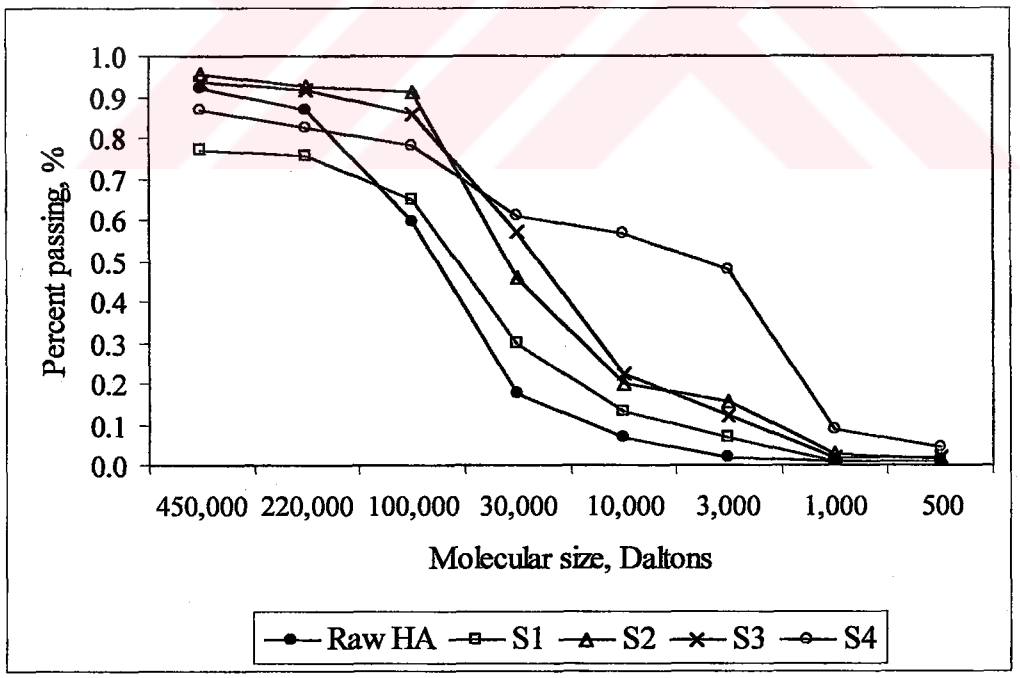

Figure 4.52. Percent passing from each filter pore size based on $Color_{400}$ measurements.

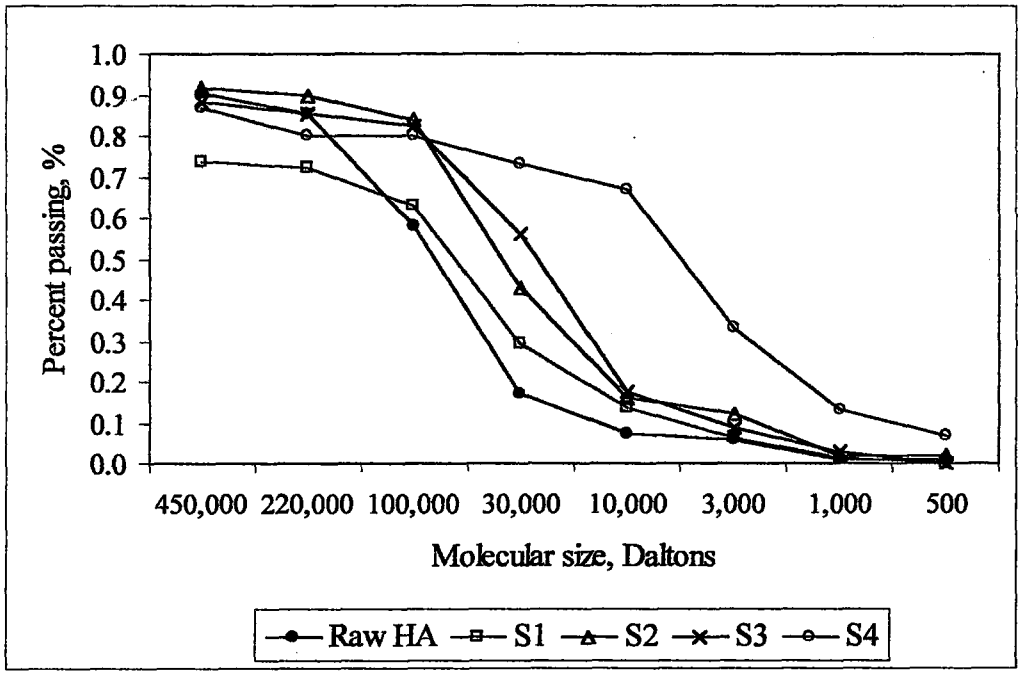

Figure 4.53. Percent passing from each filter pore size based on $Color_{436}$ measurements.

The molecular size ranges for the untreated and four ozonated humic acid samples as determined according to above presented percentage graphs are compiled in the following Table 4.22 based on UV_{254}, UV_{280}, $Color_{400}$ and $Color_{436}$ parameters.

Table 4.22. Molecular size ranges of humic acid samples.

Molecular size range, kD	Untreated humic acid	Sample 1	Sample 2	Sample 3	Sample 4
Based on UV_{254}	3 - 450	1 - 220	1 - 100	0.5 - 100	0.5 - 100
Based on UV_{280}	3 - 450	1 - 220	1 - 100	0.5 - 100	0.5 - 100
Based on $Color_{400}$	3 - 450	1 - 220	1 - 100	1 - 100	0.5 - 100
Based on $Color_{436}$	1 - 450	1 - 220	1 - 220	1 - 100	0.5 - 100

The molecular size ranges determined according to UV_{254} and UV_{280} were exactly equal to each other. According to Color data these regions showed only slight differences. Molecules greater than 220,000 D were only detected in the untreated humic acid sample based on all of the parameters and all the molecules were greater than 3000 D in this sample. Only $Color_{436}$ measurement showed molecules less than 3000 D in the untreated

humic acid sample. Increased ozone dosage resulted in shifts towards lower molecular size regions. Sample 4, which was ozonated with the highest dosage contained molecules even less than 500 D and the highest molecular size for this sample was 100,000 D.

Ozone affects humic acids basically in two ways; (i) oxidative cleavage of larger molecules to give smaller molecules, and (ii) an increase in polarity for molecules constituting partial oxidation by-products (Langlais *et al.*, 1991). The effects of various oxidants such as ozone, chlorine, hydrogen peroxide and permanganate on the molecular size distribution of aquatic humus are also reported by Myllykangas and coworkers (2002). The results revealed differing trends depending on the oxidant. The quality of the organic matter was changed significantly during the oxidation processes. Since the UV-absorption measures the intensity of the chromophores such as double bonds of the solutes the observed reductions may be due to the decomposition of the original humic acid molecule to lower molecular size fractions.

Ozonation of the humic acid samples resulted in the greatest reductions in the largest molecular size fractions. It was also reported that the greater the ozone dosage the greater the effect in this respect (Myllykangas *et al.*, 2002). These results are in good accordance with the previously published results of Amy *et al.*, 1992 and Owen *et al.*, 1995. The presented data also follow the same trend with respect to the ozonation dosage and oxidation efficiency. The pre-ozonation process effectively reduced large molecular weight organics (>10 kD) and converted them to smaller ones resulting in increases in the MW fraction <5kD. (Chiang *et al.*,2002). It was also reported that commercial humic acid (Aldrich) contained higher concentrations of DOC in the MW fraction > 30 kD (46%).

In order to determine the effects of photocatalytic oxidation in the molecular size distribution in untreated and preozonated humic acid samples, ultrafiltration through various filter sizes was applied on the photocatalytically treated samples. Recent literature covers publications about the effects of ozonation on molecular size distributions of humic substances (Myllykangas *et al.*, 2002). On the other hand, no respective data exist on the oxidative degradation achieved by direct hydroxyl radical attack on humic acids, which is the oxidation route in photocatalysis. Therefore, comparisons are only carried out within the

scope of the presented experimental work. Since the hydroxyl radicals react much faster to a greater extent and nonselectively with the organic matter in the water than molecular ozone, which is known to be selective, relatively higher reductions in higher molecular size fractions are expected. Oxidation potentials of molecular ozone and hydroxyl radicals are 2.07 and 2.80 V respectively pointing out the high oxidation efficiency of photocatalysis.

In order to make a comparison on the same bases, humic acid samples subjected to 50 minutes of irradiation period were used in molecular size distribution analysis. For the photocatalytically oxidized humic acid samples the UV-vis absorbance spectrums are plotted within a wavelength region of 200-620 nm using the samples collected after ultrafiltration through membranes. Two example spectrums for the photocatalytically treated samples are presented below for the unozonated humic acid sample and Sample 4 (Figures 4.54 and 4.55). The spectrums characterizing the ultrafiltration of other humic acid samples treated in the sequential oxidation system can be found in Appendix G.

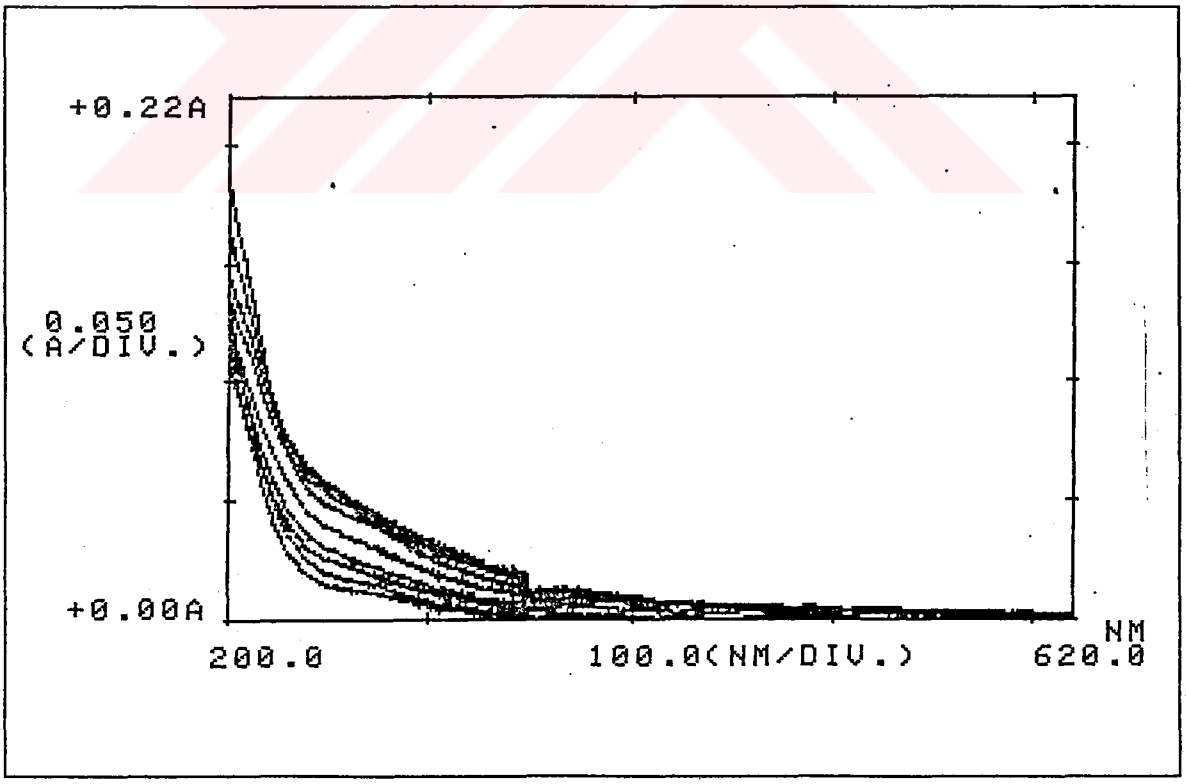

Figure 4.54. Spectrums obtained for the ultrafiltration of photocatalytically oxidized humic acid sample through membrane filters (From top to bottom: Unfiltered sample, filtrates from membrane filters 450,000 – 500 Daltons)

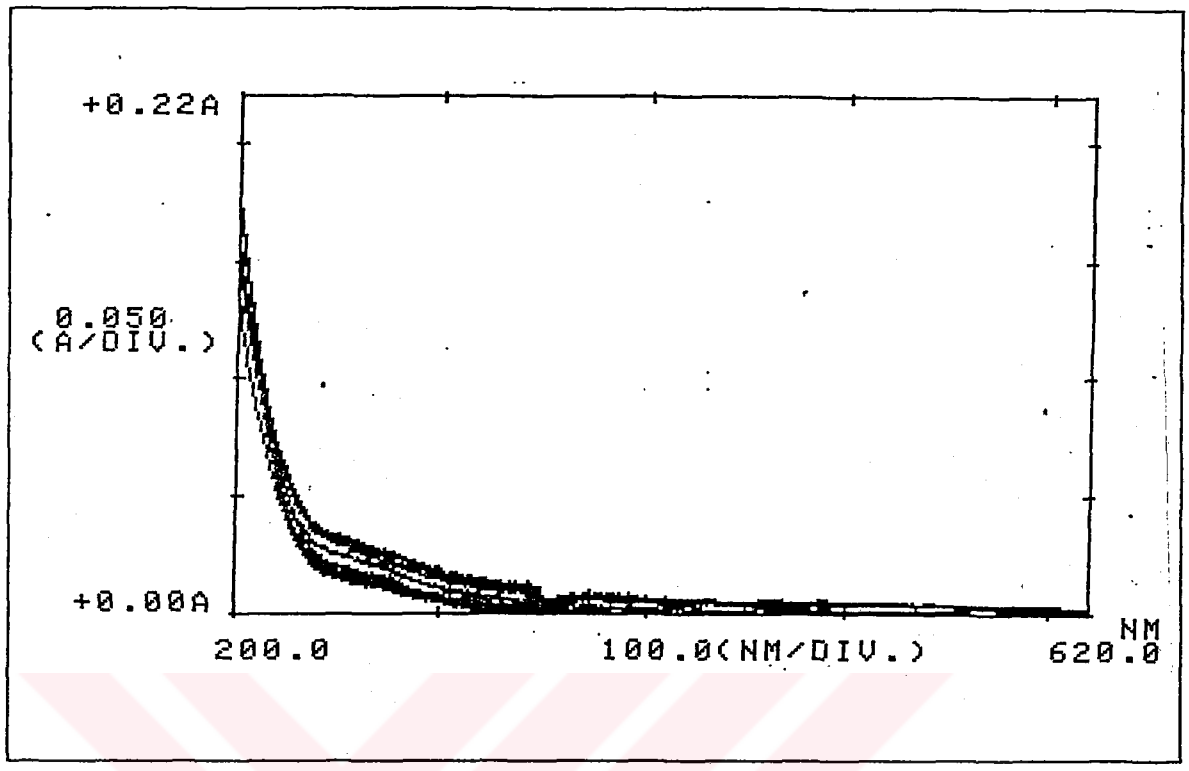

Figure 4.55. Spectrums obtained for the ultrafiltration of preozonated and photocatalytically oxidized humic acid sample through membrane filters (Sample 4) (From top to bottom: Unfiltered sample, filtrates from membrane filters 450,000 – 500 Daltons)

In the spectrum distinct separations in the absorbance trends of filtrates from different pores sizes were not observed. Shifts in the molecular sizes towards the smaller molecular size regions merged the spectrums to each other as can be followed in the plots of the spectrums obtained for the treated humic acid samples in the sequential oxidation system.

The absorbance data were used to demonstrate the molecular size distributions. Comparisons were made based on UV_{254} and UV_{280}. Molecular size distributions according to $Color_{400}$ and $Color_{436}$ could not be evaluated in photocatalytically treated humic acid samples due to very low initial color values. The color forming moieties are totally eliminated (> 98 %) from the solution at the end of 50 minutes of irradiation period during photocatalytic treatment. Molecular size distributions and percent passing values from each filter size are presented in the following figures (Figures 4.56 – 4.59) as obtained from UV_{254} and UV_{280} measurements.

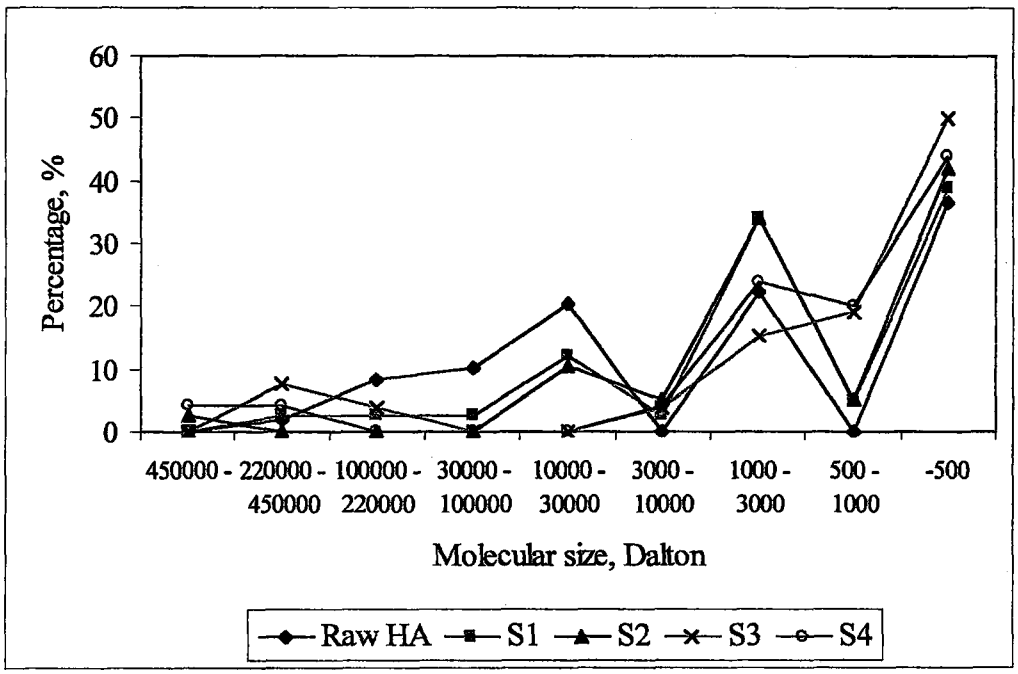

Figure 4.56. Molecular size distribution according to UV_{254} in photocatalytically treated humic acid samples.

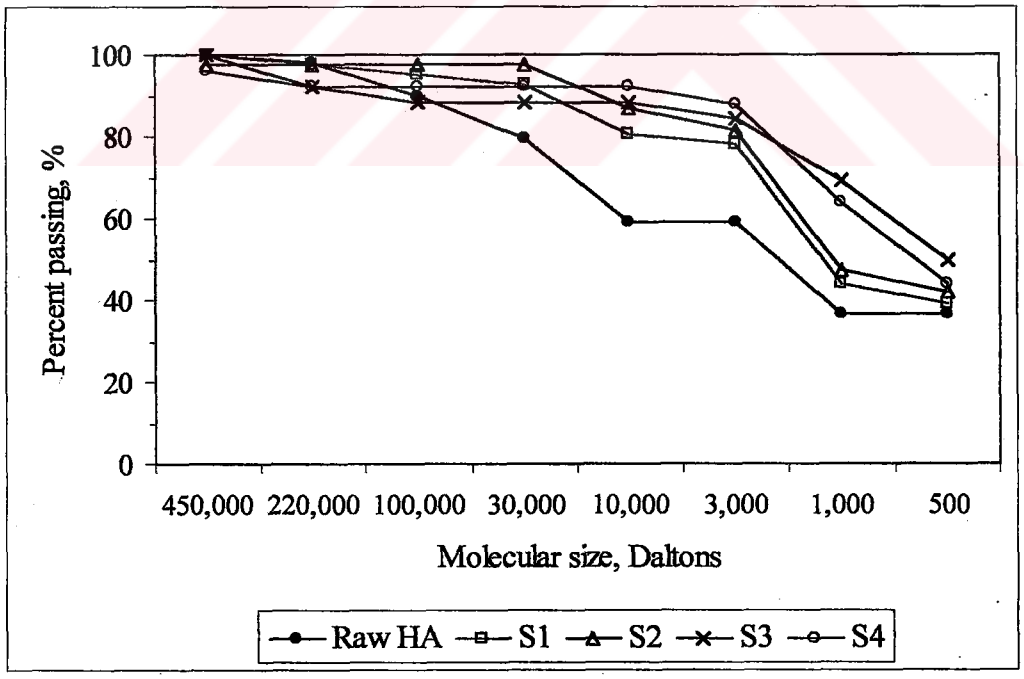

Figure 4.57. Percent passing from each filter pore size based on UV_{254} measurements in photocatalytically treated humic acid samples.

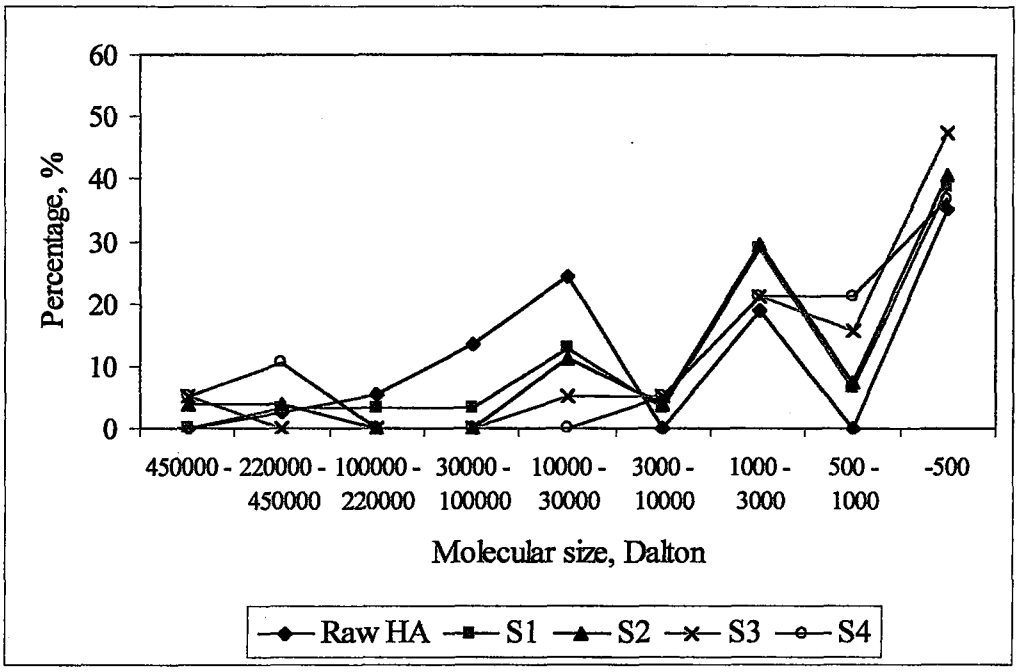

Figure 4.58. Molecular size distribution according to UV_{280} in photocatalytically treated humic acid samples.

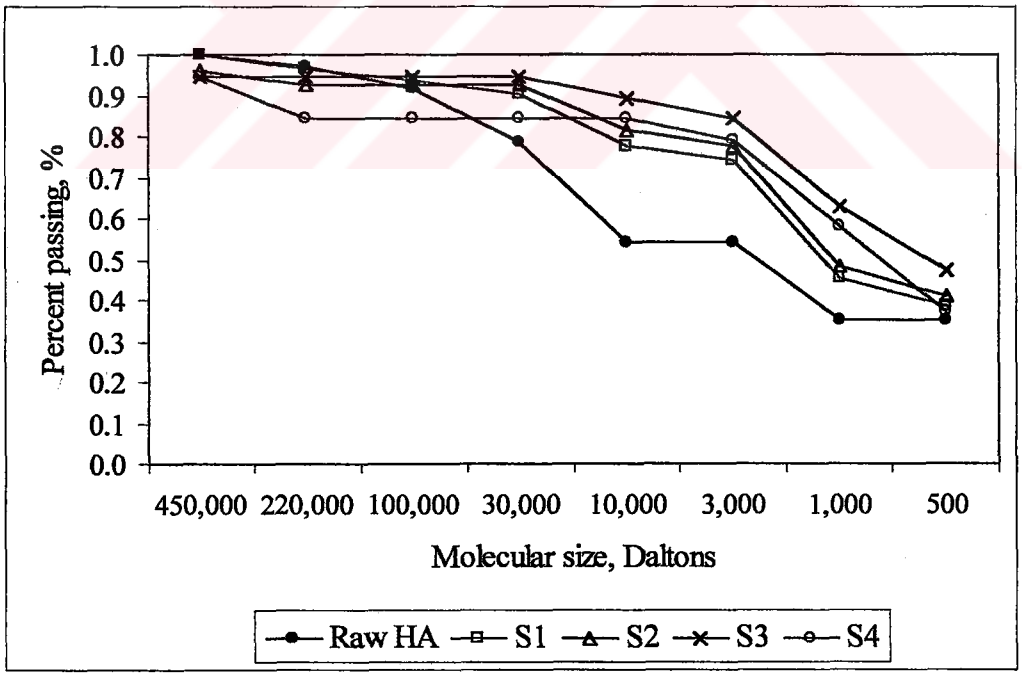

Figure 4.59 Percent passing from each filter pore size based on UV_{280} measurements in photocatalytically treated humic acid samples.

In photocatalytically treated humic acid samples, molecules greater than 30,000 D persisted only in unozonated humic acid sample. Pre-ozonated and photocatalytically treated humic acid samples exhibited molecular sizes accumulated between 10,000 – 30,000 D and 1,000 – 3,000 D. 40-50 percent of the molecules had molecular sizes less than 500 D according to both UV_{254} and UV_{280}.

The wavelength of 280 nm is the region of π-π^* transitions in substituted benzenes and most polyenes but alternatively the wavelength 254 nm should give an equally useful correlation. Therefore, the removal of olefinic/aromatic parts of the humic acid is expressed both by UV_{254} and UV_{280}. The molecular size distribution data also correlate well with these parameters depending on the oxidation route.

Similar relationships are also observed in molecular size distributions related to the $Color_{400}$ and $Color_{436}$ due to ozonation. On the other hand, subsequently photocatalytically treated samples revealed complete removal of these chromophoric groups; therefore molecular size distributions are only expressed in terms of UV_{254} and UV_{280} parameters.

4.3.7. THMFP Reduction in Photocatalytically Treated Samples

Photocatalysis is known to be an effective oxidation technology for THMFP removal in humic acid solutions (Bekbolet and Ozkosemen, 1996). The effects of ozonation on THMFP reduction in humic acid samples were previously discussed in Section 4.2.8. The THMFP analysis conducted on the photocatalytically treated humic acid samples have shown that the THMFP removal efficiency achieved by photocatalysis is irrespective of the ozonation dosage applied for the pretreatment of humic acids prior to photocatalysis. Both the unozonated humic acid sample and preozonated humic acid samples revealed ~50% THMFP removal efficiency for 50 minutes of photocatalytic oxidation in the presence of 0.50 $mgmL^{-1}$ TiO_2. As presented in the following Figure 4.60 the chlorofom formation in 24 hours in the untreated humic acid sample (as indicated "initial" in the graphics) is reduced 20 percent for a prolonged ozonation time. Photocatalytic oxidation of the same humic acid sample resulted in 52 per cent reduction in chloroform formation potential in 50 minutes. The changes in the chlorofom formation potentials for the ozonated and photocatalytically

oxidized samples (S1-S4) are also shown in Figure 4.60.

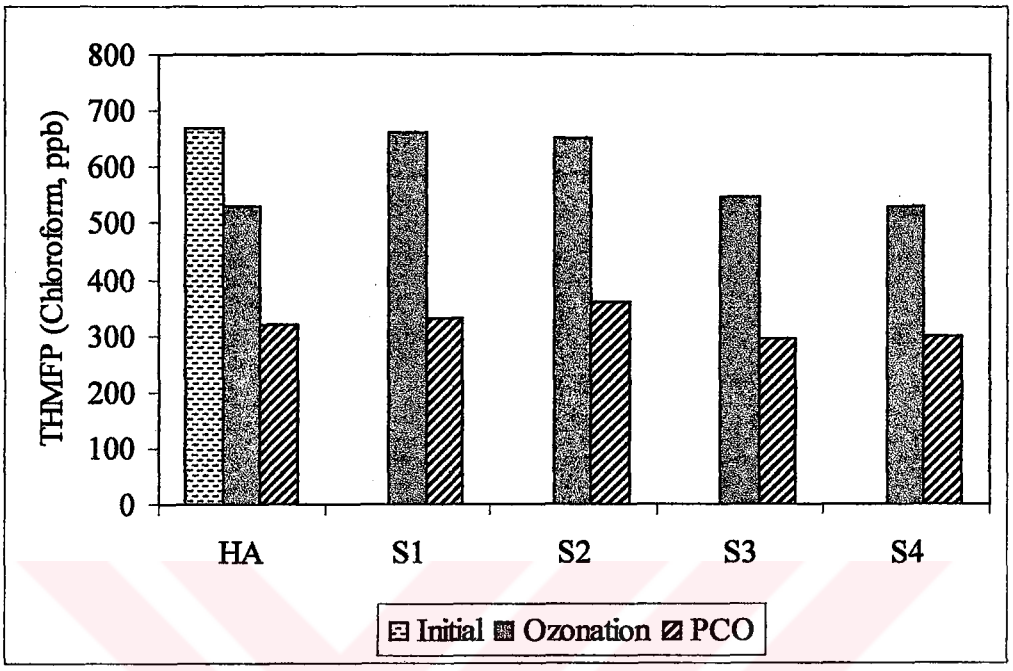

Figure 4.60. Chloroform formation potential in untreated, ozonated and photocatalytically treated humic acid samples.

The decrease in the molecular size ranges of humic acid samples was discussed in the previous section (Section 4.3.6) as the effect of sequential oxidation on the humic acid molecules. Although a consistent trend between the molecular weight and disinfection by-product (DBP) formation could not be attained by previous researchers, DBP yields are reported to increase with increasing molecular weight on a general basis (Kitis *et al.*, 2002). Reduction in THMFP values in oxidized humic acid samples determined in this study may be addressed to the decrease in molecular sizes as well as the elimination of aromaticity as expressed with reductions in UV_{280} and UV_{254} parameters.

The pathways of trihalomethane formation were previously described based on the haloform reactions of ketogroups (Figure 2.2). Since a complete elimination of the THMFP could not be achieved in the existing experimental conditions it may be concluded that the oxidation as monitored by UV_{280} and UV_{254} parameters, follows different oxidation pathways other than the elimination of ketogroups.

5. CONCLUSIONS

In this work, oxidation of humic acids was studied using ozone and photocatalysis. These two oxidation techniques are combined in a sequential systems. The effects of these oxidation systems on humic acid degradation are evaluated. The summary of the results and recommendations for further investigations can be listed as follows:

1. Simultaneous analysis of ozone concentration and humic acid as measured in terms of UV_{254}, UV_{280} and Color parameters has shown that most of the humic acid degradation takes place within the "ozone demand phase" of the ozonation process. The ozone begins to accumulate in the solution after the ozone demand is satisfied. For the design of pre-ozonation contact chambers that only aims to oxidize the natural organic matter (NOM) in drinking waters to minimize THMFP, retention time can be selected equal to the demand phase.

2. Oxidation of humic acid after the demand phase is minor. This can be observed by the UV_{254}, $Color_{400}$ data THMFP (or chloroform formation potential) measurements. THMFP is not significantly reduced for longer retention times than the demand phase duration.

3. At the beginning of the ozonation period, humic acid oxidation does not take place immediately. Within the ozone demand phase a turning point can be found where the oxidation rate significantly increases after the lag period. The ozonation systems should be designed to supply this minimum required amount (minimum retention time, minimum ozone dosage).

4. A mathematical model describing the humic acid oxidation by ozone during the ozone demand phase was proposed. The model successfully predicts the data given in the literature for the removal of organic matter by ozonation. A model that incorporates the mass transfer coefficients for the experimental set-up could be more precise.

5. The maximum oxidation efficiency obtained by ozonation was 80% for an ozone dosage of 3 mgO_3/mgC as determined according to UV_{254} elimination. 20% remaining unoxidized portion was attributed to the accumulation of carboxylic acids upon ozonation. Further treatment with photocatalysis was applied for the remaining organic materials that are recalcitrant for ozonation. In the sequential oxidation system ozonation was considered as a pretreatment stage for the partial oxidation of humic acids prior to photocatalysis.

6. The oxidative degradation of humic acids in a sequential system including ozonation and photocatalysis were found to be efficient in both UV_{254} and $Color_{436}$ removals. Pretreatment by ozonation alters the spectroscopic properties of humic acids as explained by UV_{254}, UV_{280} and $Color_{436}$. On the other hand, the complex nature of the ozonated humic acid medium could not be specifically expressed by only UV-vis properties.

7. The effect of preozonation was observed in the increased photocatalytic degradation rates as explained by pseudo-first order kinetic model. Increasing degree of pre-oxidation by ozonation resulted in increased photocatalytic oxidation rates. 50% increase was achieved in the pseudo first order degradation rate constants for the preozonated samples compared with unozonated humic acid samples for a TiO_2 loading of 0.5 mg mL^{-1}.

8. Pretreatment with ozonation affects the adsorption characteristics of the humic acids on the photocatalyst. The reasons for these changes were attributed to the alterations in the molecular structure of humic acid due to ozonation.

9. Molecular size distribution analysis using ultrafiltration was applied to assess the changes in the structure of humic acids due to oxidation. Molecular size range for the untreated humic acid was found as 1,000 – 450,000 Dalton. This range shifted to 500-100,000 in preozonated samples. After photocatalysis the largest molecular size was 30,000 D and 50% of the molecules were less than 500 D.

10. THMFP analysis conducted on the sequentially oxidized humic acid samples have shown that 50% THMFP reduction is achieved during the photocatalysis stage, irrespective of the ozone dosage applied in the first stage for pretreatment purposes.

APPENDIX A

Calibration Curves for Trihalomethane Analysis

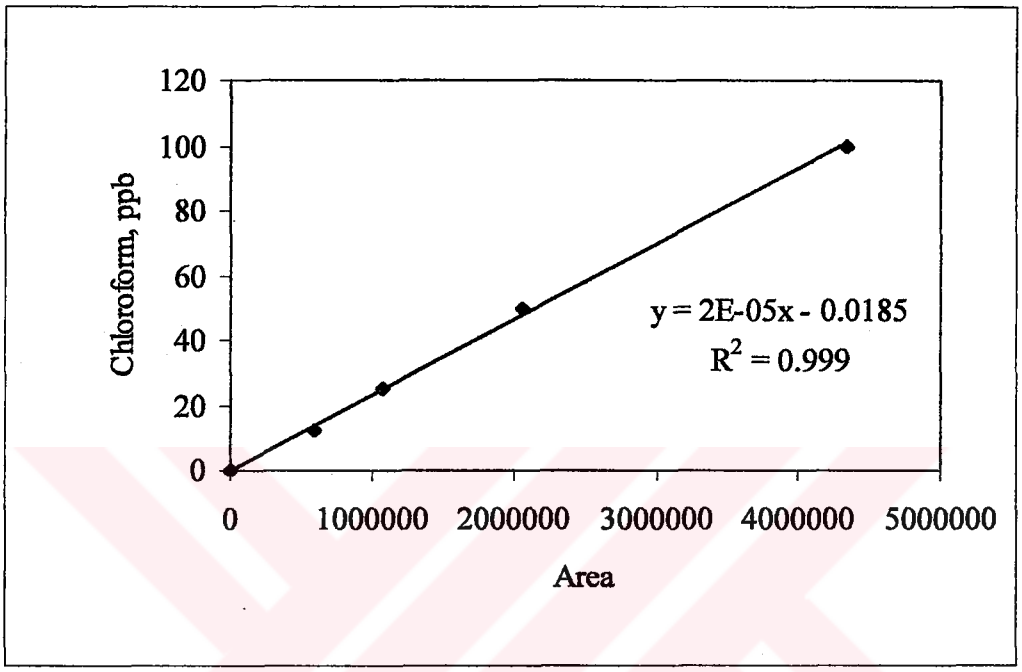

Figure A.1. Calibration curve for chloroform

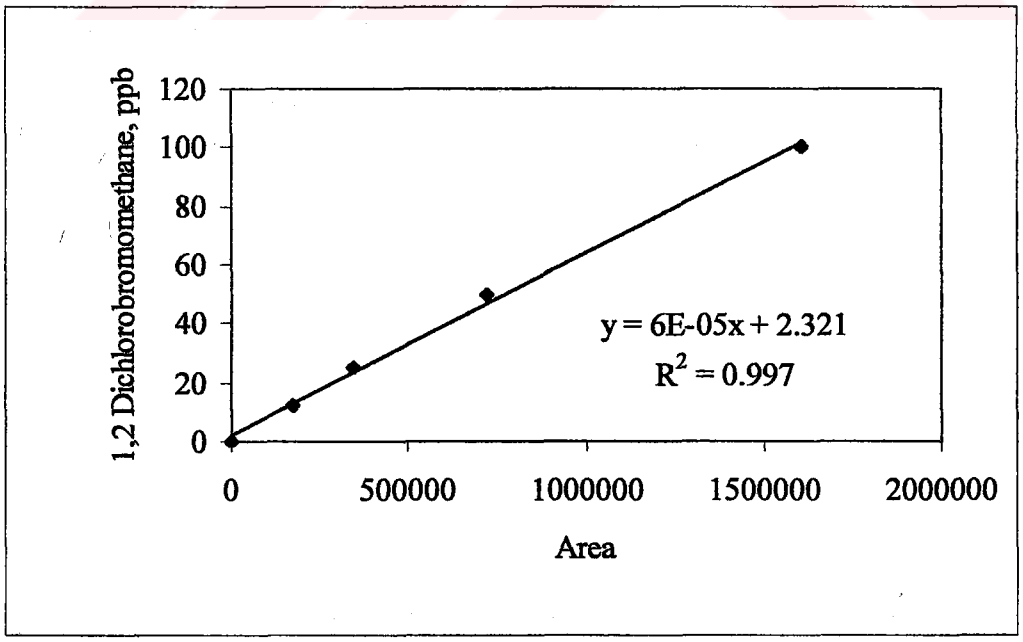

Figure A.2. Calibration curve for 1,2 dichlorobromomethane.

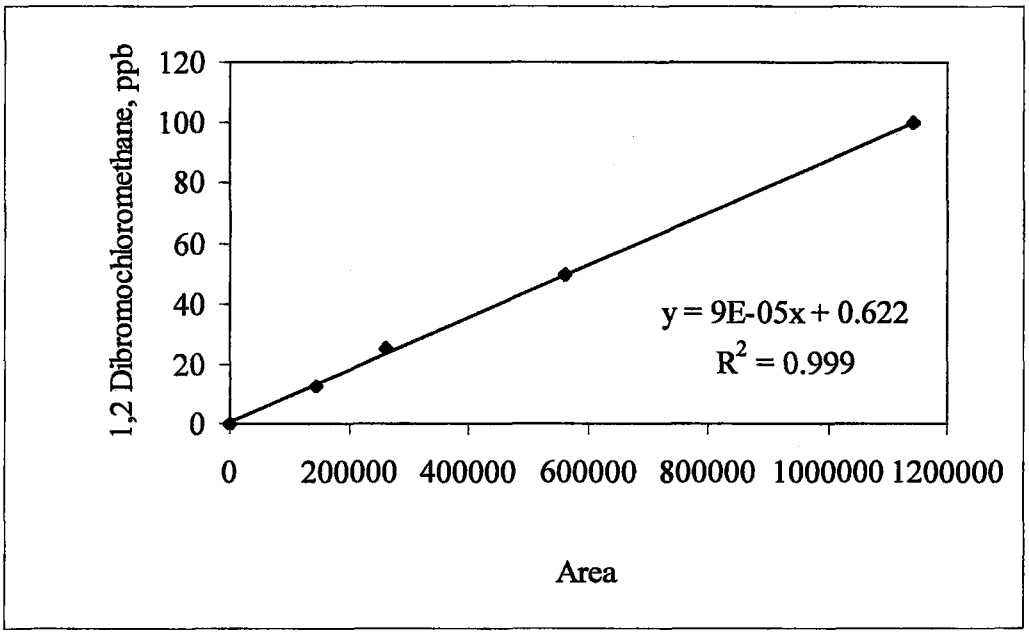

Figure A.3. Calibration curve for 1,2 dibromochloromethane.

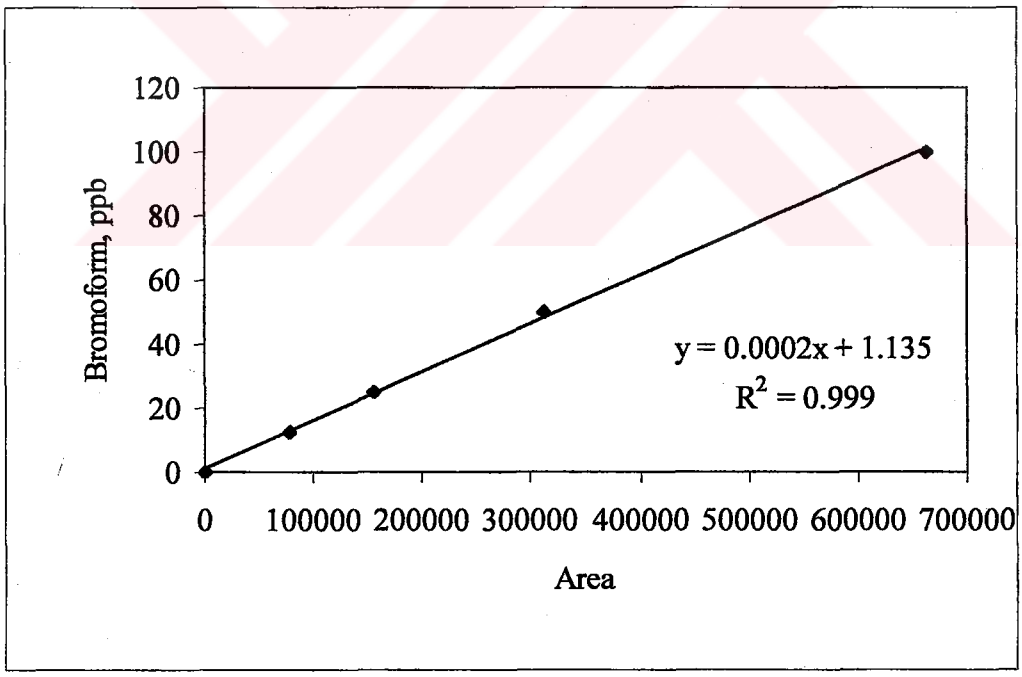

Figure A.4. Calibration curve for bromoform.

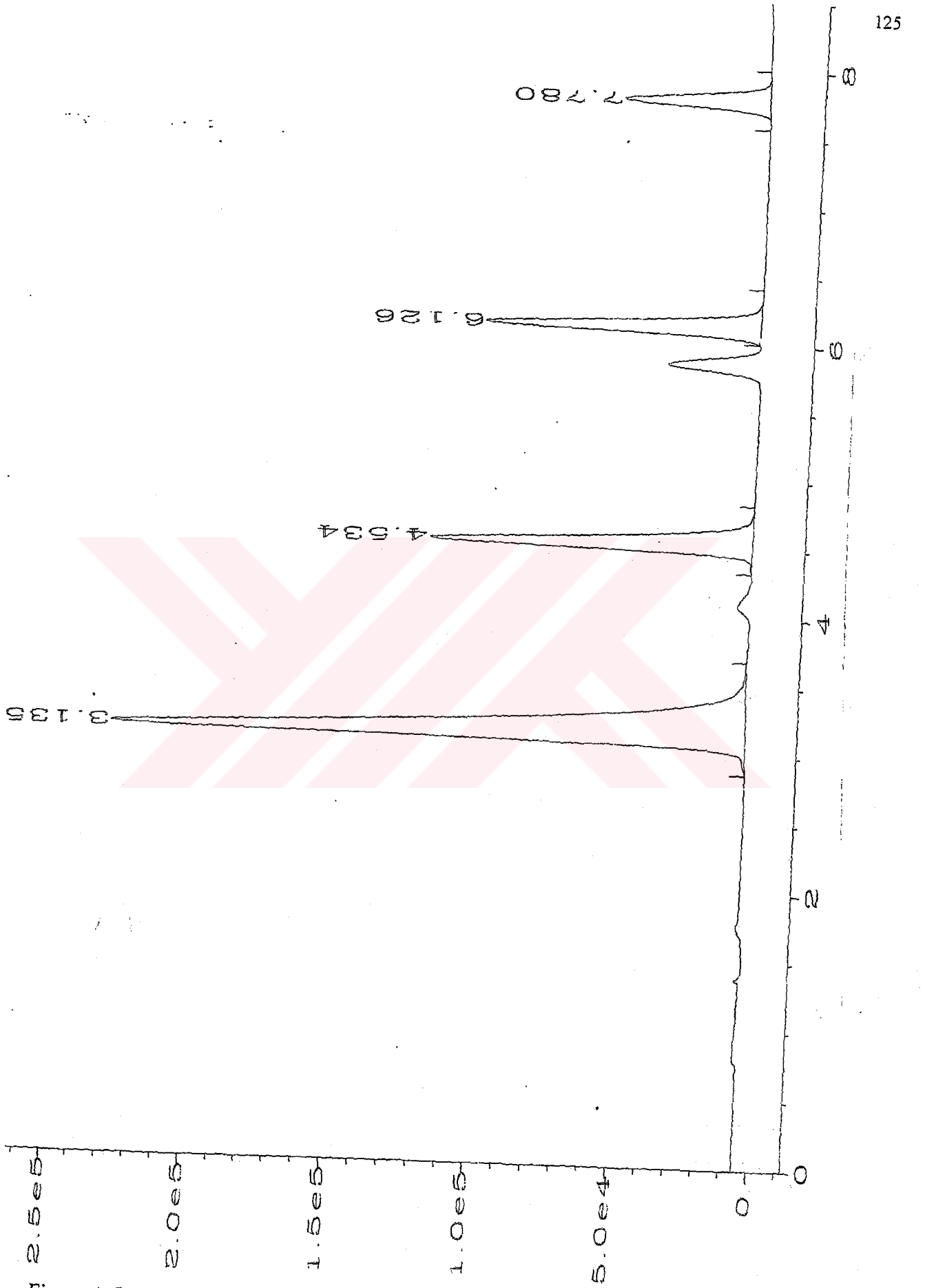

Figure A.5. Chromatogram for 50 ppb THM standard.

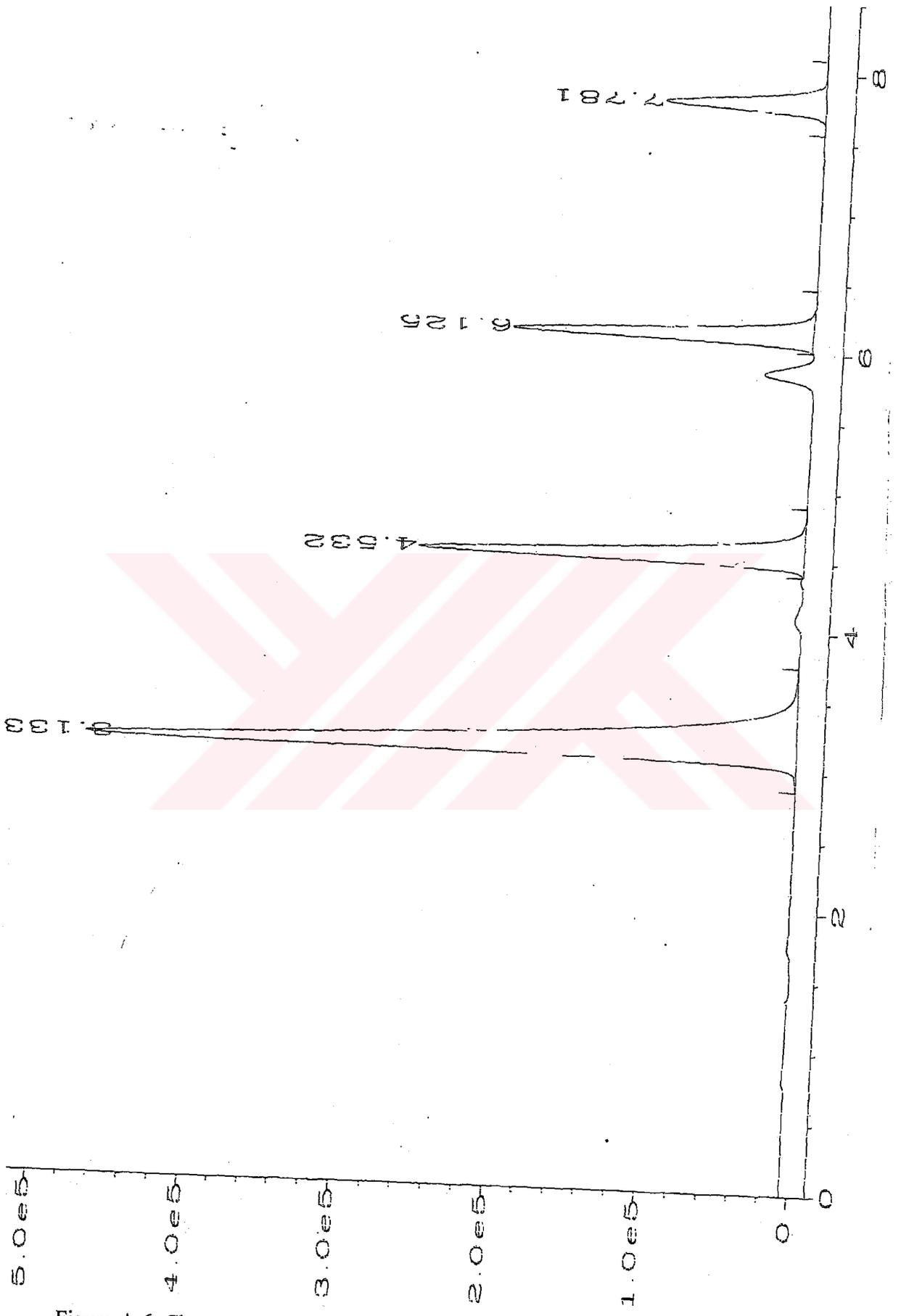

Figure A.6. Chromatogram for 100 ppb THM standard.

APPENDIX B

Calculation of Light Intensity According to Ferrioxalate Actinometry

$$n_{abs} = \frac{6.023 \times 10^{20} V_1 V_2 (OD)}{\phi_\lambda V_2 l \varepsilon t}$$

n_{abs} = the number of quanta per second per cell

V_1 = the volume of the actinometer solution irradiated (3000 mL)

V_2 = the volume of the aliquot taken for analysis (5 mL)

V_3 = the final volume to which the aliquot V_2 is diluted (25 mL)

l = the path length of the spectrophotometer cell used (2.5 cm)

OD = the measured "difference optical density" of the final solution at 510 nm,

ε = the molar extinction coefficient of the Fe^{2+} complex

(1.11×10^4 L mole^{-1} cm^{-1})

t = the irradiation time of the actinometer (sec)

ϕ_λ = the quantum yield for the Fe^{2+} formation (1.23 for 365 nm)

Intensity:

I = Number of moles of quanta per minute (Einstein min^{-1})

Irradiation time, t (sec)	Absorbance at 510 nm	Difference Optical Density, OD	Number of quanta per second, n_{abs}	Intensity, (Emin^{-1})
0 (Reference blank)	0.009	-	-	-
180	0.249	0.240	3.529×10^{17}	3.52×10^{-5}
300	0.379	0.370	3.264×10^{17}	3.25×10^{-5}
480	0.524	0.515	2.845×10^{17}	2.84×10^{-5}
600	0.635	0.626	2.762×10^{17}	2.75×10^{-5}
AVERAGE				3.09×10^{-5}

APPENDIX C

Humic Acid Characterization – Correlations Between Parameters

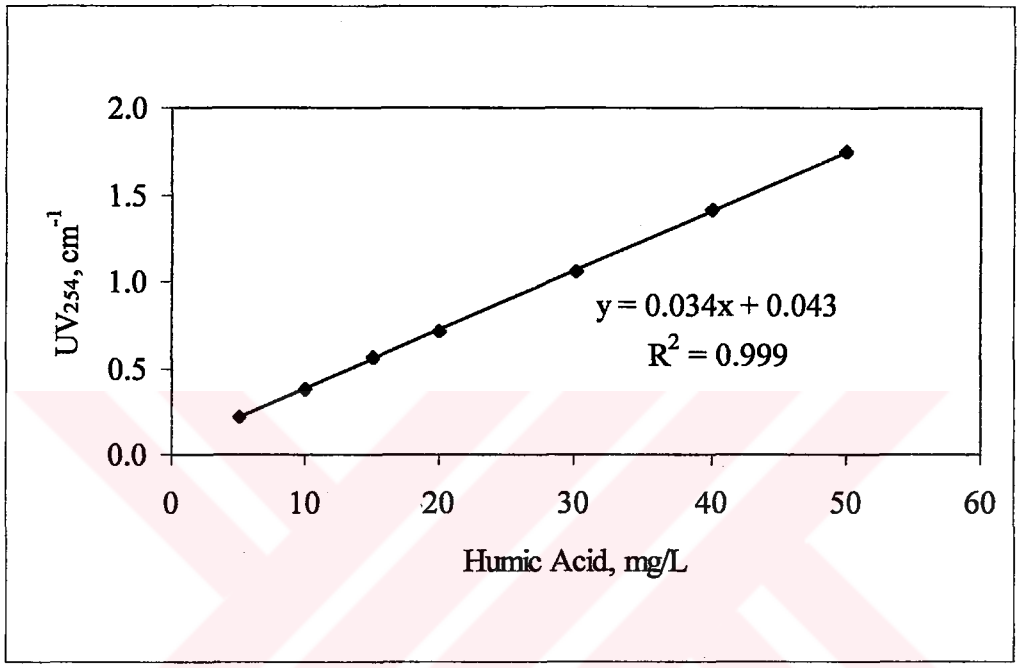

Figure C.1. Correlation between humic acid concentration and UV_{254}.

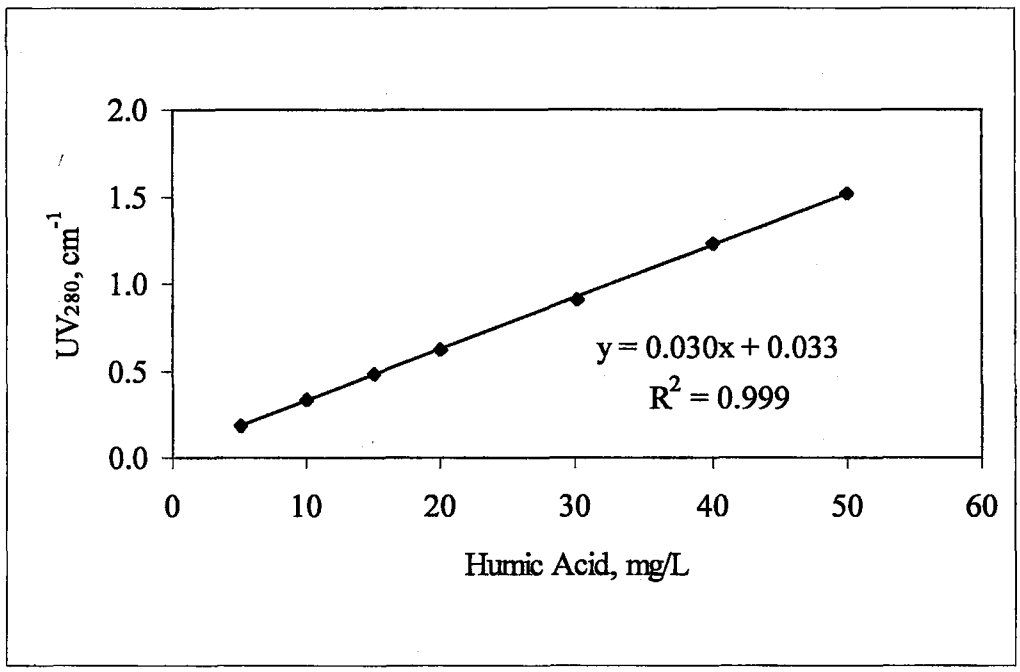

Figure C.2. Correlation between humic acid concentration and UV_{280}.

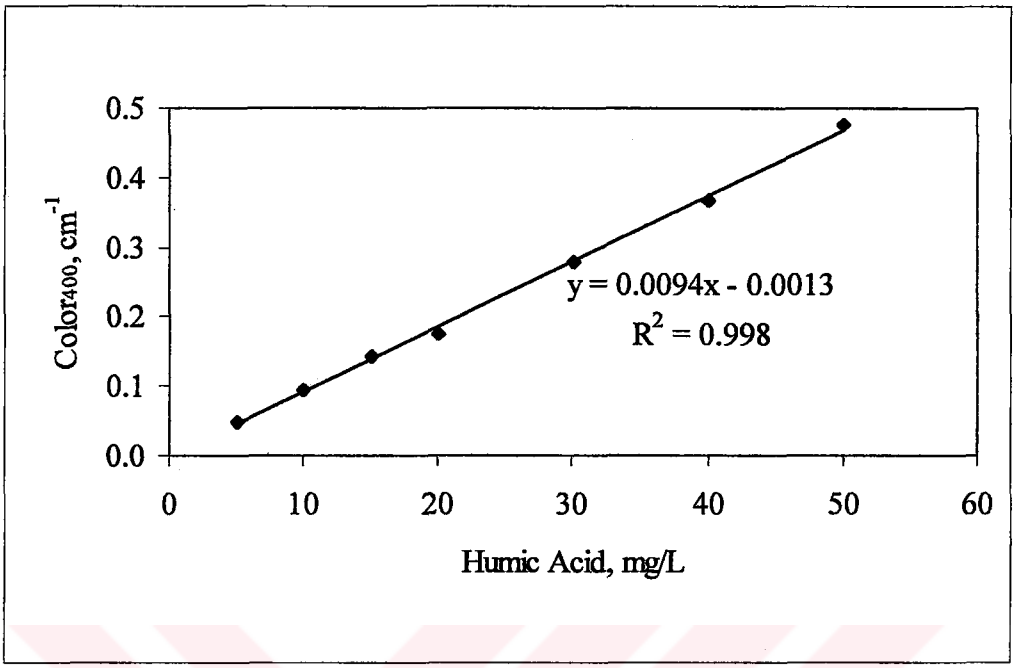

Figure C.3. Correlation between humic acid concentration and $Color_{400}$.

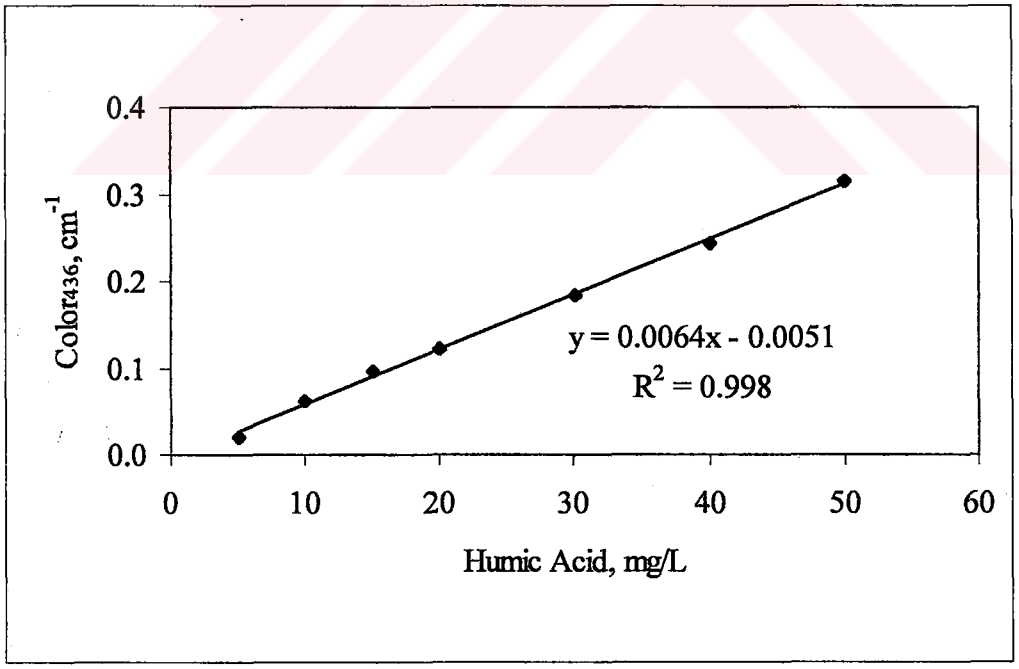

Figure C.4. Correlation between humic acid concentration and $Color_{436}$.

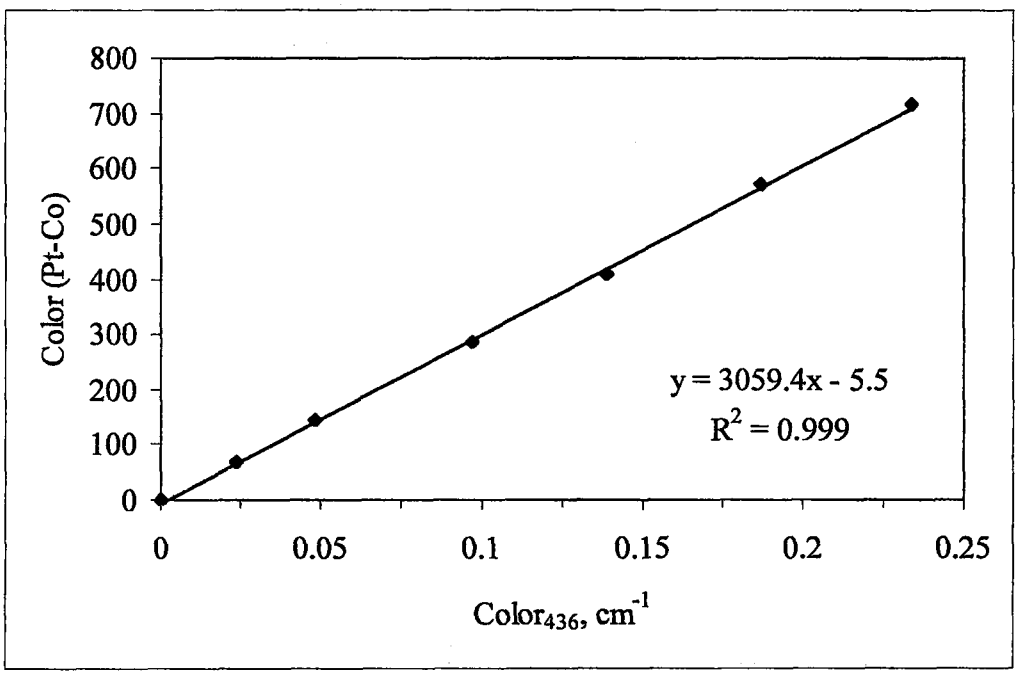

Figure C.5. Correlation between $Color_{436}$ and Color(Pt-Co).

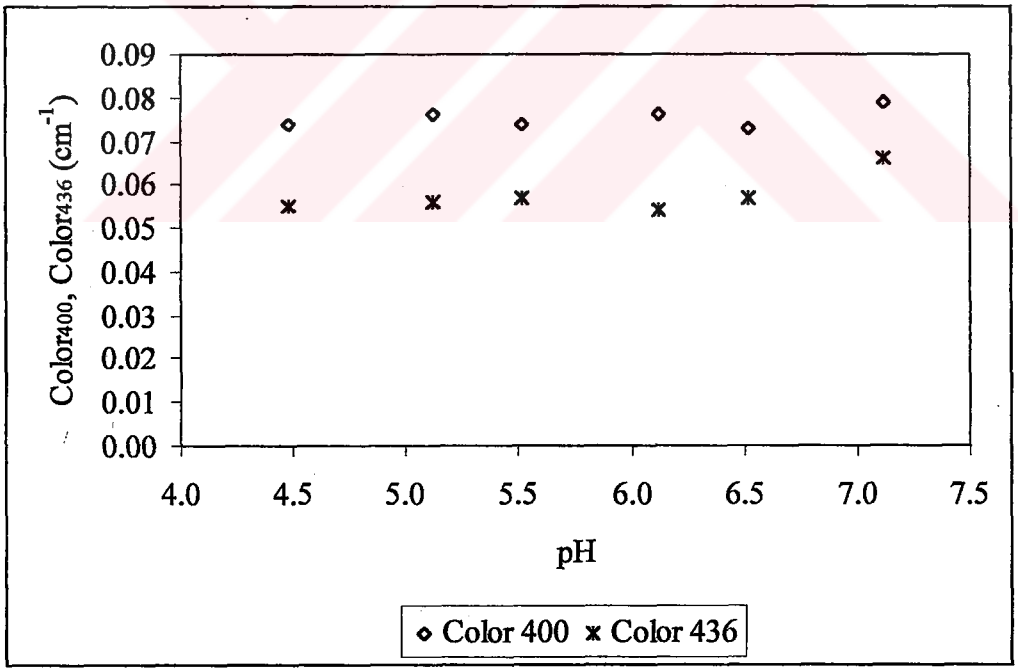

Figure C.6. Color and pH relation in 5 mgL^{-1} humic acid solution.

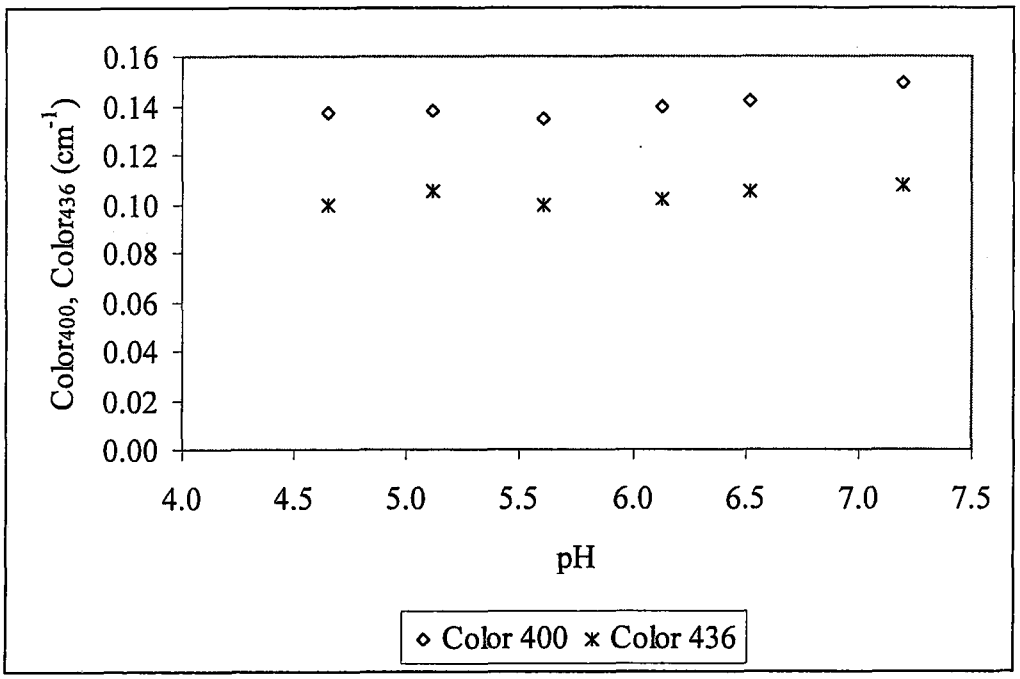

Figure C.7. Color and pH relation in 10 mgL^{-1} humic acid solution.

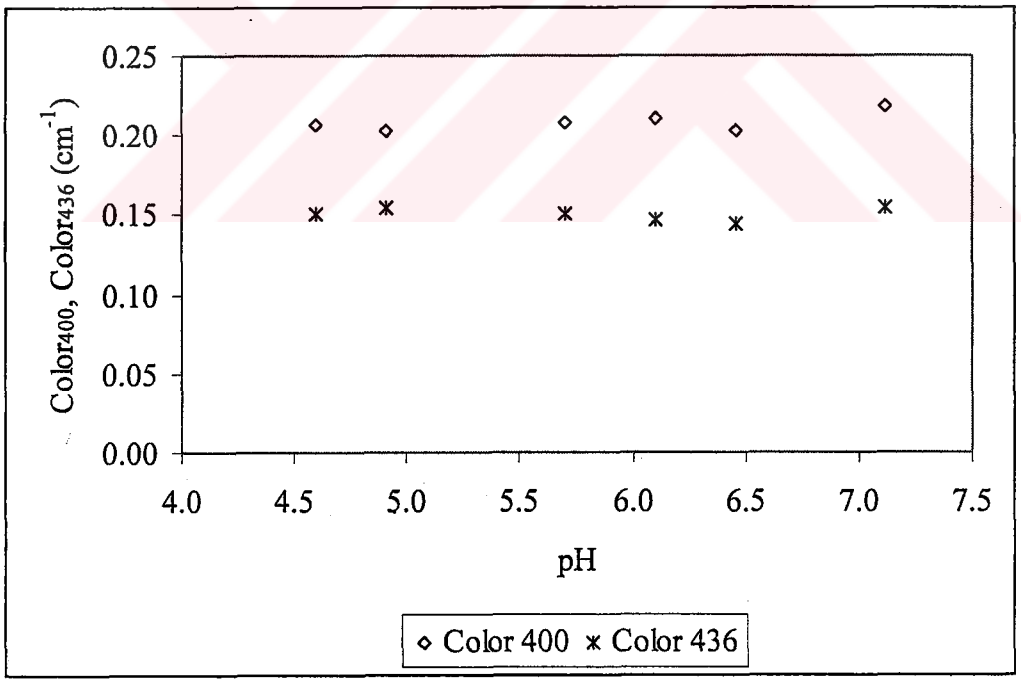

Figure C.8. Color and pH relation in 15 mgL^{-1} humic acid solution.

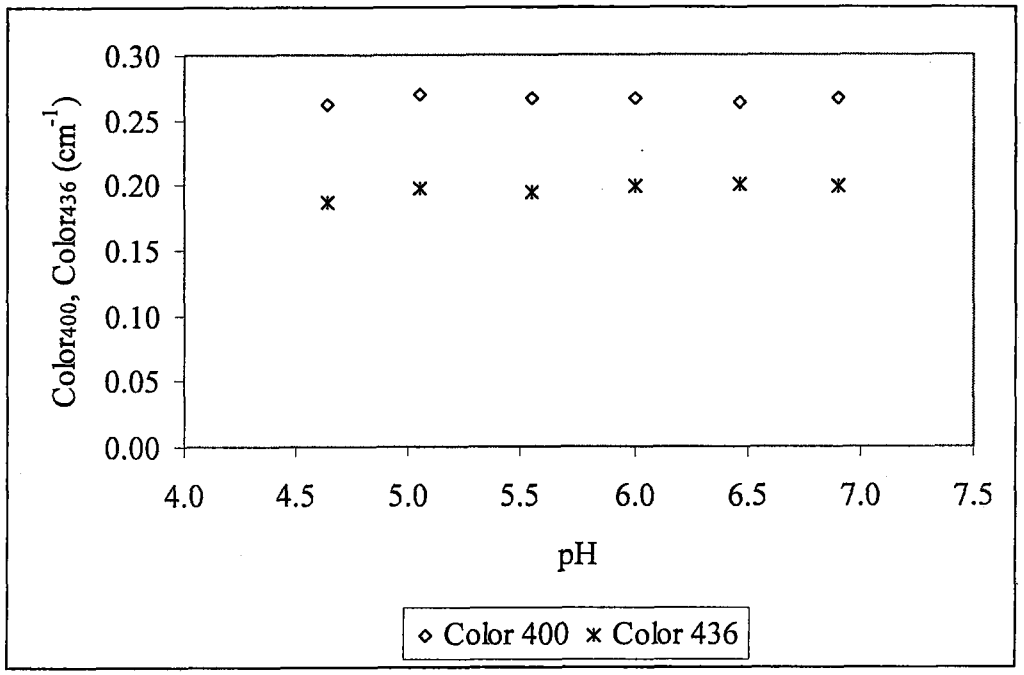

Figure C.9. Color and pH relation in 20 mgL^{-1} humic acid solution.

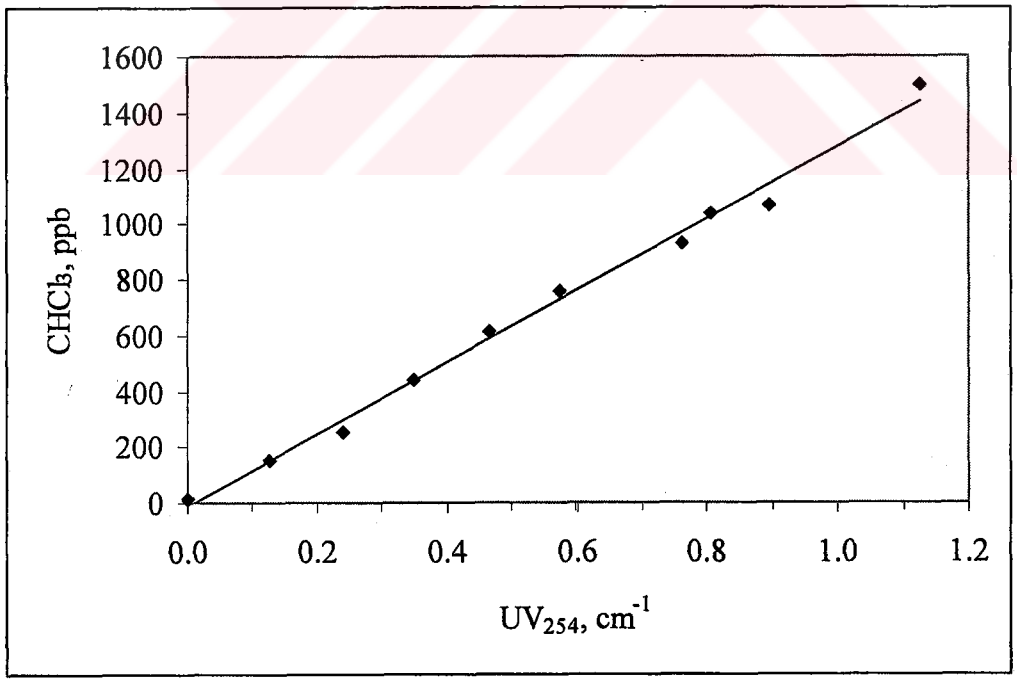

Figure C.10. Correlation between UV_{254} and $CHCl_3$ in humic acid samples

($CHCl_3 = 1293.49\ UV_{254} - 15.76$; $R^2 = 0.992$)

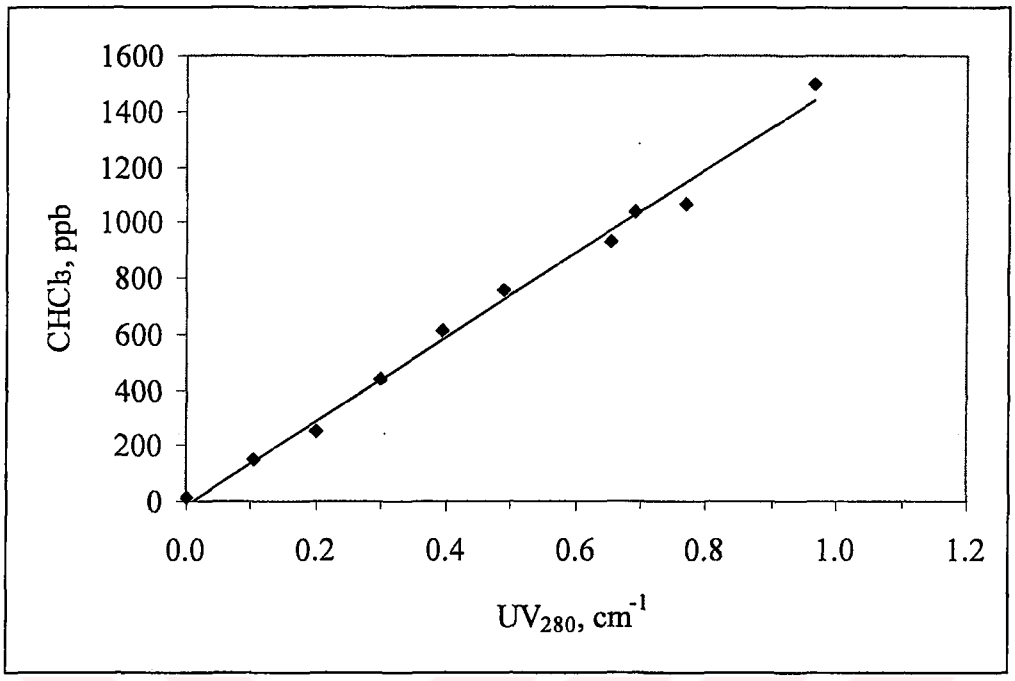

Figure C.11. Correlation between UV_{280} and $CHCl_3$ in humic acid samples

($CHCl_3 = 1503.46\ UV_{280} - 11.79$; $R^2 = 0.993$)

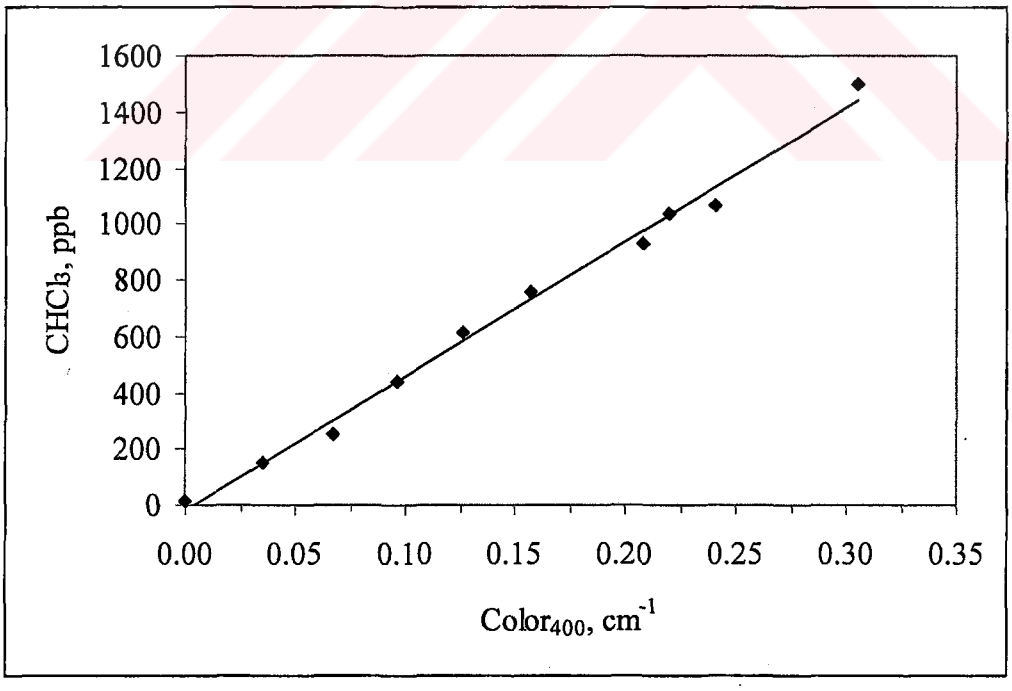

Figure C.12. Correlation between $Color_{400}$ and $CHCl_3$ in humic acid samples

($CHCl_3 = 4790.47\ Color_{400} - 21.27$; $R^2 = 0.992$)

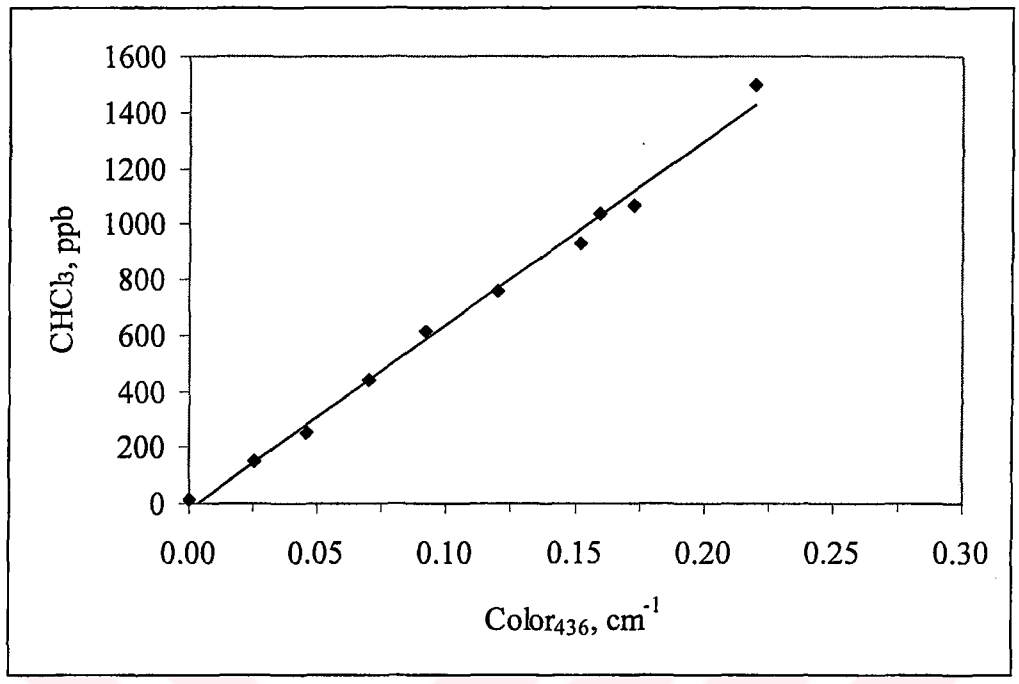

Figure C.13. Correlation between $Color_{436}$ and $CHCl_3$ in humic acid samples

($CHCl_3 = 6613.68\ Color_{436} - 24.65$; $R^2 = 0.993$)

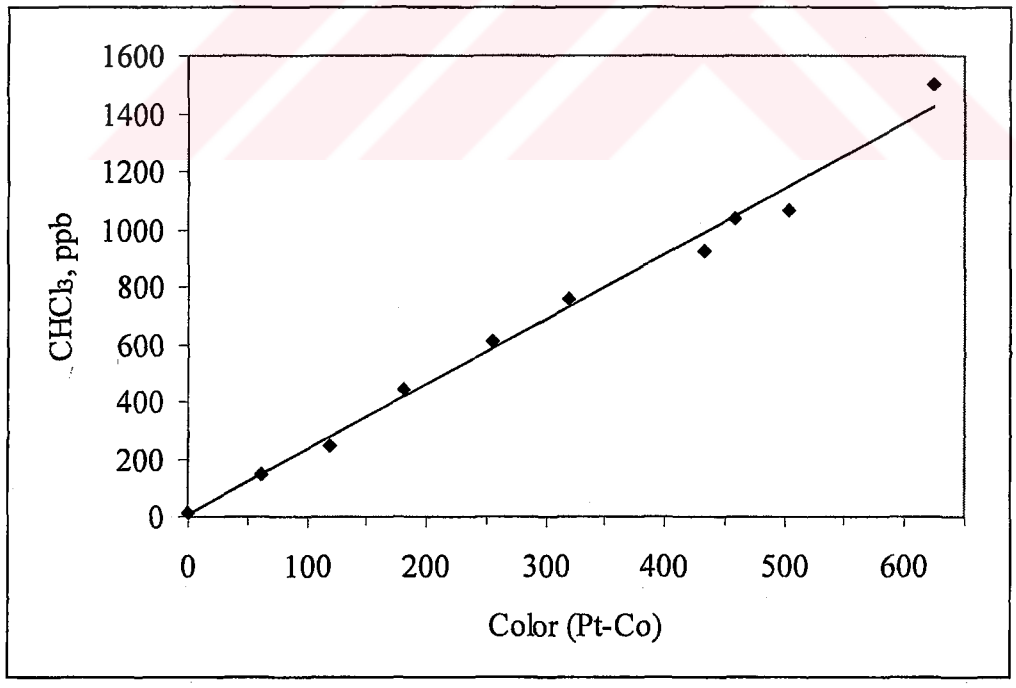

Figure C. 14. Correlation between Color (Pt-Co) and $CHCl_3$ in humic acid samples

($CHCl_3 = 2.27\ Color + 4.82$; $R^2 = 0.991$)

APPENDIX D

Reduction of THMFP with Ozonation in Humic Acid Solutions

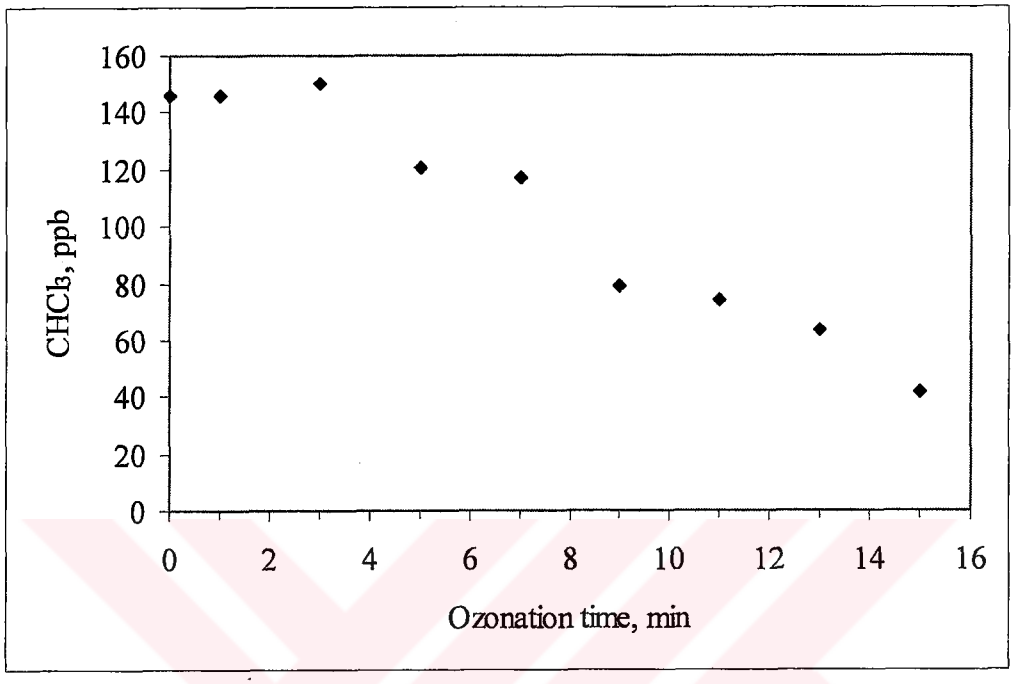

Figure D.1. Reduction of chloroform formation potential with ozonation in 5 mg L^{-1} humic acid solution.

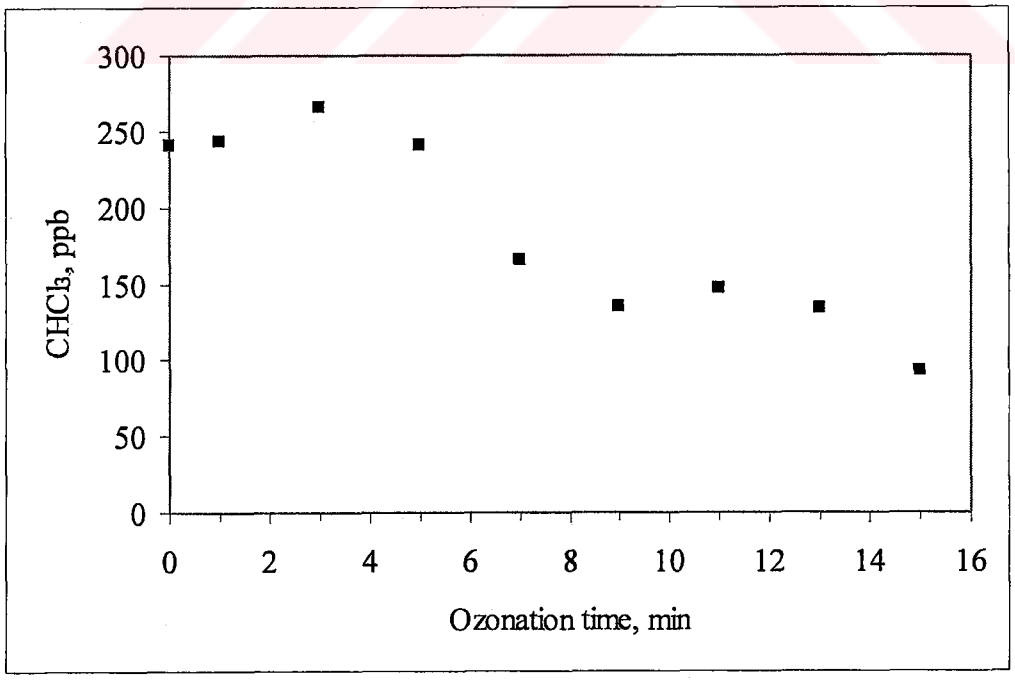

Figure D.2. Reduction of chloroform formation potential with ozonation in 10 mg L^{-1} humic acid solution.

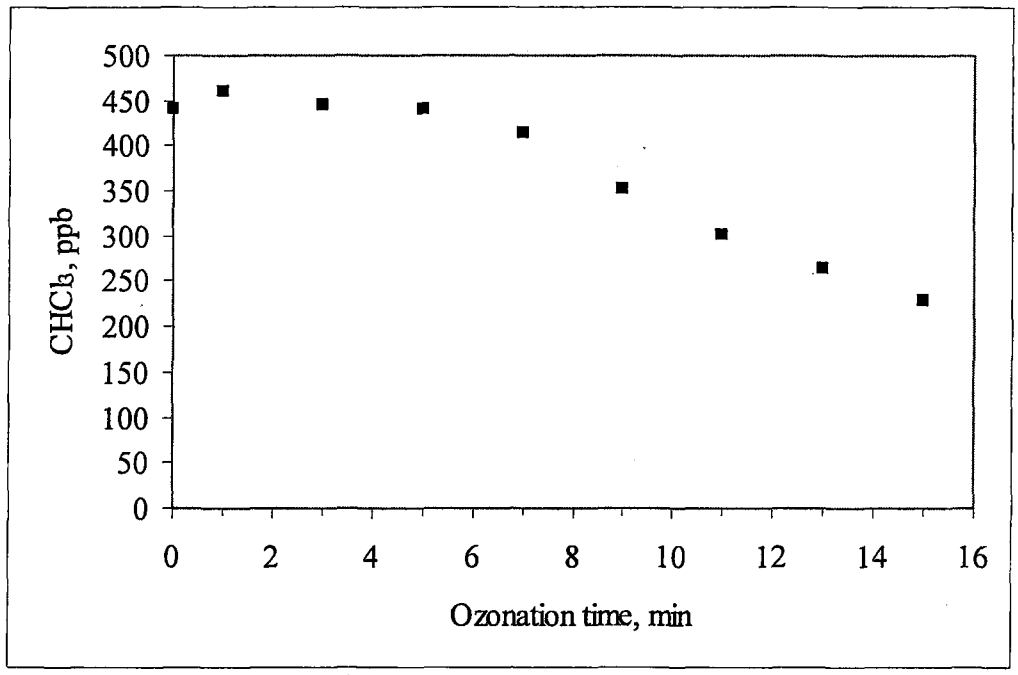

Figure D.3. Reduction of chloroform formation potential with ozonation in 15 mg L^{-1} humic acid solution.

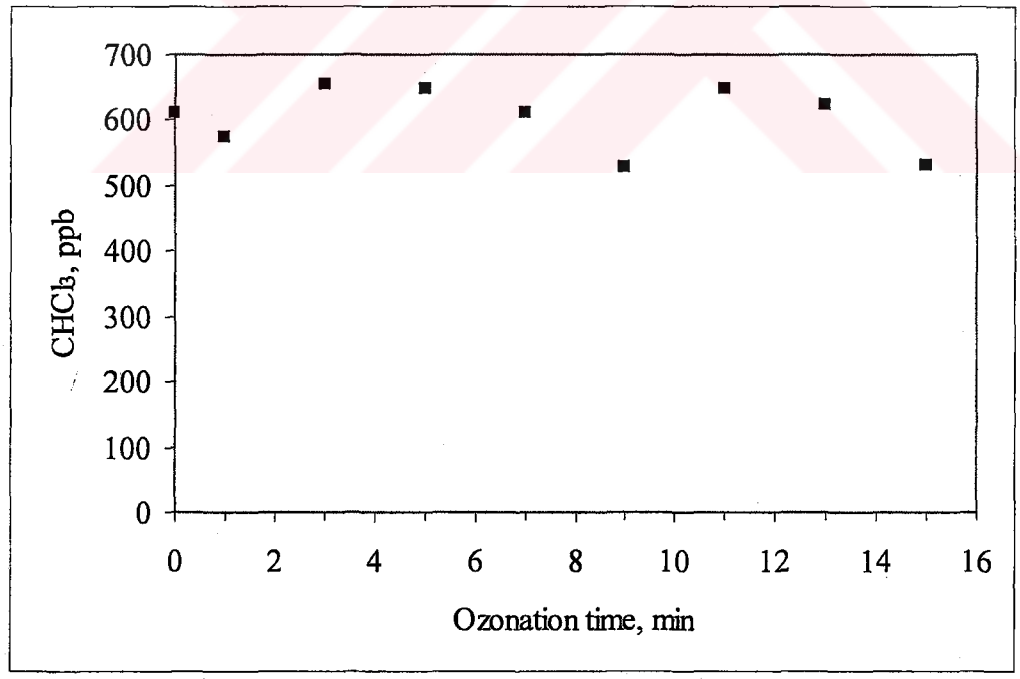

Figure D.4. Reduction of chloroform formation potential with ozonation in 20 mg L^{-1} humic acid solution.

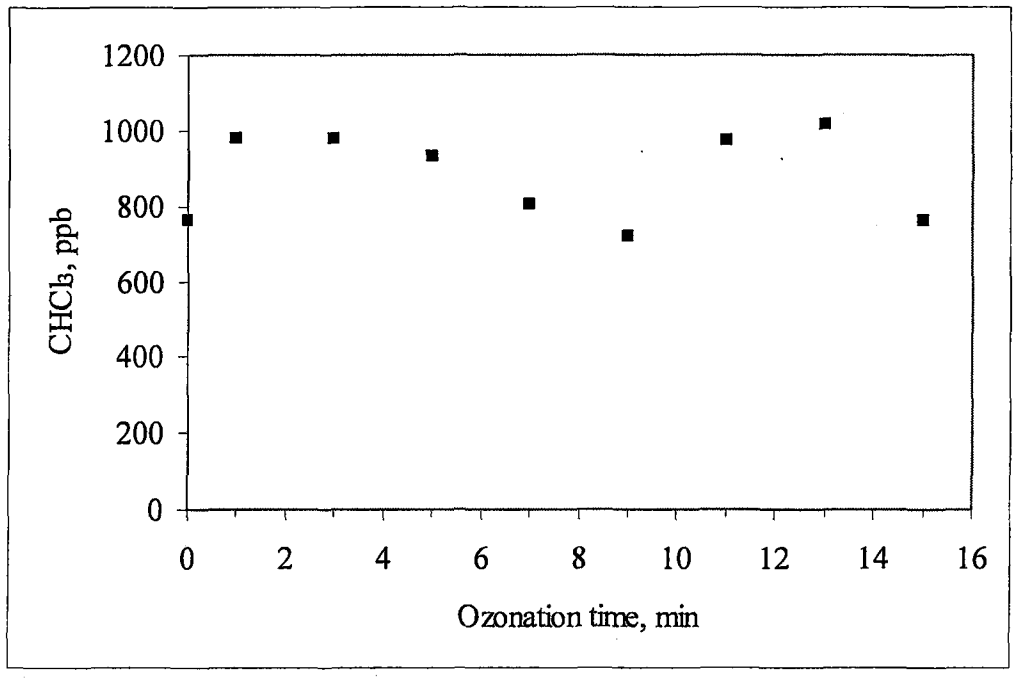

Figure D.5. Reduction of chloroform formation potential with ozonation in 25 mg L^{-1} humic acid solution.

APPENDIX E

Photocatalytic Degradation Profiles of Humic Acid Samples

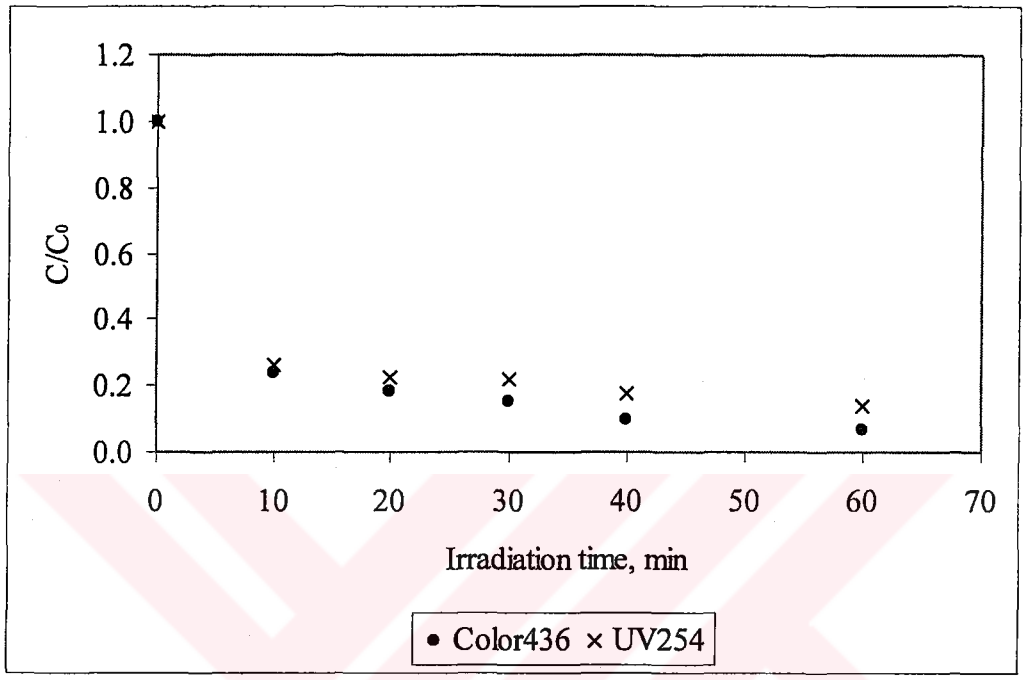

Figure E.1. $Color_{436}$ and UV_{254} degradation during the photocatalytic oxidation of 20 mgL^{-1} humic acid with 0.50 mg mL^{-1} TiO_2 loading.

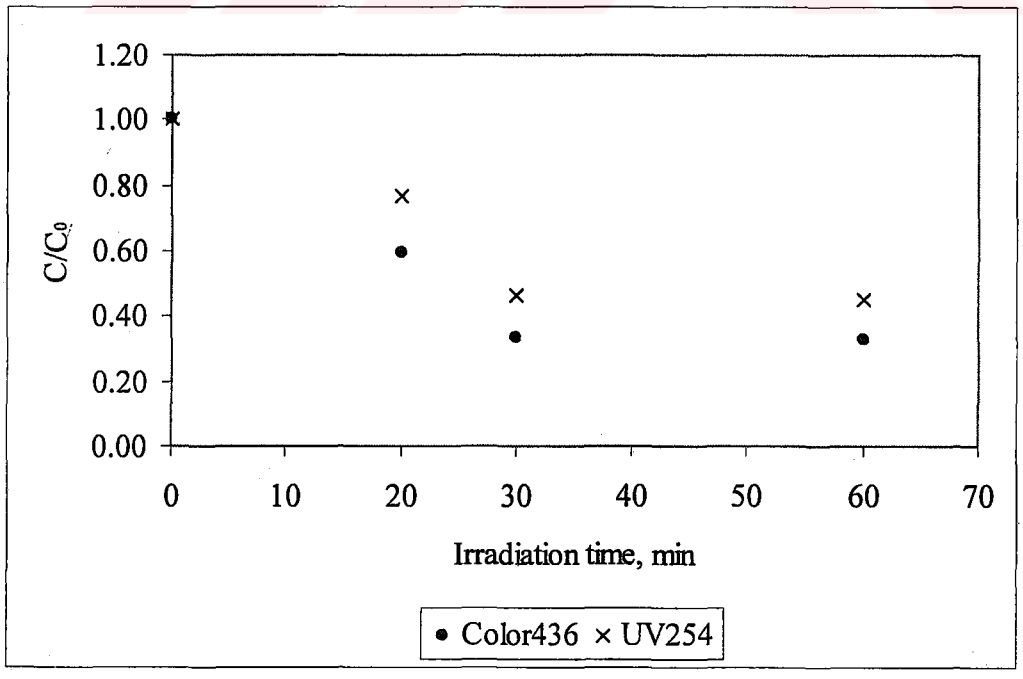

Figure E.2. $Color_{436}$ and UV_{254} degradation during the photocatalytic oxidation of 50 mgL^{-1} humic acid with 0.50 $mgmL^{-1}$ TiO_2 loading.

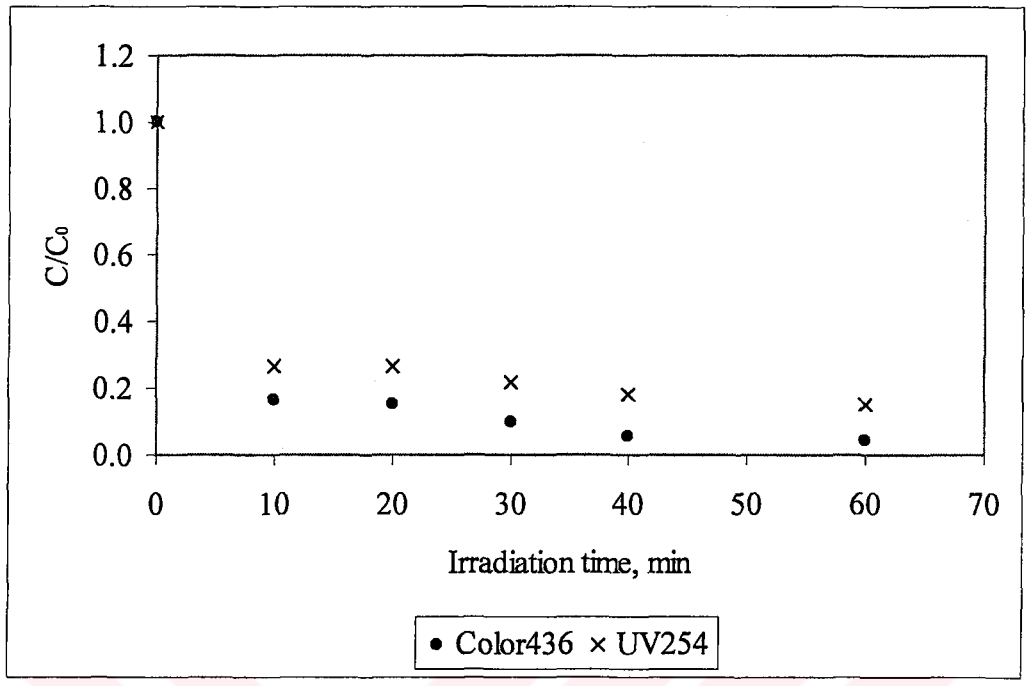

Figure E.3. $Color_{436}$ and UV_{254} degradation during the photocatalytic oxidation of Sample 1 with 0.50 $mgmL^{-1}$ TiO_2 loading.

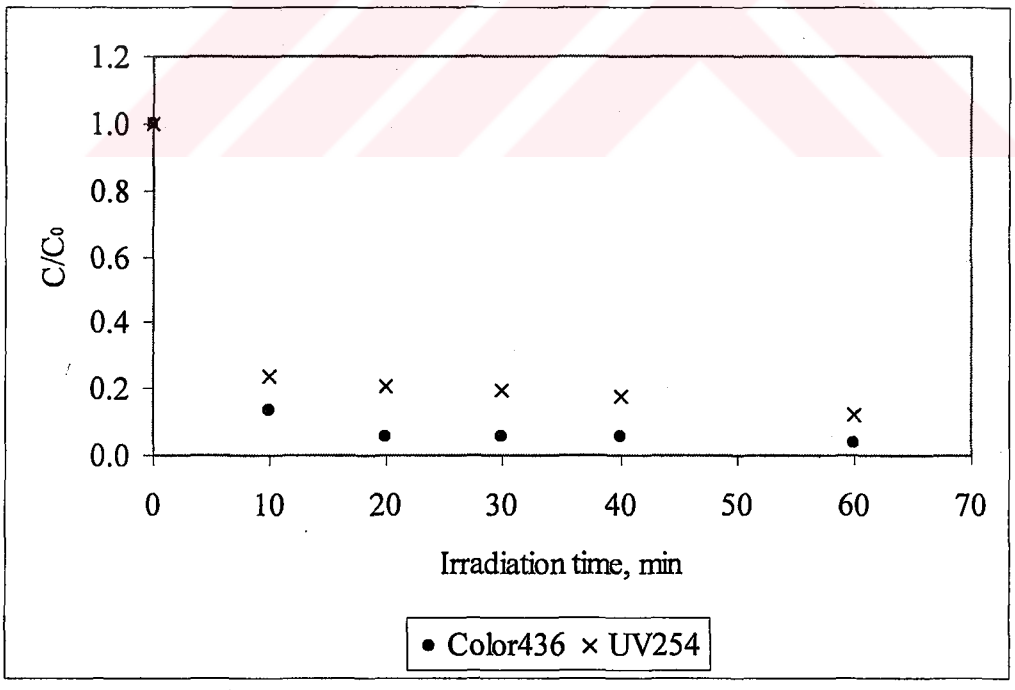

Figure E.4.$Color_{436}$ and UV_{254} degradation during the photocatalytic oxidation of Sample 2 with 0.50 $mgmL^{-1}$ TiO_2 loading.

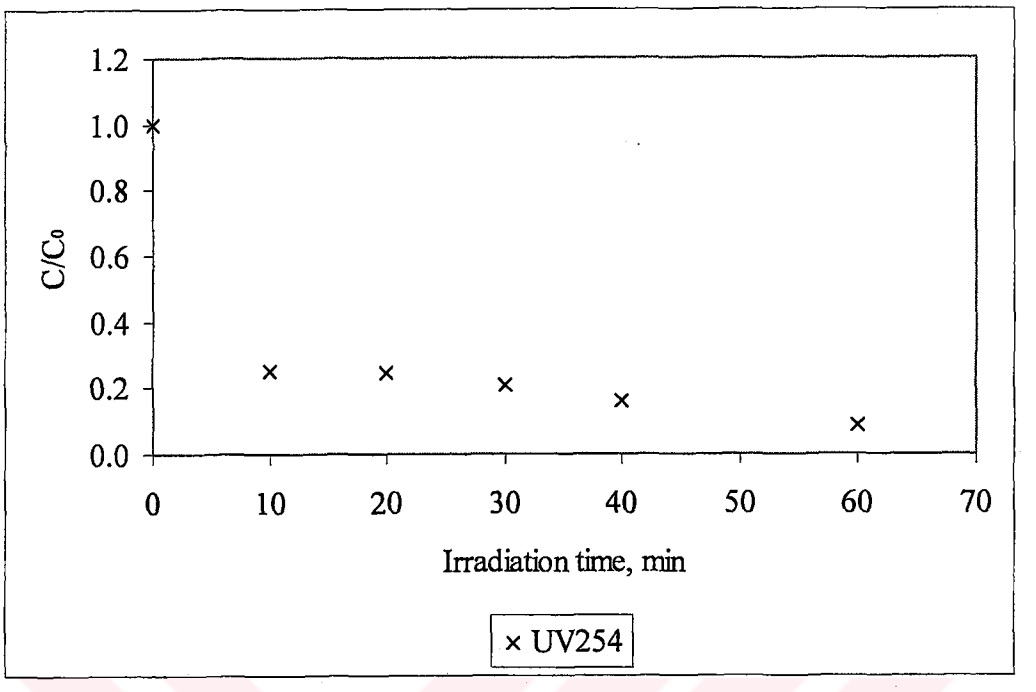

Figure E.5. UV_{254} degradation during the photocatalytic oxidation of Sample 3 with 0.50 $mgmL^{-1}$ TiO_2 loading.

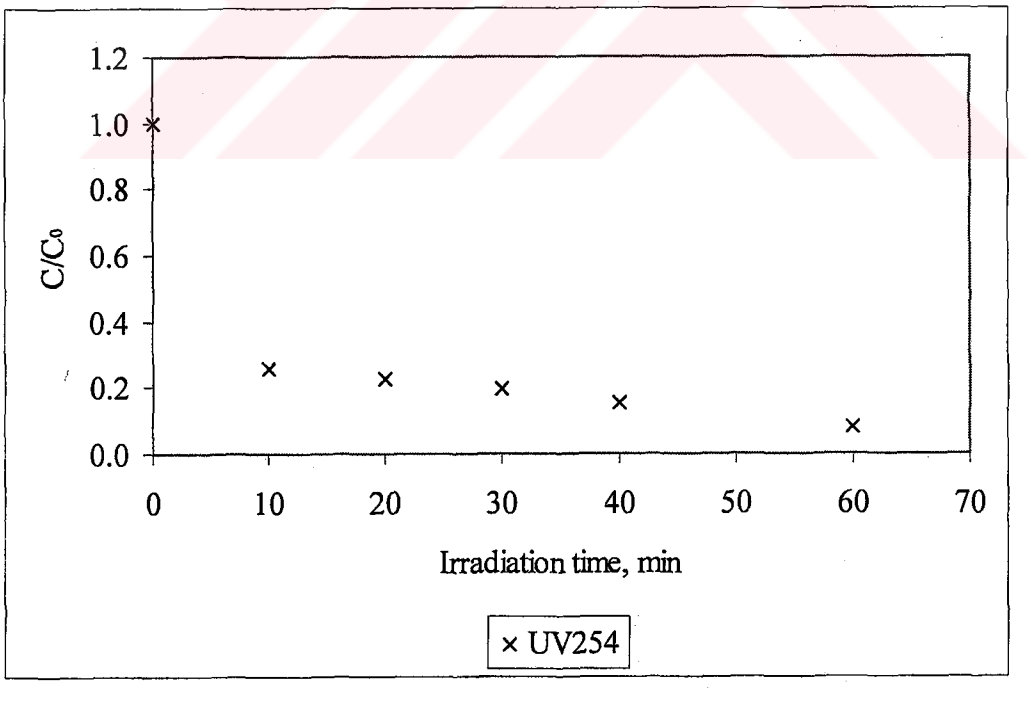

Figure E.6. UV_{254} degradation during the photocatalytic oxidation of Sample 4 with 0.50 $mgmL^{-1}$ TiO_2 loading.

APPENDIX F

Adsorption Profiles of Humic Acid Samples

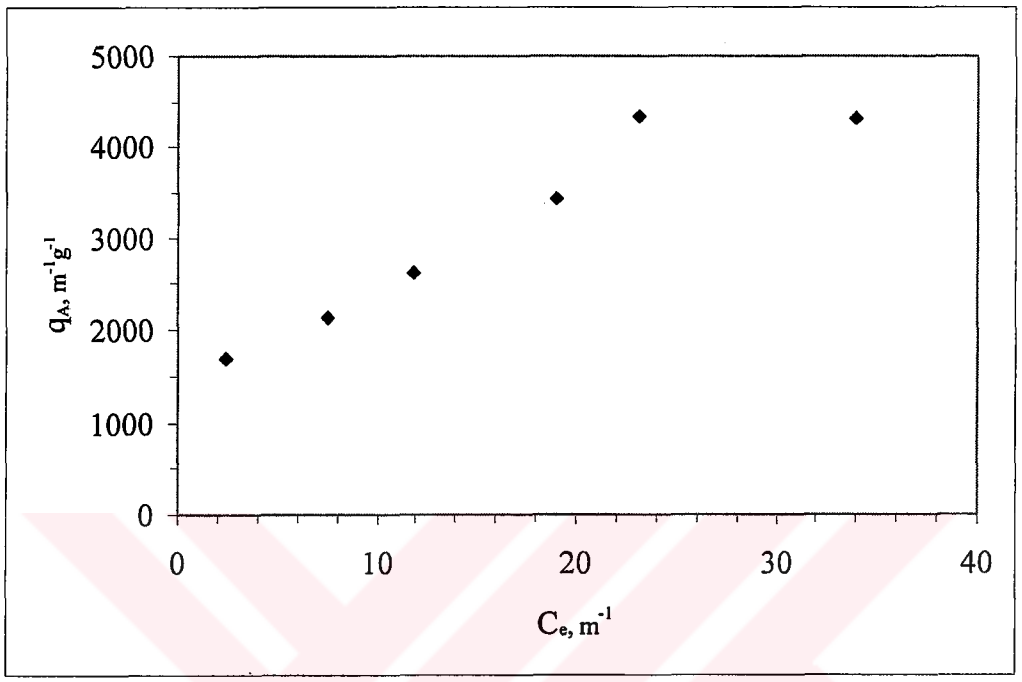

Figure F.1. UV_{254} adsorption profile for the untreated humic acid solution for TiO_2 loading between 0.1 – 1.00 $mgmL^{-1}$.

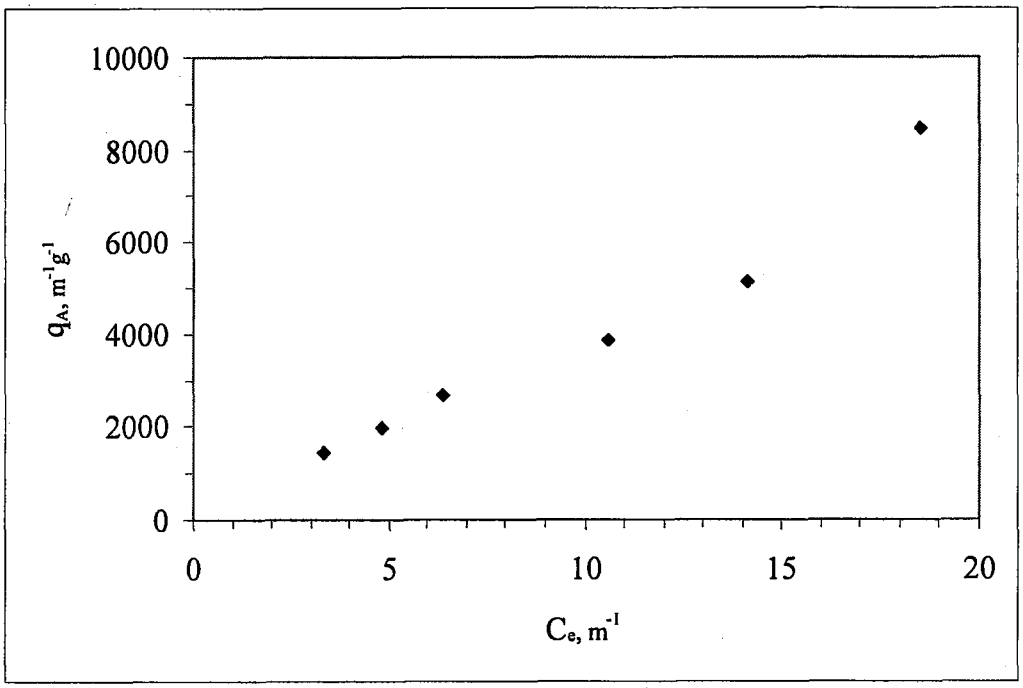

FigureF.2. UV_{254} adsorption profile for Sample 1 for TiO_2 loading 0.1 – 1.00 $mgmL^{-1}$.

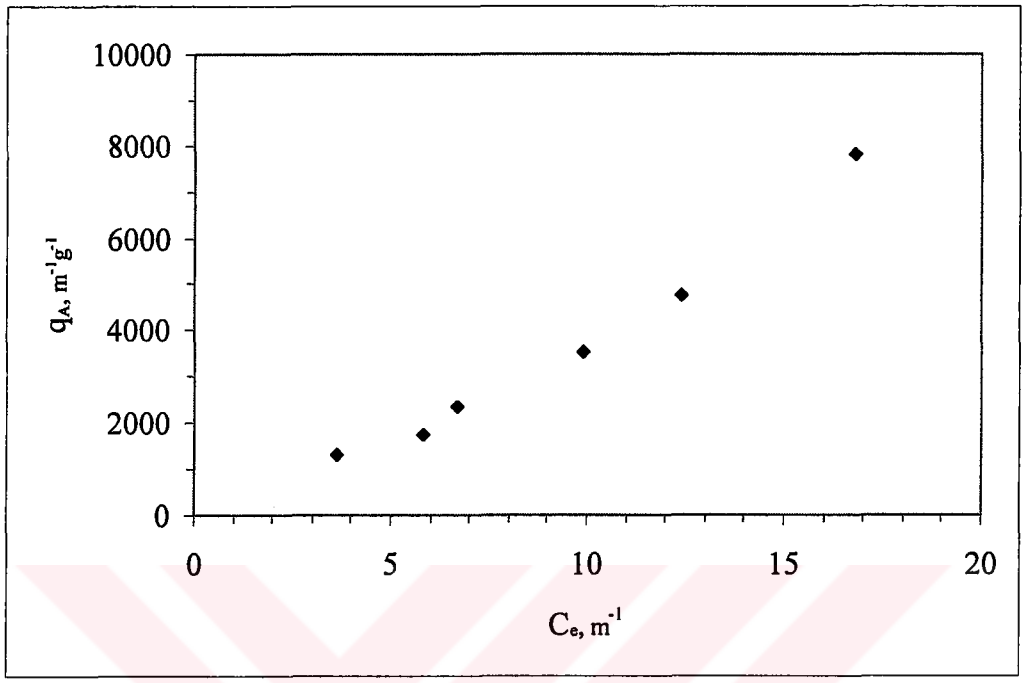

Figure F.3. UV_{254} adsorption profile for Sample 2 for TiO_2 loading 0.1 – 1.00 $mgmL^{-1}$.

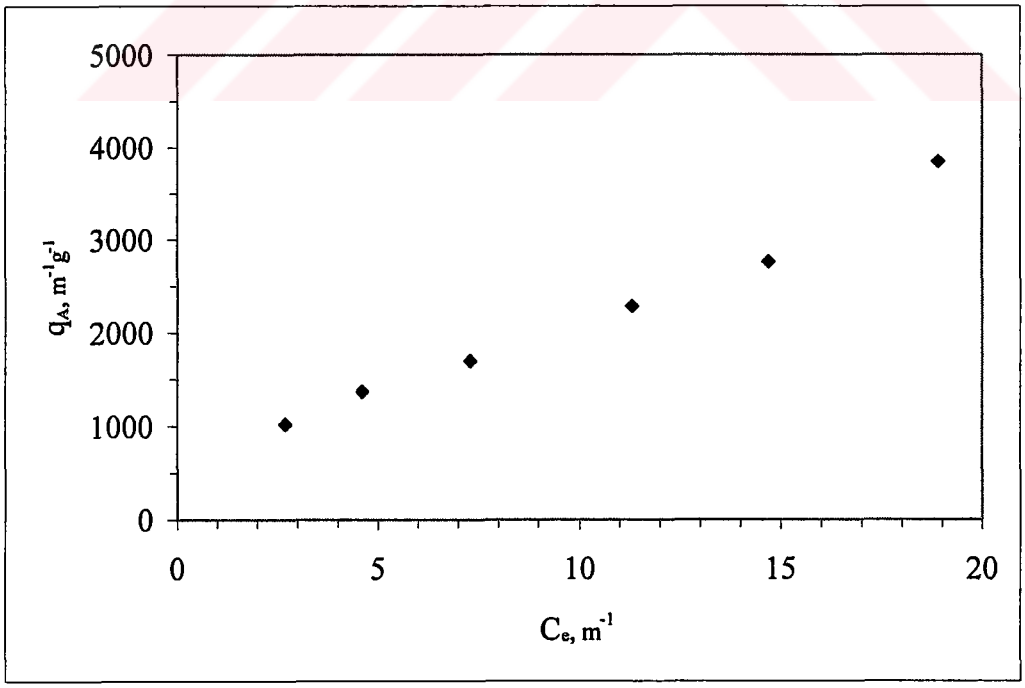

Figure F.4. UV_{254} adsorption profile for Sample 3 for TiO_2 loading 0.1 – 1.00 $mgmL^{-1}$.

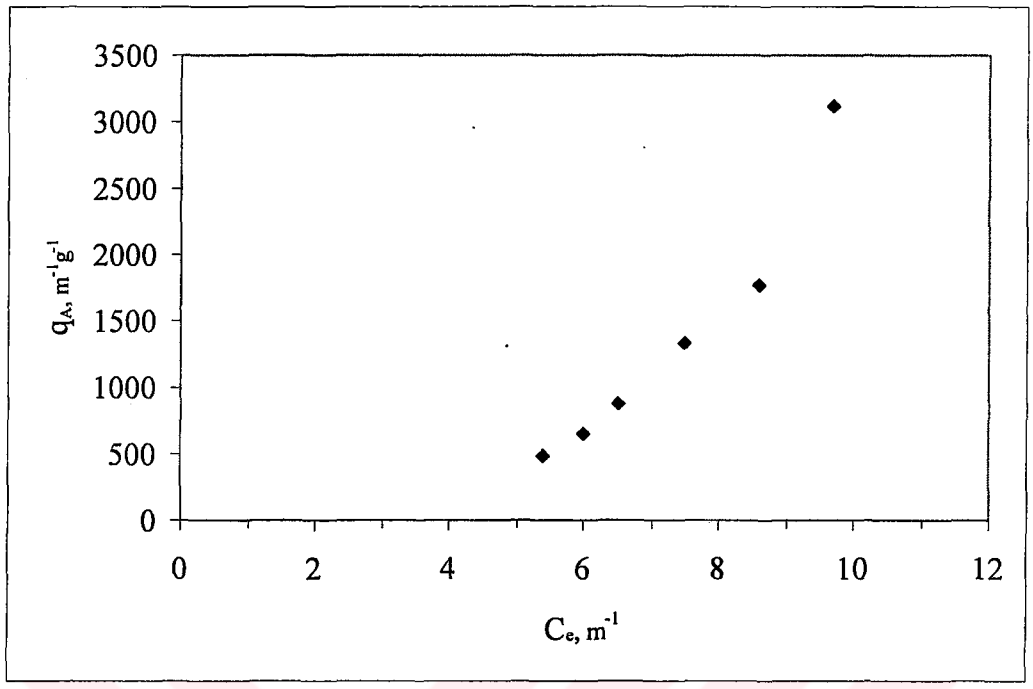

Figure F.5. UV_{254} adsorption profile for Sample 4 for TiO_2 loading 0.1 – 1.00 $mgmL^{-1}$.

APPENDIX G

Absorbance Spectrums for Humic Acid Samples Filtered Through Membranes

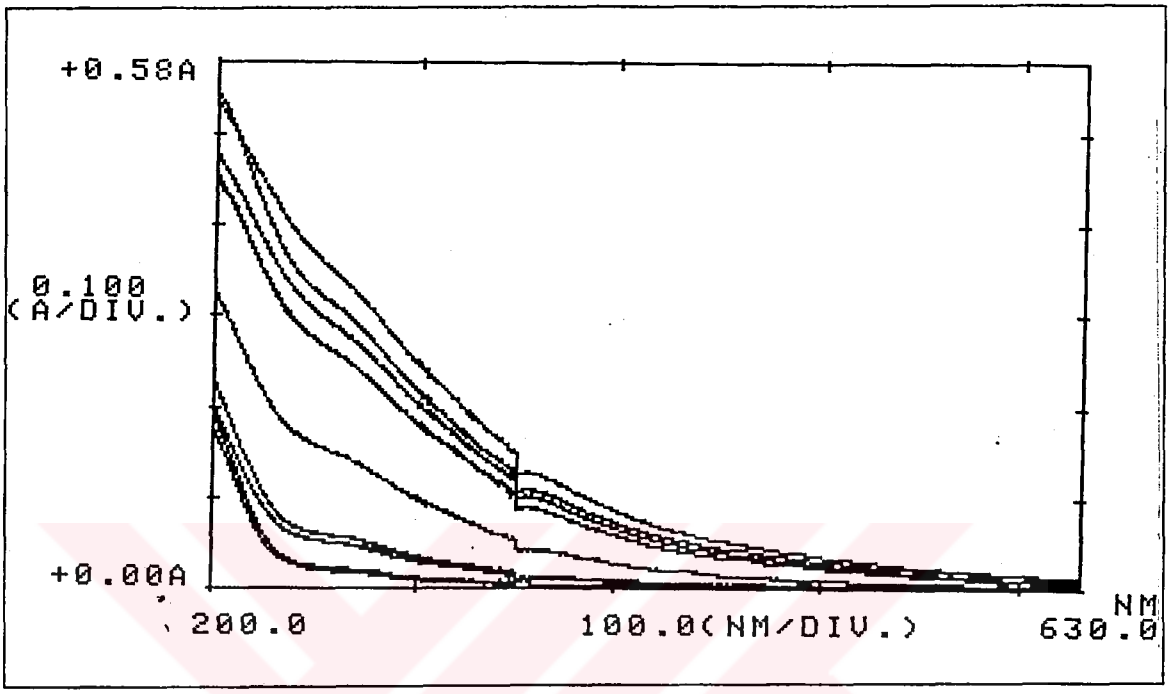

Figure G. 1. Spectrums obtained from the ultrafiltration of Sample 1 (From top to bottom: Unfiltered humic acid sample, filtrates from membrane filters 450,000 – 500 Daltons)

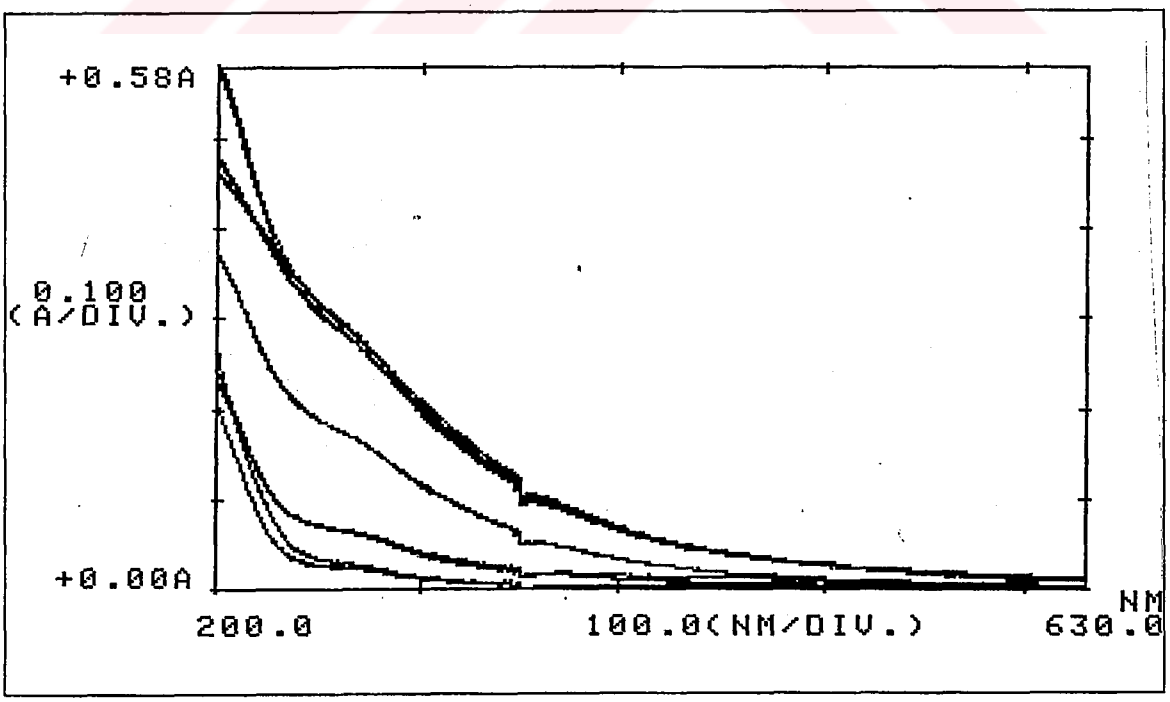

Figure G.2. Spectrums obtained from the ultrafiltration of Sample 2 (From top to bottom: Unfiltered humic acid sample, filtrates from membrane filters 450,000 – 500 Daltons)

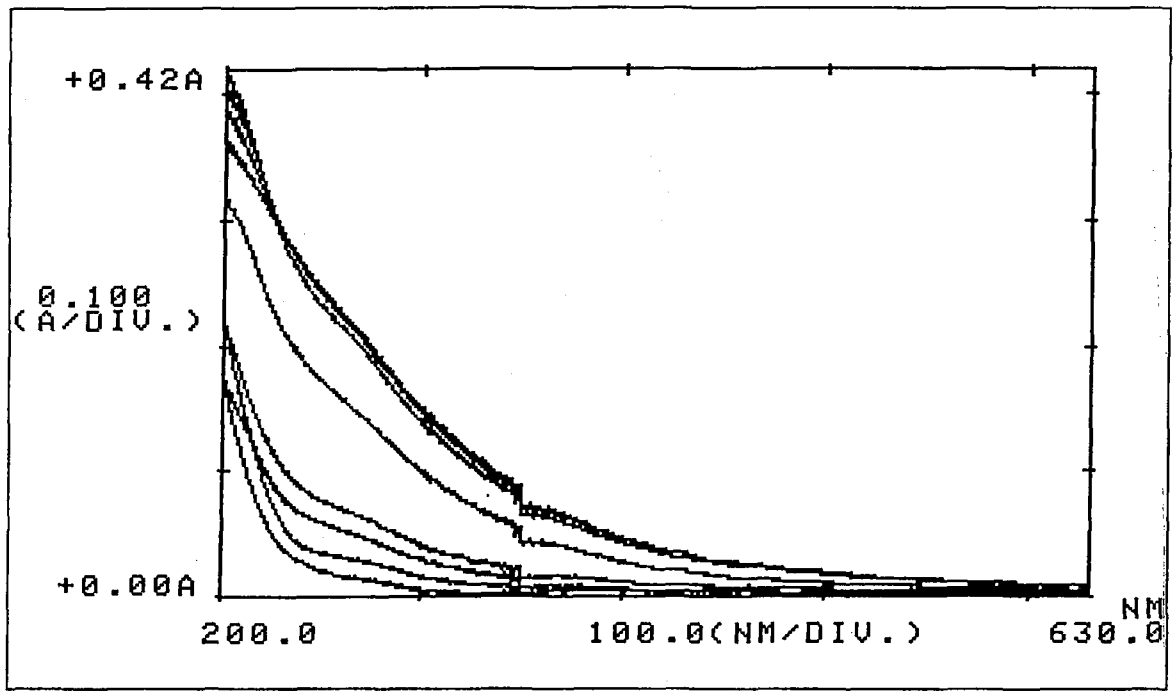

Figure G.3. Spectrums obtained from the ultrafiltration of Sample 3 (From top to bottom: Unfiltered humic acid sample, filtrates from membrane filters 450,000 – 500 Daltons)

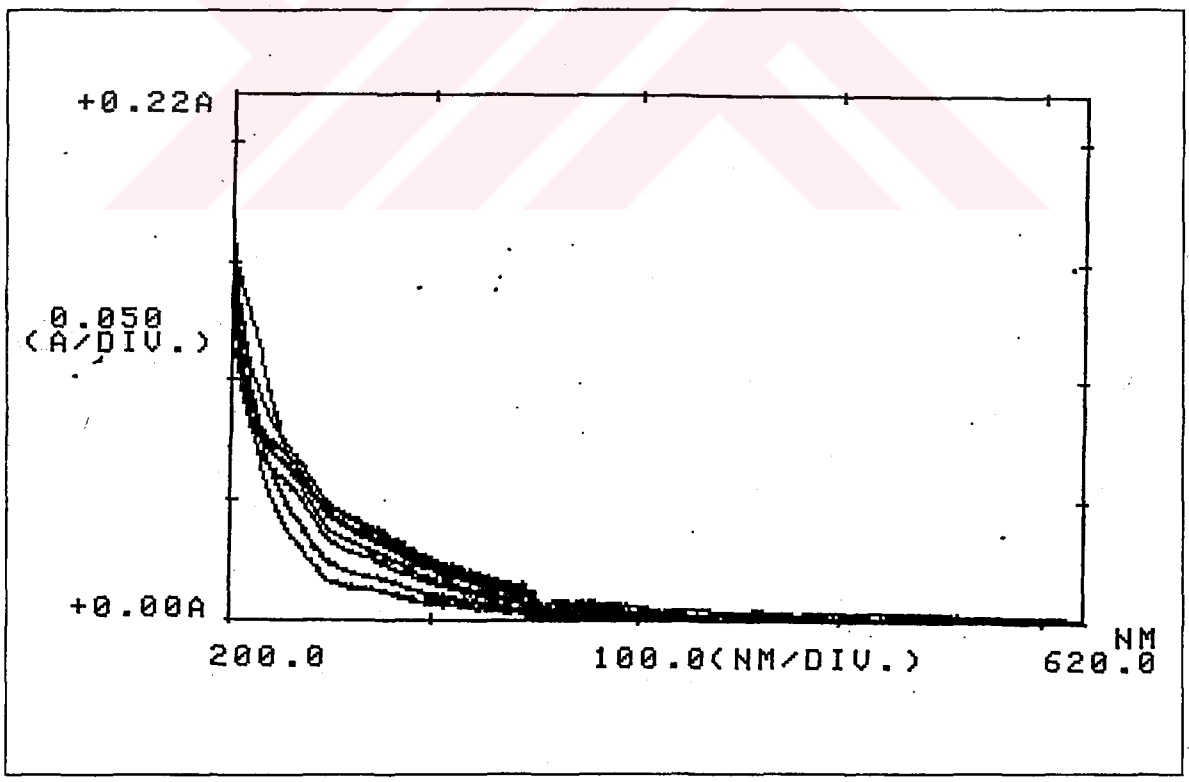

Figure G.4. Spectrums obtained from the ultrafiltration of preozonated and photocatalytically oxidized humic acid sample (Sample 1) (From top to bottom: Unfiltered sample, filtrates from membrane filters 450,000 – 500 Daltons)

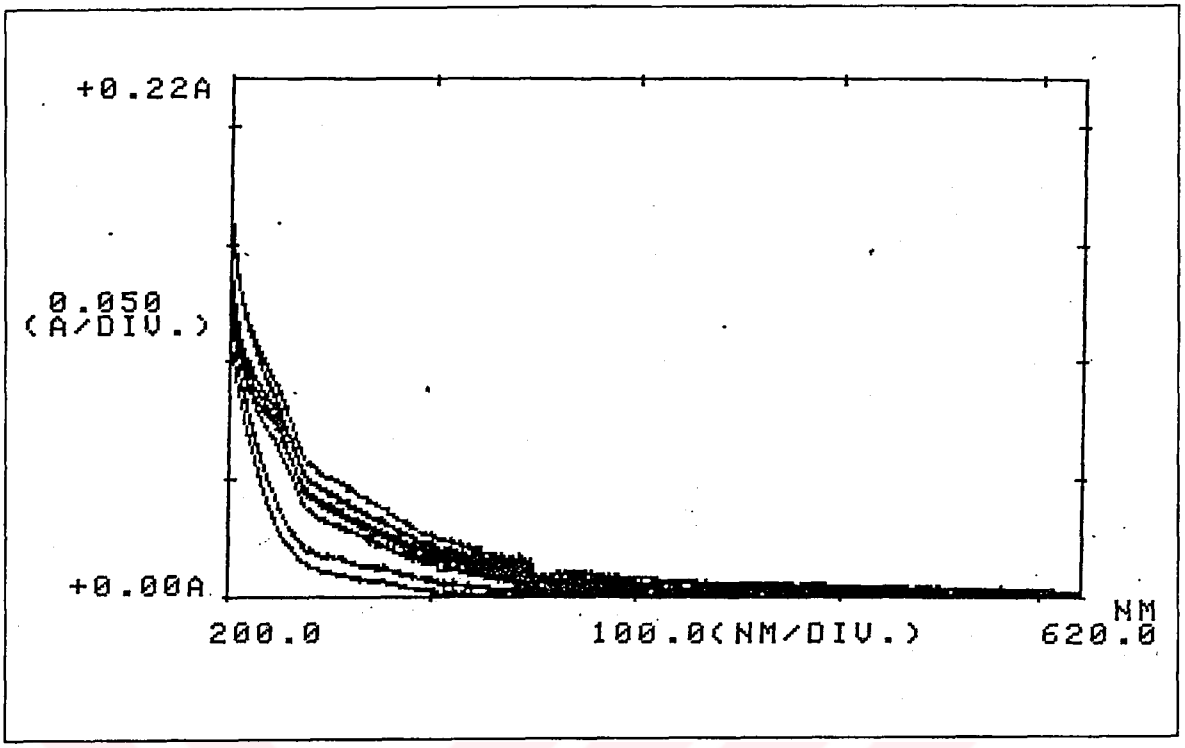

Figure G.5. Spectrums obtained from the ultrafiltration of preozonated and photocatalytically oxidized humic acid sample (Sample 2) (From top to bottom: Unfiltered sample, filtrates from membrane filters 450,000 – 500 Daltons)

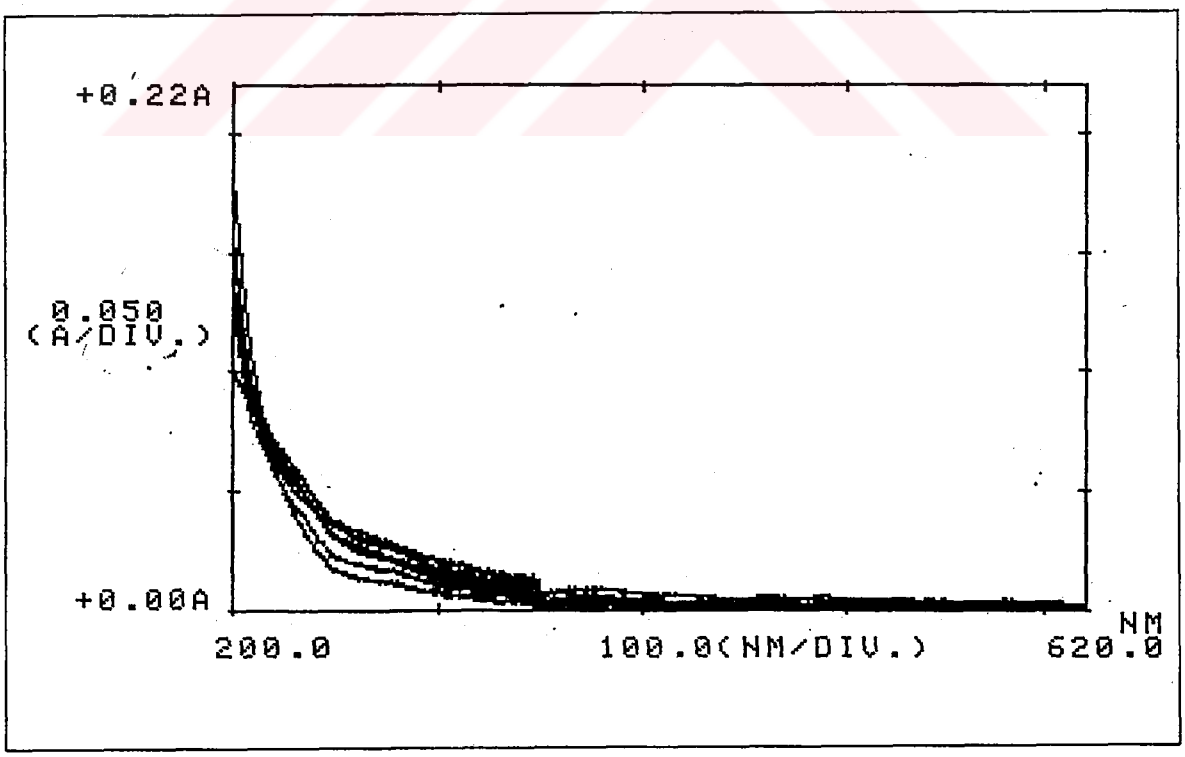

Figure G.6. Spectrums obtained from the ultrafiltration of preozonated and photocatalytically oxidized humic acid sample (Sample 3) (From top to bottom: Unfiltered sample, filtrates from membrane filters 450,000 – 500 Daltons)

REFERENCES

Allemane, H., Delouane, B., Paillard, H., Legube, B., "Comparative Efficiency of Three Systems (O_3, O_3/H_2O_2 and O_3/TiO_2) for the Oxidation of Natural Organic Matter in Water", *Ozone Sci. Eng.*, 15, 419-432, 1993.

Amy, G. L., Chadik, P. A., Chowdhury, Z. K., "Developing Models for Predicting Trihalomethane Formation Potential and Kinetics", *J. Am. Water Works Assoc.*, July, 89-97, 1987.

Amy, G. L., Kuo, C. J., Sierka, R. A., "Ozonation of Humic Substances: Effects on Molecular Weight Distributions of Organic Carbon and Trihalomethane Formation Potential", *Ozone Sci. Eng.*, 10, 39-54, 1988.

Amy, G.L., Sierka, R.A., Bedessem, J., Price, D., Tan, L., "Molecular Size Distributions of Dissolved Organic Matter", *J. Am. Water Works Assoc.*, 86, 6, 67-75, 1992.

Anderson, L.J., Johnson, J.D., Christman, R.F., "Extent of Ozone's Reaction with Isolated Aquatic Fulvic Acid", *Environ. Sci. Technol.*, 20, 739-742, 1986.

APHA, AWWA, WEF, *Standard Methods for the Examination of Water and Wastewater,* 18th Edition, Washington DC., Am. Public Health Assoc., 1992.

Arai, H., Arai, M., Sakumoto, A., "Exhaustive Degradation of Humic Acid in Water by Simultaneous Application of Radiation and Ozone", *Wat. Res.*, 7, 885-891, 1986.

Backlund, P., "Degradation of Aquatic Humic Material by Ultraviolet Light", *Chemosphere,* 23, 12, 1869-1878, 1992.

Banks, J., Wilson, D., "Use of UV_{254} to Predict the Relationship Between NOM and THMs on Upland Waters", *Proceedings of Symposium on Characterization and Treatment of Natural Organic Matter, Cranfield University,* May 15th, 2002.

Bekbolet, M., "Destructive Removal of Humic Acids in Aqueous Media by Photocatalytic Oxidation with Illuminated Titanium Dioxide", *J. Environ. Sci. Health, A.*, 31, 4, 845-858, 1996.

Bekbolet, M., Cecen, F. and Ozkosemen, G., "Photocatalytic Oxidation and Subsequent Adsorption Characteristics of Humic Acids" *Water Sci. Technol.*, 34, 9, 65-72, 1996.

Bekbolet, M., Ozkosemen, G., "A Preliminary Investigation on the Photocatalytic Degradation of a Model Humic Acid", *Water Sci. Technol.*, 33, 6, 189-194, 1996.

Bekbolet, M., Balcioglu, I., "Photocatalytic Degradation Kinetics of Humic Acid in Aqueous TiO_2 Dispersions: The Influence of Hydrogen Peroxide and Bicarbonate Ion", *Water Sci. Technol.*, 34, 9, 73-80, 1996.

Bekbolet, M., Boyacioglu, Z., Ozkaraova, B., "The Influence of Solution Matrix on the Photocatalytic Removal of Color from Natural Waters", *Water Sci. Technol.*, 38, 6, 155-162, 1998.

Bekbolet, M., "TiO_2 Mediated Photocatalytic Removal of Color from Natural Waters: Effect of Aqueous Medium", *Abstract Book of Pan-American Workshop on Commercialization of Advanced Oxidation Technologies, London-Ontario-Canada,* pp 255, 1998.

Bekbolet, M., Suphandag, A. S., Uyguner, C., "An Investigation of the Photocatalytic Efficiencies of TiO_2 Powders on the Decolourisation of Humic Acids", *J. Photochem. Photobiol. A.*, 148, 121-128, 2002.

Bian, R., Watanabe, Y., Tambo, N., Ozawa. G., " Removal of humic substances by UF and NF membrane systems", *Water Sci. Technol.*, 40, 9, 121-129, 1999.

Bose, P., Bezbarua, B., K., Reckhow, D. A., "Effect of Ozonation on Some Physical and Chemical Properties of Aquatic Natural Organic Matter", *Ozone Sci. Eng.*, 16, 89-112, 1994.

Boyce, S. and Hornig, D, "Reaction Pathways Of Trihalomethane Formation From The Halogenation of Dihydroxyaromatic Model Compounds of Humic Acid", *Environ. Sci. Technol.*, 17, 202-211, 1983.

Calvert, J.G., Pitts, J. N., *Photochemistry,* Wiley, New York, 1966.

Camel, V., Bermond, A., "The Use of Ozone and Associated Oxidation Processes in Drinking Water Treatment, *Wat. Res.*, 32, 11, 3208-3222, 1998.

Chan, Y. C., Chen, J. N., Lu, M. C., "Intermediate Inhibition in the Heterogeneous UV-Catalysis using a TiO_2 Suspension System", *Chemosphere,* 45, 29-35, 2001.

Chiang, P.C., Chang, E.E., Liang, C.H., "NOM Characteristics and Treatabilities of Ozonation Processes", *Chemosphere*, 46, 929-936, 2002.

Chin, Y-P., Aiken, G., O'Loughlin, E., "Molecular Weight Polydispersity and Spectroscopic Properties of Aquatic Humic Substances", *Environ. Sci. Technol.*, 28, 11, 1853-1858, 1994.

Cho, J., Amy, G., Pellegrino, J., "Membrane Filtration of Natural Organic Matter: Initial Comparison of Rejection and Flux Decline Characteristics with Ultrafiltration and Nanofiltration Membranes", *Wat. Res.*, 33, 11, 2517-2526, 1999.

Cooper, C., Burch, R., "An Investigation of Catalytic Ozonation for the Oxidation of Halocarbons in Drinking Water Preparation", *Wat. Res.*, 33, 3695-3700, 1999.

Eggins, B. R., Palmer, F. L., Byrne, J. A., "Photocatalytic Treatment of Humic Substances in Drinking Water", *Wat. Res.*, 31, 5, 1223-1226, 1997.

EPA, Treatment Techniques for Controlling Trihalomethanes in Drinking Water, EPA/600/2-81/156, Ohio, USA, 1981.

Evans, F., *Ozone in Water and Wastewater Treatment*, Ann Arbor Science Publishers, Inc., Michigan, 1972.

Franch, M. I., Ayllon, J. A., Peral, J., Domenech, X., "Kinetics and Mechanism of Oxalic, Maleic and Fumaric Acids Degradation by TiO_2-Photocatalysis", *Abstract Book of 2nd International Meeting on Solar Chemistry and Photocatalysis: Environmental Application, Saint-Avold (France), May 29-31,* O39, 2002.

Fujishima, A., Hashimoto, K., Watanabe, T., *TiO_2 Photocatalysis Fundamentals and Applications*, BKC, Inc. Japan, 1999.

Gaffney, J. S., Marley, N. A., Clark, S. B., *Humic and Fulvic Acids: Isolation, Structure and Environmental Role,* ACS Symposium Series No. 652, Washington DC, pp 2-16, 1996.

Gjessing, E. T., *Origin, Formation and Distribution of Humus in Physical and Chemical Characteristics of Aquatic Humus*, Ann Arbor Science Publishers Inc, Michigan, 1976.

Gjessing, E.T., Alberts, J.J., Bruchet, A., Egeberg, P.K., Lydersen, E., McGown, L.B., Mobed, J.J., Münster, U., Pempkowiak, J., Perdue, M., Ratnawerra, H., Rybacki, D., Takacs, M., Abbt-Braun, G., "Multi-method Characterisation of Natural Organic Matter Isolated from Water: Characterisation of Reverse-Osmosis Isolates from Water of Two Semi-Identical Dystrophic Lakes Basins in Norway", *Wat. Res.*, 32, 20, 3108-3124, 1998.

Glaze, W. H., Wallace, J. L., "Control of Trihalomethane Precursors in Drinking Waters: Granular Activated Carbon with and without Preozonation", *J. Am. Water Works Assoc.*, 76, 68-76, 1984.

Glaze, W., Peyton, G. R., Huank, F.Y., Burleson, J.L., Johns, P.C, *Oxidation of Water Supply Refractory Species by Ozone with Ultraviolet Radiation*, EPA/600/2-80/110, 1980.

Goel, S., Hozalski, R. M., Bouwer, E. J., "Biodegradation of NOM: Effect of NOM Source and Ozone Dose", *J. Am. Water Works Assoc.,* January, 90-105, 1995.

Gonenc, D., Bekbolet, M., "Interactions of Hypochlorite Ion and Humic Acid: Photolytic and Photocatalytic Pathways", *Water Sci. Technol.,* 44, 5, 205-210, 2001.

Gottschalk, C., Libra, J. A., Saupe, A., *Ozonation of Water and Wastewater,* Wiley-VCH, Germany, 2000.

Gracia, R., Aragues, J. L., Ovelleiro, J. L., "Study of the Catalytic Ozonation of Humic Substances and Their Ozonation Byproducts", *Ozone Sci. Eng.,* 18, 195-208, 1996.

Guittonneau, S., Thibaudeau, D. and Méallier,P., "Free Radicals Formation Induced by the Ozonation of Humic Substances in Aqueous Medium" *Catal. Today*, 29, 323-327, 1996.

Gurol, M. D., " Factors Controlling the Removal of Organic Pollutants in Ozone Reactors " *J. Am. Water Works Assoc.,* August, 55-60, 1985.

Gurol, M. D., Singer, P. C., " Dynamics of the Ozonation of Phenol-II : Mathematical Simulation " *Wat. Res.*, 17, 1173-1181, 1983.

Gurol, M. D., Singer, P. C., " Kinetics of Ozone Decomposition: A Dynamic Approach" *Environ. Sci. Technol.*, 16, 377-383, 1982.

Hatchard, C. G., Parker, C. A., "A New Sensitive Chemical Actinometer II. Potassium Ferrioxalate as a Standard Chemical Actinometer", *Proceedings of Royal Society London,* Series A, 235, 518-536, 1956.

Hoigné, J., Bader, H., "Role of Hydroxyl Radical Reactions in Ozonation Processes in Aqueous Solutions", *Wat. Res.,* 10, 377, 1976.

Hutzinger, O. (Ed.), *The Handbook of Environmental Chemistry*, Volume 2, Part A, Springer-Verlag Berlin, 1980.

Inel, Y., Okte, A. N., "Photocatalytic Degradation of Succinic Acid in Aqueous Suspensions of Titanium Dioxide: An Initial Kinetic Investigation of CO_2 Photogeneration", *Toxicol. Environ. Chem.*, 55, 115-126, 1996.

Inel, Y., Okte, A. N., "Photocatalytic Degradation of Malonic Acid in Aqueous Suspensions of Titanium Dioxide: An Initial Kinetic Investigation of CO_2 Photogeneration", *J. Photochem. Photobiol. A.*, 96, 175-180, 1996.

Inel, Y., Okte, A. N., "TiO_2 Sensitized Photomineralization Kinetics of Phthalic Anhydride", *Chemosphere*, 36, 14, 2969-2975, 1998.

Inel, Y., Okte, A. N., "Photodegradation Kinetics of Adipic Acid in the Presence of TiO_2", *Toxicol. Environ. Chem.*, 65, 123-133, 1998.

Karanfil, T., Kilduff, J. E., Schlautman, Weber, W. J. J., "Adsorption of Organic Macromolecules by Granular Activated Carbon. 1. Influence of Molecular Properties Under Anoxic Solution Conditions", *Environ. Sci. Technol.*, 30, 2187-2194, 1996.

Kavanaugh, M. C., Trussell, A. R., Cromer, J and Trussell, R. R., "An Empirical Kinetic Model of Trihalomethane Formation: Applications to Meet the proposed THM Standard", *J. Am. Water Works Assoc.*, 72, 10, 578-582, 1980.

Kerc, A. and Saatci, A. M., "Computerized Continuous Monitoring and Analysis of Ozone in Solution", *Ozone Sci. Eng.*, 18, 469-476, 1996.

Kerc, A., Saatci, A. M., Aktuz, E., "Measurement of Ozone Demand", *Abstract Book of The Fourth International Conference on Advanced Oxidation Technologies*, Orlando-USA, September 22-24, 1997.

Kerc, A., Bekbolet, M., Saatci, A., "Color and Organic Matter Removal in Humic Acid Solutions by Ozonation", *Proceedings of the 2nd International Conference on Oxidation Technologies for Water and Wastewater Treatment,* Clausthal-Zellerfeld, Germany, May 28-31, 2000.

Kerc, A., Bekbolet, M., Saatci, A., "Sequential Oxidation of Humic Acids by Ozonation and Photocatalysis", *Proceedings of IO3A- International Conference on Ozone in Global Water Sanitation, Amsterdam, The Netherlands, October 1-3,* V2 1-V2 16, 2002.

Kerc, A., Bekbolet, M., Saatci, A., "Effect of Partial Oxidation by Ozonation on the Photocatalytic Degradation of Humic Acids", *Int. J. Photoenergy,* Accepted for publication, 2003.

Kilduff, J.E., Karanfil, T., Weber, Jr. W. J., "Competitive Interactions among Components of Humic Acids in Granular Activated Carbon Adsorption Systems: Effects of Solution Chemistry", *Environ. Sci. Technol.,* 30, 1344-1351, 1996.

Killops, S. D., "Volatile Ozonization Products of Aqueous Humic Material", *Wat. Res.*, 20, 2, 153-165, 1986.

Kitis, M., Karanfil, T., Wigton, A., Kilduff, J. E., "Probing Reactivity of Dissolved Organic Matter for Disinfection By-Product Formation Using XAD-8 Resin Adsorption and Ultrafiltration Fractionation", *Wat. Res.,* 36, 3834-3848, 2002.

Ko, Y. W., Chiang, P. C., Chang, E. E., "Ozonation of p-Hydroxybenzoic Acid Solution", *Ozone Sci, Eng.,* 20, 343-360, 1998.

Korshin, G. V., Kumke, M. U., Li, C. W., Frimmel, F. H., "Influence of Chlorination on Chromophores and Fluorophores in Humic Substances", *Environ. Sci. Technol.,* 33, 1207-1212, 1999.

Krasner, S. W., Croue, J. P., Buffle, J., Perdue, E. M., "Three Approaches for Characterizing NOM", *J. Am. Water Works Assoc.*, June, 66-79, 1996.

Kuo, C., "Improved Application of Ion Chromatographic Determination of Carboxylic Acids in Ozonated Drinking Water", *J. Chromatography A.*, 804, 265, 1998.

Kusakabe, K., Aso, S., Hayashi, J. I., Isomura, K., Morooka, S., "Decomposition of Humic Acid and Reduction of Trihalomethane Formation Potential in Water by Ozone with UV Irradiation", *Wat. Res.*, 24, 6, 781-785, 1990.

Lambert, S.D., Graham, N.J.D., "Removal of Non-specific Dissolved Organic Matter from Upland Potable Water Supplies – II Ozonation and Adsorption", *Wat. Res.*, 29, 10, 2427-2433, 1995.

Langlais, B., Reckhow, D. A., Brink, D., *Ozone in Water Treatment Application and Engineering,* Lewis Publishers, Inc., USA, 1991.

Legrini, O., Oliveros, E., Braun, A., "Photochemical Processes for Water Treatment", *Chem. Rev.*, 671-689, 1993.

Legube, B., Croué, J.P., Reckhow, D.A., Doré, M., "Ozonation of Organic Precursors: Effects of Bicarbonate and Bromide", *Proceedings of the International Conference: The Role of Ozone in Water and Wastewater Treatment,* London 13-14 November, 76-86, 1985.

Legube, B., Croue, J. P., Laat, J., Doré, M., "Ozonation of an Extracted Aquatic Fulvic Acid: Theoretical and Practical Aspects", *Proceedings of the IO_3A-8^{th} Ozone World Congress*, Zurich, Switzerland, 1987.

Legube, B., Croue, J. P., Laat, J. D., Doré, M., "Ozonation of an Extracted Aquatic Fulvic Acid: Theoretical and Practical Aspects", *Ozone Sci. Eng.*, 11, 1, 69-92, 1989.

Leifer, A., *The Kinetics of Environmental Aquatic Photochemistry, Theory and Practice,* American Chemical Society, Washington D.C. Chapter 12. 1988.

Logan, E. B., Jiang, Q., "Molecular Size Distribution of Dissolved Organic Matter", *ASCE J. Environ. Eng.,* 116, 6, 1046-1062, 1990.

Maartens, A., Swart, P., Jacobs, E. P., "Removal of Natural Organic Matter by Ultrafiltration: Characterization, Fouling and Cleaning", *Water Sci. Technol.*, 40, 9, 113-120, 1999.

Malcolm, R.L., MacCarthy, P., "Limitations in the Use of Commercial Humic Acids in Water and Soil Research", *Environ. Sci. Technol.,* 20, 904-911, 1986.

Manahan, S. E., *Fundamentals of Aquatic Chemistry in Environmental Chemistry*, Lewis Publishers Inc., Michigan, 1991.

Mao, J., Hu, W., Schmidt-Rohr, K., Davies, G., Ghabbour, E.A., Xing, B., "Structure and Elemental Composition of Humic Acid: Comparison of Solid-State ^{13}C-NMR Calculations and Chemical Analysis", in Davies, G., Ghabbour, E.A. (Eds.), *Humic Substances Structures, Properties, Uses,* Royal Society of Chemistry, 1998.

Martin, C. A., Alfano, O. M., Cassano, A. E., "UV Radiation + Hydrogen Peroxide Decolorization of Waters for Domestic Supply", *Abstract Book of 5th International Conference on Advanced Oxidation Technologies for Water and Air Remediation,* Albuquerque, New Mexico, USA, pp-3, May 24-28, 1999.

Maximov, O. B., Kraskovskaya, N. P., *Geoderma*, 18, 227-228, 1977.

Mayo, P., Shizuka, H., "Measurements of Reaction Quantum Yields" in Ware, W. R. (Editor), *Creation and Detection of Excited States*, Chapter 4, Marcel Dekker, New York, 1976.

Montgomery, J. M., *Water Treatment Principles and Design*, John Wiley and Sons, New York, 1985.

Myllykangas, T., Nissinen, T.K., Rantakokko ,P., Martikainen, P.J., Vartiainen, T., "Molecular Size Fractions of Treated Aquatic Humus", *Wat. Res.*, 36, 3045-3053, 2002.

Ollis, D. F., Pelizetti, E., Serpone, N., "Heterogeneous Photocatalysis in the Environment: Application to Water Purificiation", in Serpone, N., Pelizetti, E. (Eds.) *Photocatalysis Fundamentals and Application*, John Wiley and Sons, 1989.

Owen, D., Amy, G.L., Chowdhury, Z. K., Paode, R., McCoy, G., Viscosil, K., "NOM Characterization and Treatability", *J. Am. Water Works Assoc.*, 87, 1, 46-63, 1995.

Palmer, F. L., Eggins, B. R., Coleman, H. M., "The Effect of Operational Parameters on the Photocatalytic Degradation of Humic Acid", *J. Photochem. Photobiol. A.*, 148, 137-143, 2002.

Peavy, H. S., Rowe, D. R., Tchobanoglous, G., *Environmental Engineering,* McGraw-Hill Book Company, Singapore, 1985.

Peuravuori, J., Pihlaja, K., "Molecular Size Distribution and Spectroscopic Properties of Aquatic Humic Substances", *Analy. Chim. Acta.*, 337, 133-149, 1997.

Reckhow, D. A., Singer, P. C., "The Removal of Organic Halide Precursors by Preozonation and Alum Coagulation", *J. Am. Water Works Assoc.*, April, 151-157, 1984.

Reckhow, D. A., Legube, B., Singer, P. C., "The Ozonation of Organic Halide Precursors: Effect of Bicarbonate", *Wat. Res.*, 20, 8, 987- 998, 1986.

Reckhow, D. A., Singer, P. C., Malcolm, R. L., "Chlorination of Humic Materials: Byproduct Formation and Chemical Interpretations", *Environ. Sci. Technol.*, 24, 11, 1655-1664, 1990.

Rook, J. J., "Formation of Haloforms During Chlorination of Natural Water", *Water Treatment Exam.*, 23, 234-243, 1974.

Sawyer, C. N., McCarty, P. L., Parkin, G. F., *Chemistry for Environmental Engineering*, McGraw-Hill, Inc., 4th Edition, 1994.

Serpone, N., "Relative Photonic Efficiencies and Quantum Yields in Heterogeneous Photocatalysis", *J. Photochem. Photobiol. A.*, 104, 1-12, 1997.

Siddique, M., Amy, G., Ryan, J., Odem, W., "Membranes for the Control of Natural Organic Matter from Surface Waters", *Wat. Res.*, 34, 13, 3355-3370, 2000.

Singer, P. C., "Assessing Ozonation Research Needs in Water Treatment", *J. Am. Water Works Assoc.*, 82, 78-88, 1990.

Solamons, T. W. G., *Organic Chemistry,* John Wiley and Sons, 5th Edition, 730-731, 1992.

Sonnenberg, L. B., Johnson, J. D., Christman, R. F., "Chemical Degradation of Humic Substances for Structural Characterization", *Proceedings of 193rd National Meeting of the American Chemical Society*, Denver, Colorado, April 5-10, 1987.

Sontheimer, H., Frick, B.R., Fettig, J., Hörner, G., Hubele, C., Zimmer, G., *Adsorptionverfahren zur Wasserreinigung*, DVWG-Forschungsstelle am Engker-Bunte Institut der Universitat Karlsruhe, 1985.

Staehelin, J., Hoigné, J., "Decomposition of Ozone in Water in the Presence of Organic Solutes Acting as Promoters and Inhibitors of Radical Chain Reactions", *Environ. Sci. Technol.*, 19, 1206-1216, 1985.

Stevenson, F. J., *Humus Chemistry: Genesis, Composition, Reactions,* Wiley-Interscience, New York, 1982.

Suffet, I.H., MacCarthy, P. (Eds.), *Aquatic Humic Substances*, American Chemical Society, 1989.

Takahashi, N., Nakai, T., Satoh, Y., Katoh, Y., "Ozonolysis of Humic Acid and its Effect on Decoloration and Biodegradability", *Ozone Sci. Eng.*, 17, 511-525, 1995.

Tapan, F., Turan, H., Basaran, E., "Removal of Trihalomethane Precursors by Ozonation", Senior Project, Advisor: Kerc, A, Marmara University, 2000.

Thurman, E. M., Wershaw, R.L., Malcolm, R.L., Pinckney, O.J., "Molecular Size of Aquatic Humic Substances", *Org. Geochem.*, 4, 27-35, 1982.

Thurman, E. M., Malcolm, R. L., "Structural Study of Humic Substances: New Approaches and Methods" in Christman, R. F., Gjessing, E. T. (Eds.), *Aquatic and Terrestrial Humic Materials*, Ann Arbour Science, pp. 1-23, 1983.

Trussell, R. R., Umphres, M. D., "The Formation of Trihalomethanes", *J. Am. Water Works Assoc.*, 70, 604-612, 1978.

Urano, K., Wada, H., Takemasa, T., "Emprical Rate Equation for Trihalomethane Formation with Chlorination of Humic Substances in Water", *Wat. Res.*, 17, 12, 17979-1802, 1983.

Westerhoff, P., Debroux, J., Aiken, G., Amy, G., "Ozone-Induced Changes in Natural Organic Matter (NOM) Structure", *Ozone Sci. Eng.*, 21, 551-570, 1999.

Wiszniowski, J., Robert, D., Gorska, J. S., Miksch, K., Weber, J. V., "Photocatalytic Decomposition of Humic Acids on TiO_2 Part I: Discussion of Adsorption and Mechanism", *J. Photochem. Photobiol. A.*, 5963, 1-7, 2002.

Yurteri, C., Gurol, M. D., "Ozone Consumption in Natural Waters: Effect of Background Organic Matter, pH and Carbonate Species", *Ozone Sci. Eng.*, 10, 277-290, 1988.

Zepp, R. G., Baughman, G.L., Schlotzhauer, P.F., "Comparison of Photochemical Behaviour of Various Humic Substances in Water: I. Sunlight Induced Reactions of Aquatic Pollutants Photosensitized by Humic Substances", *Chemosphere*, 10, 109-117, 1981.